Reconfigurability in Space Systems: Architecting Framework and Case Studies

by

Afreen Siddiqi

S.B in Mechanical Engineering, MIT, 1999
S.M in Aeronautics and Astronautics, MIT, 2001

Submitted to the Department of Aeronautics and Astronautics
in partial fulfillment of the requirements for the degree of

Doctor of Philosophy in Aeronautics and Astronautics

at the

MASSACHUSETTS INSTITUTE OF TECHNOLOGY

May 2006

Author .....
Department of Aeronautics and Astronautics
May 19, 2006

Certified by .....
Olivier L. de Weck
Assistant Professor of Aeronautics and Astronautics & Engineering Systems
Thesis Supervisor

Certified by .....
David W. Miller
Associate Professor of Aeronautics and Astronautics
Committee Member

Certified by .....
Jeffrey A. Hoffman
Professor of the Practice of Aeronautics and Astronautics
Committee Member

Certified by .....
Steven R. Hall
Professor of Aeronautics and Astronautics
Minor Advisor

Accepted by .....
Jaime Peraire
Professor of Aeronautics and Astronautics
Chair, Committee on Graduate Students

Reconfigurability in Space Systems: Architecting Framework and Case Studies

by

Afreen Siddiqi

Submitted to the Department of Aeronautics and Astronautics
on May 19, 2006, in partial fulfillment of the
requirements for the degree of
Doctor of Philosophy in Aeronautics and Astronautics

Abstract

Reconfigurability in engineered systems is of increasing interest particularly in Aerospace Systems since it allows for resource efficiency, evolvability, and enhanced survivability. Although it is often regarded as a desirable quality for a system, it has traditionally been difficult to quantitatively analyze its effects on various system properties in the early design stage. In order to allow for gaining an in-depth understanding of the various aspects of reconfigurability and its relationship with a system's architecture, a framework encompassing a set of definitions, metrics, and methods has been proposed. Two different modeling schemes, based on Markov models and controls theory, are first developed to show how the states and time aspects of reconfigurable systems can be naturally modeled and studied. An analytical model for quantifying the effect of reconfigurability on mission logistics, specifically spare parts demands, is formulated and it is shown through one specific example that reconfigurable parts can allow for 33-50% mass reduction. The system availability, however, becomes very sensitive to the reliability of the parts. Two case studies are then used for detailed illustration of the application of the developed framework. In the first case study, the effect of reconfigurability on a fleet of planetary surface vehicles for a surface exploration mission are analyzed. It is found that a fleet of reconfigurable vehicles can allow for a mass savings of up to 27% and their expected transport capability degradation is almost three times lower as compared to a fleet of non-reconfigurable vehicles. In the second case-study, the reconfiguration of low earth-orbit communication satellite constellations is considered for evolving to higher capacity levels. It is found that reconfiguring a previously deployed constellation can be a viable option only for certain capacity levels and multi-payload launch capability scenarios. In addition to the high level 'ility' perspectives, a lower level design assessment is also carried out through a survey of 33 representative reconfigurable systems. It is found that on average, for commercial items the cost of reconfigurability is 35%, and the average useful state occupancy time is always at least 10 times the reconfiguration time of the system. Based on the illustrative results of the case studies, and generalization of empirical data, a few principles and guidelines for design for reconfigurability are proposed.

Olivier L. de Weck
Title: Assistant Professor of Aeronautics and Astronautics & Engineering Systems
Thesis Supervisor

David W. Miller
Title: Associate Professor of Aeronautics and Astronautics
Committee Member

Jeffrey A. Hoffman
Title: Professor of the Practice of Aeronautics and Astronautics
Committee Member

Steven R. Hall
Title: Professor of Aeronautics and Astronautics
Minor Advisor

Acknowledgments

First and foremost, I am grateful to The Almighty whose help and mercy allowed me to initiate and complete this work. Alhamdolillah. I pray that He makes this work beneficial for many.

I would like to profoundly thank my advisor Professor Olivier de Weck for his guidance and advice. He helped me make sense of the new, unchartered territories of Systems Engineering. His unparalleled compassion, kindness, and generosity allowed me to cruise through the demands of graduate education and research along with new motherhood. I also want to thank my committee members for their time and support.

My dear husband Hamid Zaman deserves special thanks and gratitude for the almost superhuman strength and support he gave me during my PhD. He believed in me when I didn't, and gave me reason to keep going every time I was ready to quit. This work and dissertation would not have come about without his incredible sacrifices of time and sleep for endless months. I cannot thank him enough. My darling son Rahem, who has brought so much joy and fulfillment in my life, also deserves special praise for being the most well behaved and good natured baby. His cooperation, from sleeping through the night since he was 5 days old, to never fussing about food went a long way in helping me with my work. God bless you Rahem.

I would also like to thank my wonderful parents, Mr. F.R. Siddiqi and Mrs. Tarannum Siddiqi, whose prayers have never failed me throughout my life. I owe my successes to them, and am extremely grateful for the inspiration and encouragement they have always provided. I also want to thank my sisters Zoveen Siddiqi and Sameen Siddiqi for sharing my joys and difficulties and for being my sincere well-wishers. I am truly blessed to have them all in my life.

Many thanks also go to Christine Taylor for tips on optimization, Bill Nadir for making the CAD drawings of a planetary camper, Dan Kwon for being a study partner for the qualifying exams, Julien Lamamy for help while working on the CE&R project, Wilfried Hofstetter for providing useful references and source documents, and Matt Silver for compiling the information of launch vehicles. Special thanks to Bill Simmons for cheerfully helping through numerous Mac issues and for explaining Monte-Carlo simulations, and to Julie Finn for all her administrative help.

This research was supported by the Richard D. DuPont Fellowship, NASA's Concept Evaluation and Review (CE&R) study under sub-contract from Draper labs (contract number DL-H-551000), and through NASA's "Interplanetary Supply Chain Management and Logistics Architectures" project under contract number NNK05OA50C.

Contents

List of Figures

List of Tables

Nomenclature

Lower case

b	wheel width [m]
c	cohesion [Pa]
c_v	coefficient of variation
h	altitude [km]
l	failure rate [failures/day]
k_c	cohesive modulus of deformation
k_ϕ	frictional modulus of deformation
m_o	initial mass
$m_{P/L}$	mass of payload
m_s	structure mass
m_p	mass of propellant
m_{jk}	total number of reconfigurations/switches between states j and k in life time
p_{ij}	probability of reconfiguring from state i to j
$p(n)$	probability of n failures
q_e	# of units of a component in element e
r	range [km]
s	total number of spares
s_A	# of satellites per plane in constellation state A
s_E	maximum number of spares available from idle elements
s_I	initial number of spares in repository
$\underline{xa}_i$	state A constellation design i
z_{jk}	reconfiguration cost between state j and k
z	sinkage [m]

Upper Case

$A(t_i)$	availability at t_i
$\bar{B}(t_i)$	expected backorder level at t_i
$\bar{B}_c(s, t_i)$	expected backorder level at t_i for spares level s
$\mathbf{C}_p$	vector of capabilities
$\mathbf{C}$	vector of capacities [# of subscribers]
C_{new}	cost of new fixed/dedicated system
C_r	cost of reconfiguring existing system
D	wheel diameter [m]
D_a	satellite antenna diameter [m]
DP	Drawbar Pull [N]
E	total number of elements in mission
ETC	expected transport capability
$\mathbf{I}_o$	set of iso-performance (same capacity) designs
I_{sp}	specific impulse [sec]
J	objective function
M	cargo mass [kg]
MA	multi-access scheme
$P(s)$	probability of having s spares available
P_t	transmit power [W]
QPA	quantity per application
$\mathbf{R}$	matrix of reconfiguration costs
R_c	compaction resistance [N]
RI	reconfigurability index
S	set of finite states of a reconfigurable system
T	torque [Nm]
T_m	tow mass [kg]
T_r	reconfiguration time
T_s	average state occupancy time
V	velocity [km/hr]
W	wheel load [N]

Lower Case Greek

$\gamma(t_i)$	percentage of elements operating at t_i
γ_A	aerobrake mass factor
δ_C	percent cost savings with reconfigurable system
δ_J	performance ratio of reconfigurable and dedicated system
ϵ_{min}	min elevation angle [deg]
η_f	functional efficiency
η_p	performance efficiency
λ	mean number of failures
λ_c	coefficient of connectivity
λ_s	structure mass fraction
μ_c	combinatorial efficiency
ν	transport capability [kg-km/hr]
$\pi_i(n)$	probability of being in state i at time n
ρ	total resources
τ	shear strength [Pa]
ϕ	internal friction angle [deg]
$\phi_{ij}(m,n)$	transition probability between states i and j from time m to n
ψ	growth factor

Upper Case Greek

$\Gamma_e(t_k)$	binary variable with value 1 if element e is operating in interval t_k
Δ_e	evolvability
ΔV	velocity increment
Λ	relative degradability
Ξ_f	relative functional efficiency
Ξ_p	relative performance efficiency
$\mathbf{\Pi}$	vector of state probabilities
$\mathbf{\Phi}(m,n)$	multi-step transition probability matrix
Φ_r	relative robustness

Chapter 1

Introduction

Reconfigurability is of increasing importance in systems that require multiple capabilities, are subject to uncertainty in usage, and need to survive in the face of unknown disturbances or adverse operating conditions. This thesis explores reconfigurability from a system architectural perspective. It analyzes the high level system requirements that lead towards reconfigurability, develops key concepts and notions that can be used in studying various relevant aspects of this property, and then uses two case studies to illustrate their specific application. A more detailed view at a lower level is then undertaken in which a set of reconfigurable systems are surveyed, and common trends in their behavior and architecture are identified. The observations and analytical frameworks are then combined in proposing guidelines for Design for Reconfigurability in systems.

This chapter presents the motivation, background research, and road map of the thesis.

1.1 Motivation

Reconfigurable systems in general are understood to be those systems that can be modified or adapted in order to meet new or changed requirements. Such systems range from a box of LEGOs from which one can build different types of toys to complex manufacturing systems that can produce a variety of products. The common denominator in all of these systems is their ability to be changed so that they can fulfill a range of needs.

A common notion in the context of change in systems is *Flexibility*, a word that comes from the Latin word for bendable. Its meaning is often taken to be 'adaptable' or 'capable of change'. One particular definition is that it is "the property of a system that is capable of undergoing changes with relative ease"[26]. A comprehensive discussion of the meaning and definition of flexibility is provided in [117], where it is argued that flexible systems are those that can respond to changes in their initial objectives and requirements that occur *after* the system has been fielded, *i.e.* during the system's operation stage in its life-cycle. Given this understanding of flexibility, there are

indeed some similarities with the concept of *reconfigurability*. According to one definition from NASA, reconfigurable systems are: *Cost-effective systems that have the capability to be tuned or adapted, functionally and/or physically, either autonomously or under remote control, to optimally achieve one or more goals or objectives. These systems can adapt to events or scenarios that can be determined in advance or react to situations that were not anticipated at the time of design*[109]. A key differentiating factor for reconfigurability (versus flexibility) however, is that reconfigurable systems can *re*-configure (at least technically) which is not necessarily the case for flexible systems. The reconfigurable systems thus do not go through only a one-way change. Chapter 2 will propose and discuss a definition of reconfigurable systems and reconfigurability in more detail.

In the context of space systems, the ability to reconfigure is becoming increasingly desirable. Traditionally, spacecraft were built for pre-defined missions and fixed requirements. Some of the next generation space exploration missions, however, will be much different. They will need to last longer and explore deeper, will encounter unknown conditions, and will also be cost constrained. There will be an increasing emphasis on cost, survivability, and adaptability of missions. In a recent document authored by NASA officials it is noted that: "to enable long duration missions with minimal redundancy and mass, *system software and hardware must be reconfigurable*. This will enable increased functionality and multiple use of launched assets while providing the capability to quickly overcome components failures [90]." Given the strong interest and motivation for realizing reconfigurable space systems, this research undertakes an in-depth investigation of the implications and effects of reconfigurability.

1.2 Background

A common theme in requirements for future complex systems is their ability to adapt, and respond to new conditions. The desire to build systems that can deal with uncertainties of various kinds (economic, technical, political *etc.*) has been the incentive for developing principles, methods and technologies that will allow engineers to design for change [139]. System designs and the design processes themselves are being improved so that ambiguities can be reduced [115] and optimal designs of multi-functional and capable systems can be conceived. It is understood that system reconfigurability can be one of the key enablers of a system's ability to respond to new needs and conditions. Additionally it can allow for maximizing utility of various resources (which is particularly desirable for space systems). In recent years a significant amount of research has been focused on investigating and developing various kinds of reconfigurable systems. Figure 1-1 serves to illustrate the rapid increase in publications related to reconfigurability. The results of a keyword search in the combined databases of Compendex, and Inspec (which are large databases of engineering journal articles, proceedings and reports) are shown, in which it is clear to see the increasingly growing

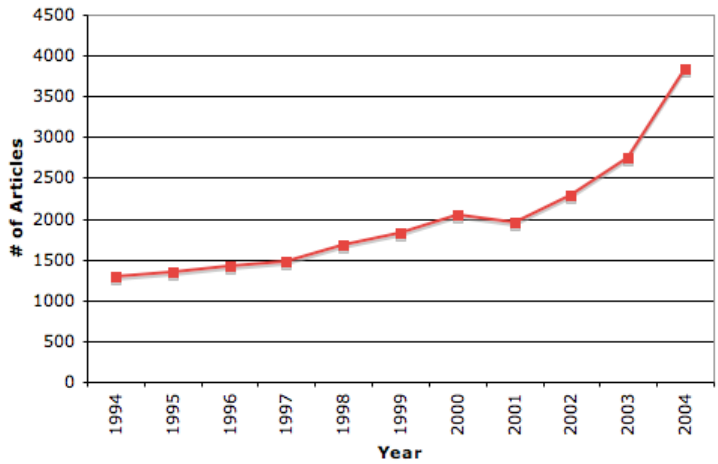

Figure 1-1: Number of Articles with keyword:'reconfig*' in their title or abstract

interest in this topic.

1.2.1 Literature Review

The existing research in reconfigurability from a technological perspective is focused very highly in the computing domain, followed by the manufacturing systems domain. An increased interest has also recently developed in morphing Unmanned Aerial Vehicles (UAV)s, and in reconfigurable modular spacecraft. The following sections review the research that has been conducted from various perspectives in these areas.

Reconfigurable Computing and Informational Systems

An area of considerable interest for reconfigurability is in computing [65] and signal processing. Field Programmable Gate Arrays (FPGAs) and other similar devices which allow circuits to be defined by software and provide for easy reconfigurations are increasingly getting attention for space systems [46, 79] in addition to manufacturing/test and many other applications. Fault-tolerant avionics requiring less redundancy and using reconfigurable generic function blocks [41], and evolvable hardware [132] that can reconfigure under different operating conditions have been proposed for enhanced survivability in long duration space missions.

Communication satellites have also received a great deal of attention in terms of making them reconfigurable in orbit. The applications range from adaptive nulling algorithms (implemented on reconfigurable hardware) to combat uplink jamming and noisy environments [88], to reconfigurable transponders in which most hardware circuit elements are implemented in software for on-orbit reconfigurations [99]. Along these lines, techniques have also been developed that allow for dynamically reconfiguring embedded software in communication satellites while ensuring quality of service

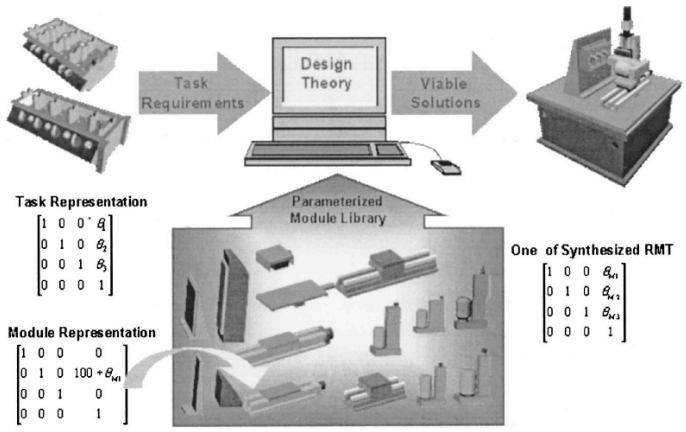

Figure 1-2: Overview of Reconfigurable Machine Tool Design [101]

to the customers [28].

Reconfigurable Manufacturing Systems

The National Research Council has identified Reconfigurable Manufacturing Systems (RMS) as the number one priority technology for future manufacturing [93]. A major effort is therefore being expended on studying RMS since responsiveness is now a new objective along with cost and quality. Reconfigurable Manufacturing Systems are considered to be those in which a machining system is created by incorporating basic process modules, both hardware and software, that can be rearranged or replaced quickly and reliably. The reconfigurability allows for adding, removing, or modifying specific process capabilities, controls, software, or machine structure to adjust production capacity in response to changing market demands or technologies [93]. Several researchers have contributed work that deals with understanding, modeling, and designing RMS. Capacity management issues in these systems have been analyzed in detail [29, 145]. First order deterministic cost models which implicitly include reconfiguration cost and time have been used to compare the life cycle cost of an RMS with that of a dedicated manufacturing system and it has been shown that economic benefits can be realized with an RMS [128]. A major aspect in RMS research has been the design process of Reconfigurable Machine Tools (RMT). Although a variety of algorithms and optimization approaches have been proposed [100, 81, 146], the general theme is that from a set of commercially available modules (that constitute a module 'library') the optimal RMT design is formulated so that it has the desired reconfigurability aspects in its Degrees of Freedom (DOF), work piece geometry variability, spindle orientation *etc.* Figure 1-2 illustrates the basic approach. The essence of the approach is to have a sufficient yet minimum set of modules that allow an RMT to have great versatility [42]. This is in contrast to the CNC machines or Flexible Manufacturing Systems (FMS) in which a lot of capabilities are always built-in. The spirit of RMS research and design is to have systems that do away with the extra all-time-present capability, and only employ appropriate resources (hardware

and software) when needed. So RMS envision using modular machines that can be installed in fractional amounts, yet perform as closely in efficiency to a dedicated system as possible at high volumes.

Morphing Aircraft

Morphing aircraft that can radically change shape are being developed and some are now in prototype stages [13]. Some examples of their geometry changes include: (1) a 200 percent change in aspect ratio, (2) a 50 percent change in wing area, (3) a 5° change in wing twist, and (4) a 20° change in wing sweep. The motivation for this effort is the high desirability of multi-capability in systems. Morphing aircraft will be able to perform multiple missions that previously required separate aircraft especially designed for different operating requirements. The goal is to have unmanned aircraft with morphable wings so that they can switch from reconnaissance missions to attack missions when needed. A way to study morphing capability as an independent design variable in architectural studies has been proposed [116]. It has also been shown how increasing reconfigurability makes the system perform better in each desired configuration [75].

Reconfigurable Modular Spacecraft

Modular spacecraft have been proposed for quite some time now. It was shown that instead of a pressurized cylinder serving as the basic module for space stations, the isosceles tetrahedron permits the construction of pressurized volumes of conceivably any shape. Spacecraft based on these modules can be reconfigured to fulfill several roles simultaneously such as orbital support craft, lander, and surface base [63]. More recently, the truncated octahedron has been proposed as a better option, in which the modules can have the highest packing efficiency (which is highly desirable for space applications) [107]. Some researchers at NASA Goddard center have been pursuing another modular architecture based on tetrahedrons [43]. The Autonomous NanoTechnology Swarm (ANTS) mission architecture is based on autonomous, addressable, self-configuring components with a tetrahedral structural framework which form tethers, struts, or shells which can be reversibly deployed or stowed from nodes. Radical changes in shape and function can potentially be achieved from these modular elements [44].

Ideas of a 'plug and play', reconfigurable architecture concept called SpaceFrame [97], and many other modular architectures have been developed recently. The motivation behind this modularity is to allow for cheaper and faster manufacturing solutions, and also potentially be able to do on-orbit reconfiguration (through easy replacement of the modules).

These are examples of cases where reconfigurability has been studied at the system level. A number of researchers have been looking at the sub-system level to improve performance, or to manage fluctuating needs. An important area of on-going research is satellite antennas and other

components associated with data transmission and reception on spacecraft. Active phased arrays [148] for flexibility in steering and reconfiguring beams, and flexible frequency generation systems [47, 50] are are few such examples.

There has also been attention given to various automotive systems and sub-systems from flexible race cars to wheels. The possibilities of improving performance of formula one race cars has been investigated by actively reconfiguring the center of gravity, roll stiffness, and the aerodynamic down force while the car is in operation [61, 106]. This allows the car to remain optimal under different regions of the track that may be straight or curved with different radii of curvatures. In traditional cases, a system is designed to operate at a single Pareto-optimal point corresponding to some acceptable level of trade off between competing objectives. Using active reconfiguration, it has been proposed that the system will be able to perform at various points along the Pareto front as the conditions change.

1.3 Thesis Contributions

From the review of research that has been conducted in various usage domains it is evident that all the work is focused on particular applications. There is no systems-level analysis for reconfigurability in general that is not application or domain specific. In each case, the research either focuses on a particular technological solution that makes a traditionally fixed system reconfigurable, or the work outlines the effect of a particular architecture on the reconfigurable system's performance, cost *etc.* There is thus a void in existing body of research in the context of reconfigurability that helps in understanding what reconfigurability essentially means, when it should be incorporated in a system's architecture or design, to what extent and how much of it should be present (if at all), and what are the implications of when and how it is implemented in the system.

It can also be noted that there has been a tremendous amount of work carried out on modularity and modular architecture, and very often it has been motivated by the need of making the system reconfigurable in various ways. However a holistic study of the end goal, *i.e.* reconfigurability itself has not been undertaken.

Furthermore, as discussed above, although computing, manufacturing and even aircraft have received considerable attention, space systems on the whole have not received that level of attention. Since the research is domain specific it is not often directly applicable to space systems. Consider for instance the research carried out for designing an RMT where it was described earlier how a 'module library' approach is used to find optimal designs. These approaches cannot be applied for space systems as-is in general (although there has been significant efforts in this regard to modular spacecraft design). In the context of reconfigurable systems, the question is usually what those modules in the 'library' should be since these are not commercially available items. Several unique

aspects, such as physical in-accessibilty, can also make the application of work done for other domains incompatible for space systems.

So while mission designers and senior officials high-light the desirability of having reconfigurable space systems, there is much work that is required in identifying and quantifying the impact of reconfigurability in these systems. This thesis, focused on space systems in particular, therefore attempts to fill these existing gaps for understanding, analyzing, and trading reconfigurability in the architecture of space systems.

Keeping these gaps in view, a comprehensive study of reconfigurability from various perspectives was carried out. Two case studies were then employed to investigate in detail some of the developed concepts and methodologies. Some of the key contributions of this work are as follows:

- A clear definition is formulated and a categorization of when and why systems need to be reconfigurable is provided. The key properties that reconfigurability enables are identified which provide the link between systems requirements, reconfigurable architectures, and enabling technologies.
- Essential concepts and notions are introduced that are key for studying and analyzing reconfigurability. Since reconfigurability is essentially a qualitative aspect of a system, it has so far not been rigorously treated as a property that can be quantitatively and analytically assessed. Several metrics and quantification schemes are proposed.
- Two methodologies for analyzing time related (or dynamical) aspects of reconfigurability are suggested and illustrated with specific detailed examples.
- An analytic model is formulated for quantifying the impact of reconfigurability on logistics (specifically spare parts) requirements for space exploration missions.
- Three fundamental architectural types for reconfigurable systems are proposed (after conducting a detailed survey of 33 different reconfigurable systems).
- Trends in the cost of reconfigurability in commercial systems, relationship between reconfiguration time and useful state occupancy time, and the impact of when and how the reconfiguration occurs are identified.
- A set of architecting principles and a framework for design for reconfigurability are proposed.

1.3.1 Research Approach

Figure 1-3 provides a summary of the main approach that was undertaken for this research. In order to gain an understanding of reconfigurability and develop a framework for its analysis, the first step involved reviewing related research. A large number of reconfigurable systems were also

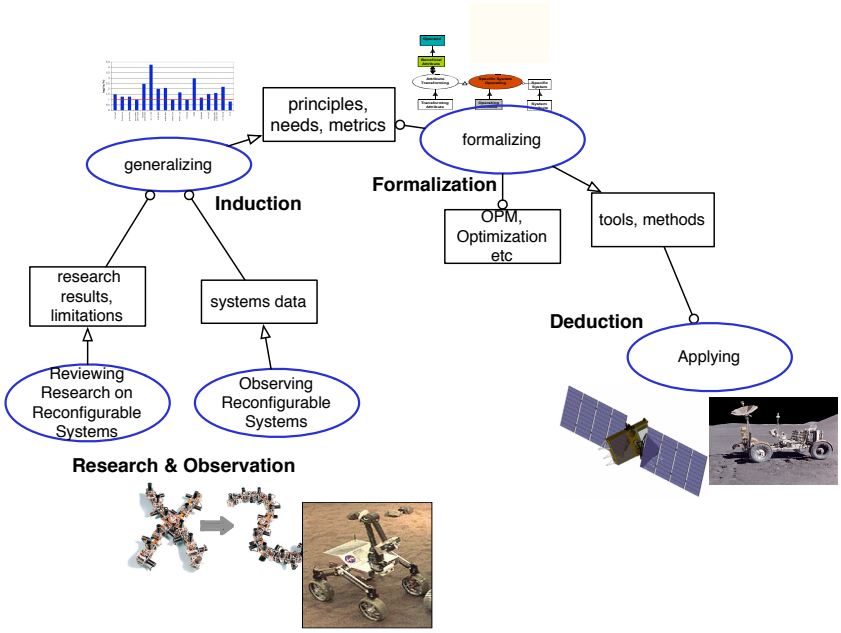

Figure 1-3: Research Approach

analyzed, and relevant data was collected so that a coherent picture could be created of the current state of research and implementation of reconfigurability. After the review and 'observation' process, the collected information was distilled to see if any general trends can be identified, and in-sights can be gained about essential characteristics of reconfigurable systems. This process of 'induction' resulted in producing several key ideas that were later on applied in this work. The essential properties that arise as a result of reconfigurability were gleaned, and a set of metrics could then be developed to quantify this 'quality'. The results were formalized using several tools employed in system architecture analyses such as Object-Process Methodology (OPM) [54], Design Structure Matrices (DSM), Optimization theory *etc.* The framework consisting of metrics, methodologies, and modeling tools was then applied in two case-studies of Planetary Surface Vehicles (PSV) and communication satellite constellations. Through this cycle of observation, induction, formalization, and application (with many iterations among these), a comprehensive approach is presented that can serve to assess the impact of reconfigurability in a system's architecture, and also aid in architecting a reconfigurable system.

1.4 Thesis Overview

Figure 1-4 provides a high-level overview of this dissertation through an Object-Process Diagram (OPD)[54]. In the first chapter, the motivations and desirability of designing and developing reconfigurable systems were highlighted (especially for aerospace systems of the future). A review of

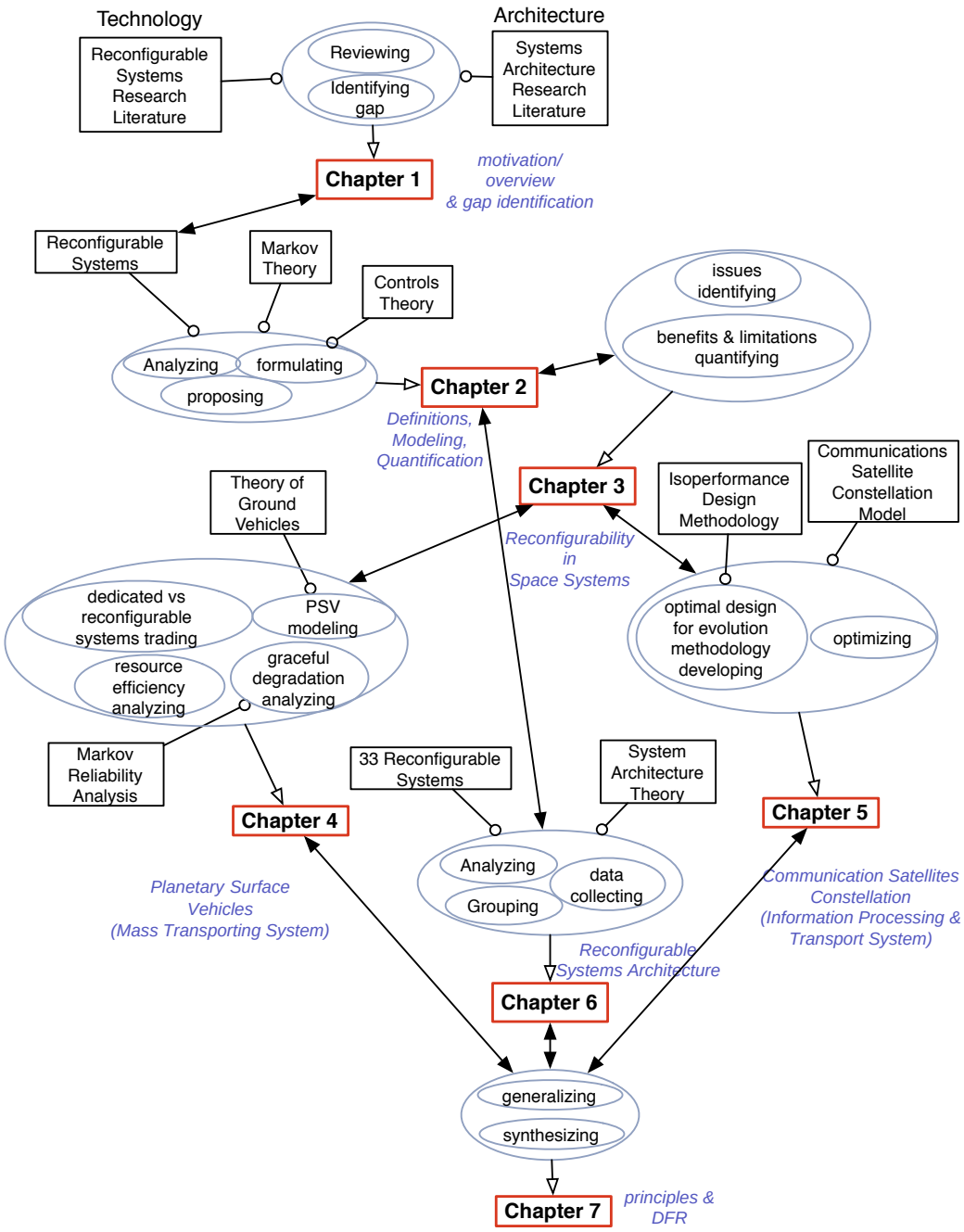

Figure 1-4: Object-Process Diagram Representation of this Dissertation (Thesis Roadmap)

research literature on reconfigurable systems and reconfigurability was then presented and a gap in existing work was identified. The need for studying and assessing reconfigurability at the system architectural and technological levels was highlighted.

In the next chapter, building up the motivation and identified gap, some essential questions about reconfigurability are addressed. A concise definition is proposed, the essential properties enabled by reconfigurability are clearly identified and reconfigurability metrics based on these driving properties are formulated. Using Markov theory and control theory two modeling methodologies are also proposed and worked through with examples.

In the third chapter, space systems are addressed in particular and their unique aspects of physical and informational accessibility are discussed. After enunciating the specific issues that pertain to these systems, and illustrating how mass efficiency is especially desirable a model is developed that can help in quantifying the impact of reconfigurability on spares requirements for space exploration missions. It is shown that through reduction of required spares, valuable mass and volume savings can be realized.

The fourth and fifth chapters use the various tools, metrics, concepts presented in the preceding chapters to study two space systems in detail. Chapter four focuses on Planetary Surface Vehicles (PSV). Reconfigurability at two different levels is separately explored. In the first case a fleet of reconfigurable vehicles is studied that can undergo reconfigurations to change system level characteristics such as tow capacity, range, speed *etc.* The mass efficiency (using models based on ground vehicle theory) and degradability considerations (using Markov models) are analyzed in-depth. At a lower level of the PSV architecture, issues of robustness in terms of having increased margin to continue traversal without getting stuck in terrain of varying soil conditions with reconfigurability is also investigated. Chapter five presents an analysis of reconfiguration of a low earth-orbit (LEO) communication satellite constellation in which evolution for higher capacity demands is investigated.

Chapter six essentially presents a look at reconfigurability from a lower level of system design. Chapters two through five explore high-level 'ility' issues such as efficiency, evolvability, degradability. In this chapter investigation of aspects such as architectural types, modules, reconfigurability cost, reconfiguration times is conducted on data obtained from 33 different reconfigurable systems. Trends and insights for object, process, agent, operand *etc.* in the architecture are addressed.

The last chapter culls the key notions and observations that result from the data of different systems and the analyses carried out in the case-studies. A set of principles are synthesized, and a general methodology for Design for Reconfigurability (DFR) is formulated.

Chapter 2

Understanding Reconfigurability

This chapter focuses on some fundamental questions about reconfigurability. Defining the demarcating boundaries of what is and is not a reconfigurable system is the first issue that needs to be clarified before any meaningful analysis of reconfigurability can take place. The first topic in this chapter therefore deals with the definitions of reconfigurability and reconfigurable systems. After describing *what* reconfigurability means, three core reasons as to *why* it maybe needed are proposed and discussed. The third topic of this chapter then deals with the issues of modeling in which Markov modeling and control-theoretic approaches are described. Lastly, a discussion about the fundamental reconfiguration processes and ways to quantify reconfigurability is presented.

2.1 Definitions

The term *Reconfigurability* means a host of different things in various contexts. Most dictionaries do not even include this word. A related term *Configure* means "to fashion by combination and arrangement; to put together in a certain form or figure" [15], and *Reconfigure* or *Reconfiguration* means "to configure again or differently" [15]. A more broad definition is given as: "to adapt (a system) to a new task by altering its configuration" [15]. It is this latter notion that will be used in this section for a general definition of reconfigurable systems and reconfigurability.

An existing general definition is hard to find. In most cases, the definitions are in the context of specific systems. For instance, Reconfigurable Computing is described as a case in which some general-purpose hardware agent is configured to carry out a specific computational task, but can be 'reconfigured' on-demand to carry out other specific tasks. A Reconfigurable Manufacturing System (RMS) is defined to be "one that is designed at the outset for rapid change to quickly adjust its production capacity and functionality in response to sudden market changes and customer demand" [94]. A definition in the context of space systems (which is also the most relevant in this thesis) can be found from NASA's description that reconfigurable systems are "Cost-effective systems that

have the capability to be tuned or adapted, functionally and/or physically, either autonomously or under remote control, to optimally achieve one or more goals or objectives. These systems can adapt to events or scenarios that can be determined in advance or react to situations that were not anticipated at the time of design"[109].

Keeping the various definitions in view from the different domains, where currently there is a lot of active interest and research in reconfigurability, a general definition can be synthesized:

Reconfigurable systems are those that can *reversibly* achieve distinct configurations (or states), through alteration of system form or function, in order to achieve a desired outcome within acceptable reconfiguration time and cost.

Following from the above definition,

Reconfigurability is a systems architectural property that defines the ease and extent to which a system is reconfigurable.

The notion of a bound on reconfiguration time and cost for reconfigurable systems should be noted here. Many systems given an infinite amount of time and resources may be able to undergo changes in their configurations (by themselves or through an agent acting upon the system). However, for a system to be considered as a truly reconfigurable one, its reconfiguration time and cost, which is the time and cost respectively that it takes to change from one configuration to another, must be within certain limits. The cost can include monetary, energy, and other types of expenditures. The extent of the bounds will depend on the type of the system. An RMS for instance will have reconfiguration times and costs that are markedly different from perhaps Field Programmable Gate Arrays (FPGAs).

The set of *configurations* of a system is taken to be the collection of specific discrete or continuous states of the system, in which there is a different form and/or functional behavior relevant to the context at hand. The difference may only be in form or functional attribute, or it may be in the externally delivered function itself. For instance, in one configuration a system may have one color, while in another it may have a different color. In this case the form attribute is different among the states. Similarly, another reconfigurable system may be able to produce product A in one configuration, while in another it can produce product B. In this case it most likely has some difference in form attributes, in addition to having difference in function attributes.

It should be noted that it is the various configurations or states of the system that allow it to respond to different needs at different times (as noted in the earlier description for reconfigurable systems [109]). However, a reconfigurable system will not be able to respond to all unexpected situations, *i.e.* the set of useful configuration (or states) of a system is usually finite or within

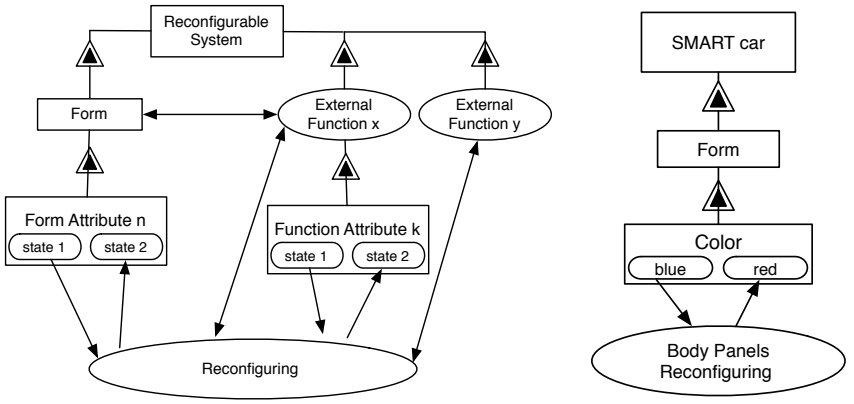

(a) OPD of a Reconfigurable System

(b) OPD of a Car with Reconfigurable Color (see also Figure B-7(c))

Figure 2-1: Object-Process Diagrams of Reconfigurable Systems

some limits. The configurations can however, be discrete or continuous. Figure 2-1(a) shows an Object-Process Diagram (OPD) [54] of a reconfigurable system as defined above. It is shown that in a reconfigurable system:

- the attributes of the system form
- the externally delivered function
- the attributes of the function

are affected by a process of reconfiguration. To illustrate with a simple example, owners of SMART cars can change the body color by easily swapping out the plastic body panels [92]. This form of reconfiguration is shown with an OPD in Figure 2-1(b) (which is a specific case of the more general OPD).

It is important to differentiate reconfigurable systems from fixed, multi-functional systems. A system may be such that it has several functions built-in that do not require any kind of change to occur in the system for their execution. That type of system will not be considered as reconfigurable. A bicycle lock (shown in Figure 2-2) that can also act as a back seat carrier is one simple example in which the product does not have to be changed in any fashion in order to be used in the two different ways. It is multi-functional, but not reconfigurable. Similarly, multi-function spacecraft can deliver a variety of services (such as telephony, transmission of video signals *etc.* through a fixed set of associated transponders). Multi-function data acquisition devices have analog input/output, digital input/output, triggering and counter channels. These types of systems are not reconfigurable. They carry out the suite of functions without undergoing any kind of *change*. The change that is referred to here is what results from a *reconfiguration process*. A detailed discussion of these processes will be

Figure 2-2: Lock N Load by Master Lock can serve as a U-lock and a carrier for bicycles

provided later. At this point it is sufficient to note that a system is reconfigurable if it goes through a process of reconfiguration before it carries out or delivers its new or modified function/objective/goal.

Systems whose configurations can undergo only a one-time change will also not be considered as reconfigurable in this study (*e.g.* spring-loaded or pyrotechnic mechanisms for one-time deployment). For the system to be considered as reconfigurable, the change it undergoes should be reversible (from a technical standpoint at least).

2.2 The Need for Reconfigurability

In general, three main reasons can be defined due to which reconfigurability may be needed in a particular system. In other words, reconfigurability is an enabler of one or more of the following properties:

1. Multi-Ability: in which the system can perform multiple, distinctly different functions at different times

2. Evolvability: that allows the system to change easily over time by removing, substituting and adding new elements and functions

3. Survivability: that allows the system to remain functional, possibly in a degraded state, despite a few failures

2.2.1 Multi-Ability

This has been the most common reason for reconfigurability in systems. When a system needs to fulfill different functions at different times from a fixed set of resources, it is often made reconfigurable in some way. The requirement for having multiple capabilities (in which each specific ability is assumed at different times) may arise due to resource efficiency requirements, such as when mass, volume, power *etc.* need to be conserved. A system may also need to satisfy multiple objectives because it has to operate in different conditions at different times, or has to fulfill new roles over

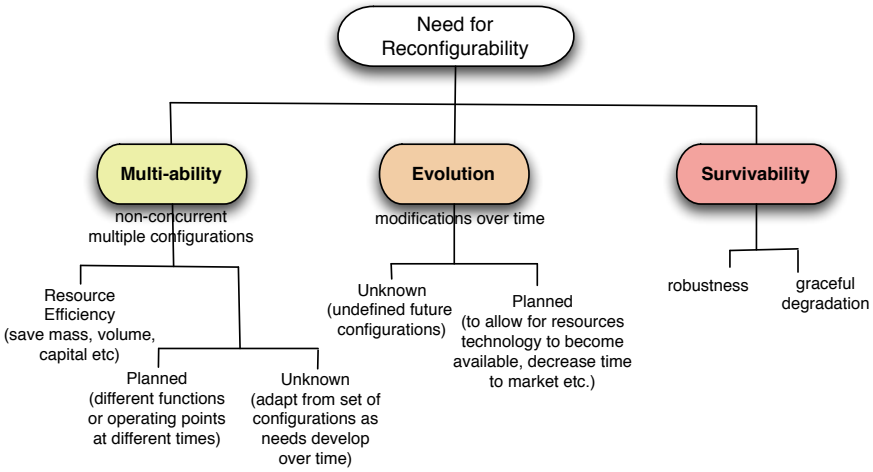

Figure 2-3: Reconfigurability enables multi-ability, evolvability, and survivability in systems

time *etc.* In both cases, the end requirement on the system is that it needs to fulfill multiple objectives/goals *etc.*, and thus should be capable of executing them collectively, but not necessarily simultaneously.

A very familiar example is a sofa-bed (that is particularly useful when space is limited and is an example of a system that is multi-capable primarily to save volume). Some types of earth-moving equipment also exhibit reconfigurability through various kinds of end-attachments that allow for different functions to be carried out. This type of system can serve as an example of both resource efficiency (it is cheaper to have one vehicle with set of attachments, then to buy a set of dedicated vehicles), and multi-role capability (since farm work perhaps requires various jobs at different times). A more recent example are morphable Unmanned Aerial Vehicles (UAVs). These aircraft have reconfigurable wings that allow for carrying out different missions (such as reconnaissance, attack *etc.*) at different times. This system is a good example of the case in which multi-objective satisfaction is needed because the system operates to fulfill different roles at different times in one flying sortie. It is not primarily driven by resource efficiency.

A key aspect for these types of systems is that the configurations are known *apriori*, and therefore are part of the design requirement of the system. The exact operational extent or usage of each particular configuration may not necessarily be known (the case in which the system adapts as new needs arise and chooses a configuration from its finite configuration set). However, the different or modified functions are part of the functional requirements, and the system design is crafted to accommodate them.

Another point to note is that in terms of design, these systems should ideally not be sized for the maximum achievable capability across all the required reconfigurations. Rather through the use of reconfiguration from one 'state' to the next these systems can achieve capabilities (or levels

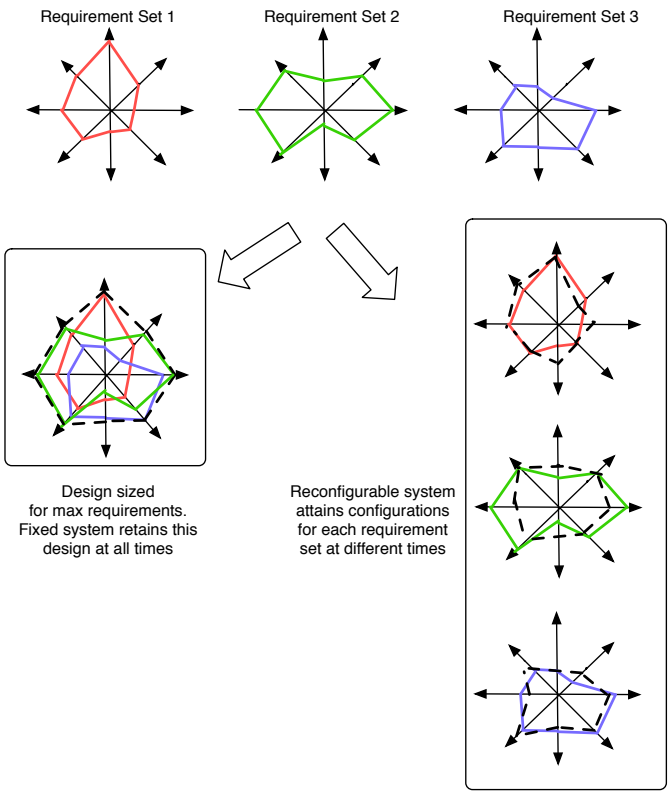

Figure 2-4: Maximum capability vs required capability design

of capabilities) they did not possess in a previous configuration. Figure 2-4 notionally illustrates this type of case. The axes represent relevant performance/design requirements such as in case of a UAV may be rate of climb, max cruise altitude, dash velocity *etc.* For different segments or stages of the mission, the desired requirements maybe different. There can therefore be sets of requirements that the system needs to fulfill at different stages/times. For an application in which different requirements exist at different times, either an all-encompassing fixed system can be produced which may very often be undesirable for a variety of reasons (cost, complexity *etc.*), or a reconfigurable system can be implemented which can be altered to meet the new needs. Each specific 'state' or configuration of the reconfigurable solution may be sub-optimal in some sense, but the overall system can be a better solution than a fixed, all-in-one implementation. This is a fundamental difference that sets a reconfigurable system apart from a multi-functional system in which all the functionality is built-in and exists all the time without undergoing a reconfiguration process.

In a space exploration program where there are severe mass and volume constraints on the amount of payload that can be delivered to a planetary surface, the ability to reconfigure a fixed set of hardware for different functions can be greatly beneficial. Maximum functionality can thus be delivered by an element of mass, relative to dedicated systems. It can be argued that reconfigurability

in space systems can primarily be driven by reasons of mass and volume efficiency alone.

2.2.2 System Evolution

Reconfigurability is needed for evolving some systems over time through expansion, upgrades *etc.* The evolution may be pre-planned, perhaps due to financial or technological constraints. A smaller, cheaper instance of the system may therefore be first deployed which may then be expanded or upgraded at a later time as more capital becomes available. In this case it can be reasonably assumed that the demand or need can be forecasted with a high degree of certainty. But the system is evolved in stages due to budgetary or technological constraints.

There are many systems however in which the needs/demands are unpredictable and the exact stages are not pre-planned. In these cases the evolution can help to manage uncertainty. Reconfigurable Manufacturing Systems are an example of such a system in which the reconfigurability is driven due to the need of adjusting the manufacturing line to accommodate varying demand levels or changing consumer tastes. RMS allow for changing both capacity and product type. The capability to reconfigure systems to manage uncertainty is most pertinent for large capital intensive systems (which most space systems are). Various researchers have shown that deploying such systems gradually, in stages, can minimize risk due to the uncertainties. In order to implement a gradual deployment strategy, and 'evolve' the system to greater or different capability, reconfigurability in the system is often required (but not always) [36, 49].

In general evolution can occur either on a particular instance of the system (*e.g.* an RMS is evolved to produce a new product), or it may occur on different instances (*e.g.* an expendable launch vehicle is reconfigured for different mission types). But here we restrict discussion to systems that get reconfigured in the operational phase, and the focus is therefore only on particular system 'instances'.

Typically, evolution can bring to mind only a one-way change that usually expands, enlarges the system in some way, but it does not necessarily have to be so. RMS are again a relevant example for this, where capacity may be increased or decreased depending on demand.

2.2.3 Survivability

The first two reasons describe situations when system architects will seek to create designs for systems that can 'live' and 'adapt' to our changing world. Reconfigurability however, can also be desirable for the basic need of survivability in the first place.

There can be two aspects of enhancing the system's survivability. In the first case the system continues functioning, even if it is on a limited scale, in the event of partial failure. In the second case, the system's stability/failure margin is increased and thus its *chances* of continuing its function (in the face of harmful inputs) are increased. In other words it becomes more robust to external

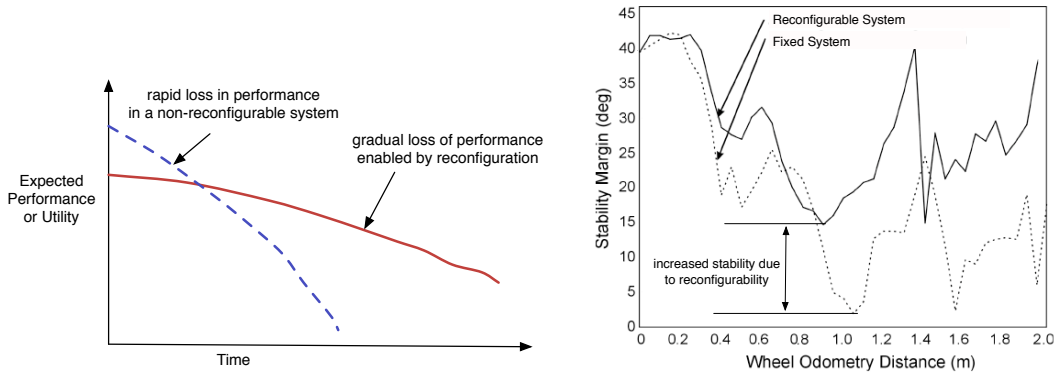

(a) Graceful Degradation

(b) Increased Robustness [72]

Figure 2-5: Survivability of a Reconfigurable and Non-Reconfigurable System

disturbances. In this second case, the system may not necessarily have 'degraded states', and may still undergo 'sudden death' if it experiences a large enough disturbing input. However, by enhancing the safety margins (through reconfigurations), it effectively reduces the probability of experiencing that failure [59]. Figure 2-5(a) illustrates notionally the difference between a reconfigurable and non-reconfigurable (or fixed) system in terms of their potential performance over time. Figure 2-5(b) shows how a reconfigurable robot can improve its stability and therefore chances of successfully traversing challenging terrain, as compared to a fixed non-reconfigurable robot [72]. The plot shows the stability margins for the two cases and it is clear to see that the reconfigurability adds to the robustness of the robot in terms of it being able to carry out its function even in the face of adverse terrain conditions.

A gracefully degrading system is one in which faults are masked and only manifest themselves in a reduced level of system functionality [102]. High cost, or highly critical systems in particular often have such requirements. Recent research, in computation of expected productivity for the Terrestrial Planet Finder Interferometer Mission, shows that reconfigurability is an enabler of graceful degradation [141]. There is also an increasing interest in having reconfiguration capability to allow for graceful degradation in automotive systems, power distribution, telecommunication, weapon systems [102] and robotics [147]. A significant amount of effort is also being directed towards avionics and other digital systems that can recover their functionality, or at least continue at a reduced level if faced with partial component failure or if experiencing operating conditions outside the design range [132].

The main cases of multi-ability, evolvability and survivability described above, either uniquely or in a combination, envelope almost all situations for which a system may need to be reconfigurable.

2.3 Reconfigurability and Operational State

One of the key things about reconfigurability is *when* it happens in the system. It can be reconfigurable while the system is carrying out its primary externally delivered function, *e.g.* if a race car, while in motion on a racetrack, reconfigures to adjust to changing track geometry. This type of reconfiguration can be termed as *on-line reconfiguration*. On the other hand, a system can also undergo reconfiguration when it is not carrying out its prime function and is either idle (but operating in some minimal way), or perhaps completely shut down. For instance, a SMART car gets its body panels changed out manually in a garage. This case can be termed as *off-line reconfiguration*. Depending on when the reconfigurations can take place, there can be direct effects on the reconfiguration time, cost, risk, value and a host of other relevant characteristics.

With the definition and elaboration of some of the basic aspects of reconfigurability in place, a discussion of its modeling and representation can now be presented. In general, most complex reconfigurable systems can be considered to exist in different configurations or 'states', at different instants of time. The next two sections describe approaches for analyzing dynamical aspects of a generic reconfigurable system. First, a Markovian modeling approach is discussed, and then a control-theoretic framework is described for assessing the temporal behavior of reconfigurable systems.

2.4 Markov Modeling of Systems

A Markov process is a probabilistic model of usually a complex system which employs the concepts of states and state transitions. Reconfigurable systems can therefore be studied with Markov models in a very natural way. Markov theory has been fairly well developed since its first introduction by the Russian mathematician A. Markov in 1907 [68]. Its basic assumptions and important results are briefly summarized in the following section, and a discussion of applicability to reconfigurable systems is then presented.

2.4.1 Discrete-Time Markov Chains

A Discrete-time Markov Chain is a process in which the system's state changes at certain discrete time instants. Suppose a system can exist in N finite and discrete states, that belong to a set $S = \{1, 2, \cdots, N\}$. A time ordered set, $T = [t_1, \cdots, t_n, \cdots, t_f]$ can be defined, and the system state at a time instant t_n can be denoted as X_n. Then, for a Markov process the following assumption holds [35]:

$$p_{ij}(n) = Pr\{X_{n+1} = j | X_n = i\}, \quad i, j \in S \tag{2.1}$$

where $p_{ij}(n)$ is the probability of transitioning from state i to j at time t_n. The probability law of the next state X_{n+1} depends on the past only through the present value of the state X_n. In other words, the Markovian property refers to a condition where memory of previously visited states between $t_1, \cdots, t_{n-1}$ is irrelevant. The $p_{ij}(n)$ are also called the single-step transition probabilities since they define the transition probabilities for one time step only. The transition probabilities from a state i sum to one.

$$\sum_{j=1}^{N} p_{ij}(n) = 1, \quad \forall\, i \tag{2.2}$$

It should be noted that p_{ii} is the probability that the system remains in state i. Using the transition probabilities between each state pair, the complete system can be described by defining a single-step transition probability matrix, $P(n)$:

$$P(n) = \begin{bmatrix} p_{11} & \cdots & p_{1N} \\ \vdots & \vdots & \vdots \\ p_{N1} & \cdots & p_{NN} \end{bmatrix} \tag{2.3}$$

This matrix provides full information regarding the behavior of the system at a particular time instant. In order to determine the individual state probabilities, a vector $\boldsymbol{\pi}(n)$ is defined where $\boldsymbol{\pi}(n) = [\pi_i(n)]_{1\,\mathrm{x}\,N}$, and $\pi_i(n)$ is the probability of being in state i at time t_n. The state probabilities at time t_{n+1} are then simply

$$\boldsymbol{\pi}(n+1) = \boldsymbol{\pi}(n)P(n) \tag{2.4}$$

If the initial state of the system is known (*i.e.* $\boldsymbol{\pi}(0)$ is given), then the above relationship allows the state probabilities to be calculated at any t_n. At any time instant, the state probabilities need to sum to one, *i.e.*

$$\sum_{i=1}^{N} \pi_i(n) = 1 \tag{2.5}$$

A multi-step transition probability between states i and j from time m to n, $\phi_{ij}(m,n)$, is defined by

$$\phi_{ij}(m,n) = Pr\{X_n = j | X_m = i\} \tag{2.6}$$

$$\phi_{ij} = \sum_{k=1}^{N} \phi_{ik}(m,n)\phi_{kj}(r,n) \tag{2.7}$$

where $i = 1, 2, \cdots, N,\ j = 1, 2, \cdots, N$, and $m \leq r \leq n$.

A multi-step transition probability matrix can then be defined as

$$\Phi(m,n) = \Phi(m,r)\Phi(r,n) \quad m \leq r \leq n \tag{2.8}$$

and for consistency, it is required

$$\Phi(n, n) = I \tag{2.9}$$

The single-step transition probability matrix, $P(n)$ is therefore

$$P(n) = \Phi(n, n+1) \tag{2.10}$$

For a system in which the single-step state transition probabilities do not depend on time, *i.e.*

$$P(n) = P \quad \forall\, n \tag{2.11}$$

the state probabilities, $\boldsymbol{\pi}(n)$ can be easily found by using the initial state probability vector $\boldsymbol{\pi}(0)$:

$$\boldsymbol{\pi}(n) = \boldsymbol{\pi}(0)\Phi(0, n) \tag{2.12}$$

$$= \boldsymbol{\pi}(0)P^n \tag{2.13}$$

This case is known as the *Time-Homogeneous Markov Chain* [127].

For systems whose state probabilities reach a limiting value as n gets large (which is when the system is not periodic and is homogeneous), the asymptotic or steady-state behavior of $\boldsymbol{\pi}$ is [68]

$$\boldsymbol{\pi}(\infty) = \lim_{n\to\infty} \boldsymbol{\pi}(0)P^n \tag{2.14}$$

Since at steady state, the relation $\boldsymbol{\pi} = \boldsymbol{\pi}P$ has to hold true, $\boldsymbol{\pi}(\infty)$ can be computed by solving the simultaneous equations given by

$$\pi_j(\infty) = \sum_{i=1}^{N} \pi_i(\infty)p_{ij}, \quad j = 1, 2, \cdots, N. \tag{2.15}$$

Since these N equations are linearly dependent, in order to get a non-trivial solution, only $N-1$ equations are used, and the Nth equation is the property that all state probabilities should sum to one:

$$\sum_{i=1}^{N} \pi_i(\infty) = 1 \tag{2.16}$$

It can be seen that Homogeneous Markov Chains are quite amenable for analysis since the state probabilities can be predicted for any future time given an initial state. This allows calculation of useful statistics such as average time spent in a particular state, mean time before a certain state maybe reached for the first time and so on. Due to these properties, a vast body of work in reliability analysis makes use of Homogeneous Markov models in which the state transition rates are given by the failure rates that produce various degraded states of the system [32].

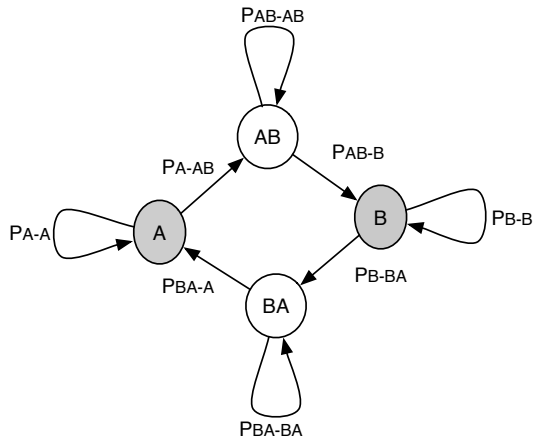

Figure 2-6: Markov Model of a Generic Reconfigurable System

2.4.2 Markov Models for Reconfigurable Systems

In case of reconfigurable systems, the homogeneous model is applicable if the single-step transition probabilities are the same over the system's operational time. This is usually true for only a small set of reconfigurable systems. A general model of a reconfigurable system is shown in Figure 2-6. Two types of states are shown, *operational states* and *reconfiguration states*. Operational states are those in which the system operates and carries out its useful function. In the figure, they are states A and B (that are shaded). The reconfiguration states are those in which the reconfiguration processes are carried out and the system may be (but not necessarily) fully or partially disabled. For the most general case it can be assumed that each operational state can configure into every other operational state after passing through a specific reconfiguration state. Thus, state A can transition to state AB (which is a reconfiguration state in which the system reconfigures from A to B), and then state AB goes on to state B (which is the state in which the system is in operational configuration B). A similar path is shown for B to BA to A. The self-transition probabilities, p_{AB-AB} and p_{BA-BA} in the reconfiguration states can be used to account for factors such as reconfiguration delay or failure in any particular attempt for example. In essence they capture the expected 'delay' in moving from one operational state to the next. In most real systems, it is usually not possible to enter each operational state from every other operational state. But the most general case is considered here for completeness. Also note that the 'reconfiguration states' are general enough that both on-line and off-line reconfigurations can be modeled in this way.

For the type of system shown in Figure 2-6, for k operational states, there are $k(k-1)$ reconfiguration states. In the general case, Figure 2-7 shows a generic operational state and a reconfiguration state. In order to clearly differentiate between the type of states, each operational state is denoted by a single variable i or j *etc.* The reconfiguration states are denoted by two variables, the first

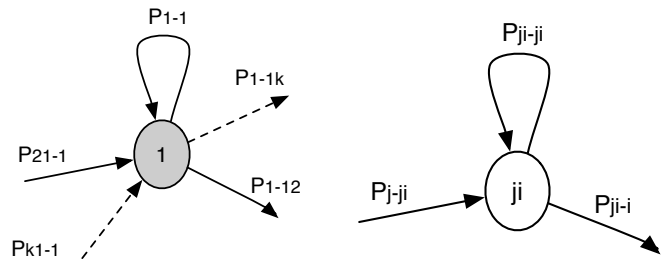

(a) Operational State (b) Reconfiguration State

Figure 2-7: Markov Model of Operational and Reconfiguration States

indicates the initial state that is reconfigured, and the second denotes the destination state that is produced as a result of the reconfiguration process, so ij is a reconfiguration state that converts state i to state j. A hyphen in the subscript of the transition probabilities serves to indicate the initial and final states between which the transition takes place. Thus, p_{i-i} is the self-transition probability of state i, while p_{i-ij} is the transition probability from i to state ij. With this notation (and omitting the argument (∞) for the πs for simplicity), for the type of systems shown in Figure 2-6 and 2-7, the results given in Equation 2.15 lead to the following equations for steady-state behavior:

$$\pi_i = p_{i-i}\pi_i + \sum_{j=1}^{k} \pi_{ji} p_{ji-i}, \quad j \neq i \tag{2.17}$$

$$\pi_i = \frac{\sum_{j=1}^{k} \pi_{ji} p_{ji-i}}{1 - p_{i-i}}, \quad j \neq i \tag{2.18}$$

where

$$\pi_{ji} = \frac{p_{j-ji}}{1 - p_{ji-ji}} \pi_j. \tag{2.19}$$

Combining the above two relations gives

$$\pi_i = \frac{1}{1 - p_{i-i}} \sum_{j=1}^{k} \frac{p_{j-ji} p_{ji-i}}{1 - p_{ji-ji}} \pi_j, \quad j \neq i \tag{2.20}$$

Since the transitions to reconfiguration states have the specific form as shown in Figure 2-7, it is also true that

$$p_{ji-ji} + p_{ji-i} = 1 \tag{2.21}$$

Using this result, Equation 2.20 becomes

$$\pi_i = \frac{1}{1 - p_{i-i}} \sum_{j=1}^{k} p_{j-ji} \pi_j, \quad j \neq i \tag{2.22}$$

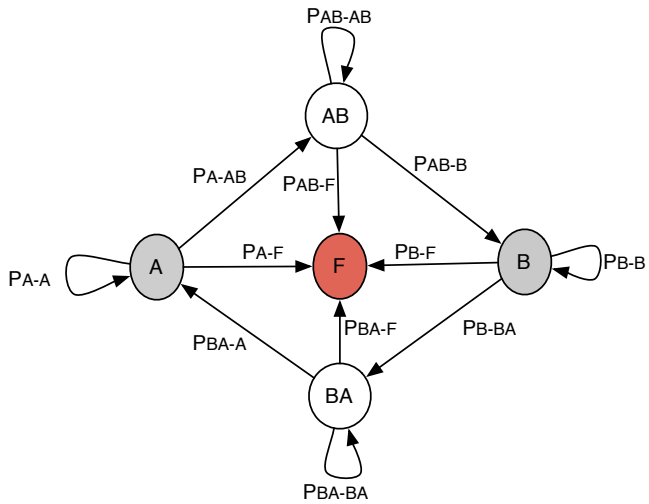

Figure 2-8: Generic Markov Model of Reconfigurable System with a Failed State

To obtain a non-trivial solution, Equation 2.16 is also used. In order to have a relation only in terms of the operational states, Equation 2.16 can be written by explicitly separating out the operational (π_j) and reconfiguration state (π_{ij}) expressions:

$$\sum_{j=1}^{k} \pi_j + \sum_{i=1}^{k} \sum_{j=1}^{k} \pi_{ij} = 1, \quad i \neq j, \tag{2.23}$$

Using Equation 2.19, it becomes

$$\sum_{j=1}^{k} \pi_j + \sum_{i=1}^{k} \sum_{j=1}^{k} \frac{p_{j-ji}}{1 - p_{ji-ji}} \pi_j = 1, \quad i \neq j, \tag{2.24}$$

Thus, the asymptotic, k operational state probabilities can be determined directly using $k-1$ linear equations given by Equation 2.22 and the kth equation given by Equation 2.24. Note, that it is assumed that the self-transition probabilities p_{i-i} and p_{ji-ji} are not one.

The above discussion focuses on a model in which only operational and reconfiguration states are considered. In many cases, it is often desirable or even required to model the failure aspects of the system as well. In such a situation, a general model of the form shown in Figure 2-8 can be employed in which a *Failed* state, F, from which the system cannot recover, is also factored in. Note that this type of model essentially describes a system in which the failed state is an *absorbing state* from which once the system enters it can never leave. There are analytical means of determining the expected number of iterations after which a system will enter an absorbing state, and those can be employed to determine failure time *etc.* [35]

A simple example of a robot can be used to illustrate how such modeling can be used notionally. It

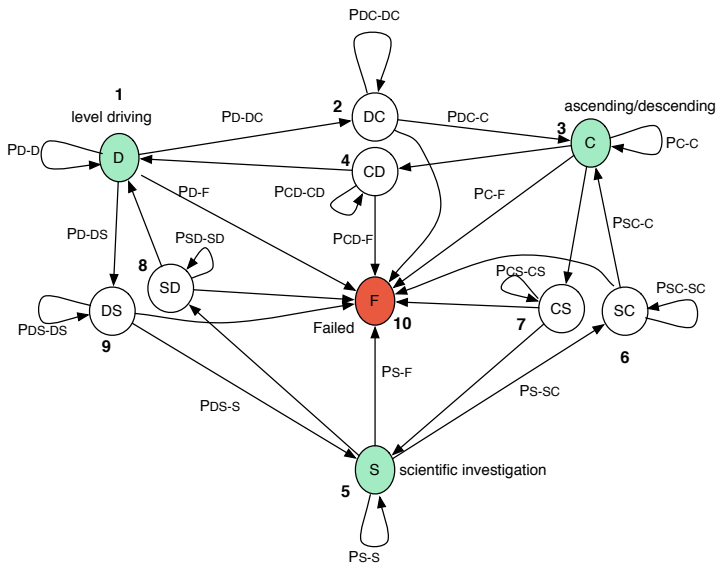

Figure 2-9: Markov Model of Reconfigurable Robot

is considered that the robot has three distinct physical (and also informational in terms of software) configurations during its operation. Suppose the three configurations, or states, correspond to its operation on flat terrain (which mainly involves driving activities and is denoted as state D), ascent or descent of a crater slope (which is denoted as C to indicate climbing up or down), and exploration of a crater floor (mainly carrying out scientific investigations and is denoted as S) respectively. As a specific example, a reconfigurable robot in development at JPL employs wheels and legs for its locomotion on an as-needed basis. Therefore, it is conceivable that the wheels are used in the flat terrain driving configuration, while the legged configuration is used when climbing/descending slopes *etc.* Suppose the terrain in which the robot will operate is fairly well known. Its characteristics (based on crater density *etc.*) are such that a Markov model shown in Figure 2-9 can be constructed. The specific transition probabilities used in the example are shown in Table 2.1. The element in the ith row and j^{th} column of the table is p_{ij}. States in Figure 2-9 are denoted with corresponding numbers. The last column shows the sum of each row from column 1 through 10. It essentially shows that the transition probabilities from each state sum to one. This is only a notional case, and the assumption is that a typical mission can perhaps be described in this way given relevant parameters such as terrain profile, robot speed, mission duration, reconfiguration processes, chances of irrecoverable failure in each state *etc.* In many actual applications, determining appropriate values for transition probabilities can be difficult.

The evolution of state probabilities, π_i, for a number of iterations is shown in Figure 2-10. Each iteration can represent a certain period of time (days, weeks *etc.*) The computation was carried out for 1500 steps, the first 20 are shown in Figure 2-10 where the probabilities of all the 10 states are

Table 2.1: Transition Probabilities Used in Simulating State Evolution of Robot

	to state										
from	1	2	3	4	5	6	7	8	9	10	$\sum$
1 (D)	0.59975	0.3	0	0	0	0	0	0.1	0	0.00025	1
2 (DC)	0	0.03	0.965	0	0	0	0	0	0	0.005	1
3 (C)	0	0	0.195	0.4	0	0.4	0	0	0	0.005	1
4 (CD)	0.945	0	0	0.05	0	0	0	0	0	0.005	1
5 (S)	0	0	0	0	0.6	0	0.3	0	0.99	0.001	1
6 (SC)	0	0	0	0	0.965	0.03	0	0	0	0.005	1
7 (CS)	0	0	0.945	0	0	0	0.05	0	0	0.005	1
8 (SD)	0	0	0	0	0.9699	0	0	0.03	0	0.0001	1
9 (DS)	0.9499	0	0	0	0	0	0	0	0.05	0.0001	1
10 (F)	0	0	0	0	0	0	0	0	0	1	1

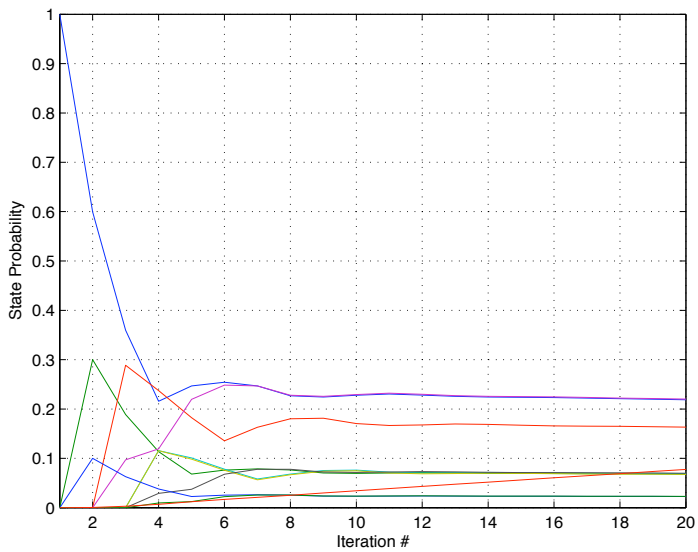

Figure 2-10: Evolution of Robot's State Probabilities

shown. Figure 2-11 shows the chances of being in an operational state (*i.e.* $p_o = \pi_D + \pi_C + \pi_S$), and the chances of being in a reconfiguration state (which is p_r, and is the sum of all the probabilities of reconfiguration states). Since the failure probability is very low initially, the p_r is almost equal to $1 - p_o$.

Figure 2-12 shows the probability of the system being in the failed state. As expected over a large number of iterations that probability approaches one. Three plots were generated by varying the transition probabilities leading to state F (such as p_{C-F}, p_{D-F} *etc*). In the first plot (from the top) the failure probabilities were increased by 50% from the values shown in Table 2.1. In the second plot, the failure probabilities are those as given in Table 2.1, while in the third plot they have been reduced by 50%. With decreasing values of those transition probabilities (denoted

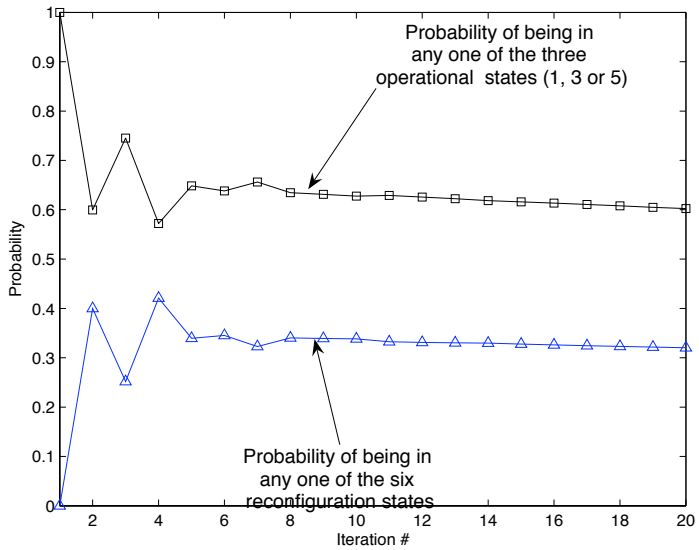

Figure 2-11: Operational and Reconfiguration State Probabilities

collectively as P_f in Figure 2-12), the chance of being in the failed state decreases. Depending on how much that decrease is, trades can be carried out between reliability and cost (since it can be expected that there will be increased cost in bringing down the failure probabilities). Note that in this simple model, there is only one irrevocable failed state considered here (since the primary aspect of interest is the multi-ability of the robot). For a more detailed analysis of survivability considerations, such as of graceful degradation, more states will need to be factored in that capture the degraded behavior/performance.

With such a model one can also determine effects of changing probabilities of self-transition of reconfiguration states. These essentially capture characteristics of the reconfiguration process and can be used to analyze effects on overall system behavior. Figure 2-13 shows how the total probability of being in any operational state D, C or S (*i.e.* $\pi_D + \pi_C + \pi_S$) is affected when the self-transition probabilities p_{DC-DC}, p_{CD-CD}, p_{SC-SC}, p_{CS-CS}, p_{DS-DS}, and p_{SD-SD} are reduced by 10% from the values shown in Table 2.1. Thus, by varying these self-transition probabilities, which correspond to design issues of the reconfiguration processes, the effect on the system performance can be determined. In this particular case the effect is negligible indicating little benefit for the specific change made.

The above example shows how Homogenous Markov Models can be used as potential tools for studying various aspects of a reconfigurable system. However, the applicability is limited to a class of systems in which no active decision rule is used to determine the state to which the system should reconfigure, rather, the probabilities are assumed to be known. There are many types of systems in which the reconfiguration to a state will depend on some exogenous variable that will make some

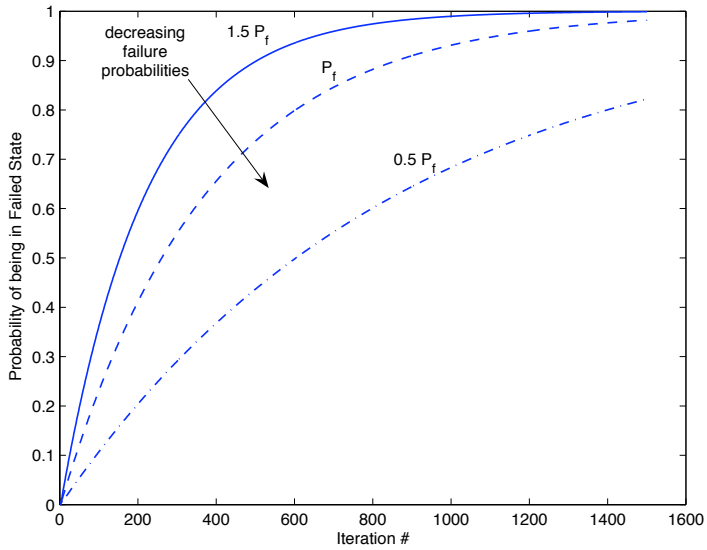

Figure 2-12: Effect of 50% Increase and Decrease in Failure Probability over Time

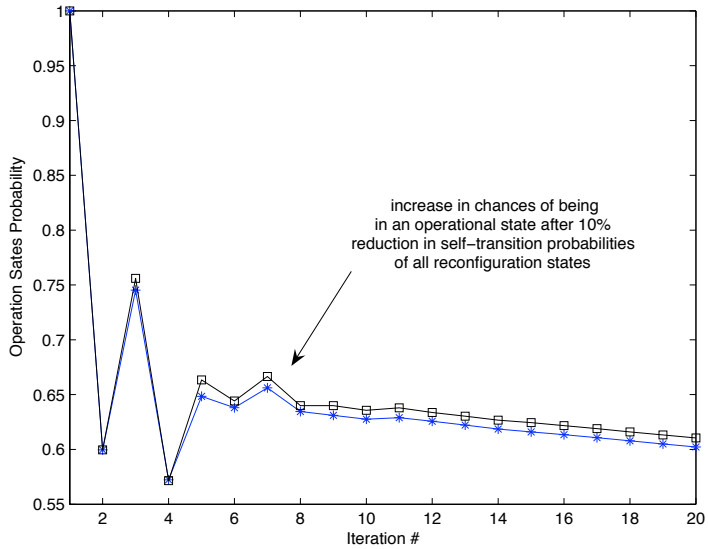

Figure 2-13: Effect of 10% change in Self-Transition Probabilities of Reconfiguration States

states desirable and some undesirable over time. Different kinds of Markov models can be used in such cases and are discussed in the following section.

2.4.3 Time Varying Markov-Based Models for Reconfigurable Systems

A more general case is one in which the single-step transition probability matrix, P, is not the same for every time step. This is known as the *Non-Homogeneous Markov Chain* [60]. In this case, Equation 2.13 does not hold, and analytical solutions to the asymptotic behavior of the system are not possible (except for the periodic cases). Indeed the system may not have a steady-state as is possible for the case of Homogeneous systems.

The multi-step transition probabilities are computed by taking a complete product of each $P(n)$ [68]:

$$\Phi(m,n) = P(m)P(m+1), \cdots, P(n-1), \quad m \leq n-1 \tag{2.25}$$

One typically has to revert to discrete-time simulation in this case.

Most reconfigurable systems, can be better described through Non-Homogeneous models, with a further assumption that the state transition probabilities at each time instant are conditioned on some external time-varying process, $u(n)$. Thus for any state-pair i and j (and using the notation with the hyphen):

$$p_{i-j}(n) = f(u(n), i, j) \tag{2.26}$$

This $u(n)$, can be mapped to a corresponding behavior of the system such that some objective J is achieved. From a given set of finite states that the system can attain in one step, there will be a state i^* that is most desirable for the system to have for a particular $u(n)$ and a particular formulation of J. In fact each state will have an associated J_i for the given $u(n)$, and the state transition probabilities will be according to this J_i. The optimal state, i^* will have the highest probability for the system to transition into, followed by the next best state and so on. The states that are worse than the existing configuration can be modeled to have extremely low transition probability for that time period (the notion of having stochasticity, rather than determinism, is discussed later on in this section). For a given input $u(n)$ the optimal operational state is

$$i^* = \texttt{argmax}\, J(u, S) \tag{2.27}$$

where J is some function that needs to be maximized, and S is the set of system states. Also as described above,

$$p_{m-mj} > p_{m-mk}, \quad J_j > J_k > J_m \tag{2.28}$$

where p_{m-mj} is the probability that operational state m will transition to reconfiguration state mj (which will then lead the system to move to operational state j) and so on. Note, that $u(n)$ could be

a vector, making $J(u, S)$ more complex however this will be explored in future work and the present discussion will only focus on a single exogenous input to which the system reacts.

As an example, consider a reconfigurable satellite constellation that is capable of changing its coverage to different locations on the globe in response to disaster relief efforts. For simplicity, it is assumed that it can attain a set of discrete states. The input to this system is the stochastic process of disaster occurrence (*e.g.* floods, earthquake, hurricane) in various regions of the globe. Given a certain demand at a particular time, $u(n)$, there is an optimal state (among the discrete and finite set) that the satellite constellation should adopt so that it maximizes its communication service to the required region. The function J can thus be the revenue (or perhaps some metric of service), and the state that maximizes J should get the highest transition probability for that time step. Thus, the transition probabilities will be such that p_{j-ji^*} are high (*i.e.* the probability of moving from a sub-optimal state to its corresponding reconfiguration state that leads to i^* will be high). Also, if the system is already in the optimal state, it will stay there, *i.e.* $p_{i^*-i^*} = 1$ and $p_{i^*-i^*j} = 0$. In other words, it will be an absorbing state but only during the period of time when its optimal. Since in the non-homogeneous case, the absorbing states change with time (with the exception of irrevocable failure), the long-term behavior cannot be predicted analytically (unless $u(n)$ is periodic).

Although in many reconfigurable systems, the state transitions are thought of as deterministic processes (based on several factors of cost and benefit), the 'stochasticity' is modeled here to reflect the fact that not all the parameters required to make the optimal decision maybe known with certainty. Assigning probabilities to the states essentially implies that there is some chance of each state being adopted given its relative performance and other real-world considerations. The assumption is that the optimality selection is based on a J which captures most but not all criteria of evaluation (since certain things are hard to quantify or include in analysis). So cost, performance *etc.* perhaps maybe part of the formulation for J, but other changing factors such as social, political, regulatory may cause for the 'optimal' state (determined through its J) to not be adopted, and some other 'less-optimal' state can possibly be adopted due to a variety of reasons.

So in summary, if one state has very poor performance as compared to other states, it will have a low probability of being adopted, and if there is one that is especially better it will have a higher chance of being adopted. If the difference in performance is not very large among the states, then the π_i will be almost evenly distributed. The problem will be 'diffused' since there are many options with almost similar benefits to chose from. So a way of determining how many states/configurations the system should have can be based on how sharply the performances of the configurations differ from each other.

Example: Planetary Surface Vehicles

A simulation model based on the approach described above can be used to analyze various aspects of the system. The external process, the states of the system, and other parameters can be varied to assess the impact on system performance.

In order to illustrate how a reconfigurable system can be studied with this method, a planetary surface vehicle (PSV) similar to the robot example in Section 2.4.2 with reconfigurable wheels was considered. A model that allows analysis of wheel-terrain interaction for a vehicle moving on unprepared terrain was employed [70]. This model computes several forces such as the ground reaction normal to the plane of contact, maximum thrust that soil of a particular type can provide under given wheel load *etc.*

It was assumed that in a future human exploration mission to Mars, a PSV that can carry an astronaut along with some small amount of cargo will have to traverse terrain whose soil characteristics may not be fully known. Robotic missions to Mars have shown that the soil conditions vary widely even within a small radius of exploration [91]. A PSV on an exploration mission can thus be expected to encounter terrain of varying characteristics over the course of its movement on the Martian surface.

From a performance and cost perspective for wheel motion, the two main quantities of interest are usually the Drawbar Pull, DP, and the necessary torque, T, required for the loaded wheel to turn. The DP is the difference between the maximum thrust that the soil can provide and all the resistance forces that the wheel has to overcome. If the DP is zero, the vehicle has just enough force to propel only itself forward, and if it is negative, then the vehicle cannot move because the wheel will slip. The torque is directly related to the energy consumption, E, of the vehicle through angular velocity ω (as shown in the following equations).

$$P = T\omega \tag{2.29}$$

$$E = \int_{t_o}^{t_f} T(t)\omega(t)dt \tag{2.30}$$

Therefore, for a fixed speed requirement it is desirable to minimize T.

A detailed discussion of the equations and the model will be presented in Chapter 4. For the discussion at hand about modeling system states, it is sufficient to note that wheel dimensions affect the DP and T. Therefore, for a given sprung mass of the vehicle (which defines the load on the wheel), an alteration of the wheel width and diameter can be a means of changing the resultant DP and T. Thus, in order to optimize performance in terms of DP, and at the same time to improve energy consumption, the PSV is considered to have reconfigurable wheels. Such wheels can alter their width, b, or diameter, D within certain limits of their normal dimensions. It is assumed that the various dimensions that the width and diameter can achieve are discrete and define the 'state'

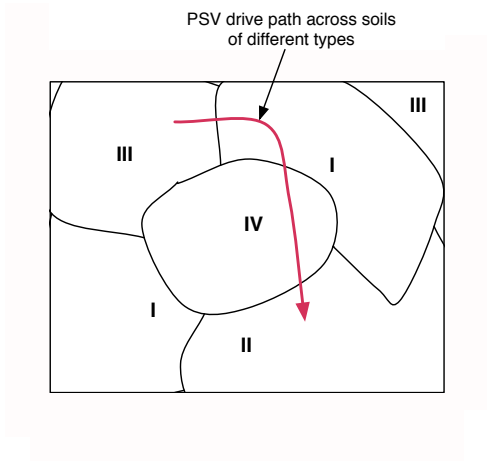

Figure 2-14: Regions of Different Soil Types

of the wheel at any given time. As the PSV moves over terrain of varying soil characteristics, the wheels try to achieve a configuration that maximizes an objective J where

$$J = \alpha DP - (1 - \alpha)T \tag{2.31}$$

The α is a constant and determines the weight for the two opposing objectives of maximizing drawbar pull (DP), and minimizing required torque (T).

In this analysis the PSV was modeled with 4 independently driven wheels, and carried a load of a suited astronaut, and 50 kg of cargo. The sprung mass of the un-loaded vehicle was estimated to be 200 kg. The total load per wheel in martian gravity was computed to be 367.5 N. The normal diameter, D_o, of each wheel was set to 1 m and width, b_o, was 0.5 m. The PSV speed was set to 5 km/hr, and the simulation was performed for a period of 30 minutes of travel. The vehicle traveled over different types of soil conditions characterized as sand, sandy loam type I, sandy loam type II, and clayey soil (detailed info about the soil data is given later in Table 4.11 in Chapter 4). Figure 2-14 shows a notional path of a PSV in which it encounters regions of different soil types while traversing a planetary surface.

In the first case, the reconfigurable wheels were allowed to vary their diameters by $\pm 15\%$ of D_o, and for each value of D, the corresponding width could be between 30% to 60% of D. As a rule of thumb, wheel widths are usually not allowed to exceed more than 60% of the diameter in order to avoid turning issues, and that is why the limit of 60% was imposed here.

The initial definition of the states was made by assuming that only three different diameter sizes were possible (each within the $\pm 15\%$ range), and only 2 different widths for each diameter size. A total of six different states were thus allowed for each reconfigurable wheel, and all four wheels were assumed to reconfigure together. Table 2.2 shows the values of b and D in each state. At each time

Table 2.2: Set S of Wheel Dimensions' States, $m = 6$

#	$b[m]$	$D[m]$
1	0.34	0.85
2	0.51	0.85
3	0.4	1
4	0.6	1
5	0.46	1.15
6	0.69	1.15

step as the vehicle was simulated to move forward and encountered some particular soil type, the 'performance' of each of the six states was computed using Equation 2.31. Thus, for a particular time t_n, a set $\mathbf{J}(n) = [J_i(n)]_{1\mathrm{x}m}$ was obtained, where $J_i(n)$ was the value of the objective function for state i at t_n, and m was the total number of states. In this case m was 6. The probability of being in each state was then defined as:

$$\pi_i(n) = \frac{[J_i(n) - J_{min}(n)]^2}{\sum_{k=1}^{m} [J_k(n) - J_{min}(n)]^2} \tag{2.32}$$

where $J_{min}(n) = \min[\mathbf{J}(n)]$. With this formulation, the worst state (the one with J_{min}) will essentially have zero probability. Note, that the state probabilities are directly defined here. In other analyses, a state transition probability matrix (as described in the preceding section for definitions of $p_{ij}s$) can be produced and then Equation 2.25 can be used to determine the evolution of state probabilities. Additional improvements can be also made by including consideration of reconfiguration costs, energy, time *etc.* For a first order analysis for illustrative purposes however, Equation 2.32 is used.

In this case, the soil conditions, which act as the $u(k)$ of the system here, can be assumed to be not known exactly. They perhaps are measured on-line as the vehicle moves [70], so only an approximate knowledge of the terrain is at hand to the system. In future analysis, Kalman filter estimates of $u(k)$ can be incorporated.

An expected measure of the performance, $\bar{J}$ can be determined at each time step, where $\bar{J}(k)$ is given by

$$\bar{J}(k) = \mathbf{J}(k)\boldsymbol{\pi}^T(k) \tag{2.33}$$

Figure 2-15 (a) shows $\bar{J}$ as compared to the ideal performance, $J^*(k)$, which would we be achieved if the optimal state, i^*, was selected at every instant k. The comparison is also made with a fixed case in which the wheel cannot attain different states (is not reconfigurable) and has a fixed diameter of 1 m and width of 0.5 m (throughout the drive cycle).

For the specific set of allowable states, S shown in Table 2.2, the probability of being in each state at every time step was computed using Equations 2.31 and 2.32. Figure 2-16 shows these

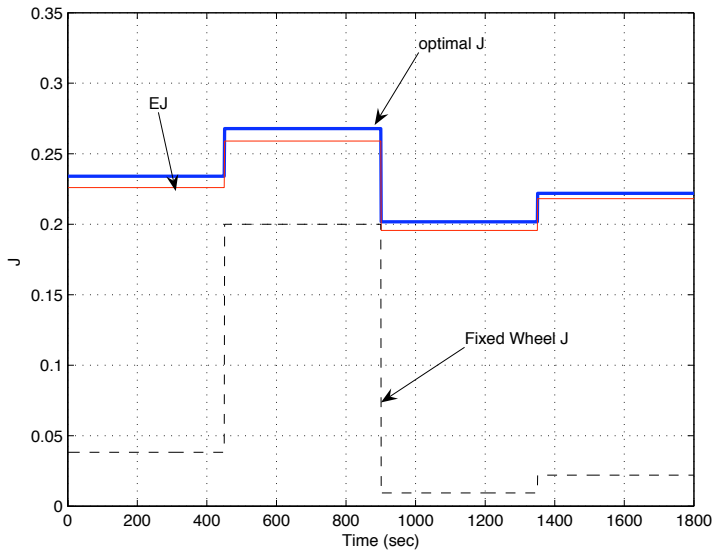

Figure 2-15: J^* and $\bar{J}$ (denoted as EJ in figure) for reconfigurable case compared with J of a fixed case

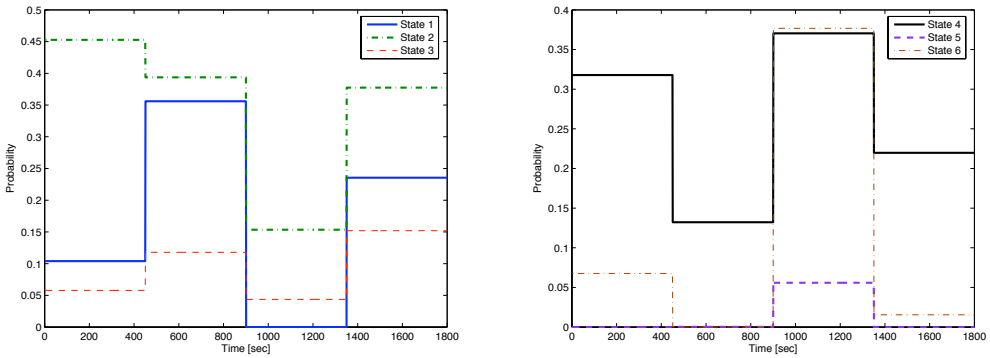

(a) Probabilities of States 1, 2, and 3

(b) Probabilities of States 4, 5, and 6

Figure 2-16: State Probabilities vs Time

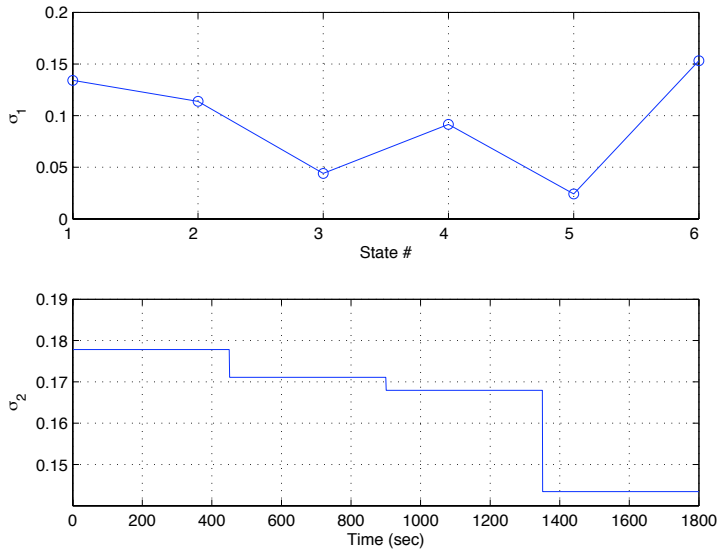

Figure 2-17: Time Variation of State Probabilities

values for the six states. It can be seen that the states exhibit various types of behavior. There are some that have large variation in their probabilities indicating that their performance varies widely relative to others over the course of travel. On the other hand there are other states that do not vary much in their relative performance over the course of the system's operation in a range of environmental conditions. There are still others whose performance is poorer than the rest and have a lower probability on average throughout. Figure 2-17 shows a graph of the standard deviation of each state's probability over the course of the simulation time (in the top plot). State 1 and 6 show the greatest variability (highest value of σ). These are the extreme case diameter and width, and therefore are either very good or very bad in the different conditions. Figure 2-17 also shows the standard deviation among the state's probabilities at each time step (in the bottom plot). A large value at any particular time step indicates a bigger spread in the state's probabilities (indicating the presence of states with widely varying performances). A small value means that at the time instant all states perform relatively the same and thus have more equal chances of being adopted.

When the wheels are allowed to have more states, it can be expected that the probabilities will 'spread' out. This is confirmed by Figure 2-18 that shows the state probabilities when the wheels can have 12 different states. Table 2.3 shows the specific values of b and D used. This problem essentially becomes diffuse and has many states with more or less similar chances of getting adopted partly because of the specific example and also because of the decision rule used in Equation 2.32 to assign the probability values. Selecting the subset of reconfigurable states that give the most distinct capabilities, or a more sophisticated decision strategy can help to mitigate this issue.

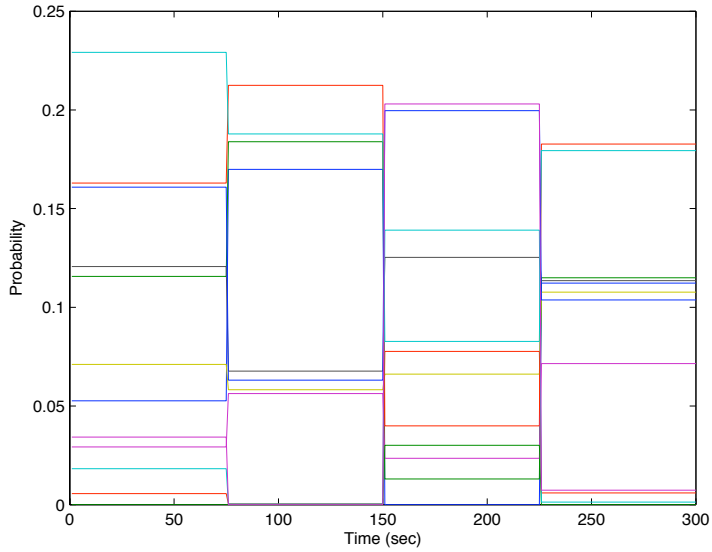

Figure 2-18: Extent of Variation in State Probabilities

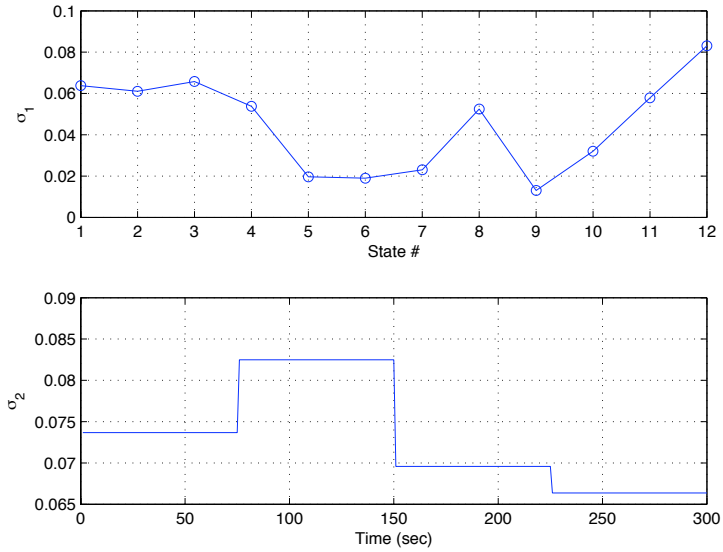

Figure 2-19: Extent of Variation in 12 State Probabilities

Table 2.3: Set S of Wheel Dimensions' States

#	$b[m]$	$D[m]$
1	0.34	0.85
2	0.39	0.85
3	0.45	0.85
4	0.51	0.85
5	0.4	1
6	0.46	1
7	0.53	1
8	0.6	1
9	0.46	1.15
10	0.53	1.15
11	0.61	1.15
12	0.69	1.15

2.4.4 Markov Representation of Reconfigurability Cases

For the three cases discussed in Section 2.2 previously, simple Markov representations can be used to clarify and highlight their main aspects. Both Figure 2-8 and 2-9 essentially represent a reconfigurable system that is multi-capable. It exists in different operational states and can carry out different or modified functions. Figure 2-20(a) shows this case for completeness here. Figure 2-20(b) shows how evolution can be conceived in a Markov sense. In this situation, the system exists in some particular way (perhaps has two operational states), and at a later time during its life cycle it can acquire a new state (through changes made to the system). Another possibility is that it does not acquire a new state entirely, but perhaps undergoes some modification in its existing states (shown as A' and B' in the figure). In many systems, the evolution may be a mix of these two situations. There has been work done on Non-Homogeneous Markov models for phased systems by several researchers [127], which can be applied here.

As discussed previously in some systems reconfigurability is required for graceful degradation. Figure 2-20(c) notionally shows how a system may behave in such a case. The main thing to note is that there is not a direct connection to the failed state from every other state. The system goes through a few different degraded states before it fails entirely. In the case when the system is robust through increased failure margins from reconfigurability, from a Markov perspective, there may not be any 'degraded states' in which the system exists, rather the *transition probabilities* to the failure state get lowered. So in graceful degradation there are potentially a number of states in which the system exists before complete failure, while if failure margins are increased, the chances of entering the failed state are reduced (but degraded states may not necessarily be present).

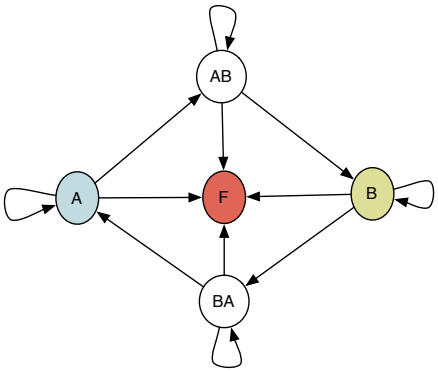

(a) Multi-Ability

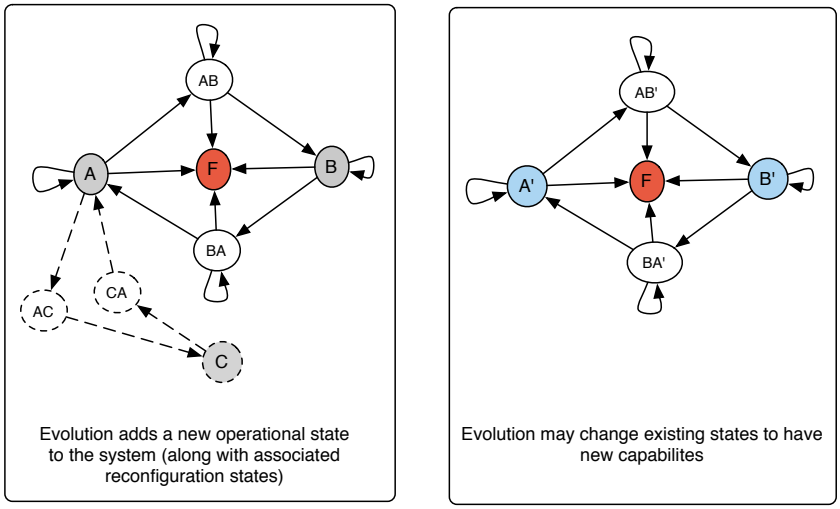

(b) Evolution

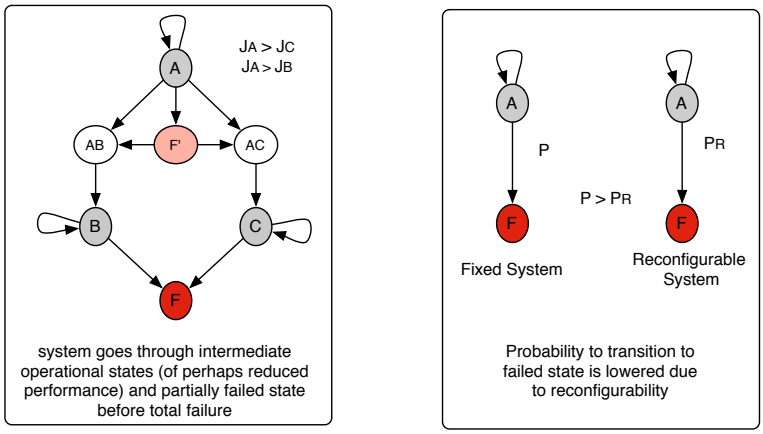

(c) Survivability

Figure 2-20: Markov Representation of Multi-Ability, Evolution and Survivability

2.5 Control-Theoretic Framework

Another scheme of modeling and representing reconfigurable system can be based on concepts and tools of classical control theory. Many complex reconfigurable systems are capable of undergoing two kinds of reconfigurations: an active or *on-line* reconfiguration during which the system's main functions continue to operate, and a passive or *off-line* reconfiguration in which the system is made idle while the reconfiguration takes place. In this context, a reconfigurable system can essentially be modeled as a system that tries to produce a *desired* output (much like a servo) at various points during its operation by undergoing some form of *on-line* reconfiguration. When the desired output requires a change in the system that is outside its existing capability or *on-line reconfiguration bandwidth*, it then undergoes a more radical form of reconfiguration which may require the system to be 'shut down' but alters its capabilities to meet the new objectives when it is operational again after the reconfiguration process. Modeling the dynamics of these processes allow for estimation of accrued 'losses', or cost (either in terms of money, or other relevant metrics such as energy *etc.*). They also allow for studying the effects of changing the extents of the systems on-line and off-line reconfigurability, thereby enabling system designers to determine the extent and type of reconfigurability the system should possess.

Control-theoretic approaches have been used in a meta-sense for a variety of applications ranging from modeling organizational dynamics to human-machine interaction [122]. These are systems that cannot be described through physical dynamical equations, none-the-less the tools of control theory lend themselves to studying certain basic time-related characteristics of these systems. It is proposed that a control-theoretic approach can also be applied to a class of reconfigurable systems (in a variety of domains) that alter certain attributes in response to changing needs.

Traditionally, what is being referred to as *on-line* and *off-line* reconfigurability has been studied separately in detail by various researchers [61, 30]. This work however combines these two aspects to present a more comprehensive method.

2.5.1 Meta-Controls Model of Reconfigurable Systems

Many systems are usually reconfigurable so that they can meet new needs that may arise over time. These systems are capable of modifying some of their key characteristics such as their *functional attributes* in order to produce a desired outcome. Figure 2-21 shows how these systems can be modeled in a generic manner. Typically, there is some change in the system's environment (it maybe a physical environment such as terrain or some other non-physical entity such as market conditions *etc*). Those changes are 'sensed' and can be mapped to some corresponding 'desired attribute' of the system (such as characteristics of a rover's wheel in response to some conditions of the terrain, or coverage area of a satellite in response to some market demand). This mapping

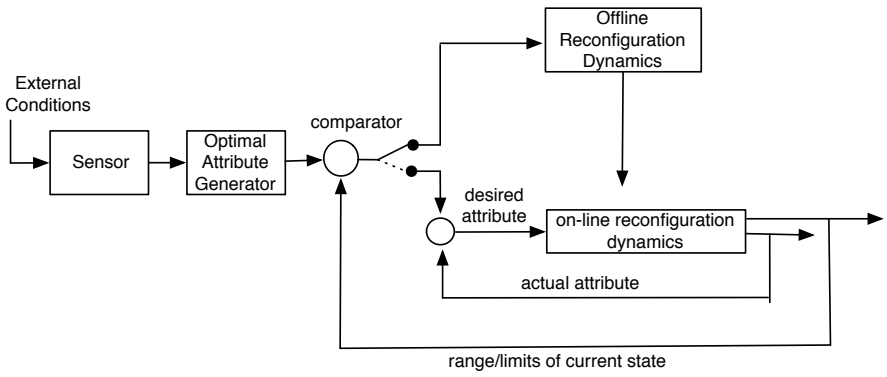

Figure 2-21: Generic Reconfigurable System

is often based on some criterion such as minimization of lost profit, expended energy *etc.* The reconfigurable system tries to achieve this desired attribute through its reconfiguration process as best as it can. Typically, the system will possess the capability of altering its operational attribute within a certain range, primarily driven by actuator dynamic range (*e.g.* a satellite maybe able to steer its antenna through some fixed range). This is essentially the traditional type of 'active control' that many modern systems employ. For instance, active suspensions in automobiles that respond to changing road conditions, temperature and humidity controllers in buildings *etc.* These types of systems essentially can continue to operate while some attribute is adjusted in order to meet some desired goal (*e.g.* smooth ride, or comfortable temperature *etc.*) For many of these systems the envelope of operation is fairly well-defined and the 'band-width' or limits of their reconfigurability is thus designed into and fixed in the system *e.g.* in case of cars that are meant for urban use, the conditions of roads can be characterized within a well defined range, the temperature profile of a city is well known and environment control systems are designed accordingly for living spaces *etc.*

There are a class of systems, however, that can experience either unknown, or known but widely varying needs over the course of time. In such a case, the system may need to under-go substantial changes that cannot either technologically or economically be implemented through on-line reconfiguration. In order to stay optimal, and in some cases even functional, the system must undergo off-line reconfiguration. Thus, if the desired attribute is within the range or 'reconfiguration band-width', then the system will reconfigure on-line to achieve that desired level. On the other hand, if the required attribute level needs a change from the system that is greater than its existing band-width, then the system can achieve the new level by undergoing an off-line reconfiguration process (*e.g.* the satellite may need to under go an orbital reconfiguration if simply steering its antenna from its existing orbit is not sufficient). Figure 2-22 illustrates these concepts.

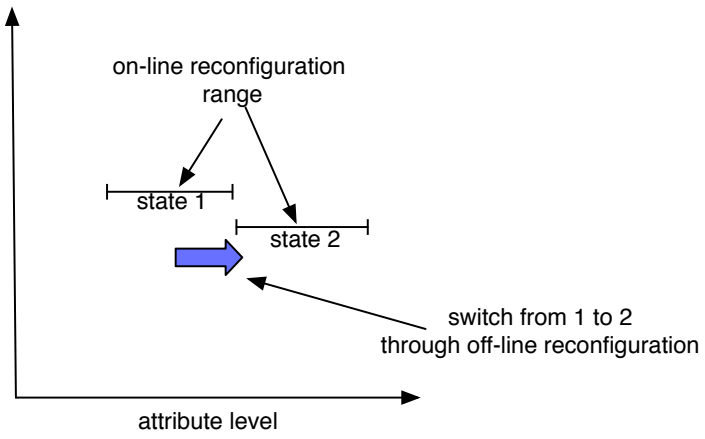

Figure 2-22: On-line and Off-line Reconfiguration

2.5.2 Classes of Inputs

When the reconfiguration process in a reconfigurable system is distinguished along lines of *when* and *how* it takes place relative to the operation of the system, the input to which the system is responding can be categorized into two main classes.

In the first class, the input can be thought of as being stationary during the time the system reconfigures off-line (*i.e.* is non-operational). Examples of these types of situations are when a rover may need to reconfigure in response to some terrain condition. When the rover stops moving, and undergoes the off-line reconfiguration, the terrain conditions are not changing, they remain the same as before. The 'input' to this system, which is the condition of the terrain, therefore remains constant while the system reconfigures. When the rover resumes its motion, the input too resumes from its previous point. This type of case is illustrated in Figure 2-23. The top plot shows how the input may look like without consideration to the reconfiguration processes. It is shown that for certain ranges of the input, there is a specific state that the system needs to adopt in order to continue functioning properly. Initially the system is in state 1, then at time t_1 it should switch to state 2 and so on. The bottom plot shows how the input to the system will actually appear when reconfiguration is factored in. The states cannot be achieved instantaneously, and the system has to undergo some kind of reconfiguration process that has an associated reconfiguration time Td_i for switching to state i. The input maintains its value at the point the reconfiguration needs to occur, and then resumes after the system is on-line again after reconfiguration.

In the second type, the input cannot be considered to be at hold while the system undergoes a reconfiguration. This is a more common case, and also more challenging to deal with. This case is shown in Figure 2-24. The shaded regions show the time durations during which the system is not active. An example of this type of situation is a manufacturing system where the input is

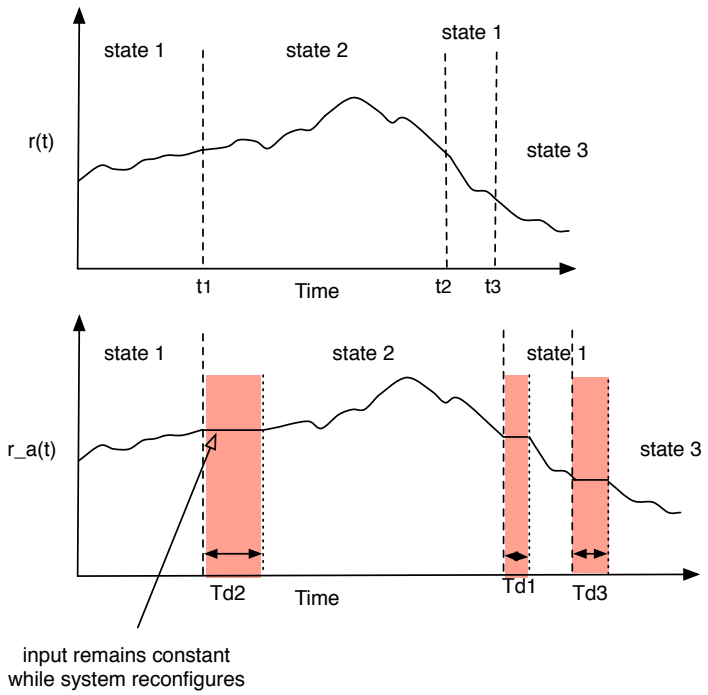

Figure 2-23: Stationary input during off-line reconfigurations

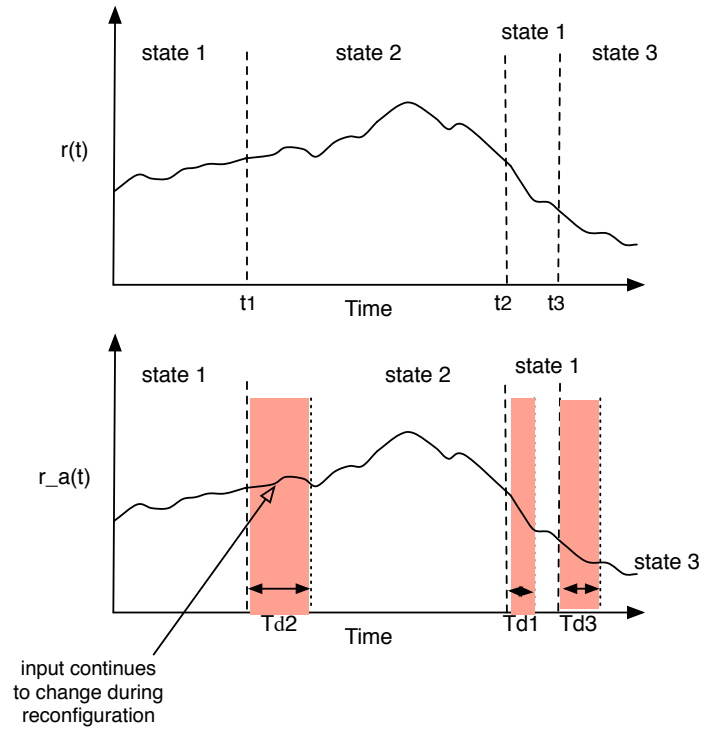

Figure 2-24: Evolving input during off-line reconfigurations

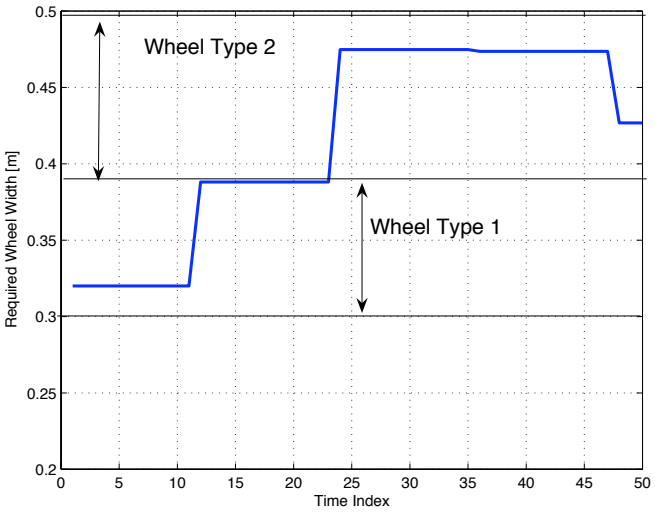

Figure 2-25: Optimal Wheel Width Required for Sortie

perhaps market demand for a particular product. During the time the system reconfigures off-line, the market demand will continue to evolve, and when the system comes on-line, it needs to respond to the current demand and not the demand that existed when the reconfiguration was triggered. This makes the reconfiguration decision very challenging, since the system must reconfigure to a state that is *expected* to be required of the system when it comes back on-line, and the cost of being off-line and reconfiguring should get compensated by the benefit of being in the new state.

Example: Reconfigurable PSV

The reconfigurable PSV introduced in the previous section that is capable of altering its wheel dimensions in order to respond to terrain conditions can serve as an illustrative example. Figure 2-25 notionally shows the ideal wheel width that the system should have as it travels over a certain stretch of planetary surface. The PSV is assumed to have two types of wheels, each of which has a range between which it can reconfigure on-line as the vehicle moves (*i.e.* adjust its width). The first type has a range of 30 cm to 39 cm, and the second type has a range of 39 cm to 50 cm. These are its on-line reconfiguration limits. Since there are two wheels, each has its own (perhaps similar, but slightly different transfer functions). It is clear from Figure 2-25 that in some instances the first type of wheel will be needed, while in other cases the second type will be required if the vehicle is to carry out its sortie. Figure 2-26 shows how this specific system can be modeled on a high-level.

This type of input is treated as being stationary during the off-line reconfiguration process. Figure 2-27 shows the simulated output. While the output is zero during the off-line reconfiguration process, the input remains at the value that it had when the reconfiguration started. The dynamics of the wheels were modeled as simple first order systems with a lag, and a free integrator was also

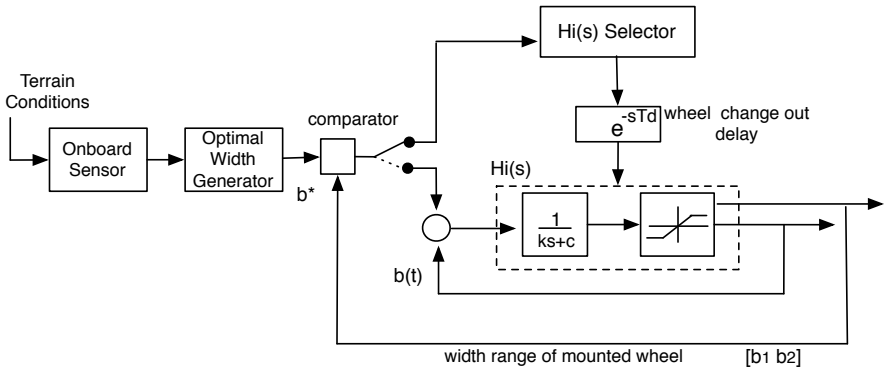

Figure 2-26: On-line and Off-line Reconfiguration of Wheels on PSV

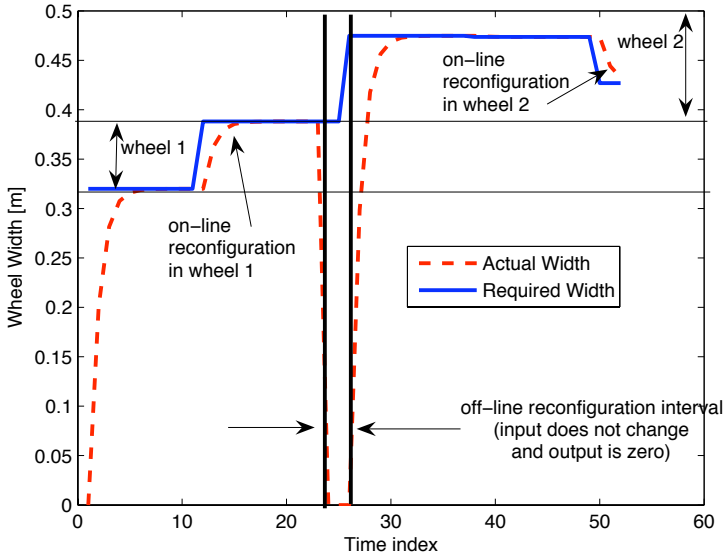

Figure 2-27: On-line and Off-line reconfiguration of wheel

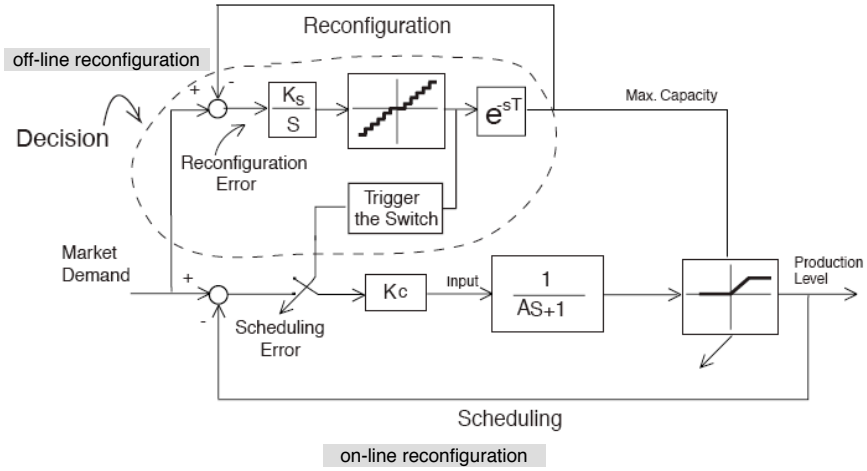

Figure 2-28: Online and Offline Reconfiguration of an Manufacturing System [30]

added in the loop to remove steady state errors. The time delay is implemented as a first order Pade approximation.

Example: Reconfigurable Manufacturing Systems (RMS)

For the case in which the input continues to evolve while the system reconfigures, reconfigurable manufacturing systems are a relevant system for discussion. The actively adjusted scheduling done on a manufacturing line is essentially the on-line reconfiguration, while the off-line reconfiguration is when the system is reconfigured to undergo a more radical change in which perhaps its capacity is altered. Previous research in this area has already shown how the dynamics of reconfiguration of an RMS can potentially be modeled [30]. That model is used here as an illustrative example. Figure 2-28 shows the two on-line and off-line reconfiguration loops that are present in an RMS. If the dynamics of scheduling are sufficiently fast, only the capacity reconfiguration loop can be considered for first order analysis. A manufacturing system in which the production capacity can be scaled to different levels in order to match demand requirements is therefore considered. This system can reconfigure to adopt different capacity levels as desired. Figure 2-29 shows the dynamical model for RMS capacity. The input $r(t)$ is the required capacity level (in units of parts/time unit). The output $y(t)$ is the actual capacity, and $e(t)$ is the difference between the desired capacity and the actual capacity of the system. The constant K_1 is the cost in dollars of one part *i.e.* it is \$/part, while K_2 is number of parts/unit time/\$. The system time delay, or dead-time, is T_d, and represents the reconfiguration time. When T_d is small the system can react to market demand more quickly. The product of K_1 and K_2 is the total gain, and represents how large a change in $y(t)$ can be made in response to a difference between actual and desired capacity levels. It is assumed here that during the reconfiguration time production level on average remains same (and does not fall to zero). After

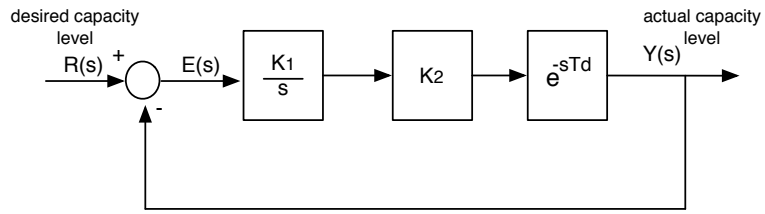

Figure 2-29: Laplace Domain Dynamical Model of Capacity Reconfiguration [30]

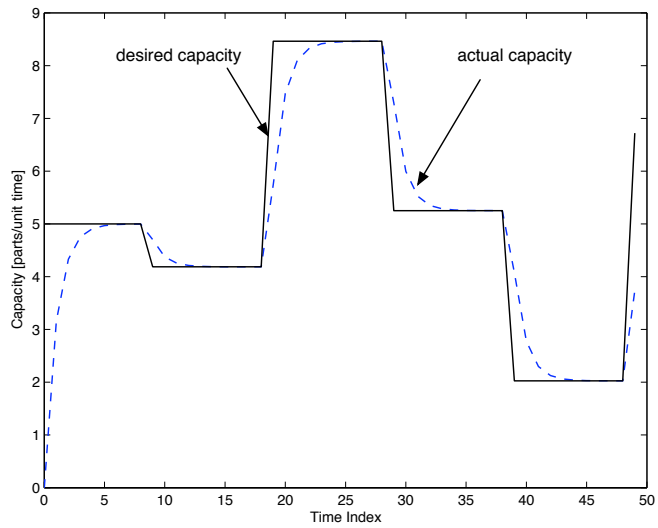

Figure 2-30: Slowly varying capacity requirement

the reconfiguration time is over the ramping up or ramping down begins (which is governed by the product $K_1K_2e(t)$), and the system tries to achieve its target capacity level.

Figure 2-30 shows how the system will respond when the capacity requirements change slowly. The value for K_1 and K_2 is set to 1 and T_d is 0.01. It can be seen that the system scales its capacity up or down and follows the demand with some lag and delay (according to the model). It can however eventually reach its target goal and remain in production at the desired level for a significant period of time. If however the demand changes more rapidly, then the system may never catch up or spend very little time at the desired level. Figure 2-31 illustrates this situation in which the T_d is same as the one used in previous figure, but the input is varied more quickly.

A possible metric for measuring the performance is the cumulative 'error' [30]:

$$J = \int_{t_o}^{t_f} |e(\tau)| d\tau \tag{2.34}$$

where t_o is initial time when system is installed and t_f is final time when the system is retired. This

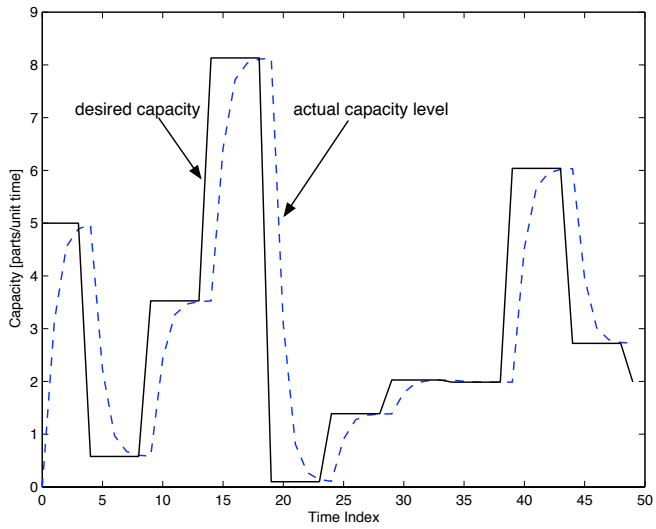

Figure 2-31: Rapidly varying capacity requirement

measure is essentially the combined error of over-production (over capacity) and lost opportunity (under capacity). Figure 2-32 illustrates this for a notional case for increasing T_d. The capacity demand was varied every 10 units of time, and the integration was done over a period of 50 time units. Plots such as these can be used in trading the costs and benefits of reducing T_d.

The purpose of this example is to simply highlight the fact that in the types of systems where the requirements/needs/demand *etc.* evolve over time during the reconfiguration process, the reconfiguration time and the rate of the change of input are key in ensuring reasonable performance of the system. A system that has been specifically designed to be able to undergo rapid changes (as is the philosophy of RMS) can achieve better performance through lower reconfiguration times and therefore lower 'errors' or 'losses'. From a technical stand-point, the reconfiguration time will depend on the design and technologies, in addition to operational processes *etc.* It might however be more costly to implement a design that allows rapid reconfiguration as compared to one that remains fixed. Detailed analyses will thus be required for each specific system in which both recurring and non-recurring costs will have to considered. The reconfiguration costs (that can be driven by reconfiguration time), along with the frequency of reconfigurations (driven by the frequency of change in the demands) will all have to be factored in.

2.6 Reconfiguration Processes

Depending on the system, the reconfiguration process can be fairly simple (*e.g.* turning a knob) to a highly complex procedure involving both humans and machines (for instance reconfiguration

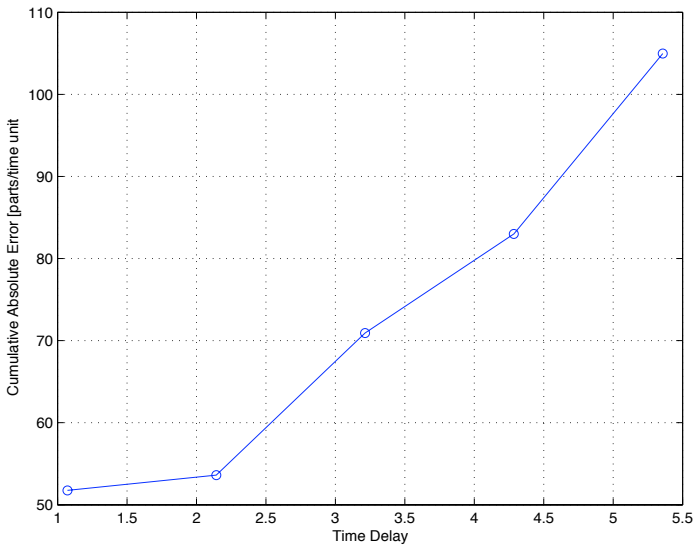

Figure 2-32: Cumulative Absolute Error

of a manufacturing line). Fundamentally however, in any reconfiguration, one or more of the three entities, Matter, Energy, and Information, is:

- Increased/Added
- Decreased/Removed
- Transformed/Re-arranged/re-distributed

Any kind of system reconfiguration can be described by these three primitive or base processes that combine in different ways (in time and extent). The entity that is reconfigured will mostly be (but not necessarily always) related to the nature of the system, *e.g.* in informational systems, it will be information that will mostly be subject to these processes, while in mechanical systems it can be either mass or energy. All of these processes can be viewed from a discrete and continuous sense. Figure 2-33 shows an illustration of these processes. The following sections explain each in more detail.

2.6.1 Extension/Addition

In this process matter, energy, or information can be added to the system. Installation of a component, addition of a module in a software application, increasing the size (for instance in an inflatable structure) are all examples of this process.

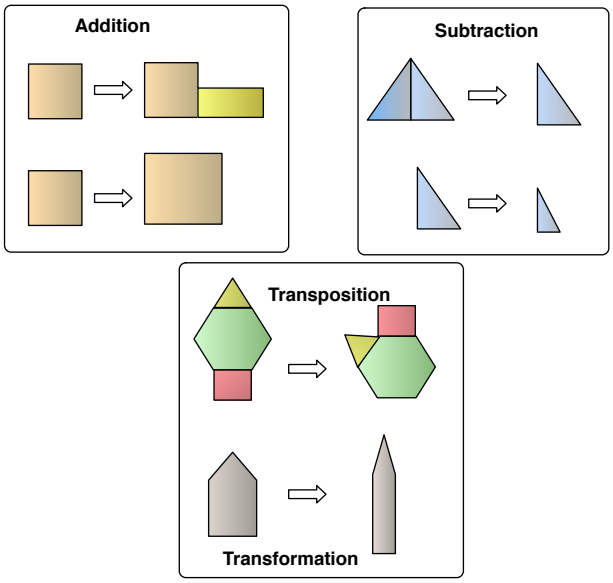

Figure 2-33: Fundamental Processes of Reconfiguration

2.6.2 Reduction/Substraction

This is the opposite or reverse case of the above described process. In this matter, energy or information are removed from the system. This can often occur as part of a substitution procedure, or may be required in a graceful degradation scenario (when failed parts or elements may be discarded from the system).

2.6.3 Transformation/Transposition

In many reconfigurations, the system changes shape, form, content etc without any addition or subtraction, but rather through re-arragement of its existing components/elements *etc.* The re-arragement can be discrete (*e.g.* in many modular furniture pieces shelves or tables can be reconfigured in different shapes), or continuous (the shape of the wing in a morphing UAV, or the position of spacecraft modules in formation flight). A car in which the seats can be reconfigured by stowing away to make room for cargo is also an example of transposition.

Note, that even some common processes such as swapping out a component with a different one are simple combinations of the base functions of removal (of the installed component) and addition (of the new component). There might be multiple ways in which a reconfiguration from an operational state A to state B maybe technologically achieved. It can be expected that the reconfiguration processes will inherently drive the cost and complexity of a reconfigurable system.

2.7 Quantification

Quantifying a 'quality' is usually very difficult. Reconfigurability is inherently a qualitative attribute, consequently it is not immediately obvious what the best metrics for quantitatively measuring its extent can be. It is however, highly desirable to have such means since they would allow for easy comparisons and trades between various architectures.

It is proposed that reconfigurability can be measured both in the performance and design space. In the performance domain, various aspects such as the system capability, reliability *etc.* are of relevance. The effects on these characteristics can be captured to obtain a quantitative sense of reconfigurability that essentially brings about those effects.

Depending on the life-cycle stage of the system (whether it is in the early conceptual stage versus perhaps at the detailed design stage), the level of available information will be different and will thus directly impact the types of metrics that can employed. The following sections elaborate in detail some of the proposed quantitative measures that are in the performance and design/component domains.

2.7.1 Performance Metrics

At the most general level, reconfigurability may be quantified based on the three categories of multi-ability, evolution, and survivability introduced in Section 2.2 earlier. This section introduces two metrics that can be used for multi-ability assessment, one metric for evolution and two metrics for survivability (one each for graceful degradation and robustness respectively). All of these are based on measures relative to fixed/non-reconfigurable systems (that do only one thing in a multi-ability sense, or cannot evolve over time from an evolution sense, or cannot exist in a degraded state in a survivability sense *etc*).

A. Relative Functional Efficiency

This measure captures the relative efficiency of a reconfigurable system as compared to an equivalent collection of dedicated systems. It is most applicable for the case of multi-capability for resource efficiency.

First, the Functional Efficiency, η_f is defined as the ratio of the functional capability (output) to resources (input):

$$\eta_f = \frac{\textit{Total Functional Capability}}{\textit{Resources}} \tag{2.35}$$

The functional capability will be based on the context of the system under analysis. For instance, for vehicles it can be the transport productivity [144], or for RMS it can be the expected production rate [58] *etc.* The resources can be monetary in nature, or some other relevant quantity such as mass or energy.

For a reconfigurable system the total functional capability is the sum of the capabilities of all the states in which the reconfigurable system can exist, and the resources are the total mass or cost of the reconfigurable system. Typically, a reconfigurable system will be compared with a dedicated fixed-functionality system to conduct trades. In such a case, a set of dedicated systems will be used that will correspond in functionality to various states of the reconfigurable system under study. Then, for the dedicated system set the total functional capability is the sum of the capability of all the dedicated systems in the set and the resources are the cost or mass *etc.* of all the dedicated systems combined.

The Relative Functional Efficiency ratio, Ξ is then defined as

$$\Xi_f = \frac{\textit{Functional Efficiency of Reconfigurable System}}{\textit{Functional Efficiency of Dedicated System Set}} \tag{2.36}$$

$$= \frac{\eta_{f\,R}}{\eta_{f\,D}} \tag{2.37}$$

where functional efficiency of the reconfigurable system is computed using Equation 2.35 as

$$\eta_{f\,R} = \frac{\sum_{i=1}^{m} \nu_i}{\rho} \tag{2.38}$$

where m is the number of states, ν_i is the capability of state (or configuration) i, and ρ represents the resources (such as cost, mass *etc*) of the complete system. The functional efficiency of the dedicated system set is computed as

$$\eta_{f\,D} = \frac{\sum_{j=1}^{k} \nu_j}{\sum_{j=1}^{m} \rho_j} \tag{2.39}$$

where k denotes the total number of dedicated systems in the set (being compared against the reconfigurable system). The quantities ν_j and ρ_j here are the capability and cost (resource) of the jth dedicated system.

For a reconfigurable system to be favorable, the functional efficiency ratio should be greater than 1. When $\Xi_f > 1$, it means that the reconfigurable system can provide more functionality per unit resource then the set of dedicated systems.

It should be noted that this quantitative measure essentially captures the *non-recurring* cost. In reconfigurable versus dedicated system comparisons, it can be important to incorporate both the non-recurring and recurring costs in the analysis. For resource efficiency purposes, the non-recurring cost of a reconfigurable system might be less as compared to a dedicated systems set (*e.g.* mass of reconfigurable system may be lower then combined mass of dedicated systems), however if the reconfigurable system is highly sub-optimal its recurring costs may end up being more depending on the extent of usage. The 'cost of sub-optimality', *i.e.* the additional cost incurred by the

reconfigurable system during its operation due to it being sub-optimal, may tilt the balance in favor of dedicated systems. For a more inclusive assessment in which the operational aspect is also incorporated, a Performance Efficiency, η_p, can be used:

$$\eta_p = \frac{\textit{Total Life Cycle Performance}}{\textit{Total Resources over Life Cycles}} \tag{2.40}$$

There can be several context appropriate definitions for 'Total Life Cycle Performance'. One definition for it can be the integral of functional capability and the duration of use. For vehicles, this can be the integral of transport productivity and the duration of travel, or for manufacturing systems it can be the integral of production rate and duration of production. If the duration of use is not known explicitly, an expected total life cycle performance can be computed using probability distributions. The 'Total Resources' here include both recurring and non-recurring costs. For instance, for planetary surface vehicles the non-recurring cost could be mass of the vehicle and recurring cost could be mass of fuel consumed. For RMS the non-recurring cost will be the cost of the machines/plant etc while the recurring costs will be the cost of electricity/energy, raw materials *etc.*

The Relative Performance Efficiency ratio of a reconfigurable and dedicated system set can be defined (in a similar fashion as before):

$$\Xi_p = \frac{\textit{Performance Efficiency of Reconfigurable System}}{\textit{Performance Efficiency of Dedicated System Set}} \tag{2.41}$$

$$= \frac{\eta_{p\,R}}{\eta_{p\,D}} \tag{2.42}$$

In this case also, for the reconfigurable system to be favorable (when life cycle considerations are made), the Ξ_p should be greater then one. Chapter 4 will illustrate how these metrics can be applied in an actual trade study.

B. Evolvability

In the case of evolution, the system changes or reconfigures to meet some new need/requirement *etc.* That need may or may not have been anticipated at the time of design. A savings perspective can be used in quantifying evolvability. The cost of reconfiguring an existing system from its present state to a new state versus the cost of deploying a new system to meet the changed requirements can therefore be considered. Additionally, performance aspects also need to be included in. This is because a reconfigurable system due to inherent limitations of its design may not be able to ideally fulfill the new need/requirement even when it reconfigures to some best achievable state. So while it is possible that the reconfiguration cost may be lower as compared to fielding a totally new system, the performance that would be achieved after the reconfiguration may also be lower. The capability or performance achieved from the new state after reconfiguration should therefore also be factored

in to get a more accurate assessment.

Suppose the cost of a new system is C_{new} while the reconfiguration cost is C_r. The performance of the new system (which can be assumed to be equal to the desired performance or need requirement) is J_{new}, while the performance of the existing system after it reconfigures to its most suitable state (for the new need) is J_r. Then evolvability can be defined as the product of two quantities:

$$\Delta_e = \left(1 - \frac{C_r}{C_{new}}\right) \frac{J_r}{J_{new}} \tag{2.43}$$

$$= \delta_C \, \delta_J \tag{2.44}$$

The δ_C is the percent cost savings that can be achieved if C_r is lower than C_{new}, while δ_J gives the relative measure of performance between the reconfigurable system and possible new system. There can be four cases in any given situation. In the first case the cost of reconfiguration is less, but the resulting performance is also less as compared to that of a new system that can be deployed. From Equation 2.44 it means that δ_C and δ_D will both be between 0 and 1, and therefore the following implication holds:

Case I:

$C_r < C_{new} \Rightarrow 0 < \delta_C < 1$

$J_r < J_{new} \Rightarrow 0 < \delta_J < 1$

$\Rightarrow 0 < \Delta_e < 1$

In this case as shown above, the value of Δ_e will be between zero and one. In the second situation, the reconfiguration cost is less and the performance is more from the reconfigurable system. This is the ideal case for reconfigurability.

Case II:

$C_r < C_{new} \Rightarrow 0 < \delta_C < 1$

$J_r > J_{new} \Rightarrow \delta_J > 1$

$\Rightarrow \Delta_e > 0$

Here Δ_e will always be positive for sure. It will be greater than one if J_r is significantly higher. However it might be between zero and one also depending on how much C_r and J_r differ from the new system cost and performance. From these two cases, it can be seen that at the very least, Δ_e is a positive quantity if C_r is less. If Δ_e is greater than one, it means for sure that the performance of the reconfigurable system is also better (along with lower cost). So reconfiguring the existing system is definitely the better option if $\Delta_e > 1$.

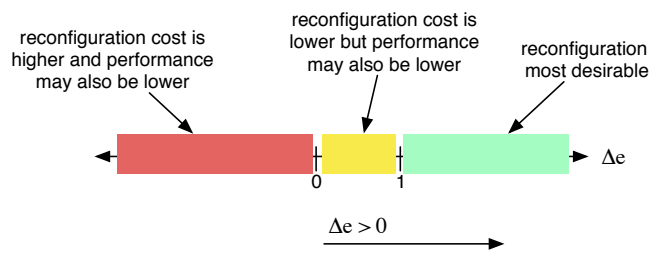

Figure 2-34: Evolvability Axis

In the third case, the cost of reconfiguration is higher, but the performance achieved is also higher.

Case III:

$C_r > C_{new} \Rightarrow \delta_C < 0$

$J_r > J_{new} \Rightarrow \delta_J > 1$

$\Rightarrow \Delta_e < 0$

In the fourth case, the cost of reconfiguration is high and the performance is lower as compared to a new system. In such a situation reconfiguration will not make sense, and it is better to deploy a new system.

Case IV:

$C_r > C_{new} \Rightarrow \delta_C < 0$

$J_r < J_{new} \Rightarrow \delta_J < 1$

$\Rightarrow \Delta_e < 0$

From the third and fourth case it can be seen that Δ_e will be negative if reconfiguration costs more. However one cannot definitively know whether the performance is also poor or not, and δ_C and δ_J will have to inspected in addition to simply computing Δ_e. These cases are summarized in Figure 2-34. Chapter 5 illustrates the use of this metric.

C. Survivability

The rate of change of a system's expected productivity/capability *etc.* with time, $\frac{d\bar{C}}{dt}$ can give a measure of how rapidly it's usefulness changes. The Relative Degradability, defined as the ratio Λ, of the rate of change of expected capability of a reconfigurable system and dedicated system can be

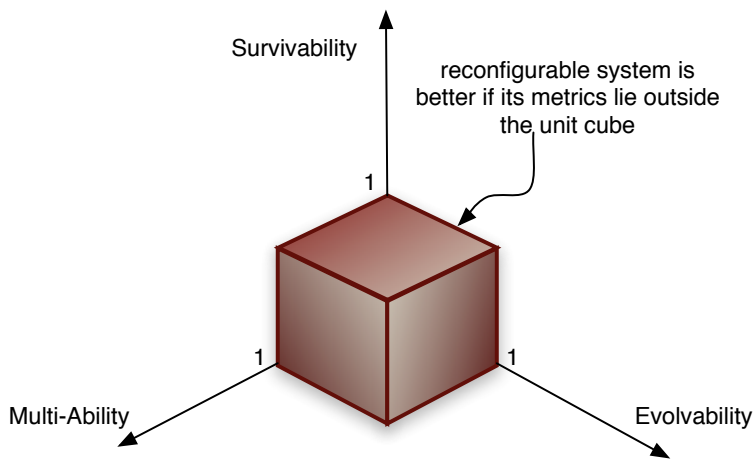

Figure 2-35: Reconfigurable and Fixed systems can be evaluated in this space

used as a measure of comparison:

$$\Lambda = \frac{\left(\frac{d\bar{C}_D}{dt}\right)}{\left(\frac{d\bar{C}_R}{dt}\right)} \tag{2.45}$$

For the reconfigurable system to be favorable, Λ should be greater than 1. The Λ is essentially the ratio of the slopes of the lines shown in Figure 2-5(a) illustrating how the expected functionality or productivity varies with time for the reconfigurable and dedicated systems.

A related measure can also be based on the ratio of stability margins or failure probabilities between the reconfigurable and dedicated cases for a system. This is more of an evaluation of the system's robustness:

$$\Phi_r = \frac{\phi_R}{\phi_D} \tag{2.46}$$

The variable ϕ denotes the stability margin or failure probability and the subscript R and D denote the reconfigurable and dedicated systems respectively. For the reconfigurable system to be favorable Φ should be greater than one.

Depending on the particular system under study, one or both of the measures can be employed in evaluating graceful degradation and robustness. Chapter 4 illustrates the use of both of these metrics.

Based on these metrics, the Degrees of Reconfigurability (DOR) in a 3D space, with axes of multi-ability, evolvability, and degradability, can be envisioned (see Figure 2-35). This can serve to define where a particular concept/design lies and can be used in trades between potential concepts for a particular system. The exterior region of a three dimensional unit cube in the all-positive axes space will be the space where reconfigurability is favorable. In that exterior region, all the metrics η_n (or η_p), Λ and Φ_r will be larger than one. The strongest case for a system to be reconfigurable may then be when it occupies a spot far out in the 3D space (meaning it has all three reasons for

requiring reconfigurability).

2.7.2 Design Metrics

In the design space, the relevant things are components, interfaces *etc.* In this context the issues for reconfigurability are things like how easy it is to carry out the reconfiguration processes (of adding, removing or transposing components for instance), or how much variability does a sub-system or part provide in terms of its functional/form attributes *etc.* The following sections describe a set of metrics that can be employed for capturing the reconfigurability in a quantitative sense.

Reconfigurability Index

In case of the performance space, it is proposed that the extent of reconfigurability of a system can be measured by the maximum amount of change in the systems capability among all of its viable configurations. In other words, the capability 'bandwidth' of a reconfigurable system can be used as a measure of the extent its of reconfigurability.

The capability can be quantified through metrics that are based on the high level performance parameters related to the value delivering function of a system. For example, for transportation systems the Transport Productivity metric [144] can be utilized. This will be discussed further in Chapter 4.

In general, a reconfigurable system will have capability C_i when it is in its configuration or state i. For a total of m possible configurations (or viable states) a set $\mathbf{C}_p$ can be defined for the system as:

$$\mathbf{C}_p = [C_1, \cdots, C_i, \cdots, C_m] \tag{2.47}$$

A *Reconfigurability Index*, RI, for the system is then

$$RI = \max(\mathbf{C}_p) - \min(\mathbf{C}_p) \tag{2.48}$$

Consider for instance a vehicle design that is reconfigurable into three different states. Its transport capabilities in each state are

$$\mathbf{C}_p = [2000, 3000, 3500]$$

The RI for this will therefore be $3500 - 2000 = 1500$. Note, that since this is not a relative measure, rather an absolute measure, it is only applicable for comparison between similar systems/elements. It is essentially the extent, range or *bandwidth* of capability. Note, that there might be 'gaps' in that range depending on the capabilities of the specific states.

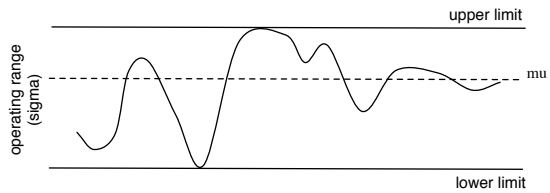

Figure 2-36: Operating range and nominal operating point

Coefficient of Variation

This metric is similar to RI, however it is more applicable to situations where there is a nominal point of operation. It can therefore be best used at the component/sub-system level rather than at a system level. It is defined as the ratio between the range of operation, σ, and the nominal (or mean) operating point, μ (see Figure 2-36).

$$c_v = \frac{\sigma}{\mu} \tag{2.49}$$

The reconfigurability of wings, antennas *etc.* can be described with this metric.

Combinatorial Efficiency

It is the ratio of number of distinct configurations, n_c, of the system and the total number of modules or building blocks, N_m [107].

$$\mu_c = \frac{n_c}{N_m} \tag{2.50}$$

It is called 'combinatorial efficiency' since it provides a measure of how many *unique* configurations can be achieved (which can be thought of as the output) through a given 'input' set of modules.

Coefficient of Connectivity

It is defined as the ratio of the number of links changed, l_c, to the total number of links in the initial and final configurations, l_t.

$$\lambda = \frac{l_c}{l_t} \tag{2.51}$$

The links can be physical, informational *etc.* In order to make use of this metric, detailed information about the system connectivity relationships (such as through Design Structure Matrices) will be required. It is thus only applicable for cases where enough information about the system design is available. In general, it can be expected that the reconfiguration cost will be directly related to the λ. Reversibility of the reconfiguration relates primarily to whether the link changes, l_c, can be reversed.

A more inclusive and related metric has been previously proposed in which the changes that

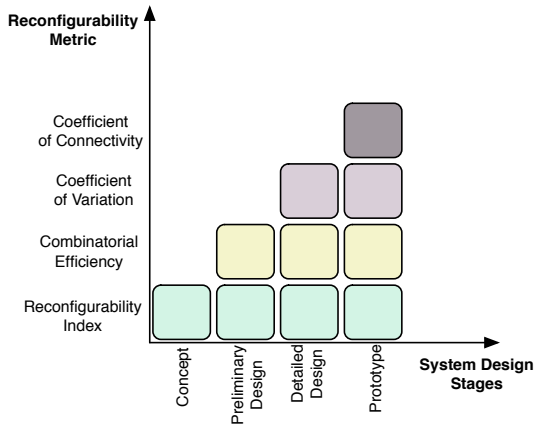

Figure 2-37: Reconfigurability Needs for Selected Systems

occur in the system's DSM over its various configurations are analyzed in the context of introducing new technology into a system's design [126]. This 'delta DSM' approach essentially provides information about how much the DSM changes (and therefore the connectivity links). A measure of reconfigurability can be based on a similar metric. *Ideally, the most reconfigurable system is one that can undergo very little change in its DSM but produce a large change in its form/functional attribute or relevant performance measure.* So one form of comparison can be the ratio of the change in performance and of the corresponding 'delta DSM'. The higher this ratio, the more reconfigurable a particular design will be.

Figure 2-37 shows how these metrics can be expected to be usable at different design stages of a system. In the initial stage when only concepts of the system are generated, perhaps the only metric that can be used is the reconfigurability index if a general idea of the capabilities of the various concept configurations is known. In the later preliminary design and detailed design stages, when more information is added, the combinatorial efficiency and coefficient of variation metrics can be expected to be usable. Since in these stages, detailed information regarding the system's modules, their capabilities, component operation regimes etc will be known. Although a fair knowledge of the system's DSM would be at hand at this point, the connectivity coefficient is marked as truly being useful in the prototype stage when an actual prototype can provide the exact information needed to accurately compute this metric.

Chapter 3

Reconfigurability in Space Systems

This chapter focuses on space systems, and discusses their unique aspects and special issues that many other types of systems do not commonly encounter. A detailed analysis of the various factors that relate to reconfigurability considerations in space systems is presented. In the last section a model is developed to quantify some of the effects of reconfigurability on space mission logistics requirements.

3.1 Distinctive Issues in Space Systems

There are several technological, economical, and political aspects that set space systems apart from other types of systems. Space systems often incorporate highly sophisticated materials, components, and other technologies customized or specifically produced for the space environment. They have to exhibit a high degree of reliability and robustness. They are mostly produced in either single or very small quantities, are high in cost and complexity. Most of them are strongly connected with government agencies and national policies.

Most space systems also face various kinds of uncertainties ranging from budget variations (from their conception to actual deployment and operation), to technical issues related to environmental conditions and space weather [139].

The basic issue, however, that sets space systems apart from all other technical systems is their location. Space systems are deployed, operated, and (often also retired) at the largest distances from their point of origin (Earth) as compared to any other human engineered system[1]. Because of this location aspect, at the heart of all the issues related to space systems are two fundamental physical limitations: the Earth's gravity well (which dictates issues of mass transportation) and the speed of light (which drives the issues of information transmission).

[1] In case of future planetary outposts one can argue on more subtle issues of their origins.

Table 3.1: Launch Costs to LEO for Different Vehicles[73]

Vehicle	Max to LEO [kg]	Cost (FY 2004) [$ Million]	$/kg [Thousand]
Athena I	820	19.18	23.39
Athean II	2065	29.34	14.21
Atlas IIA	7316	95.93	13.11
Atlas IIAS	8618	118.51	13.75
Atlas IIIA	8640	118.51	13.71
Atlas IIIB	10718	118.51	11.05
Atlas V400	12500	101.58	8.12
Atlas V500	20050	124.15	6.19
Delta II	5140	67.7	13.17
Delta III	8290	95.93	11.57
Delta IV Medium	8600	101.58	11.8
Delta IV Medium +	13600	124.15	9.12
Delta IV heavy	25800	191.87	7.43
Minotaur	636	14.10	22.18
Pegasus XL	443	16.93	38.21
SSLV Taurus	1320	22.57	17.10
Commercial Taurus	1380	22.57	16.35
Titan II	1900	45.14	23.76
Ariane 40	5000	95.93	19.18
Ariane 42P	6600	101.58	15.39
Ariane 42L	7900	112.86	14.2
Ariane 44LP	9100	124.15	13.64
Ariane 44L	10200	141.08	13.83
Ariane V	18000	203.16	11.23
H-II	10060	191.87	19.07
H-IIA 202	9940	84.65	8.51
M-V	1800	67.72	37.62

The cost of escaping the Earth's gravitational pull with current technology is very high. The physical accessibility (through either robots and/or humans) of a space system, after it has been deployed, is therefore extremely difficult and costly. Table 3.1 shows the maximum payload capacity to low Earth orbit of various launch vehicles and the upper range of their launch costs. Based on this data, the average cost of transporting one kg of mass to LEO with the existing capabilities is a little over $15,800. This large cost of physical transport from the Earth's surface to low Earth orbit and beyond is a principal issue for modern space systems. It leads to severe constraints on mass and volume of the system that can be fielded. Furthermore, since deployment alone is so expensive and difficult, the service/and or supply lines of these systems are either non-existent or very thin. This contributes to requirements of increased reliability and robustness. Because it is hard to repair or service the systems (and due to their expensive nature it is highly desirable for them to continue operation in face of anomalies and failures), space systems are built with various redundancies and contingency aspects (and therefore usually end up with trade-offs between the mass and volume constraints on one hand and increased reliability and robustness on the other).

The second limiting factor is the speed of light, which puts the ultimate limits on informational accessibility. As the systems go further away from Earth, time delays in communication become an increasingly important issue that affect the architecture, design, and technologies of the systems. The mass and volume constraints (due to limitations of mass transportation) further add to the informational accessibility constraints since the systems have limited power and therefore have limitations on their bandwidth. The informational access is thus affected both in terms of quantity and speed due to the issues of mass and energy transportation. The limitations on time and extent of informational exchange between the ground and the deployed space system at long distances, drives systems to have greater autonomy and intelligence which adds to the requirement of having sophisticated software which is costly to develop.

Another important factor that drives several technical issues (and also arises due to the location aspect) is the harsh environment of outer space and planetary surfaces. Physical human access/presence is particularly affected by this, since the hostile conditions add to the cost aspect (a lot of support systems are needed to ensure human survivability). Furthermore, it sets an inherent limit to the extent of using commercial of-the-shelf (COTS) components and technologies in space systems (which again adds to cost). Since the environmental conditions of space and planetary surfaces are not found naturally on Earth in many cases, the system can never be fully tested. This then leads to issues of robustness and reliability (which again add to the cost).

The transportation difficulty and costs, reliability requirements, and expensive technology (for the unique environmental conditions) all combine to produce high total costs (and also high risks) in developing and deploying space systems. Figure 3-1 provides a high-level and simplified view of these interactions. The full dynamics at play in space systems are much more inter-twined and complex. There are several additional factors ranging from policy and regulation, to economic aspects that bear in on the design, implementation and operation of these systems and affect their costs and performance. The purpose of the schematic in Figure 3-1, however, is to simply illustrate how the two fundamental physical limitations of transfer of mass and electromagnetic waves affect space systems. These two factors along with harsh environmental conditions (primarily but not solely) generate a host of issues and requirements for these systems. So while the natural limits of environment and location cannot be changed, a greater focus on new ways of designing and using space systems can help in overcoming the cost barriers. Reconfigurability in ways that have previously not been incorporated in the design of space elements can play a very significant role in realizing systems that reduce over all mission costs, enhance element survivability and provide for evolution over time.

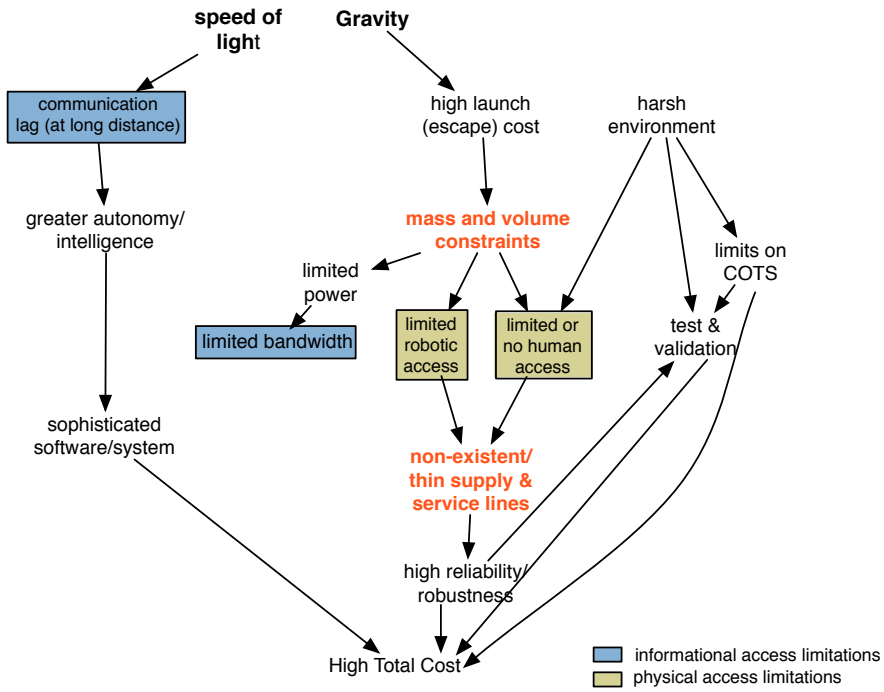

Figure 3-1: Main factors affecting technical aspects and costs of space systems

3.2 Reconfigurability for Mass and Volume Efficiency

From an architectural and design perspective, the issue of mass and volume constraints is very important. Since the costs are so high (currently more than $15800 per kg on average), it is highly beneficial to extract as much utility as possible from every kilogram of mass transported from the Earth's surface.

The future missions to Moon and Mars, as outlined by NASA's Vision for Space Exploration, can be expected to employ several large elements. For chemical propulsion, the initial mass in LEO (IMLEO) is driven by the rocket equation. For a propulsive stage, the high-level mass breakdown is given by

$$m_o = m_{P/L} + m_s + m_p \tag{3.1}$$

where m_o is the initial mass before a burn, $m_{P/L}$ is the mass of payload to which a velocity increment must be imparted, m_p is mass of propellant, and m_s is structure mass also known as dry mass (which includes the engines and vehicle sub-systems). The final mass, m_f, is the mass after a complete burn but before discarding the tanks and is given by

$$m_f = m_{P/L} + m_s \tag{3.2}$$

From the rocket equation the mass of propellant is

$$m_p = m_f \left(e^{\frac{\Delta V}{I_{sp} g}} - 1 \right) \tag{3.3}$$

Substituting Equation 3.2 in Equation 3.3, and denoting the term $e^{\frac{\Delta V}{I_{sp} g}}$ with β

$$m_p = \left(m_{P/L} + m_s \right) (\beta - 1) \tag{3.4}$$

$$m_p = \left(m_{P/L} + \alpha m_p \right) (\beta - 1) \tag{3.5}$$

where $\alpha m_p = m_s$, and α is the structure mass fraction. Re-arranging the terms gives

$$m_p = m_{P/L} \left(\frac{\beta - 1}{1 - \alpha(\beta - 1)} \right) \tag{3.6}$$

A quantity λ_s, which relates to the structure mass fraction, can now be defined as:

$$\lambda_s = \frac{m_s + m_p}{m_p} = \alpha + 1 \tag{3.7}$$

Then

$$m_p = m_{P/L} \left(\frac{\beta - 1}{1 - (\lambda_s - 1)(\beta - 1)} \right) \tag{3.8}$$

$$m_p = m_{P/L} \left(\frac{1 - \beta}{(\lambda_s - 1)\beta - \lambda_s} \right) \tag{3.9}$$

Using Equation 3.7, Equation 3.1 can be written as:

$$m_o = m_{P/L} + \lambda_s m_p \tag{3.10}$$

Substituting Equation 3.9 in the above equation gives

$$m_o = m_{P/L} + \left(\frac{(1 - \beta)\lambda_s}{(\lambda_s - 1)\beta - \lambda_s} \right) m_{P/L} \tag{3.11}$$

Re-arranging the above expression yields

$$m_o = \left(\frac{(1 - \beta)\lambda_s}{(\lambda_s - 1)\beta - \lambda_s} + 1 \right) m_{P/L} \tag{3.12}$$

The term in parenthesis is essentially the 'growth factor' ψ that relates the initial mass before the

burn and mass of payload. The expression for ψ can be further simplified to get:

$$\psi = \left(\frac{(1-\beta)\lambda_s}{(\lambda_s - 1)\beta - \lambda_s} + 1 \right) \tag{3.13}$$

$$= \frac{\beta}{(1-\lambda_s)\beta + \lambda_s} \tag{3.14}$$

Note from Equation 3.7 that λ_s depends purely on the type of propellant chosen and the structural efficiency, *i.e.* technology of the rocket. The variable β on the other hand depends on propulsive efficiency (I_{sp}) and the depth of the gravity well *i.e.* how large the ΔV requirement is.

For each stage i, with Δv_i, there is a corresponding β_i, and the growth factor is thus:

$$\psi_i = \frac{\beta_i}{(1-\lambda_s)\beta_i + \lambda_s} \tag{3.15}$$

If a one-way trip to the Moon is considered (for deploying surface assets for instance), the primary propulsive maneuvers from LEO will be [82]

- Trans-Lunar Injection (TLI), with ΔV of around 3.36 km/s
- Lunar Orbit Insertion (LOI), with ΔV of 0.84 km/s
- Lunar Landing (LL), with ΔV of 1.87 km/s

If the vehicle stack is considered to have just one cargo module, of mass m_c, that will be delivered to the surface, it has to undergo all the above three listed events. The initial mass in LEO (IMLEO) for this trip is then

$$m_{IMLEO} = m_c \psi_{moon} \tag{3.16}$$

$$\psi_{moon} = \psi_{TLI}\psi_{LOI}\psi_{LL} \tag{3.17}$$

where the ψ's are computed from the associated ΔV's.

For a one-way Mars trip, the main maneuvers for a conjunction class mission are usually assumed to be [136]

- Trans-Mars Injection (TMI) with ΔV of 3.506 km/s
- Aerobraking
- Mars Landing (ML) with ΔV of 0.625 km/s [82]

For the aerobraking, a ratio γ_A can be defined as

$$\gamma_A = \left(\frac{m_{AB}}{m_{P/L}} + 1 \right) \tag{3.18}$$

where m_{AB} is usually 15% of $m_{P/L}$, thus γ_A is 1.15 [136]. The IMLEO for Mars is then

$$m_{IMLEO} = m_c \psi_{mars} \tag{3.19}$$

$$\psi_{mars} = \psi_{TMI} \gamma_A \psi_{ML} \tag{3.20}$$

ψ_{TIM} and ψ_{ML} are computed using ΔV for TMI and ML respectively.

Since the ψ's depend on the I_{sp} and number of stages (through β), there can be a great deal of variability depending on the specific architecture and technology of the chemical transport system *e.g.* hypergolics versus LH_2/LOX. Figure 3.2 shows how the growth factor (ψ_{moon} and ψ_{mars}) varies as a function of I_{sp} and number of stages in the TLI. The calculation is based on assuming the structural mass to be 10% of the propellant mass (*i.e.* a value of 1.1 for λ).

Three different scenarios for staging, in the TLI or TMI phase, were analyzed. In the first scenario only one stage for TLI or TMI is assumed. In the second scenario two stages are assumed (and each stage has half the total ΔV required for TLI or TMI), and in the third case there are three stages (with each stage having a third of the total required ΔV for the trip segment). It can be seen that there is marked improvement from single stage to double stage, however a third stage does not bring too much benefit. Furthermore, the absolute difference in mass growth factor is more pronounced between a single stage and double-stage scenario for lower I_{sp} cases, while it is much smaller for higher I_{sp} values.

For the lunar mission, it can be observed that for an I_{sp} of 460 sec and two stage TLI, the growth factor is approximately 4.5. Thus for each kilogram on the lunar surface 4.5 kg must be brought to LEO. In those 4.5 kg in LEO, 1 kg is the actual payload while the remaining 3.5 kg are the transport vehicle's hardware and propellant). For a lower I_{sp} of 320 sec, the IMLEO (for unit mass on lunar surface) is as high as 10 kg (for single stage TLI). The growth factor would be even higher if we accounted for Earth-to-Orbit launch.

For the Mars mission the growth factor for two-stage TMI and I_{sp} of 460 sec is approximately 3.3 (as can be seen from Figure 3.2). It is lower as compared to a Lunar mission since aero-braking is assumed for the Mars case which eliminates the need to do a major burn to do Mars orbit insertion. The landing ΔV is also small based on the assumption that parachutes and other devices will be used to assist in the descent. In the Lunar case the landing is completely powered (hence has a large ΔV of 1.87 km/s). The total cost however for a Mars mission (even with possibly lower growth factor) will most likely be much higher than the cost for a Lunar mission, since the long mission (both in terms of travel and surface stay times) will contribute to higher cost vehicles and support systems. Equations 3.17, 3.20, and 3.15 can be used to approximately compute the mass required in LEO for lunar or martian missions for a payload mass of 1 kg. Using the maximum and minimum values of the growth factors (which also is the mass in LEO for unit mass on a planetary surface), and

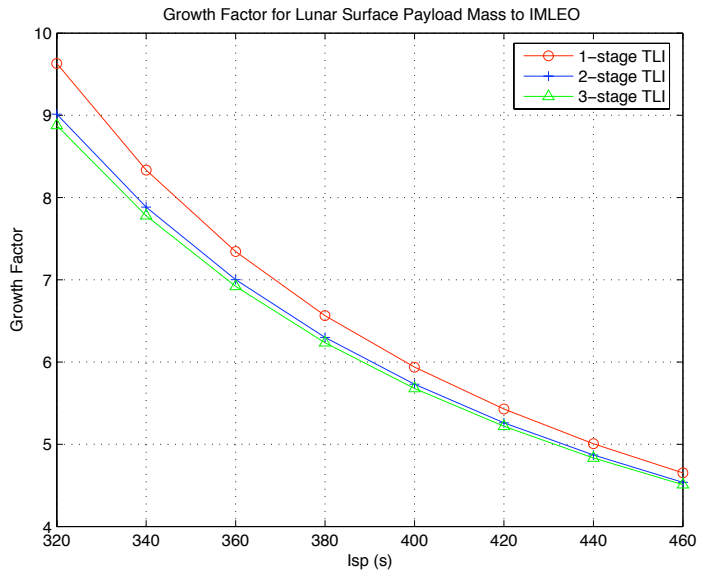

(a) Growth Factor for Lunar Mission

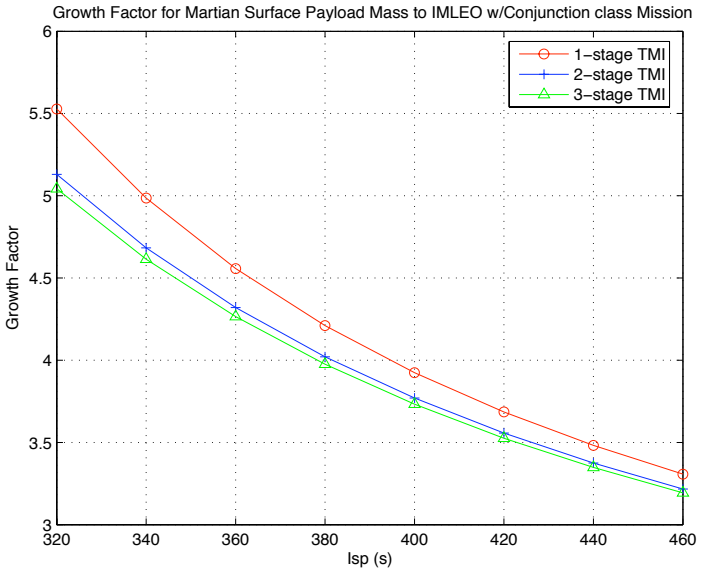

(b) Growth Factor for Martian Mission

Figure 3-2: Growth factors in LEO for payloads to be delivered on surface of Moon and Mars

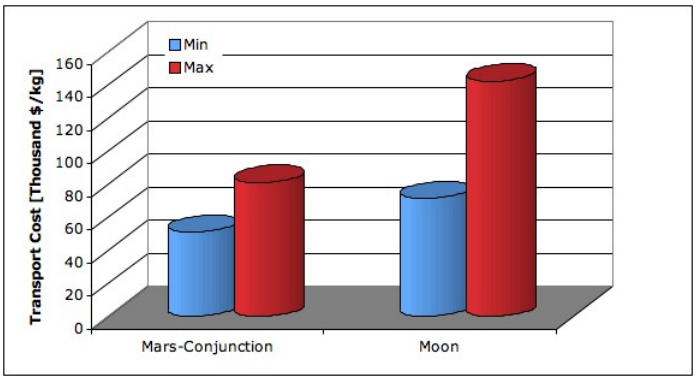

Figure 3-3: Specific Cost of Transport from Earth Surface to Planetary Surface

multiplying with the average cost of transport to LEO, that cost of transport to a planetary surface is obtained and shown in Figure 3-3. It should be noted that this is only the cost of transporting the required amount of mass in LEO, using current launch vehicles filled to capacity, for unit mass landed on Moon or Mars surface. Total program costs of a Lunar or Mars exploration program will run in billions of dollars and a more sophisticated cost analysis will be needed to assess the true cost of landing payload on the surface of Moon and Mars. However, even focusing on transportation cost alone, using current launch prices, is enough to illustrate how valuable each kilogram (and also cubic meter) is on the Moon and Mars. It can be seen from Figure 3-3 that each kilogram costs upwards of $40,000 (reaching even up to $140,000).

Reconfigurable systems that can perform different or modified functions at different times as required over a mission, thereby allowing reduction of total mass and volume that needs to be deployed, can greatly benefit space exploration. Reconfigurability for multi-ability (functionality) is therefore highly desirable and needs to be seriously considered for space systems where mass and volume are at the utmost premium.

3.3 Spares Estimation Model for Exploration Missions

As illustrated through Figure 3-3, mass efficiency from all avenues of a mission should be explored since its payoff can be immense in terms of dollar costs. The Vision for Space Exploration being pursued by NASA since 2004, makes it even more relevant and important to be able to quantitatively assess the mass (or other resource) savings that can be realized with reconfigurability. With new vehicles and space elements to be designed for future missions, it is highly desirable to have models that can help in making high level design decisions regarding the various '-ilities' of the system such as it commonality, reconfigurability, reliability *etc.* On this note, this section presents an attempt to address this issue by looking at logistical resource requirements. The future human missions to the Moon and Mars can be expected to use several elements, where in typical elements comprising

a surface mission may include ascent/descent vehicles, rovers for surface mobility, habitats for long duration surface stays *etc.*, see Figure 3-4.

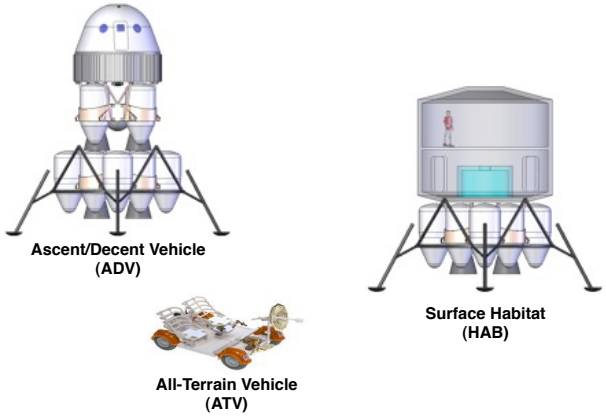

Figure 3-4: Typical space exploration mission elements

In such large missions, the required logistics resources can become significant. Common or reconfigurable spare parts, that can be configured to function in different systems as required, can potentially be of great benefit since the mass and volume of logistics resources (spare parts) needed for an exploration mission can be greatly reduced through the use of such components. Furthermore, other maintenance and operation procedures can become easier due to commonality of components in different elements.

In order to assess the impact of having reconfigurable (or common parts) on the mass requirement, an analytical model was developed. Several models have been produced previously for analyzing spare parts inventory requirements. Caglar and Simchi-Levi [38] have shown how a two-echelon spares parts inventory system can be modeled and optimally solved for a given service time constraint. Shishko [123] has modeled costs of spares and repairs in estimating operations costs for the International Space Station. Bachman and Kline [31] have developed a model for estimating spare parts requirements for space exploration missions (which is is discussed in the next section in detail). An enhanced model that explicitly accounts for the reconfigurability is then formulated to show how reconfigurable spares can affect mass and volume requirements.

3.3.1 Model for Estimating Spare Parts Requirements

A total of E, co-located elements are considered to be part of the mission. Although each element is composed of several sub-systems and parts, for simplicity only one type of part is considered first here (the extension for several parts is discussed at the end of the section). It is assumed that there is no re-supply (which is conceivable for a mission to Mars for instance), so no additional parts can be made available during the course of the mission. Furthermore, no repair capability is assumed.

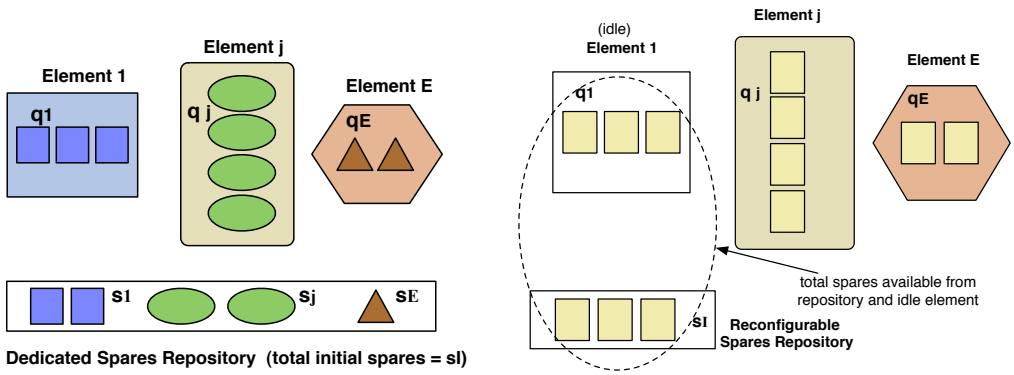

(a) Dedicated spares for particular elements

(b) Reconfigurable spares for any Element

Figure 3-5: Dedicated and reconfigurable spares usability by elements

Thus, once a part fails it cannot be employed for use at a later time.

Figure 3-5 illustrates the usage model assumed for dedicated and reconfigurable parts. It shows that if elements are using dedicated components, then only particular spares designed for a particular element can be utilized from a spares repository. On the other hand, operating elements in need of reconfigurable (or common) spares can obtain the parts from either a spares repository or an idle element (as indicated with the dashed oval).

Dedicated Spare Parts

In this case the component used in each element will be for the dedicated use of only that element. For simplicity, consider that there is only one type of component installed on element j (Fig. 3-5(a)). The 'quantity-per-application' (QPA), which is the number of units of the component used, will be denoted as q_j. It is assumed that there is a spare parts repository which is a collection of spares for the various mission elements. The spares level for each element's component in that repository is s_j. The sum of all s_j is s_I which is the total number of spares initially in the repository at the start of the mission.

It is considered that the components fail according to a Poisson process described by

$$p_j(n) = \frac{e^{-\lambda_j}\lambda_j^n}{n!} \tag{3.21}$$

$$\lambda_j = \int_{t_o}^{t_f} l_j \, dt \tag{3.22}$$

where $p_j(n)$ is the probability of having exactly n failures of the component in element j in interval $[t_o \; t_f]$ for a process that has a failure rate of l_j, which is the inverse of its Mean Time to Failure, (MTTF). The mean of such a Poisson process can be shown to be equal to λ_j. If there are

q_j units, and l_j is independent of time, then the mean number of failures in interval $[t_o\, t_f]$ is simply

$$\lambda_j = q_j l_j (t_f - t_o) \tag{3.23}$$

and is sometimes referred to as "outstanding orders" [38], or as the "number in the pipeline" [31]. Note that the interval $[t_o t_f]$ is the duration the component has operated for. The expected backorder level, $\bar{B}_j$, is the expected value of the difference between actual number of spares that are available and the required number of spares (as driven by the number of failed components). It is therefore computed as [31]

$$\bar{B}_j = \sum_{n>s_j}^{\infty} (n - s_j) p_j(n) \tag{3.24}$$

In reality the upper bound on the summation is the total failures that can occur of the component.

In this case redundancy in an element is ignored, and it is assumed that an element is operational if it does not have any outstanding requests for replacing its failed component, *i.e.* its $\bar{B}$ is zero. If it is assumed that the backorders of the part are uniformly distributed across the elements, then the probability that there is an outstanding request for a component in a particular element is $\bar{B}_j/q_j$. The failures of the components in the different elements are considered to be independent, and thus the availability (of the element that uses this component) is

$$A_j = \left(1 - \frac{\bar{B}_j}{q_j}\right)^{q_j} \tag{3.25}$$

It should be noted that A is the availability that can be expected at the end of time t_f since it was used for evaluating λ given in Equation 3.23. The *system* availability can be defined as the probability of *all* the elements that should be operating to be actually operational. The overall availability is then simply the product of availability of all the elements (assuming that all the elements need to be fully operational for the entire mission)

$$A_{sys} = \prod_{j=1}^{E} A_j \tag{3.26}$$

If more than one component needs to be considered in the analysis, this model is easily extended by using Equation 3.25 for each component and then taking the product to get element availability (assuming that all of those components have to be operational for the element to be considered 'available'). However, this can get more complex if redundancy is also modeled.

Reconfigurable Spare Parts

The above approach is the traditional analysis in which it was assumed that elements use dedicated components, and hence have corresponding dedicated spares for maintenance. A spares inventory

stock level for a repository can be estimated by analyzing failure rates and operation duration, and other desired constraints (such as mean delivery times *etc.*) for a mission.

Now consider the case where it is assumed that reconfigurable components are used, and a particular component can be either reconfigured (or utilized as-is) for use on a variety of different elements in the mission (Fig. 3-5(b)). A specific instance of the component installed on one element that is not operating for a period of time during the mission, can therefore be employed on a different element that may need it (which is also referred to as *temporary scavenging* or *cannibalization*) when all the spares from the inventory have been depleted. In such a scenario, an element e, during its idle time, *i.e.* the time when it is not operating, can then be viewed as a potential 'spares repository' that can supply a maximum of q_e spares if required (where q_e is the QPA of that component in element e). In such a situation (and assuming the elements are co-located) there is not just one warehouse of spares, but also other temporal repositories that can supply limited quantities of spares at certain points over the course of the mission. It needs to be emphasized that the existence of those repositories is a function of the mission time. Furthermore, the 'spares' from these temporal repositories are not necessarily new, rather they may have operated for a period of time.

The system availability will be based on the number of potential spares that can be obtained from the initial spares repository as well as idle mission elements and will thus be affected by the operational scenario. The operating time profile of each element over the course of the mission therefore has to be first considered. Using this information, a set of time instances can then be defined:

$$T = [t_1, \cdots t_i \cdots, t_n] \tag{3.27}$$

where t_i is a time instant in which there is a change in the operating mission elements. Note that the t_i's are not necessarily equally spaced in time *i.e.* $t_i - t_{i-1} \neq t_{i-1} - t_{i-2}$ for some i. Figure 3-6 illustrates this graphically where a few elements are shown with a specific operation profile. The status of each element is *one* when it is operating, and *zero* when it is idle. The instants where there is a change in the operating elements are marked as t_1, t_2 *etc.*

Assuming that each element comes initially equipped with its full set of functioning units of the component (meaning it has its q_e units installed), the maximum number of spares that can be available from idle elements at time t_i is then

$$s_E(t_i) = \sum_{e=1}^{E} q_e[\neg\Gamma_e(t_i)] \tag{3.28}$$

where $\Gamma_e(t_i) = 1$ if element e is operating in interval starting at t_i and is zero if idle. The symbol $\neg$ is for the logical NOT operation.

Note that the element is considered to be 'operating' in this context if it carries out functions that require the component to be installed, and is idle if it is in a state that does not require its presence.

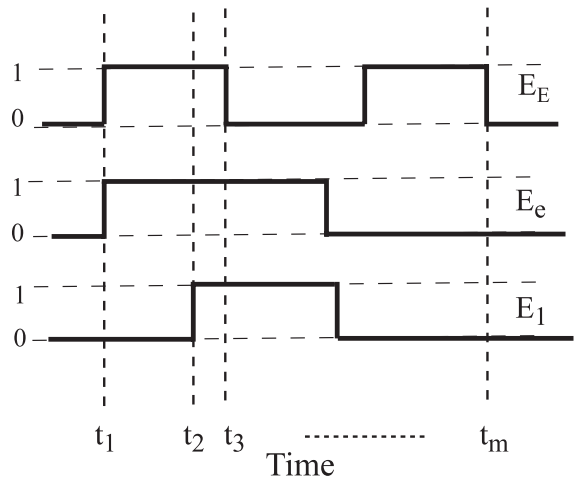

Figure 3-6: Notional operational profile Γ_e of various mission elements over time

Thus, in reality each element can potentially have different Γ for each component at any instant of time depending on its particular operational state (since all components may not be required for each state). Therefore, when several components are being considered Γ should be determined at the component level for a better assessment of the impact of reconfigurablity (or commonality). Here, since only one type of part is being analyzed, the Γ is taken at the element level.

It is assumed for simplicity that the failure rate is the same for all the reconfigurable components in the elements and is denoted as l. In more detailed analyses the failure rate is often adjusted for each particular element with various factors (so called 'K-factors'[31]), that account for environmental and other relevant aspects. However, these are also ignored for simplicity here. For each element, e, the mean number of failures is then

$$\lambda_e(t_i) = q_e l \sum_{k=1}^{i} [t_k - t_{k-1}] \Gamma_e(t_k) \tag{3.29}$$

This is the mean number of failures the element has experienced over interval $[t_o\ t_i]$ based on its particular operational time history (which gets accounted for through the use of Γ).

The above equation is applicable when the operational history of each component (or part) is equal to the operational history of the element to which it belongs. However, in the case when failed parts can be replaced by new spares in an inventory, then the computation of the mean number of failures of a part type using q_e in the calculation will be conservative. This is because if we suppose that there is a fresh spare among the q_e parts on an element (the fresh spare has not operated previously), then $q_e - 1$ parts have the same operation time as the element, while the new spare has operated for a shorter time. For an analysis in which only dedicated spares are considered along with possibility of replacement with new spares, this is a reasonable way to compute the mean number of failures for a given duration of time.

In the situation when some parts are allowed to be cannibalized from other elements (after the new spares have been depleted), then a particular part on an element may have operated for a longer period of time than the element it may temporarily be installed in. Figure 3-7 shows the three types of parts (based on how their operational history compares with that of the element on which they are installed).

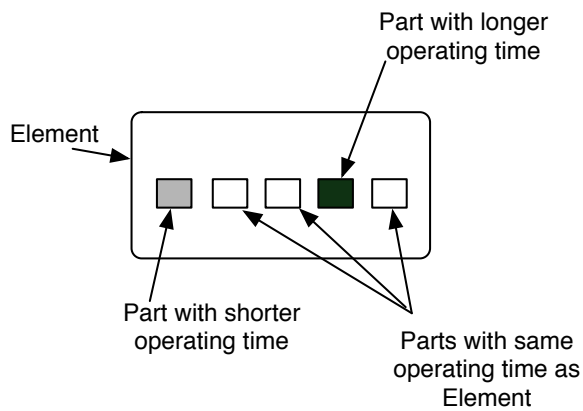

Figure 3-7: Types of parts that can exist in an element

In this case, Equation 3.29 is appropriate if the cannibalization would occur very rarely. In that situation, the possibility of having a part on an element that has operated longer than the element it is installed on will be very low, and Equation 3.29 can still be applicable with some degree of caution. However, if the cannibalization can happen frequently (perhaps due to a combination of high failure rates and fewer new spares *etc.*), then the problem can be analyzed in two ways. In the first case it can be simulated in which the operational and element installation history of each part will be known explicitly (this requires modeling of a decision rule in terms of prioritizing replacement of spares). In the second method a more conservative estimate of the mean failures is made by noting that the operation time of any part at a time instance cannot exceed the total mission time elapsed up to that time. In that case

$$\lambda_e(t_i) = q_e l \sum_{k=1}^{i} [t_k - t_{k-1}]. \tag{3.30}$$

Note that this bound can give significantly conservative results if the operation duration of an element is much less than the total mission time. However, this simplification allows an analytical assessment (instead of simulation) and establishes a conservative bound when the chances of cannibalization are great enough that the subsequent effect on part failure rate cannot be ignored.

The mean number of failed components of a particular type from all the elements in interval $[t_o\ t_i]$ is

$$\lambda(t_i) = \sum_{e=1}^{E} \lambda_e(t_i) \tag{3.31}$$

If the total number of failures (which is a random variable) up to a given time instance is n_F, then the number of total spares (which is also a random variable) is

$$s(t_i) = s_I + s_E(t_i) - n_F \tag{3.32}$$

The term s_I denotes the initial quantity of spares in an actual repository, whereas $s_E(t_i)$ as described earlier is the additional spares that can be provided by the various idle elements (which act as pseudo repositories). If $n_F > s_I + s_E(t_i)$, then $s(t_i)$ is zero.

The number of failures, n_F, can assume integer values ranging from 0 to N, where N is the total units of the component in the mission (summed over all E elements)

$$N = s_I + Q \tag{3.33}$$

$$Q = \sum_{e=1}^{E} q_e. \tag{3.34}$$

The random variable $s(t_i)$ can also take integer values that are according to Equation 3.32. For zero failures it can have a maximum value of $s_I + s_E(t_i)$, or it can have a minimum value of zero if no spares are available.

In the dedicated case each element has its own set of spares, and therefore the spares level s_j for each element j is used to determine its particular backorder level. In the augmented model with reconfigurable or common parts, since *all* the elements are supplied with replacement parts from a total of $s(t_i)$ spares, the backorder levels are computed at the mission level (across all elements). The expected back-order level at t_i, for the condition when the total spares level is s, is then

$$\bar{B}_c(s, t_i) = \sum_{n_F=s+1}^{N} [n_F - s]\, p(n_F) \tag{3.35}$$

The expected backorder level after accounting for all the possible values of s is then

$$\bar{B}(t_i) = \sum_{s=0}^{S} \bar{B}_c(s, t_i) P(s) \tag{3.36}$$

$$\bar{B}(t_i) = \sum_{s=0}^{S} \left(P(s) \sum_{n_F=s+1}^{N} (n_F - s) p(n_F) \right) \tag{3.37}$$

where S is the maximum value of the total spares level at time t_i (corresponding to zero failures). The probability $P(s)$, is equal to the probability of n_F failures occurring which result in a spares level s (as given by Equation 3.32). For instance, if the possible values of $s(t_i)$ in an interval are 0, 1, and 2, then the conditional backorder levels $\bar{B}_c(0)$, $\bar{B}_c(1)$, and $\bar{B}_c(2)$ which correspond to each possible value of s are computed. The values are then multiplied with $P(0)$, $P(1)$, and $P(2)$ and

summed to get the overall backorder level $\bar{B}(t_i)$

The probability of a total of n_F failures taking place up to a time t_i in the mission across all the elements is computed by considering all the possible ways in which that number of failures can occur. For instance, if there are two mission elements and n_F is 2. There are three possible ways in which a total of two failures can occur. In the first case there can be two failures in the first element, and none in the second, or in a second case there can be no failures in the first element and while two in the second, or in the third case there can be one failure each in the two elements. In all these scenarios the total number of failures is the same, however each individual element has different number of failures. The number of failures that an element e experiences in a particular scenario w will be denoted as n_e^w. The probability of any individual scenario, w, occurring is the product of the probabilities of the specific failures occurring in each element in that particular scenario (assuming the failures are independent).

$$P_w = \prod_{e=1}^{E} p(n_e^w) \tag{3.38}$$

For instance in the example described above, the probability of the first scenario taking place is the product of the probability of having two failures in the first element and probability of having no failures in the second element. The probability of having n_e^w failures in element e is the poisson probability

$$p(n_e^w) = \frac{e^{-\lambda_e} \lambda^{n_e^w}}{n_e^w!} \tag{3.39}$$

The argument t_i has been omitted from λ_e for simplicity here. The probability of having n_F failures occur across all the mission elements is then the sum of probabilities of all the various ways in which it can happen. Therefore

$$p(n_F) = \sum_{w=1}^{W} P_w \tag{3.40}$$

where W is the number of all the combinations in which a total of n_F failures can occur from among E elements with a total of Q components.

Using Equation 3.37, the overall availability at t_i is then simply

$$A_{sys}(t_i) = \left(1 - \frac{\bar{B}(t_i)}{Q}\right)^Q \tag{3.41}$$

It can be observed that now the 'end-of-mission' availability is not directly relevant (which is usually the case in traditional studies). A is no longer a monotonically decreasing function of time due to the explicit consideration of making use of components from other elements. The end-of-mission availability may be higher due to more spares being potentially available if fewer elements are operating, while the availability at some intermediate mission time maybe lower when more elements are operating at the same time. The availability for each interval can be computed using the above

equation. Since the worst case scenario is often of interest, the mission level availability for this reconfigurable spare parts case can then be taken as the minimum system availability that occurs at any time during the mission duration.

$$A_{sys} = \min\left[A_{sys}(t_i)\right] \quad t_i \in T \tag{3.42}$$

3.3.2 Monte-Carlo Simulation

The validity of this model for reconfigurable or common spares can be tested through a discrete-event simulation. Furthermore, as discussed previously, a simulator can serve to assess the conservativeness of the assumptions regarding part operation times for Equation 3.30.

In the simulation, the failure of parts installed on a set of given mission elements (Fig. 3-4) is simulated as a Poisson process (with the details as discussed in the previous section). Each part is allowed to be in one of three different states. It can either be operating (if it is on an operating element), it can be idle (if it is either installed on an idle element, or is in the spares repository), or it can be in a failed state. Once the part has failed, it cannot be repaired.

If a part fails, it is replaced immediately with a spare part from the repository if one is available. These spares are new and therefore have not operated for any duration of time until they are installed on an element. Their probability of failure at any day will therefore be different (and lower) than the failure probability of other parts that have been working in the element for longer periods of time. Note, that as failures occur during the mission, the 'fresh' spares from the repository are first used. If there are more failures and the spares repository is empty, only then parts from idle elements are taken away to be installed on operating elements that need them. The cannibalization of idle elements is thus done as a last resort when all the new spares have been used up. In the simulation the cannibalization is done randomly from the first idle part that is found. In a more realistic case, priorities can be assigned to elements so that relatively less critical elements can be more readily cannibalized than the more critical ones (because cannibalization can lead to new problems and potential failures of other parts in the element).

If at any time instance, there are more spares required than are available, then the spares are allocated to the elements in an optimal way such that the mission level availability is maximized. Another algorithm for assigning the spares can be based on the priority level of the mission elements. The elements with higher priority (*e.g.* those that are critical for crew survivability *etc.*) can be assigned spares before low priority elements are given the left over parts.

For each simulation, a uniformly distributed random number is generated which is then used to determine if a part fails or not at each time step (*e.g.* each day of a mission). A part is allowed to fail if its probability of failure is greater than the random number, otherwise it is allowed to continue operation and its operational time is incremented by one time step.

If there is a failure, the part is replaced with either new or used spares according to the procedure described above. If there are no parts that can be installed in place of the failed one, the element on which the part failed is considered to be 'un-available' or down.

Even if a failure does not occur in a particular time step, but an element is down (when it should be operational), the availability of spares is checked and appropriate assignments are made if possible. Since the spare parts are a function of time due to the operational scenario of the elements, an element maybe down due to lack of spare parts for some duration of the mission, but it may be able to function again later on if some other element becomes idle and its parts become available for temporary cannibalization.

Each simulation run of a specific mission (over a certain mission time-line) plays out one particular outcome that can unfold. Hundreds of such simulations therefore need to be carried out so that a statistical analysis can be done to assess how the availability of the elements compares with the analytical predictions. Section 3.3.4 will discuss the results of a case study, in which the model predictions and simulated results will be compared for a sample exploration mission.

3.3.3 Sensitivity Analysis

It can be seen that the system availability (Eq. 3.42) is a function of failure rate l, QPA, operational scenario Γ, and spares level, s_I. For a given value of s_I (which are the number of spares brought initially at start of mission), it can be useful to assess how the availability varies with the other parameters.

Availability and Quantity

For finite values of q, Equation 3.25 can be used for determining how A changes with q. However, using the general relation (for a variable x)

$$\lim_{n\to\infty}\left(1+\frac{x}{n}\right)^n = e^x, \tag{3.43}$$

it can be seen that if q becomes large (*i.e.* many units of the same component are used) then the availability is simply an exponential function of the backorder level.

$$\lim_{q\to\infty} A = \lim_{q\to\infty}\left(1+\frac{-\bar{B}}{q}\right)^q \tag{3.44}$$

$$= e^{-\bar{B}} \tag{3.45}$$

Thus, availability can decrease extremely rapidly if the backorder level makes even a modest climb.

Availability and Failure Rate

Dedicated Case

For the case of dedicated components, the availability of an element is given by Equation 3.25 which is reproduced below.

$$A = \left(1 - \frac{\bar{B}}{q}\right)^q$$

The subscripts i and e have been dropped since we are considering only one element and one component in that element. The derivative of A with respect to the failure rate l can be expressed as

$$\frac{dA}{dl} = q\left(1 - \frac{\bar{B}}{q}\right)^{q-1}\left(-\frac{1}{q}\frac{d\bar{B}}{dl}\right) \tag{3.46}$$

$$= q\frac{A}{\frac{q-\bar{B}}{q}}\left(-\frac{1}{q}\frac{d\bar{B}}{dl}\right) \tag{3.47}$$

$$= \frac{Aq}{(\bar{B}-q)}\frac{d\bar{B}}{dl} \tag{3.48}$$

$$= \frac{Aq}{(\bar{B}-q)}\left[\frac{d}{dl}\left(\sum_{n>s}(n-s)p(n)\right)\right] \tag{3.49}$$

$$\tag{3.50}$$

Since l is the variable of interest, a constant α in this context can be defined

$$\alpha = q\Delta t \tag{3.51}$$

where Δt is the total duration of time for which the element operated. The number in the pipeline is then

$$\lambda = \alpha l \tag{3.52}$$

Equation 3.49 can then be written as

$$\frac{dA}{dl} = \frac{Aq}{(\bar{B}-q)}\left[\sum_{n>s}\frac{(n-s)}{n!}\frac{d}{dl}\{e^{-\alpha l}(\alpha l)^n\}\right] \tag{3.53}$$

$$\frac{dA}{dl} = \frac{Aq}{(\bar{B}-q)}\left[\sum_{n>s}(n-s)p(n)\left(\frac{n}{l}-\alpha\right)\right] \tag{3.54}$$

As expected, the rate of change of A with respect to l is negative since $\bar{B}$ cannot be greater than q. Thus the availability decreases with increasing failure rate.

Reconfigurable Case

In the reconfigurable case, a similar procedure for determining the derivative from the availability equation can be followed. In this case it should be recalled that the number of failures and spares available was computed for all the elements combined at the mission level. Therefore in order to be able to compare the dA/dl at the element level between the two cases, it is assumed for the reconfigurable case that the variable s denotes the spares level that a particular element can use. Since the objective of this analysis is to simply compare the sensitivity expressions of availability with failure rate, this assumption is reasonable in this context. If subscript r is used for the reconfigurable case, then the following expression can be written for the availability of a particular element at time t_i:

$$\frac{dA_r}{dl} = \frac{A_r q}{\bar{B}_r - q} \frac{d\bar{B}_r}{dl} \tag{3.55}$$

Using Equation 3.37, the above expression can be written as

$$\frac{dA_r}{dl} = \frac{A_r q}{\bar{B}_r - q} \left[\sum_{s=0}^{S} \left(P(s) \sum_{n>s} (n-s) \frac{d}{dl} p(n) + \bar{B}_c(s) \frac{d}{dl} P(s) \right) \right] \tag{3.56}$$

Using the development of Equation 3.53 for the derivative of $p(n)$, the above equation becomes:

$$\frac{dA_r}{dl} = \frac{A_r q}{\bar{B}_r - q} \left[\sum_{s=0}^{S} \left(P(s) \sum_{n>s} (n-s) p(n) \left(\frac{n}{l} - \alpha \right)) + \bar{B}_c(s) \frac{d}{dl} P(s) \right) \right] \tag{3.57}$$

From the above equation and Equation 3.54 it is sufficient to see that the rate of change of A with respect to l is different for the dedicated and reconfigurable cases. There is an additional term in Equation 3.57, due to the formulation of the $\bar{B}_c$, which makes the change rates different for the two cases. This difference in the sensitivities of A to l (as evident from Equations 3.54 and 3.57) can become important in studying the tradeoffs between reconfigurable components and dedicated components versus different reliabilities. Section 3.3.4 provides an example of such a case.

Availability and Operation Time

The model developed for the reconfigurable case makes the backorder levels and thus availability dependent on the number of idle elements at a given instance of time. The operational scenario can greatly affect mission level availability. In order to assess the impact of operational times a quantity, γ, can be defined such that it is the fraction of operating elements out of the total mission elements at a particular time. Thus

$$\gamma_i = \frac{1}{E} \sum_{e=1}^{E} \Gamma_e(t_i) \tag{3.58}$$

With this definition γ varies between 0 (when no element is operating) and 1 (when all elements are operating simultaneously). If a simplifying assumption is made that all elements in the mission have the same QPA of the component, *i.e.* $q_e = q \, \forall \, e$, then the maximum number of spares that can

be obtained from the elements s_E at time t_i (shown in Equation 3.28) is

$$s_E(t_i) = q \sum_{e=1}^{E} \neg\Gamma_e(t_i) \tag{3.59}$$

The summation term is simply the number of idle elements at t_i, so

$$s_E(t_i) = qE(1 - \gamma_i) \tag{3.60}$$

From Equation 3.32, it follows that the spares $s(t_i)$ available at instant t_i is now also a function of γ and is

$$s(t_i, \gamma_i) = s_I + qE(1 - \gamma_i) - n_F \tag{3.61}$$

The first term is the initial inventory or fresh spares, the second term represents the pseudo-inventory of spares from idle elements, and the third term in the sum is the total cumulative number of failed parts across all elements up to time t_i in the mission. The derivative of the availability A_r of an element with respect to γ at time t_i can now be expressed (in a similar fashion as Equation 3.55 and with the same assumptions) as

$$\frac{dA_r}{d\gamma} = \frac{A_r q}{\bar{B}_r - q} \frac{d}{d\gamma} \bar{B}_r \tag{3.62}$$

The above equation can be expanded further as

$$\frac{dA_r}{d\gamma} = \frac{A_r q}{\bar{B}_r - q} \left[\sum_{s=0}^{S} P(s) \frac{d}{d\gamma} \bar{B}_c(s) + \bar{B}_c(s) \frac{d}{d\gamma} P(s) \right] \tag{3.63}$$

Now, in the dedicated case the availability is not dependent on which other elements are operating at a given instant of time. Therefore there is no dependence on γ and

$$\frac{dA}{d\gamma} = 0. \tag{3.64}$$

In order to show that the variation of the availability with γ is different for the dedicated and reconfigurable/common case, it is sufficient to see that Equations 3.63 and 3.64 are not the same.

3.3.4 Example: Mars Exploration Mission

A case study of a planetary exploration mission can be developed for assessing the spare parts requirements for reconfigurable and also dedicated components. Furthermore, in order to test the validity of the model, Monte-Carlo simulations are carried out using a discrete-event simulation of the mission.

A surface exploration mission of Mars is considered in which the mission elements are an Ascent/Descent Vehicle (ADV), a surface habitat (HAB), an un-pressurized all-terrain vehicle (ATV) and a pressurized rover (PR). It is assumed that there is no re-supply or repair and all the spares that may be required during the course of the mission have to be brought in along with other cargo. In the Hubble Space Telescope, in addition to several rate sensors (gyros), a few of its electronic control units (ECU) also failed.[108, 76] Thus, as a realistic example an ECU is taken to be the component under consideration here. This ECU is assumed to be reconfigurable such that it can be employed for use in any of the mission elements described above. The QPA of this ECU for the ADV, ATV, HAB and PR are 1, 1, 3, and 2 respectively. The Mean Time To Failure (MTTF) of this ECU is assumed to be 100,000 hours of operation (which is a realistic number). The failure rate, l is then simply the reciprocal of this MTTF. Since this is a Mars mission, a surface stay of 600 days [66] is assumed (therefore the mission time starts at day 1 on the surface and ends at day 600 when the crew departs).

A specific operational scenario is assumed, and the operation time profiles for the elements are shown in Figure 3-8. At each time instant, a value of 1 indicates that the element is operating, while a value of zero is shown when the element is idle. Based on these operation profiles, the instance of time in which a change in the operating elements occur are determined.

It can be observed that the the time instances in Figure 3-8 vary widely in duration, with some intervals being very small (a few days), while others are very large (hundreds of days).

As discussed earlier, in the reconfigurable case the system availability may not necessarily be the lowest at the end of mission since the number of available spares are derived from idle components in addition to a spares repository (Equation 3.32). This can be seen in this case also where Figure 3-9 shows that the availability is lowest in the 5th interval. This interval happens to be the longest and also has the most elements concurrently operating, thus making its s_e the lowest (as shown in Figure 3-10). Since the potential number of spares are the lowest in this interval, the availability is also the lowest. The availability could have been relatively higher, however, if this occurred earlier in the mission since the chances of part failure would have been lower. As discussed in Equation 3.42, this minimum value of availability over the mission duration is considered for comparison with dedicated cases (in which only the end-of-mission availability is evaluated).

In addition to applying the analytical model for this particular case study, a discrete-event simulator was also used to compare the results for the reconfigurable case. Figure 3-11 shows the outcome of 5000 simulations for an inventory spares level, s_I of 0 for the reconfigurable case. It can be seen that in some cases, all four elements were not 'available', despite their ability to use scavenged parts. Overall, the availability was found to be 78.08% for this particular spares level.

The system availability as a function of inventory spares level, s_I, was then determined using the analytical model (with Equations 3.26 and 3.42) and the simulator. The system availability for the

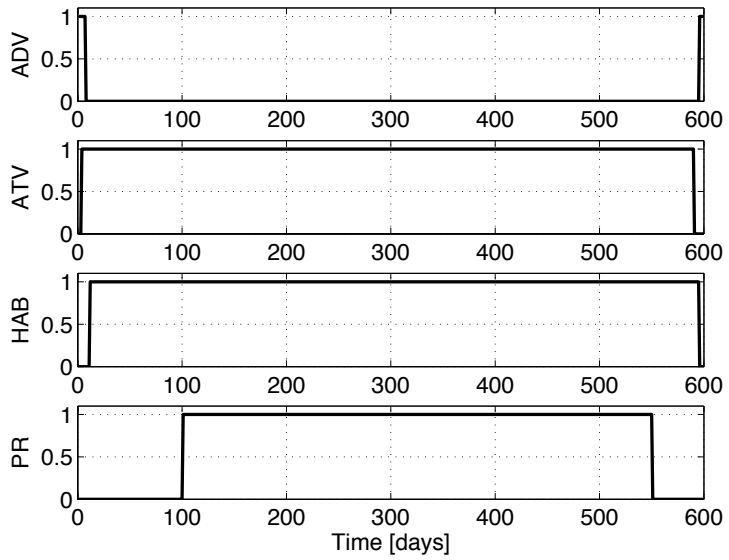

(a) Operation time profile

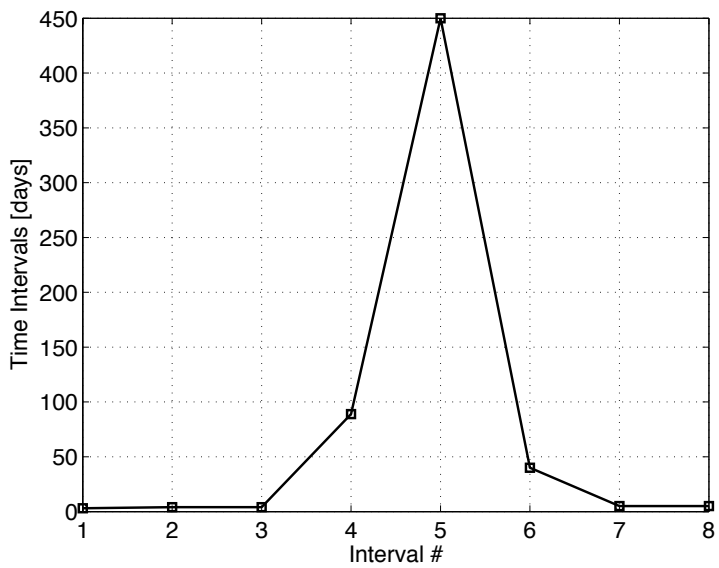

(b) Time Intervals $(t_i - t_{i-1})$

Figure 3-8: Operation time profiles of the mission elements.

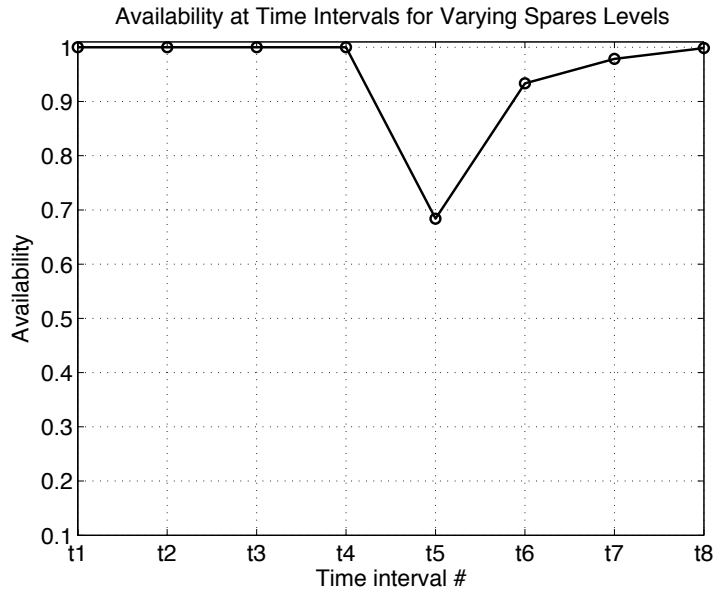

Figure 3-9: Availability in various time intervals for reconfigurable case (computed analytically)

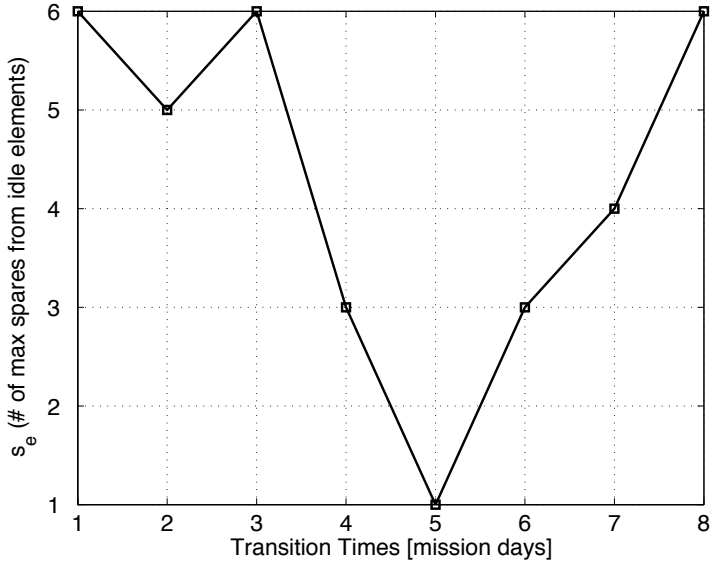

Figure 3-10: Max spares from idle elements in various time intervals

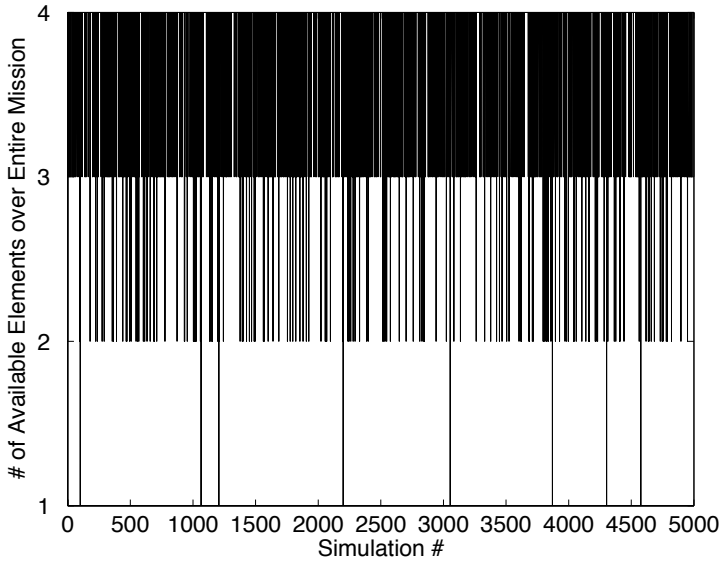

Figure 3-11: Simulated results of system availability (5000 runs, s_I=0)

reconfigurable case was computed in two ways using both the conservative assumption (Equation 3.30), and relatively non-conservative assumption (Equation 3.29), respectively.

In the dedicated case, the assumption was that each element had its own particular ECU which cannot be used in the other elements. Furthermore, for each given spare level, the optimal spares combination (for each element) that maximized the system availability was used. The optimal combination was computed by simply doing a full-factorial analysis (since the number of elements and the spares level was small). All the possible combinations for a total spares level (s_I) to be distributed among the E elements were determined and the corresponding level of availability was computed. The combination that produced the highest overall availability at the mission level was chosen for each particular value of s_I. So for instance, if a total of 3 spares were part of the repository ($s_I = 3$), the optimal combination of having spares for the ADV, ATV, HAB and PR was determined such that the system availability was highest for the total spare level of 3. In this case it worked out to be one spare each for the ATV, HAB and PR, while none for the ADV. Details of the optimal combinations of the dedicated spares are given in Table 3.2.

Table 3.2: Optimal spares allocation for the dedicated case and operational scenario shown in Figure 3-8

Total Spares (s_I)	ADV	ATV	HAB	PR
1	0	0	1	0
2	0	0	1	1
3	0	1	1	1
4	0	1	2	1

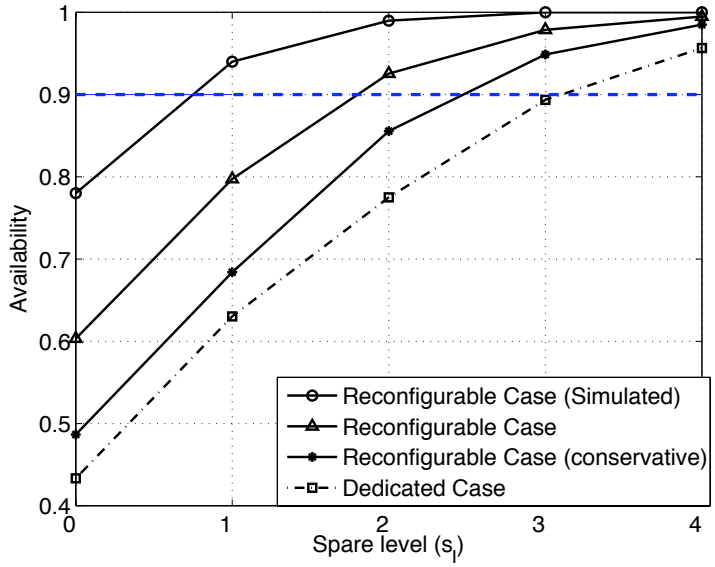

Figure 3-12: Availability vs inventory spares levels for reconfigurable/common and dedicated spares

Figure 3-12 shows how the reconfigurable and dedicated cases compare in terms of system availability as a function of initial spares level. A total of four lines, each corresponding to a particular case, are shown. The first line from the top is the simulated result obtained for each spares level for the reconfigurable case. The second line from the top shows the analytical result from the model using the non-conservative approach for computing λ_e (Equation 3.29). As expected, it gives a lower prediction for the availability as compared to the simulated case. However, the third line which is the analytical prediction using the conservative value for λ (Equation 3.30), is the most stringent in the availability prediction. The fourth line is for the dedicated case and is always lower in availability as compared to the reconfigurable scenario. It should be noted that for the zero spares level case, the reconfigurable scenario can offer significant benefits in terms of increased system availability. It can be expected that spares will not be carried along for all subsystems/components due to overall cargo mass and volume capacity constraints. The advantage from the reconfigurable case for the zero spares level therefore indicates the benefit that can be achieved for the type of parts for which there will be no spares.

In the case of the Hubble Space Telescope, the mass of its ECUs was 8 kg. If several components in several mission elements are reconfigurable or common, the total mass savings can become significant, or for a given spares mass the system availability can be increased. Plots such as the one shown in Figure 3-12 can thus be used to quantify the impact of reconfigurability or commonality on the sparing requirements (and subsequently mass and volume). For instance, in this particular example if a 90% availability target is to be achieved (dashed line), only one reconfigurable or common spare (as shown for the simulated result), or two spares (as shown for the non-conservative result) are

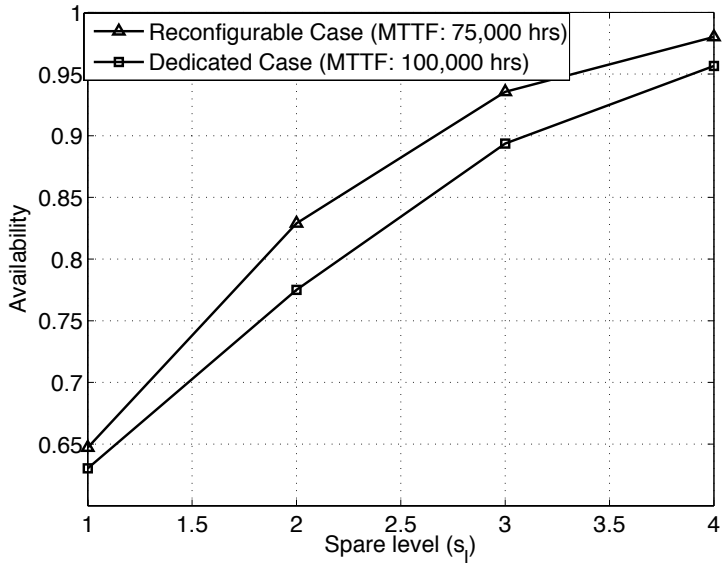

Figure 3-13: Availability for reconfigurable versus dedicated spares with different MTTF

needed versus three spares for the dedicated case. There can thus be a saving of at least 33% or even 50% in the number of required spares for a given system availability target.

The advantage in mass and volume can also potentially be traded with component reliability. Extremely stringent reliability requirements are often a significant cost driver in both manned and un-manned missions. Figure 3-13 shows how the availability compares for different spares levels between the two cases in which the dedicated case has ECUs with MTTF of 100,000 hours, while the reconfigurable ECUs have MTTF of 75,000 hours. For one spare, the two cases are almost identical, and for more spares the reconfigurable case offers an advantage. The reconfigurable case can allow for lower reliability and therefore potentially lower cost.

The availability of the system as a function of failure rates is also examined using the assumptions of this case study. It was analytically shown in Section 3.3.3 that the availability for the reconfigurable and dedicated case changes at different rates with changing failure rate l. Figure 3-14 shows how the availability decreases with increasing failure rate (with s_I set to 1), and graphically shows the trade-off that exists between the two cases.

Trade studies can therefore be conducted to find the cross-over failure rates that make one case favorable over the other. It is interesting to note that reconfigurable/common parts can actually perform worse because of risk pooling when failure rates are large. In that case, a low reliability common part introduces a vulnerability that now affects all elements in the mission, whereas in the dedicated case elements are somewhat protected from such systemic problems by virtue of their separate spare pools. However, if reliability is reasonably good (in this example if $l < 0.0006$) the reconfigurable case will always be better.

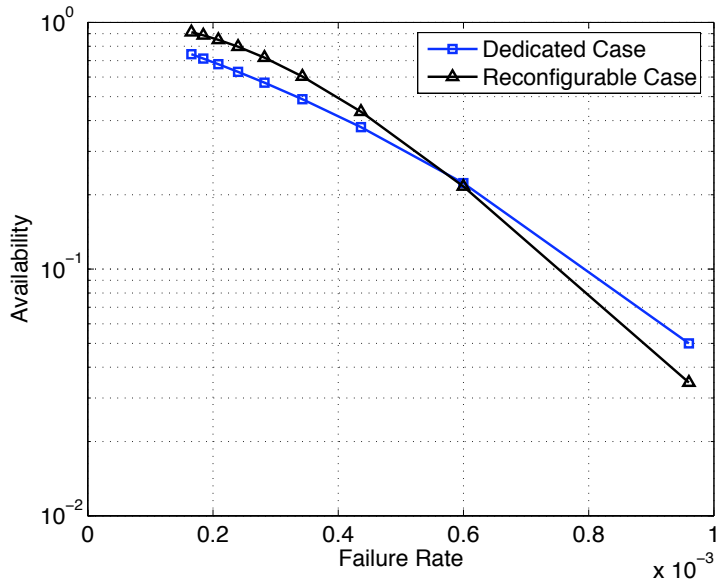

Figure 3-14: Availability vs failure rates for reconfigurable and dedicated spares, spares level $s_I = 1$

The variation of the Availability with γ can also be explored by varying the operational scenarios. The scenario shown in Figure 3-8 was not used in this computation. Four different scenarios were considered instead, with one, two, three, and all four elements operating at a given time, corresponding to a γ of 0.25, 0.50, 0.75, and 1, respectively. The inventory spares level, s_I was set to 2. Figure 3-15 shows how the availability decreases with increasing γ.

It is seen that the availability changes very rapidly for the reconfigurable case with increasing γ since there are fewer spares that can be counted in the total spares pool (due to few idle elements). In the four scenarios constructed for the different γ's, the total operational time of the individual elements is gradually increased. In the dedicated case, as γ increases, there is thus a more gradual decrease in the availability. If the total operational time remains the same between the various γ's, then there will be no change in availability (as shown through Equation 3.64) for the dedicated case.

It can also be noted that the reconfigurable case has appreciably higher availability even for scavenging in the case of $\gamma = 1$. This is because although there are no elements that can lend any extra spares (since all elements are operating at all times), the fact that the spares are reconfigurable or common means that any failure in any element can be fixed if there is any spare available in the repository. Whereas in the dedicated case, a failure in a particular element can only be fixed if a spare for that particular element is available. Thus, even if there are no elements that can be temporarily cannibalized, reconfigurable (or common) components can offer advantages in terms of required spares for a desired level of system availability.

In summary, it can be seen from the simple example analyzed here that the capability to cannibalize parts from idle elements when no other spares are available can be very valuable since it allows

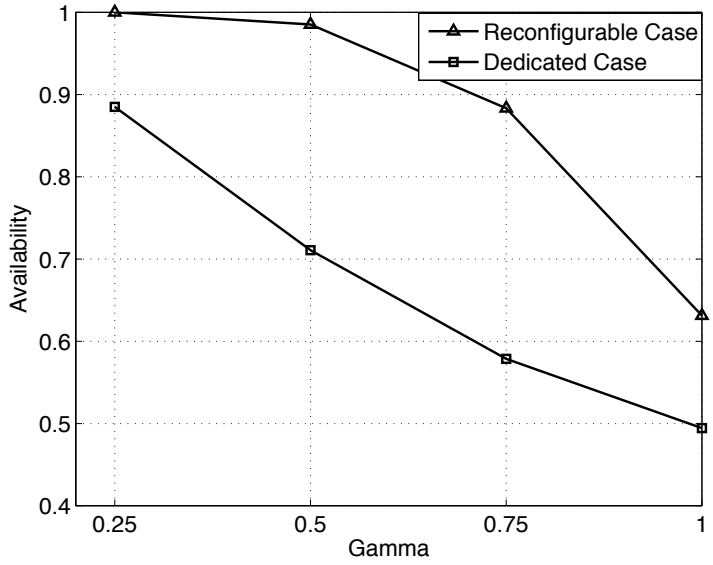

Figure 3-15: Availability vs Gamma for Reconfigurable Case

for the reduction in the total spares requirements. In order to have this capability, commonality and interchangeability throughout system designs and across mission elements will be needed.

The tradeoff in having such a capability however, might be that the increased complexity required for each reconfigurable component could result in increased costs and reduced reliability. This model can thus be used in studying tradeoffs between the architectural qualities (of reconfigurability/commonality *etc.*) with component reliability and element operational scenarios.

Another point to note is that the reconfigurability/commonality is treated here at a low level of the system (namely specific parts). At a higher level, in which perhaps larger sub-systems between the elements are reconfigurable, a few other factors will have to be considered. For instance, the 'scavenging' aspects may get somewhat limited (with increasingly large sub-systems). Also, even though in this case it was assumed that all QPA number of parts are required for the element to be considered 'available' it can generally be relaxed at the part level (in which the system can still perform although at a degraded level). For larger and larger sub-systems however it will be harder to make such an assumption, which in turn will impact the availability computations. Also, the impact on crew time was not factored in. In future enhancements to this model an explicit consideration for this will be made.

Chapter 4

Case Study-I: Planetary Surface Vehicles

In a space exploration enterprise that is geared towards human exploration of Moon and Mars, a fundamental and arguably perhaps the most important component will be the surface exploration system. This is because one of the principal benefits from an exploration program is knowledge or information. In the case of planetary exploration, this knowledge will primarily be produced as a result of traversing a large and varied area of interest. Consequently planetary surface vehicles will play a crucial role, since they will directly enable the crew to extend their radius of exploration and thus achieve many exploration goals and objectives. Figure 4-1 shows the maximum distance of the astronauts from the Lunar Module in the Apollo missions and the samples that were collected for return [16]. It is is striking but not surprising to note that Apollo 11, 12 and 14 are clustered together, and there is a sudden jump in the distance traversed and the samples collected in Apollo 15, 16 and 17. In the last three missions the Apollo Lunar Roving Vehicle (LRV) was used, and it can be clearly seen that a surface vehicle greatly enhanced the value of the missions (by enabling exploration of a larger area and allowing more samples to be collected, and returned). It can be expected that future missions to Moon and Mars will also employ surface vehicles as one of the key elements for exploration.

Planetary Surface Vehicles (PSV) have many requirements that make them particularly relevant for reconfigurability:

- A fair amount of mass (hundreds to thousands of kilograms) and volume (few cubic meters) is involved in these systems. It is therefore desirable to analyze how they can provide multiple capabilities. If a single vehicle along with some set of components can deliver new or modified functionality, the mass and volume efficiency might be greatly improved which can directly impact mission costs.

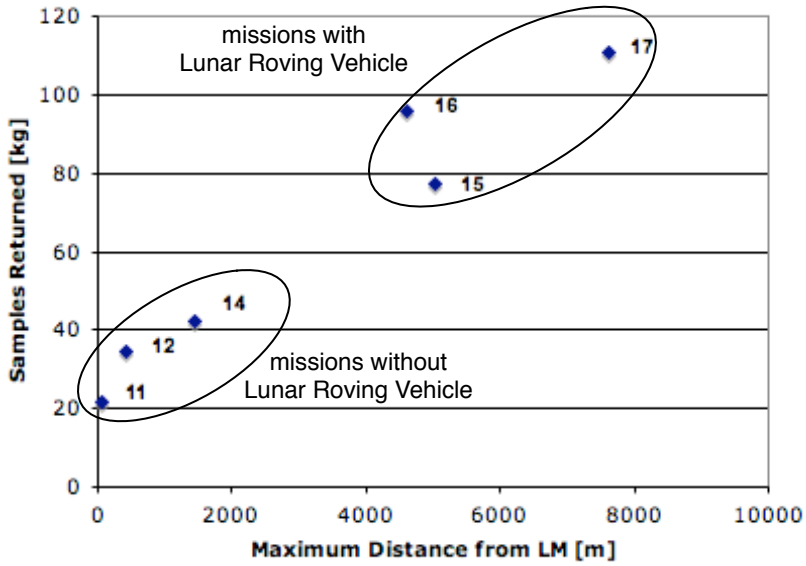

Figure 4-1: Mass of samples returned to Earth and max distance from Lunar Module in various Apollo missions [16]

- The evolution of these vehicles on the planetary surface over the course of multiple missions can also be of interest. A long term base or outpost may necessitate modifications and changes to the vehicles already deployed on the surface to adapt efficiently to new needs and requirements.

- Large uncertainties on the terrain in which the vehicles will operate make it highly desirable for these systems to be robust and maintain basic functionality to some minimum level. Furthermore, since they will serve many vital needs for the mission, graceful degradation will be very important.

4.1 PSV Modeling Framework

A tool was developed in MATLAB to model various kinds of open and pressurized vehicles. The model is based on physics of off-road vehicle motion and terrain interaction [144], and uses parametric models of component masses (such as wheels, motors *etc.*) to get mass estimates. Figure 4-2 shows the N^2 diagram of the various modules that are in the model. The diagram only shows the interconnections between the modules, but not the specific variables that are exchanged for simplicity and readability. Each major sub-system has been implemented as a separate module, and consequently there are a few feedback loops due to the dependance of the various sub-systems on each other. A detailed description of each module is provided in Appendix A with key equations, assumptions and references. There are several input parameters and outputs of the model, and few

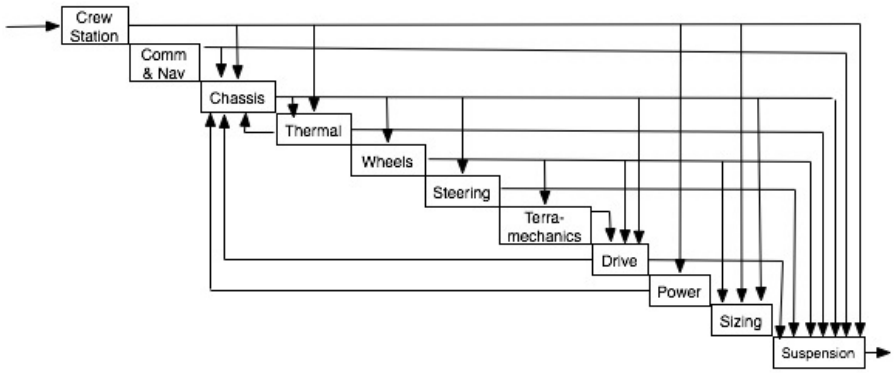

Figure 4-2: N^2 diagram of PSV model implemented in MATLAB

Table 4.1: Main inputs and Outputs of Model

Inputs	Outputs
# Crew	Mass [kg]
Cargo [kg]	Power [kW]
# Wheels	Energy [kW-hr]
Power Source	Wheelbase [m]
Drive Type	Track [m]
Average Speed [km/hr]	Wheel Diameter [m]
Range [km]	Motor Torque [N-m]
Tow Capacity [kg]	Motor Power [W]

primary input and output variables are shown in Table 4.1. Figure 4-3 shows some types of PSVs that the tool can model.

4.1.1 Benchmarking of PSV Model

In order to verify the model estimates, the Lunar Roving Vehicle (LRV) that was used in Apollo 15-17 [119], and Northrop's concept vehicle, the Lunar Surface Vehicle (LSV) [103] were used for benchmarking.

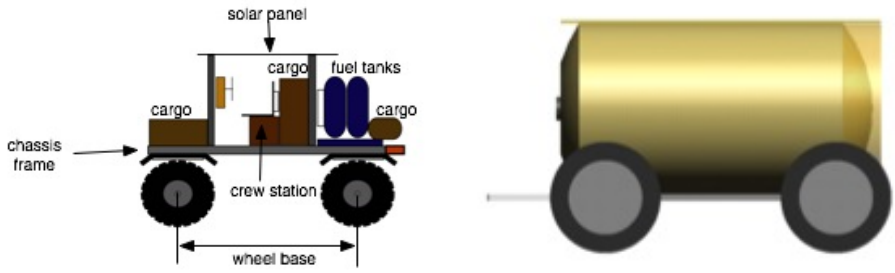

(a) Generic Open PSV

(b) Pressurized Vehicle

Figure 4-3: Types of vehicles that can be analyzed with the PSV modeling framework

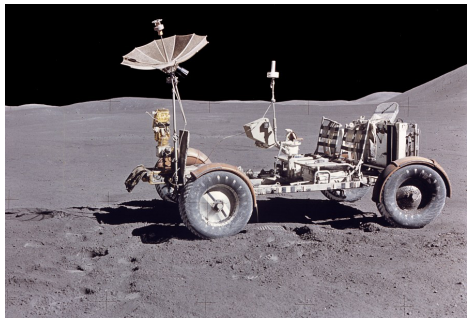

(a) LRV on Lunar Surface[2]

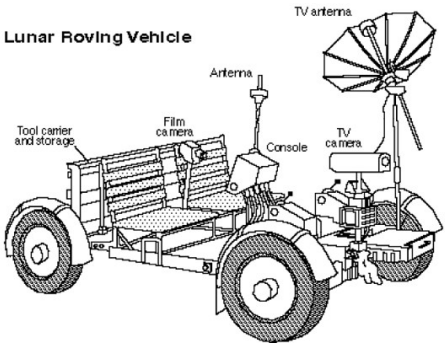

(b) LRV Schematic

Figure 4-4: Lunar Roving Vehicle used in Apollo 15-17

Table 4.2: Input Parameters for LRV Benchmark

Vehicle Type	open
Passengers	2
Total Payload [kg]	490
Range [km]	40
Operating Duration [hrs]	12
Power Source	batteries
Power Source Type	Ag-Zn
Motor Type	DC brush
Drive Type	independent
No. of Wheels	4
Obstacle Height [m]	0.3

The LRV was an open vehicle, very much like a dune-buggy that allowed the astronauts on the Moon to easily carry equipment and samples, and explore a larger area around their landing sites. It seated two crew members, had independently driven wheels, and dual steering. It was powered by Ag-Zn batteries and could carry a total payload (including the weight of the passengers) of about 490 kg. Figures 4-4(a) and 4-4(b) show a picture of the LRV on the lunar surface, and a labeled schematic. The parameters used for benchmarking the model against the LRV are given in Table 4.2. Table 4.3 shows the output data for the LRV comparison. It can be seen that the difference between the actual data and the model estimates for the total mass and power is within 10%. The dimensions are a bit different since the tool uses an empirical model based on dimensions of sports cars and dune buggies to estimate the wheelbase and track based on the number of passengers. There is a difference in the mass of wheels as well since the LRV had wire-mesh wheels while the model uses an empirical estimate based on mass of wheels used for race cars (made of light alloys such as aluminum). The turning radius is computed in the model for single Ackermann steering, while the LRV had dual-Ackermann steering (which is why it had a much smaller turning radius). So there are differences at the sub-system level, but in terms of gross mass and power estimates the model is fairly reasonable.

Table 4.3: Comparison of Actual and Estimated Data for Apollo LRV

	Actual	Estimate	% Difference
Wheel Diameter [m]	0.82	0.7	14.6
Wheel Width [m]	0.23	0.18	21.7
Wheel Mass [kg]	5.4	13.2	144
Wheelbase [m]	2.29	2.64	15.3
Track [m]	1.83	1.7	7
Length [m]	3.1	3.34	7.74
Width [m]	2.06	1.8	12.6
Height [m]	1.14	1.7	49
Battery Capacity [W-hr]	8280	7400	10.6
Drive Motor Power [W]	191.5	193	0.8
Gradeability [deg]	23	15	34.7
Turning Radius [m]	3.1	4.73	52.5
Total Mass [kg]	210	226	7.6

Table 4.4: Input Parameters for LSV Benchmark

Vehicle Type	pressurized
Passengers	2
Payload [kg]	364
Range [km]	240
Speed [km/hr]	5
Operating Duration [days]	14
No. of EVAs	14
Power Source	fuel-cells
Motor Type	AC
Drive Type	central
No. of Wheels	8
Max Obstacle Height [m]	0.5

The parameters used for benchmarking the model against the LSV are given in Table 4.4. The number of EVAs is an input since it is used to determine the additional consumables and energy requirements that are levied. Table 4.5 shows the data for the LSV comparison. In this case also there is overall good agreement between the gross mass estimate. The power estimate is almost half because in the LSV a redundancy was assumed for the power system, while in the model no redundancy was assumed. The crew habitable volume also compares very well (although the dimensions are different).

4.2 Reconfigurable System Design for Multi-Ability

This section develops a method for determining a good design for the class of systems in which multi-ability is required, and the different functions or modified functions/capabilities are known in advance. In this case the system needs to reconfigure between a small set of discrete configurations (or states). A more general design for reconfigurability process is formulated later on in Chapter 7.

Table 4.5: Comparison of Actual and Estimated Data for Northrop LSV

	Actual	Estimate	% Difference
Wheelbase [m]	3.15	5.12	62.5
Track [m]	3.3	2.4	27
Height [m]	2.7	2.9	7.4
Length [m]	4.35	6.42	47
Crew Volume [m^3]	11.48	13.57	18.2
Hab Width [m]	2.25	2.28	1.3
Power [kW]	5.13	2.92	43
Total Unloaded Mass [kg]	3182	2902	8.7

Consider a system defined by a design vector, $\mathbf{x}$. Let the ith configuration (state), in which the system can exist, be denoted as $\mathbf{x}_i$. Each configuration will be defined by specific values of a set of n design variables, and can thus be expressed as

$$\mathbf{x}_i^T = [x_{1i}, \cdots, x_{ji}, \cdots, x_{ni}] \tag{4.1}$$

If a total of m configurations are possible, then a larger vector $\mathbf{X}$ can be defined which is essentially a super set of all the configurations and will be expressed as:

$$\mathbf{X}^T = \left[\mathbf{x}_1^T, \cdots, \mathbf{x}_i^T, \cdots, \mathbf{x}_m^T\right] \tag{4.2}$$

where $\mathbf{X} \in \Re^{nm \times 1}$.

An optimization problem can now be formulated in which the goal is to find $\mathbf{X}$ such that some desired criterion, $\mathbf{J}$ is maximized subject to constraints $\mathbf{g(X)}$.

It should be noted that this method essentially expands the design space to include all the required configurations for the complete design, not just a single design for a particular state. If the number of configurations/states, m, is large, or the number of design variables, n, in each state is large, then nm will be large, and the problem can quickly become computationally prohibitive. However for many systems where the configurations can be expected to be only a few, and at the conceptual design stage (the number of design variables will be small), this method can be fruitfully employed.

A useful criterion for the design objective can be to minimize reconfiguration cost over the system life cycle and minimize the cost due to non-optimality (that may potentially result due to the system being reconfigurable). In this case only the cost minimization is factored in for simplicity. If z_{jk} is the cost of reconfiguration between states j and k, and m_{jk} is the total number of reconfigurations (state transitions such as those discussed earlier in Markov models) between states j and k over the

system's life, then

$$\min \mathbf{J} = \sum_{j=1}^{p} \sum_{k=1}^{p} m_{jk} z_{jk} \tag{4.3}$$

$$s.t \quad g_i(X_i) \leq 0 \tag{4.4}$$

In many situations m_{jk} may not be known (because the usage scenario, for instance as defined through $\Gamma's$ in Section 3.3.1, may not be known exactly), and the designer may only have a probabilistic estimate at best. In that case the expected reconfiguration cost, $\bar{z}_{jk}$ can be used to obtain results.

4.3 Mars Exploration Mission

For long-term missions to Moon and Mars a number of researchers have analyzed the types of vehicles that will potentially be needed for surface operations and exploration [114, 57, 56]. The various types include survey vehicles, science vehicles, site preparation vehicles, transport and assembly vehicles, astronaut transport vehicles, service and maintenance vehicles, and mining vehicles [57]. Each type is based on the primary function performed by the vehicle.

For simplicity, in this case study we consider a surface operations scenario in which five crew members land on a planetary surface and use a vehicle for setting up some basic infrastructure. The tasks in that operation will include moving and placing large equipment and modules (such as the lander, a habitat *etc.*) in a desired location so as to set up a long term base. The towing and cargo carrying capacity of such a vehicle will thus have to be large. However, its speed can be expected to be fairly slow since its operations will be performed with utmost care and may also require a reasonable degree of accuracy (especially if various surface modules need to be connected together). Its total range (the distance it can traverse before it needs to be refueled) will also be small since it is expected that the modules will be delivered to the planetary surface in close proximity (a few hundred meters or few kilometers apart).

Once the base set up operations are over, the astronauts will start the exploration phase of the mission in which they will make both short and long range sorties from the main base. The short range sorties (that do not require extended stay away from the base) can be conceived to be carried out by vehicles that can transport one crew member and basic field equipment and tools. The cargo carrying capacity will not need to be large; however its top speed and range should ideally be higher than for the infrastructure-setup vehicles (SPVs).

For long range excursions, that will require the crew to be away for several days from the base, a *planetary camper* will be used. The camper would essentially be a vehicle that provides a pressurized, habitable volume to a crew of 2 for a few days. In each long excursion, the camper will be hauled by

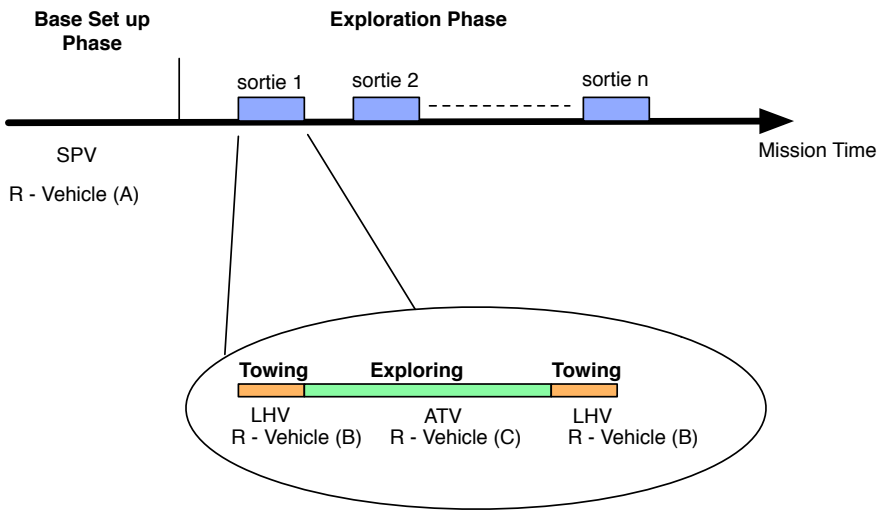

Figure 4-5: Mission Scenario

an un-pressurized vehicle with sufficient towing capacity, to a 'camping site'. An additional vehicle is also brought along to help scout the way. Once at the site, the camper will be parked, and the two un-pressurized vehicles will be used to explore the surrounding area. After the exploration, the camper will be hauled back to the main base. For the scenario described above, there can be two options in the context of reconfigurability for architecting the mobility system. In the first option, the different operations are carried out by a fleet of vehicles in which each performs a dedicated task. The fleet will consist of the following three types of vehicles:

- Site Preparation Vehicle (SPV) for transporting and placing modules, shelters, and lander to desired locations.
- Long Haul Vehicle (LHV) for towing a camper to various planetary sites for over-night excursions.
- Astronaut Transport Vehicle (ATV), to be used for high speed, long range, traverses for exploration.

Figure 4-5 illustrates the mission scenario schematically and shows when the three types of vehicles will be used along the mission time line. The desired specifications of range, tow capacity, cargo capacity, and speed for each type are shown in Table 4.6. Figure 4-6 shows the specification in a radar plot to illustrate how the three different vehicles vary in terms of their capabilities. It is assumed that the exploration operations consist of two teams of two people each that explore the surface at a given time. Each team brings a dedicated camper, and two LHVs for the trip. One person stays on the base for maintenance and support and uses an ATV. Aside from the camper (which is not factored in as being reconfigurable), for this scenario a total of six vehicles will be

Table 4.6: Performance Specifications for Dedicated Vehicles

	SPV	LHV	ATV
Range [km]	5	50	100
Speed [km/hr]	3	8	12
Tow Capacity [kg]	5000	2500	5
Cargo Capacity [kg]	500	200	50

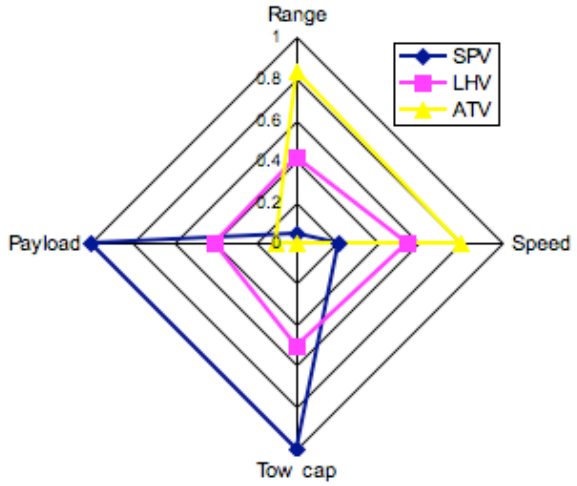

Figure 4-6: Radar plot showing specifications of dedicated vehicles required for different tasks

Table 4.7: Design Details of Dedicated Vehicles

	SPV	LHV	ATV
Total Power [kW]	2.68	3.47	0.94
Fuel Capacity [kg]	2.7	11.4	4.1
Wheelbase [m]	2.54	2.54	2.54
Track [m]	1.52	1.52	1.52
Wheel Diameter [m]	1.13	1.12	1.09
Wheel Width [m]	0.34	0.28	0.27
Max Torque [Nm]	34.6	16.65	2.7
Traction Drive Power [W]	646	842	211
Total Mass [kg][1]	358	401	245

needed: 1 SPV, 2 LHVs and 3 ATVs.

In the second alternative, a set of identical reconfigurable vehicles is used. The reconfigurable vehicles can undergo changes in their capabilities so that any one vehicle can be configured or morphed, between states A, B and C, to carry out any of the three types of tasks at a given time (see Figure 4-5). This will thus be a case in which the system needs to be reconfigurable in order to have multi-ability. For the exploration operations scenario described above, this would require 5 reconfigurable vehicles. One vehicle will be used by the person at base, and the two teams out on exploration will use two vehicles each.

4.3.1 Dedicated Vehicle Designs

The PSV MATLAB model (described in Section 4.1) was used to model various vehicles. The model is essentially an 'inverse design' model, in which performance specifications are given as inputs and the outputs are design details such as mass, power, energy, dimensions *etc.* Table 4.7 shows the details of the SPV, LHV, and ATV that were described in the previous section, and designed for minimum mass. The power system consists of fuel cells and solar panels. The vehicles are modeled, using inputs in Table 4.6, to be used on Mars (0.38g), with four independently driven wheels using harmonic drives of gear ratio 1:30, and each having one crew seating capacity. For modeling simplicity, the vehicle dimensions are estimated based on only the number of passengers. The consideration for cargo capacity is made in computing the structural aspects (such as thickness and size of chassis frame cross-section), and power and energy requirements (to carry the load), but not in the vehicle's size. The wheelbase and track values are therefore the same for each of the three types of vehicles in this case because the number of passengers is the same in each.

[1] A Polaris 700 single passenger, All-Terrain Vehicle with 135 kg cargo, and 680 kg tow capacity weighs 350 kg (for use on Earth) [10]

4.3.2 Reconfigurable Vehicle Design

A 'good' reconfigurable vehicle design was obtained by using the methodology presented in Section 4.2. In this problem, the vector that described the ith configuration (or state) was defined as:

$$\mathbf{x}_i^T = [r_i, V_i, T_{mi}, M_i] \tag{4.5}$$

where r is the range [km], V is the speed [km/hr], T is the mass [kg] the vehicle can tow, and M is the mass [kg] the vehicle can carry as payload. It was assumed that the reconfigurable vehicle needs to exist in three different configurations, A, B, and C in order to carry out the three types of tasks discussed earlier. The full design vector that needed to be determined through optimization consisted of 3 sub-vectors (each with 4 variables) for a total of 12 variables. It was denoted by:

$$\mathbf{X}^T = [\mathbf{x}_A^T \, \mathbf{x}_B^T \, \mathbf{x}_C^T] \tag{4.6}$$

The problem was formulated as

$$\min \mathbf{J} = z_{AB} + z_{BC} \tag{4.7}$$

$$\begin{aligned} s.t \\ 0.5 \leq r_A \leq 8, \quad 60 \leq r_B \leq 80, \quad 50 \leq r_C \leq 100 \\ 0.5 \leq V_A \leq 5, \quad 4 \leq V_B \leq 10, \quad 6 \leq V_C \leq 15 \\ 4000 \leq T_{mA} \leq 7000, \quad 2500 \leq T_{mB} \leq 4000, \quad 5 \leq T_{mC} \leq 5000 \\ 500 \leq M_A \leq 800, \quad 100 \leq M_B \leq 200, \quad 30 \leq M_B \leq 180 \end{aligned}$$

The objective function $\mathbf{J}$ was the sum of reconfiguration costs in changing from state A to B, z_{AB}, and in changing from state B to C z_{BC}. It was assumed that $z_{AB} = z_{BA}$ and $z_{BC} = z_{CB}$.

PSV Reconfiguration Cost

The reconfiguration costs, z_{ij}, were computed on the simplifying assumption that the cost is directly related to the amount of mass that is interchanged during a reconfiguration process. Thus, greater the mass of the components that need to be substituted, higher will be the costs. In reality, other costs such as energy crew time etc. will also be involved.

The determination of which components are substituted and which are transformed was based on the type of the component. It was assumed that the chassis frame, fuel tanks, and thermal system could only be altered through discrete addition and removal *i.e.* an off-line reconfiguration will be performed. Thus in order to reconfigure an LHV to an ATV, the necessary modules will have to be carried as payload during the sortie. The wheels and traction drives were considered to have

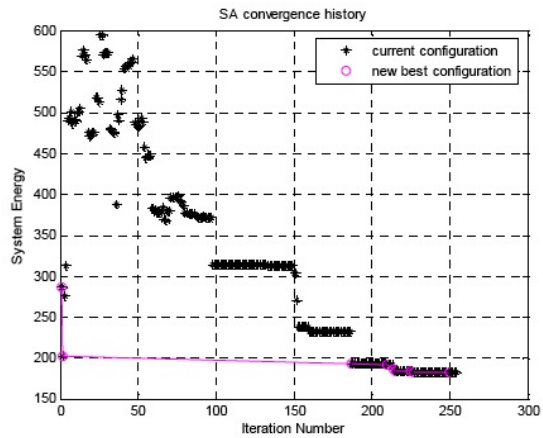

Figure 4-7: Convergence History of Optimal Design Determination Through Simulated Annealing

the additional capability of undergoing transformation, so on-line reconfiguration is possible. For the case of transformation, the coefficient of variation, c_v (as described in Equation 2.49), was set to 10% for both the wheels and drives. This effectively meant that the wheel diameter and width could vary by 10%, and the max power level of the traction drives could be altered by 10% (perhaps by channeling extra-power from non-essential devices when needed). If the required change in the component characteristics in configuring from one state to another was greater than what could be achieved with the given c_v, then substitution (*i.e.* a sequence of subtraction and addition) would be carried out. The mass of the component removed and that of the one installed are both summed up to get the total mass that is inter-changed. In case a component was found to be reconfigurable through on-line reconfiguration, then no additional mass was added. The reconfiguration cost is therefore a lower bound on the actual costs that may be incurred. Other considerations of cost such as crew time spent in carrying out the reconfigurations, and energy and other consumables required for the reconfiguration processes have not been factored in.

The optimization was carried out by using a heuristic method, Simulated Annealing [80], which is suitable for problems with both continuous and discrete variables. Although in this specific analysis only continuous variables were involved, in other more general analyses discrete variables are also involved such as number of wheels, power source type, drive type *etc.* Hence simulated annealing instead of a gradient based algorithm has been implemented in this MATLAB framework for studying PSVs. Figure 4-7 shows the convergence history of the algorithm. The optimal solution found for the given objective function and constraints (as shown in Equation 4.6) was: $\mathbf{J}^* = 182$ kg, and $\mathbf{X}^* = [8, 0.67, 5527, 501, 60, 4.5, 2522, 118, 95.7, 12.5, 42.2, 171]^T$. The total mass of the reconfigurable vehicle system (with all the required parts/modules) was computed to be 330 kg. Table 4.8 shows this solution. Each configuration was modeled with the same number of passengers (*i.e.* one), drive system, power system *etc.* as the fixed/dedicated vehicles. It can be seen from Table 4.8 that the

Table 4.8: Optimal Configurations for Reconfigurable Vehicle

	A	B	C
Range [km]	8	60	95.7
Speed [km/hr]	0.67	4.5	12.5
Tow Capacity [kg]	5527	2522	42.2
Cargo Capacity [kg]	501	118	171

Table 4.9: Design Details of Reconfigurable Vehicles

	A	B	C
Total Power [kW]	0.73	1.92	1.36
Fuel Capacity [kg]	4.48	13.1	5.4
Wheelbase [m]	2.54	2.48	2.48
Track [m]	1.52	1.52	1.48
Wheel Diameter [m]	1.13	1.11	1.11
Wheel Width [m]	0.32	0.27	0.28
Max Torque [Nm]	37.5	15.7	3.9
Traction Drive Power [W]	156.8	455.6	315.3
Total Mass [kg]	245	311	270

cargo capacity for configuration C is fairly high (than is necessarily needed). This is because the results were obtained by only minimizing reconfiguration cost (and not penalizing deviations from the 'target' specification set given in Table 4.6).

Reconfiguration Details

The detailed design specifications for each of these configurations are given in Table 4.9. It is observed that the fuel tank sizes need adjustment in changing from configuration A to B and B to C. The changes are needed in order to reduce the mass of the vehicles. In calculating the mass of the power subsystem of each configuration it was assumed that the tank size and other hardware elements are sized according to its maximum fuel capacity. Thus, if the largest tank size (which is used in B) is used on other configurations as well with partially filled fuel, the mass of configuration A (245 kg) and for C (270 kg) in that case will be higher. The traction drive powers are markedly different in all the three states so they are also changed. The wheel diameters and widths do not undergo a change larger than their c_v so they can simply be reconfigured through transformation (on-line reconfiguration). These results can aid in making architectural decisions about the interface designs between the sub-systems that would allow for installations, removals, and transformations. Figure 4-8 shows an OPD of the key features of the reconfiguration. For simplicity only a reconfiguration from state A to B is shown. All the three states A,B,C however are indicated in the various objects.

An 'all-size fits all' approach can be compared in which a vehicle is designed for the maximum specs so that it can be used for all of the different tasks (so it has 100 km range, 12 km/hr average speed, 5000 kg tow capacity and 500 kg cargo capacity). The mass of such a vehicle is determined

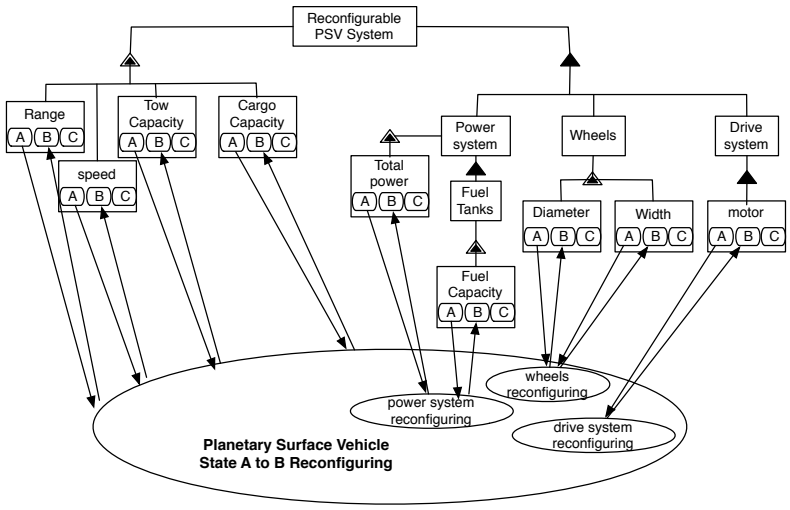

Figure 4-8: Object-Process Diagram of PSV Reconfiguration

to be 800 kg which is significantly more than the reconfigurable vehicle system.

4.4 Fleet of Reconfigurable vs Dedicated Vehicles

Using the specific designs for the dedicated and reconfigurable vehicles, a fleet of vehicles was considered that can deliver all the required functionality as required by the mission (discussed in Section 4.3). Various comparisons for mass (and volume) efficiency, evolvability, and reliability were made.

4.4.1 Mass Efficiency

In the most general case, it is easy to see that since one reconfigurable PSV can do the functions of three different dedicated PSVs, some significant mass savings can be realized. The combined dry mass of 1 SPV, 1 LHV and 1 ATV is 985 kg, while one reconfigurable vehicle is 317 kg. So in terms of pure mass savings the ability to configure a single vehicle to perform multiple functions is clearly very beneficial.

An important aspect, however, is the time at which the various functions are required (similar to Γ in the previous chapter). A reconfigurable system, that can perform one type of task at a time, will not be able to provide multiple concurrent functions that may be required (as noted earlier in the definitions discussion in Section 2.1). The time requirement of the various functions will thus play a critical role in determining the extent of benefit that can be obtained through reconfigurability. So, for instance if the site preparation task is done initially, and then later both an LHV and an ATV are required at the same time, then at least 2 reconfigurable vehicles will be needed.

If the whole exploration mission scenario is considered along similar lines, for the initial base setup phase at least one SPV is required. Then for two simultaneous EVA teams, a total of 2 LHVs

and 2 ATVs required. Furthermore it was assumed that the fifth crew member who stays at the base (while the other four are out on EVA) has an ATV available at the base for local work and rescue operations. The whole fleet of surface vehicles will thus at a minimum consist of 1 SPV, 2 LHVs and 3 ATVs. For the reconfigurable case however, at any given time a total of five vehicles need to be available (two each for the two EVA teams and one at the base). Therefore 5 vehicles can deliver the same functions at the required times instead of 6 for the dedicated case.

The different usage scenarios are shown in Figure 4-9(a). Three different cases are plotted. In the first case there is only 1 R-PSV (reconfigurable PSV) for 3 D-PSVs (dedicated PSVs which are 1 SPV, 1 LHV and 1 ATV). This is the case when none of the tasks are required simultaneously. So in principle one R-PSV is sufficient. The second case is for 2 R-PSVs and 3 D-PSV (which is when both LHV and ATV are required for operation simultaneously). The third case is of the fleet described above with 5 R-PSVs and 6 D-PSVs. It is clear that in a multi-ability reconfigurable system, the amount of benefit (in terms of mass savings here) that can be realized is closely tied to the usage/operation scenario.

Relative Functional Efficiency

The reconfigurable and dedicated vehicle fleets can also be assessed from the Relative Functional Efficiency, Ξ_f, perspective. The Ξ_f was determined by first computing the functional efficiency, $\eta_{f\,D}$, of a set of dedicated vehicles (consisting of 1 SPV, 1 LHV and 1 ATV). The $\eta_{f\,D}$ had been defined in Equation 2.39 as

$$\eta_{f\,D} = \frac{\sum_{j=1}^{k} \nu_j}{\sum_{j=1}^{n} \rho_j}$$

Here the ν_j is the transport capability [144] and ρ_j is the mass of each vehicle. The ν is defined as the product of a vehicle's average speed with the payload it transports. In this case the total transported payload is the sum of cargo mass (carried on the vehicle) and the mass towed by the vehicle. Therefore:

$$\nu = V \times (T + M) \tag{4.8}$$

The specific equation used for calculating $\eta_{f\,D}$ was

$$\eta_{f\,D} = \frac{\nu_{SPV} + \nu_{LHV} + \nu_{ATV}}{m_{SPV} + m_{LHV} + m_{ATV}} \tag{4.9}$$

The $\eta_{f\,R}$ for the reconfigurable vehicle, with states A, B, and C was also computed in a similar manner using Equation 2.38:

$$\eta_{f\,R} = \frac{\nu_A + \nu_B + \nu_C}{m_R} \tag{4.10}$$

where m_R is mass of total reconfigurable vehicle system (with all the parts required for the various configurations along with the base vehicle). The ratio of $\eta_{f\,R}$ and $\eta_{f\,D}$ was then computed which

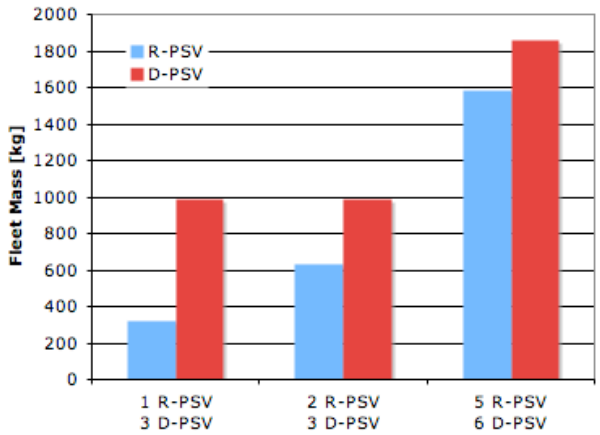

(a) Dry mass comparison

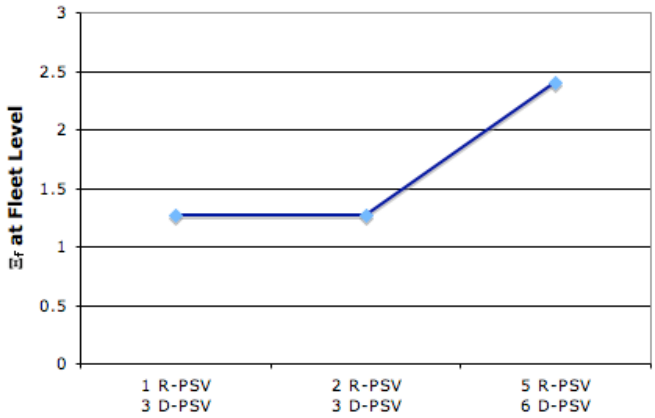

(b) $\Xi_f (= \frac{\eta_{f\,R}}{\eta_{f\,D}})$ comparison

Figure 4-9: Comparison between Reconfigurable and Dedicated PSV fleets

was the Ξ_f, and was found to be 1.275. This indicates that the reconfigurable system offers more efficiency (by 27%) in terms of delivering unit transport capability per unit of mass as compared to the dedicated system. A similar computation was carried out for the other two cases described above. Figure 4-9(b) summarizes the results. It should be noted that the masses of the reconfigurable system give a lower bound since any mass penalty of having components that can transform, or be installed and removed easily has not been factored in. The difference of mass thus provides the limiting value of reconfigurability, *i.e.* the reconfigurable option is better strictly in terms of mass if the mass penalties due to having reconfigurable components/sub-systems are lower than the difference. However, even if all the mass difference were consumed by the heavier reconfigurable components, there still is a benefit to the reconfigurable fleet because as failures occur components can be swapped out more easily and multi-functionality is retained longer at the fleet level (see Chapter 3).

In addition to the mass savings, the volume savings are implicit. If there are fewer vehicles that

can do the job, there will be volume savings as well. It is however difficult to quantify those at this stage since they will depend on the stowage capabilities of the vehicles, and the design of the PSVs did not have that level of detail as they were primarily parametric.

Another important aspect is the extent of usage. Not only is the operational scenario important (*i.e.* which function/capability is required when), but also to what extent. This is because any difference in performance (usually worse for the reconfigurable system as compared to its ideal dedicated case) may weigh out over its life cycle if it is used extensively. So if the usage is going to be extensive, it may be better to have dedicated systems. An assessment based on the Relative Performance Efficiency Ξ_p of the reconfigurable and dedicated vehicles was therefore carried out.

The vehicles have been modeled to use $H_2 - O_2$ fuel cells, both of which are not found in free states on Moon or Mars. In the event that the total fuel for the mission has to be transported (considering the fuel cells are not regenerative for the worst case), then the total mass associated with the mobility system will be the mass of the vehicles plus the fuel they will use over the course of the entire mission. The total resources are then the mass of the vehicles (non-recurring cost) along with the fuel mass of H_2 and O_2 (recurring cost).

Figure 4-10 shows the relative performance efficiency, Ξ_p. This was obtained by first computing the performance efficiency, $\eta_{p\,D}$, of the dedicated set of vehicles (consisting of 1 SPV, 1 LHV and 1 ATV). Recall from Equation 2.40, the Performance Efficiency was defined as

$$\eta_p = \frac{\textit{Total Life Cycle Performance}}{\textit{Total Resources}}$$

The transport capability of each vehicle was multiplied with the total time it was used for in the mission to get the total life cycle performance. The specific equation used was:

$$\eta_{p\,D} = \frac{\nu_{SPV} T_{SPV} + \nu_{LHV} T_{LHV} + \nu_{ATV} T_{ATV}}{m_{SPV} + m_{LHV} + m_{ATV} + m_{H2} + m_{O2}} \tag{4.11}$$

where T is the time of use of each vehicle and is computed by dividing the distance traversed by the vehicle with its speed. The m_{H2} and m_{O2} are the mass of fuel. Similarly for the reconfigurable system:

$$\eta_{p\,R} = \frac{\nu_A T_A + \nu_B T_B + \nu_C T_C}{m_R + m_{H2} + m_{O2}} \tag{4.12}$$

Note that the mass of fuel comes out differently since the vehicle designs are different for the reconfigurable and dedicated case, so even for equal distance of travel the fuel consumption is different.

In order to do a trade over different usage extent, the distances traversed over the total mission by the LHV (the towing vehicle) and ATV (which is the light astronaut transport vehicle) were varied between several thousand kilometers. The total distance traversed by the SPV (used for base

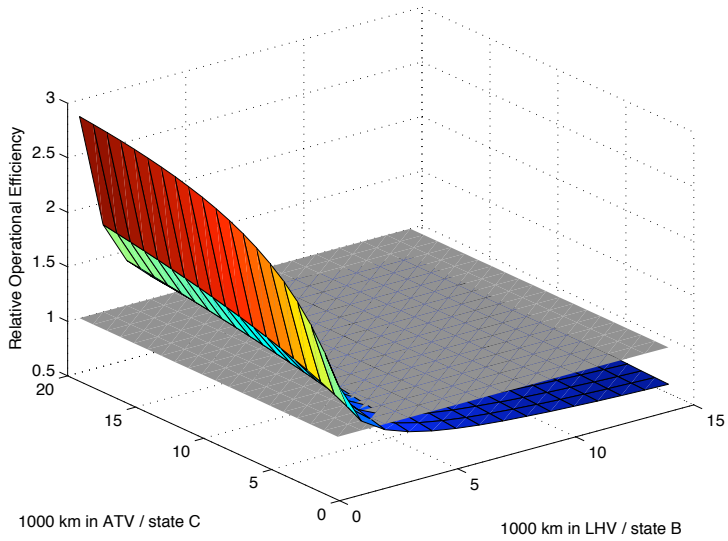

Figure 4-10: Relative Performance Efficiency of Planetary Surface Vehicles fleet

set up is fixed to 50 km over the two year Mars surface mission). Then for each set of distances (axes X and Y in Figure 4-10) a corresponding value of η_{pD} was calculated. A similar procedure was carried for computing η_{pR} for the reconfigurable vehicle that could adopt states A, B and C. The ratio of the two efficiencies was then take to obtain Ξ_p and was plotted on the z-axis in the figure. For values of greater than 1 of the Relative Performance Efficiency, the reconfigurable system offers an advantage. It is clear to see from Figure 4-10 that the reconfigurable vehicle is better for small traverses of configuration B (that corresponds to the LHV). After approximately more than 5000 km of travel, the fuel consumption gets high enough to make the dedicated system better in terms of over all mass (resources) involved. The implicit assumption here is that the fuel is transported to the surface, and it is therefore very costly to consume more fuel. This figure illustrates the typical trade-off that may exist in many systems when subjected to analysis for reconfigurability. The reconfigurable system may give benefits in terms of using less non-reccurring resources, but over the long run it may end up being more expensive due to sub-optimalities.

In a 600-day mission to Mars it maybe unlikely that this much distance will be traveled cumulatively by the vehicles, however, if the vehicles are to be used in subsequent missions (that maybe part of a long exploration campaign) then a dedicated fleet may merit a more closer look.

4.4.2 Reliability and Robustness

A major concern, especially for critical systems is robustness in continuity of function in the face of disturbances, and high reliability of components and sub-systems.

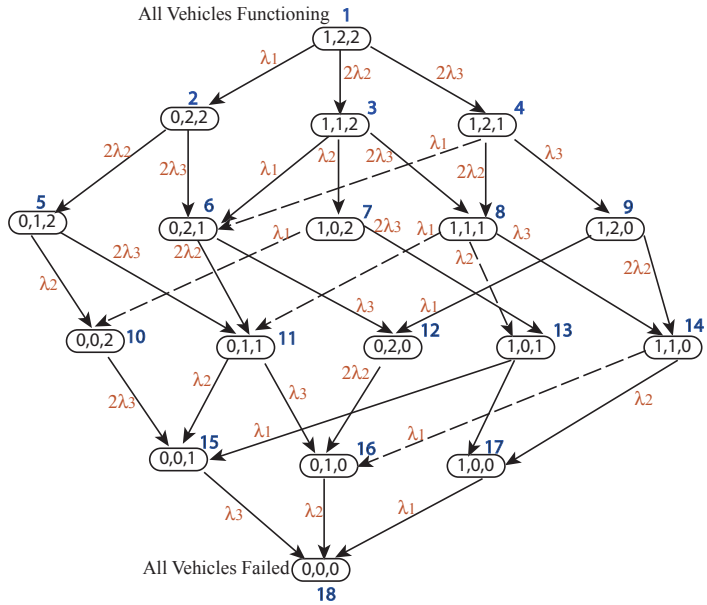

Figure 4-11: Markov Model of Dedicated Vehicle Fleet

Markov Reliability Analysis for Functional Availability

In the PSV case study a Markov reliability analysis was conducted on the reconfigurable and dedicated vehicles at the fleet level. Each 'state' of the fleet was defined by the number of vehicles of each type that are functional. The initial 'state' at the start of the mission was denoted as $[1, 2, 2]$ for 1 SPV, 2 LHV, and 2 ATVs. The failures were modeled at the vehicle level (not at the component level as in Chapter 3), and each vehicle was assumed to have a specific Mean Time To Failure (MTTF). The transition rate, λ_{ij}, between each state i and j was then simply the reciprocal of the MTTF of the vehicle that fails as the fleet moves from state i to j. Figure 4-11 shows the Markov model for the dedicated fleet. The initial state is 1, and the transition rate of moving to state 2 (which is [0,2,2]) is λ_1 which is the failure rate of the SPV. State 3 is [1,1,2] and can be attained from State 1 if one of the LHVs fail. The transition rate is $2\lambda_2$ since there are two LHVs and if the first or the second LHV fails, the fleet will be in state 3. The final state 18 is [0,0,0] in which all three vehicles have failed. Based on this Markov model the probabilities of the fleet of being in any particular state at a specific time were computed by defining a vector Π, of 18 elements in which the ith element π_i was the probability of being in state i. Thus at any time the sum of the elements

of Π would be 1. For this continuous time model, the following equations hold:

$$\frac{d}{dt}\Pi(t) = A\Pi(t) \tag{4.13}$$

$$\Pi(t) = e^{At}\Pi_0 \tag{4.14}$$

where $\Pi_0^T = [1, 0, \cdots, 0]$ (and is the initial state at time 0) and $A \in \Re^{nxn}$ is given by

$$A = \begin{bmatrix} -(\lambda_1 + 2\lambda_2 + 2\lambda_3) & 0 & 0 & \cdots & 0 \\ \lambda_1 & -(2\lambda_2 + 2\lambda_3) & 0 & \cdots & 0 \\ \lambda_2 & 0 & -(\lambda_1 + \lambda_2 + 2\lambda_3) & \cdots & 0 \\ \vdots & 0 & 0 & \cdots & \vdots \\ 0 & 0 & 0 & \cdots & 0 \end{bmatrix} \tag{4.15}$$

In the reconfigurable fleet, each vehicle could deliver the functionality of an SPV, LHV or ATV. Since there were two LHVs and ATVs in the dedicated case, two reconfigurable vehicles were considered for a somewhat equal comparison in a functional sense. The failures were assumed to be at the configuration level (instead of vehicle level). So a reconfigurable vehicle could for instance have a particular failure so that it could only be operate in states of an SPV and an LHV but not as an ATV. This can happen if some specific part fails that was needed for the ATV configuration but not required for the SPV and LHV configurations. The initial state was set to [2,2,2] since at the start of the function, the fleet could deliver the functionality of 2 SPVs or 2 LHVs or 2 ATVs. A Markov model was made and the state probabilities were computed in a similar way as for the dedicated case discussed above (see Figure A-4). A value of 10 years for the MTTF for each dedicated vehicle (and configuration in the reconfigurable vehicle case) was assumed. Although more realistically, the MTTF for the configurations would be higher since it would occur due to partial failure of the vehicle (so that for instance it can only operate in two out of its three possible configurations). The estimate for the reconfigurable case will be therefore conservative.

Figure 4-12 shows the probability of having at least one of each kind of vehicle (or configuration) being available. This essentially means that all the different functions/tasks can be carried out since each type of vehicle is functional. This was computed by summing the probabilities of all the states (given in general by $[i, j, k]$) in which i, j, and k were greater than or equal to 1. It can be seen the that chances of having the capability to perform all the types of tasks is improved for the reconfigurable case. For a two-year mission the dedicated fleet has a probability of 60% that all types of tasks can be performed as compared to the 82% chance for the reconfigurable vehicles fleet. In order to assess the performance degradation over time of the fleet, the transport capability metric, ν [144] was used. The ν of a fleet is simply the sum of the ν of each vehicle in the fleet. Figure 4-13 shows how the *Expected Transport Capability* of the fleet degrades over time.

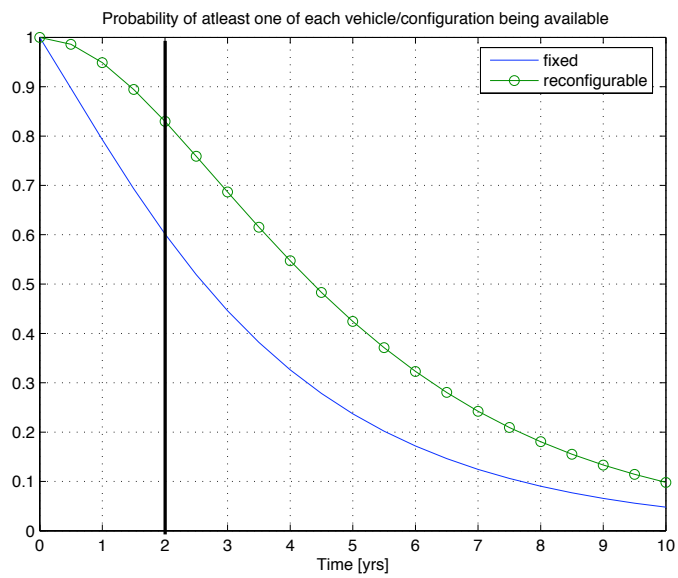

Figure 4-12: Probability of Having Functional Capability of Each Type

The Expected Transport Capability is defined as

$$ETC = \boldsymbol{\nu}^T \Pi(t) \tag{4.16}$$

where $\boldsymbol{\nu}^T = [\nu_1 \cdots \nu_i \cdots \nu_n]$ (for n states) and ν_i is the transport capability of the fleet in state i. It can be seen that the plots are not linear, and the derivatives vary as a function of time. The derivatives of the ETC for each case, were therefore computed by the taking the mean derivative between two sets of points each along the line. It is clear to see simply from the plots alone that the reconfigurable system degrades more slowly as compared to the fixed system. However, in numerical terms, for the dedicated case, the mean $\frac{dETC}{dt}$ was found to be $-4.80 \times 10^3 [kg - km/hr/year]$, and for the reconfigurable case it was $-1.76 \times 10^3 [kg - km/hr/year]$. The ratio, which is the relative degradability, Λ was thus 2.72 showing that the reconfigurable system is almost three times more favorable from a degradability perspective.

Terrain Uncertainty Management

A key uncertainty that planetary surface vehicles encounter is the terrain condition. Recent troubles experienced by Opportunity, one of the Mars Exploration Rovers, in spring of 2005 serve to highlight this fact. The rover got stuck over the course of its explorations due to an unanticipated change in soil conditions. It took five weeks of painstaking operation to free all six wheels of the rover, which were mired up to their rims in the soft sand of a small martian dune [12]. In future human missions, it will be highly desirable to manage this inherent uncertainty in terrain. A vehicle with a robust

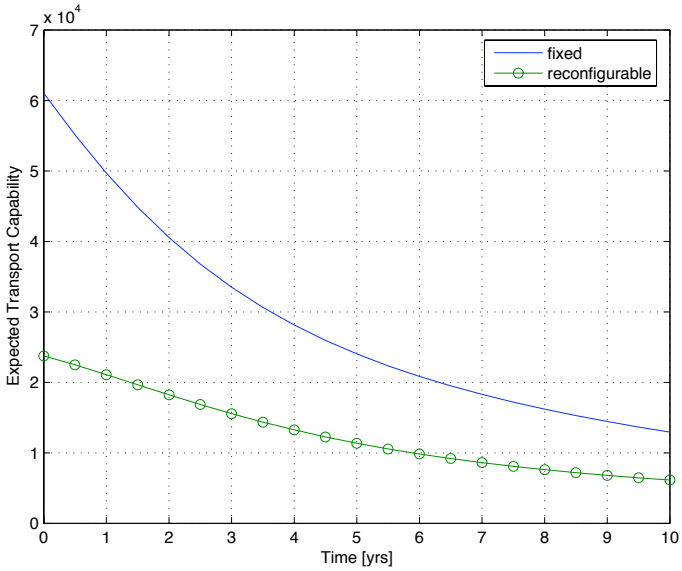

Figure 4-13: Expected Transport Capability of Fleet

(a) Opportunity stuck in a sand trap on Mars[121]

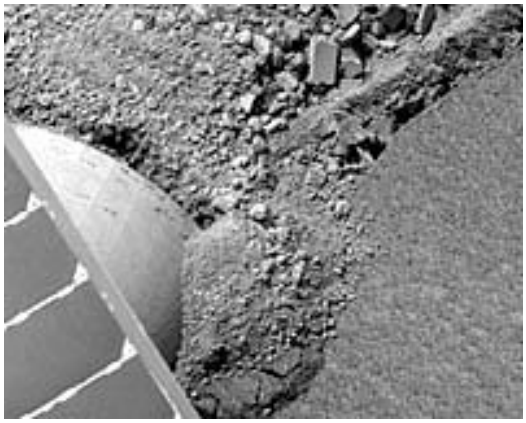

(b) A close up of one stuck wheel among five others [131]

Figure 4-14: Opportunity was stuck on Mars for five weeks

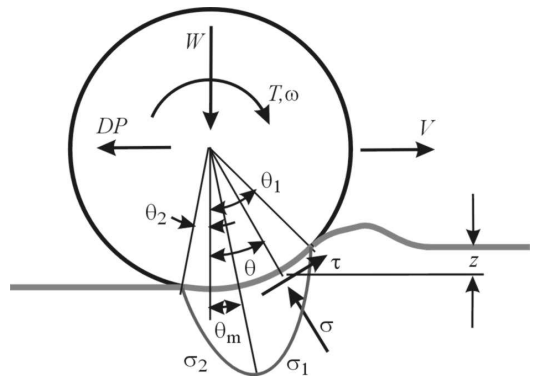

Figure 4-15: Free Body Diagram of a rigid wheel on deformable terrain[70]

locomotive system that can reconfigure according to soil conditions in order to maintain necessary tractive ability can be greatly beneficial. Wong [144] has studied the mechanics of a driven wheel and soil interactions. Iagnemma [72] *et al.* have further developed those results that allow accurate modeling of the interactions of a rover wheel with terrain (see Figure 4-15). The results of these studies are used in this analysis.

From a traction point of view for wheel motion, the main parameter of interest is the Drawbar Pull (DP). The DP is the difference between the thrust (H) provided by the soil and the necessary force required for the loaded wheel to move [144].

$$DP = H - \sum R \tag{4.17}$$

$$\sum R = R_c + R_b + R_g + R_r \tag{4.18}$$

The $\sum R$ represents the total of all resistances that need to be overcome by the wheel. On soft, loose terrain they can include compaction resistance, R_c, bull-dozing resistance, R_b, grade resistance R_g (if the wheel is on a slope), and rolling resistance R_r among others. The soil thrust, H, is dependent on the characteristics and composition of the soil, along with wheel loading and dimensions. Typically, on loose flat terrain the compaction resistance, R_c is the largest (as compared to R_b, and R_r). For a driven wheel on soft terrain, it is given by [144]

$$R_c = \frac{z^{n+1}}{n+1}\left(k_c + bk_\phi\right) \tag{4.19}$$

$$z = \left[\frac{3W}{(3-n)(k_c + bk_\phi)\sqrt{D}}\right]^{2/(2n+1)} \tag{4.20}$$

where z is the sinkage of the wheel, W is the wheel load, b and D are the wheel width and diameter,k_c is the cohesive modulus of deformation, k_ϕ is the frictional modulus of deformation, and n is the sinkage coefficient. For different types of soil, the values of k_c, k_ϕ, and n are different and the R_c

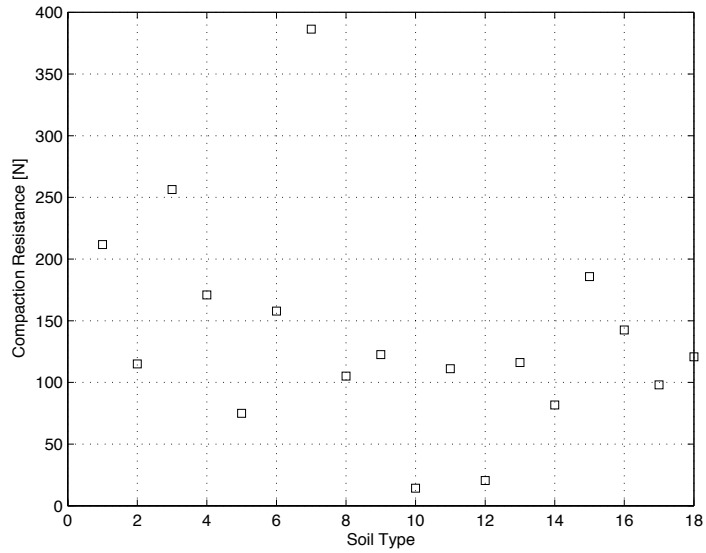

Figure 4-16: Compaction Resistance in Varying Soil Conditions

can vary significantly. Figure 4-16 shows the compaction resistance experienced by a wheel of 1 m diameter, 0.3 m width and supporting a load of 150 kg for soil types ranging from dry sand to heavy clay. The values of the soil parameters used are given in Table A.11 in Appendix A. It thus clear that the DP can be greatly affected depending on the type of soil the vehicle traverses over. The thrust the soil can provide (H) before it experiences shear failure (and the wheels will lose traction) is fundamentally dependent on its shear strength. There are a number of criteria proposed for the failure of soils and other similar materials. One of the widely used and simplest is due to Mohr-Coulomb [144]:

$$\tau = c + \sigma \tan \phi \tag{4.21}$$

where τ is the shear strength, c is the cohesion, and σ is the normal stress on the sheared surface, and ϕ is the angle of internal shearing resistance of the material. Cohesion of the material is the bond that cements particles together irrespective of the normal pressure exerted by one particle upon the other. On the other hand, particles (with frictional masses) can also be held together when a normal pressure exists between them. Granular masses, covering trafficable surfaces, usually have both cohesive and frictional properties. There were several experiments conducted by the Soujourner rover during the Path Finder mission to determine the soil characteristics on Mars [91]. Table 4.10 shows the values of c and ϕ that were empirically determined at different locations. It is clear that the terrain on Mars is highly varied even within a fairly short radial distance (of few kilometers). Figure 4-17 shows the shear strength of these different soil types. In order to ensure that a vehicle can successfully traverse terrain with varying (and unknown) characteristics, the DP must be able

Table 4.10: Parameters for Various Soil Types Found by Soujourner[91]

c [kPa]	0.21	0.09	0.34	0.15	0.09	0.36	0.27	0.3
ϕ [deg]	37	34.4	41.5	33.3	42.4	26.4	37.1	36.9
c [kPa]	0.26	0.19	0	0.27	0.4	0.18	0.43	0.26
ϕ [deg]	41.2	36.9	28.2	41	34.7	35.1	40.6	38.1

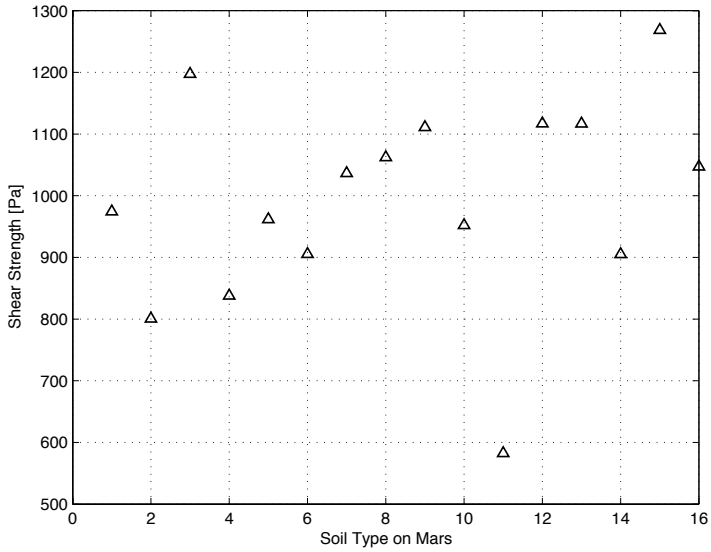

Figure 4-17: Shear Strength of Soil at Different Locations Traversed by Soujourner

to stay at a positive level at all times. Equation 4.17 shows that if the DP is positive the soil has the capability of providing equal or more thrust than is required for the vehicle's motion. If the DP is negative, then it means that the soil cannot develop enough thrust for the vehicle to move forward, and thus the PSV will be stuck. From Equation 4.17 it can also be seen that the DP can significantly change (due to H and R_c changing), and thus it would be desirable to have PSVs that can adapt to varying soil conditions to maintain near constant DP.

If it is assumed that the primary resistance to wheel motion on soft terrain is due to soil compaction, then the following integral equations can be used to compute the DP along with the required Torque, T that would be needed for a wheel [144].

$$DP = \frac{D}{2}b\left(\int_{\theta_1}^{\theta_2} \tau(\theta)\cos(\theta)d\theta - \int_{\theta_1}^{\theta_2} \sigma(\theta, b)\sin(\theta)d\theta\right) \tag{4.22}$$

$$T = (\frac{D}{2})^2 b \int_{\theta_1}^{\theta_2} \tau(\theta)d\theta \tag{4.23}$$

Figure 4-15 shows how the various θ are defined.

From a design point of view, the three main variables that affect the trafficability of the vehicle are the wheel load, wheel diameter and wheel width. If it is assumed that the wheel load cannot be altered, (and considering that the number of axles remain the same and/or no additional wheels are added on to distribute the load per wheel) then only the diameter and width of the wheels can be subject to reconfiguration. Figure 4-18 shows how the DP and sinkage of a wheel are affected for varyings values of its diameter and width. For each value of the diameter, the wheel width was allowed to be between 30% and 50% of the diameter, to ensure feasible and realistic dimensions. The calculation was based on a four-wheeled vehicle on Mars carrying a total load of 250 kg. The soil parameters were assumed to be $c = 1[kPa]$, $\phi = 35^o$, $k_c = 10[kN/m^{n+1}]$, $k_\phi = 850[kN/m^{n+2}]$, $K = 0.3[m]$ and $n = 1$ [71]. It is clear to see that an increase in width and diameter leads to increasing DP. But it also leads to increased energy consumption of the vehicle. It was thus assumed that a PSV can use reconfigurable wheels that can alter their dimensions (width and diameter) subject to varying soil conditions so that some objective of DP and energy consumption is fulfilled. In Section 4.5 some technologies related to development of reconfigurable wheels for vehicles will be discussed.

Reconfigurable Wheels and Locomotion Robustnesss

In order to assess the impact of having such a wheel with reconfigurable dimensions versus a wheel with fixed dimensions, a simulation of a few drive cycles of a 4-wheeled PSV on Mars was carried out. It was assumed that the vehicle travels for 30 minutes over terrain with varying soil conditions at a constant velocity of 5 km/hr. The vehicle sprung mass was assumed to be 200 kg. It also

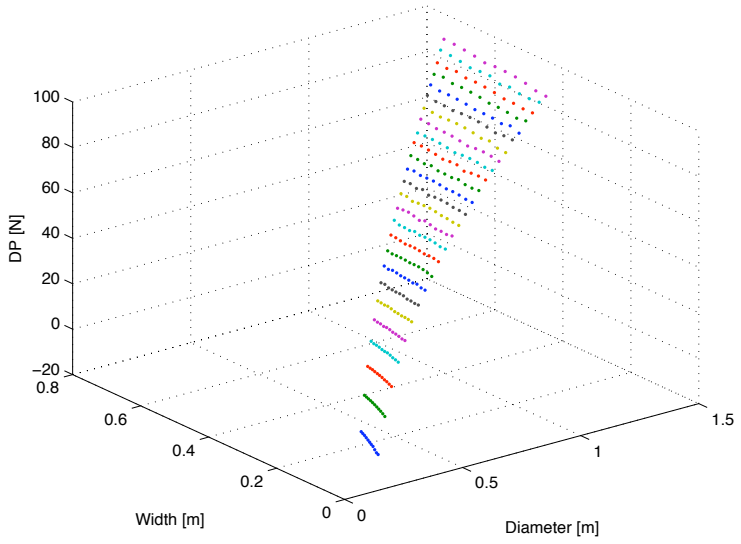

(a) Variation of DP

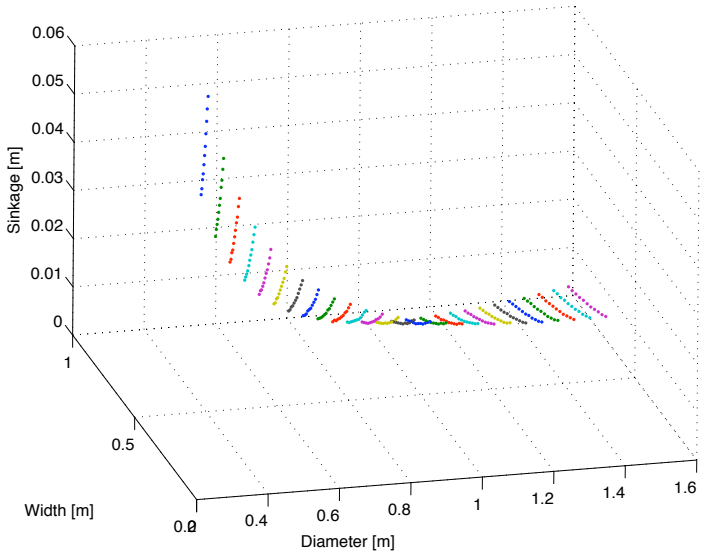

(b) Variation of Sinkage

Figure 4-18: DP and sinkage as a function of wheel diameter and width

Table 4.11: Soil Parameters Used in Simulation

Type	K_c $[kN/m^{n+1}]$	K_ϕ $[kN/m^{n+2}]$	c [kPa]	ϕ [deg]	n	K [m]	Density $[kg/m^3]$
LETE sand	6.49	505.8	1.15	31.5	0.705	1.15	1600
Clayey soil	13.19	692.15	4.14	13	0.5	1.15	1520
Sandy loam I	2.79	141.11	15	25	0.3	1.13	1500
Dry sand	0.99	1528.43	1.04	28	1.1	2.54	1600
Sandy loam II	74.6	2080	0.22	33.1	1.1	2.54	1350

carried one suited astronaut and cargo. The total supported mass was thus set to 450 kg. A set of different soil parameters were used to simulate the varying conditions the vehicle experiences during its course of travel. Table 4.11 shows the soil data used in the simulation. Since mostly the data available for Mars was only of c and ϕ, representative data (of a few different types of soil) from [144] was employed. Figure 4-19 shows how the data was varied in the simulation. As the vehicle moves over soil of different characteristics, its DP also varies. The DP was computed from Equation 4.23 for each time step using the corresponding soil condition. For a wheel with fixed dimensions and having a width of 0.3 m and diameter of 1.0 m, Figure 4-20 shows how the DP changes over time. The minimum DP that is developed over the course of travel is of most interest since it defines the capability of the vehicle to keep moving without getting stuck. The threshold is at DP of zero (after which the vehicle will not be able to get enough thrust from the soil). It can be seen that the DP drops to a value of 62 N over one region during the course of its travel.

A similar simulation was then carried out for a vehicle that had wheels with reconfigurable dimensions. The wheel load, and soil conditions were the same as discussed earlier. There were five cases in total that were analyzed for the reconfigurable wheel case. In the first case, the wheel was allowed to vary only its width (b) and only by a small amount: it could essentially vary between 0.3 and 0.4 m. The variation was assumed to be discrete in steps of 3.33 cm. So the allowable values for b were 0.3, 0.33, 0.367, and 0.4 m. At each time step, the specific value to be used for b was obtained by minimizing a cost function J (similar to that used earlier in Section 2.4.3 in Equation 2.31):

$$J = \alpha J_1 - (1 - \alpha) J_2 \tag{4.24}$$

where α is a constant between 0 and 1, J_1 is the scaled DP and J_2 is the scaled torque. The goal was thus to have as large a DP as possible while at the same time reducing the required Torque (which is directly related to the energy consumed during driving). In the simulation α was set to 0.8 (to weigh the maximization of DP more). Since the optimization problem was fairly tractable and small, a full factorial analysis was done at each step in which the cost function was evaluated for each possible value of b. The best value of b was then picked that had the minimum value of J. Note that no time delays were assumed, and at each time step as soil parameters changed,

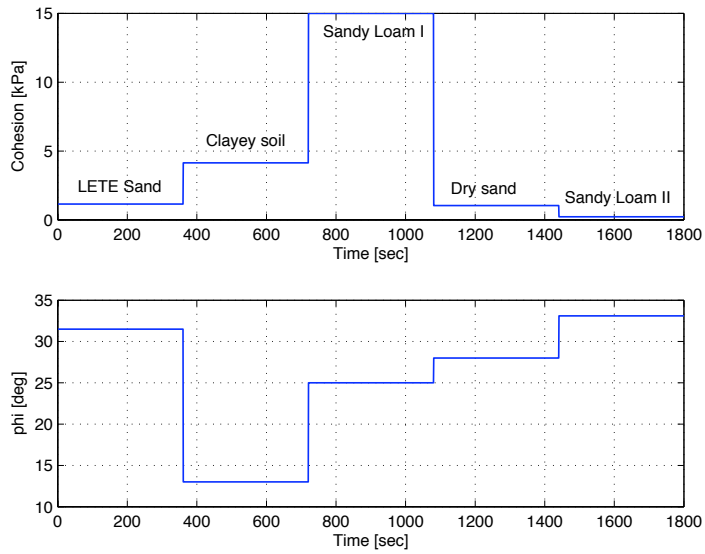

(a) c and ϕ over time

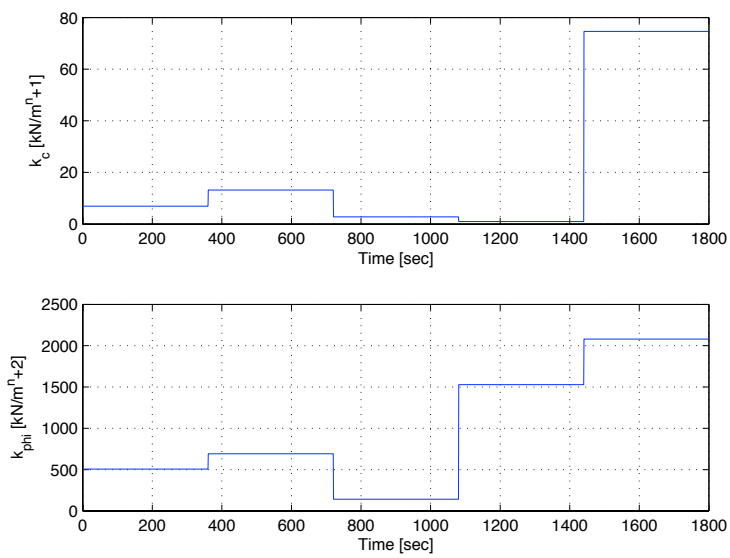

(b) k_c and k_ϕ over time

Figure 4-19: Variation of Soil Parameters with Time

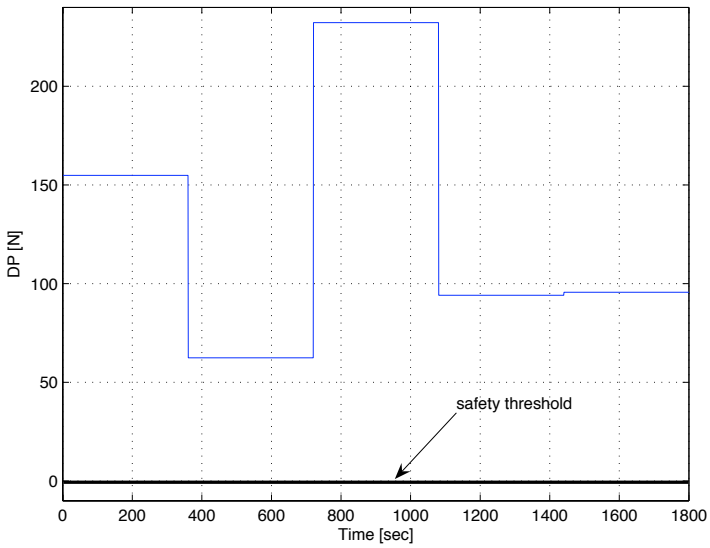

Figure 4-20: Variation of Drawbar Pull of a Wheel over Varying Soil Conditions

the b was allowed to change instantly. The DP was computed at each time step using the optimal value of b. The simulation thus modeled the response of an ideal wheel in which the changes in soil conditions could be sensed and the corresponding reconfiguration could be made instantaneously (through on-line reconfiguration). In the second case, the wheel width was allowed to reconfigure by a larger amount, and could assume values between 0.28 m and 0.55 m. The diameter, D, was the same as before of 1m. The number of discrete states (of b) was allowed to be 5 in this case. In the third case, reconfigurability in the diameter was allowed (but was reduced for the width). The diameter could assume values between 1.15 and 0.85 m and width could be between 0.28 and 0.35 m. In the fourth case, the diameter was also between 1.15 and 0.85, but the width was allowed to vary more, *i.e.* between 0.28 and 0.55 m. In the fifth case the allowable values for D were 1.25 and 0.75 m, while that for b were the same as in case four (between 0.28 and 0.55 m). In summary, case 1 was for small reconfigurability in width, case 2 for larger reconfigurability in width, case 3 for small reconfigurability in diameter (but very little in width), case 4 for larger reconfigurability in diameter and width, and case 5 was for very large reconfigurability in diameter and width. In the cases where D was reconfigurable, b was also made reconfigurable to ensure realistic dimensions. For each case the simulation was run and the DP was found as a function of time. Figure 4-21 shows how the fixed wheel simulation and reconfigurable wheel (case 5) compare. The wheel reconfiguration process is modeled in an OPD and shown in Figure 4-22. A summary of all the five cases of reconfigurable wheels as compared to a fixed wheel is shown in Figure 4-23. The Φ_r (discussed in Section 2.7.1 earlier) is plotted which is the ratio of the $\min DP_R$ (minimum DP for reconfigurable case) and $\min DP_{FX}$ (minimum DP for fixed case). It provides a measure of the relative 'survivability' of the

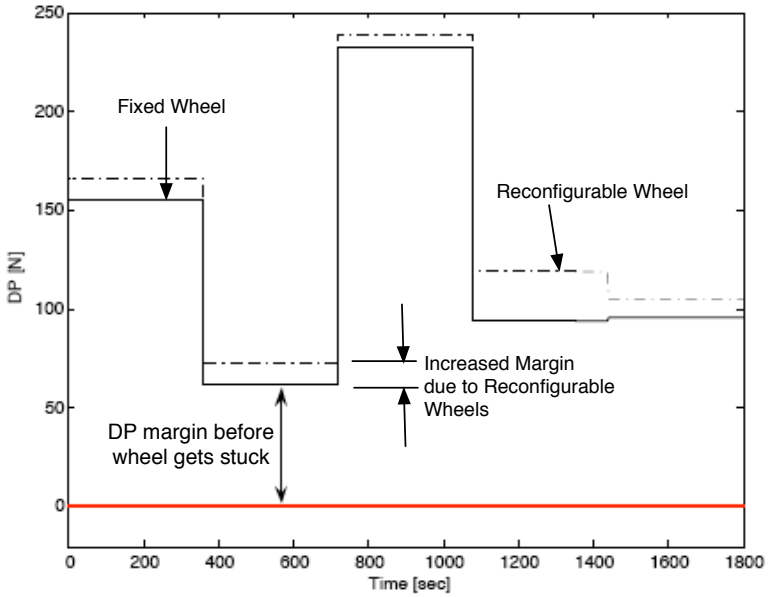

Figure 4-21: Comparison of DP of wheel with fixed and reconfigurable dimensions

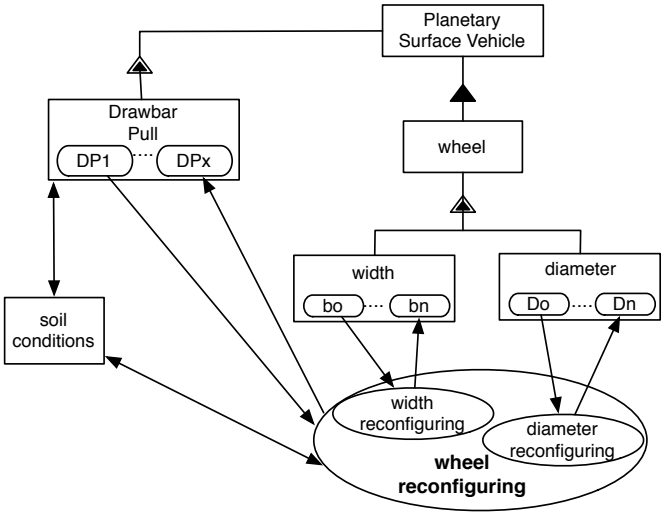

Figure 4-22: Object-Process Diagram of Wheel Reconfiguration

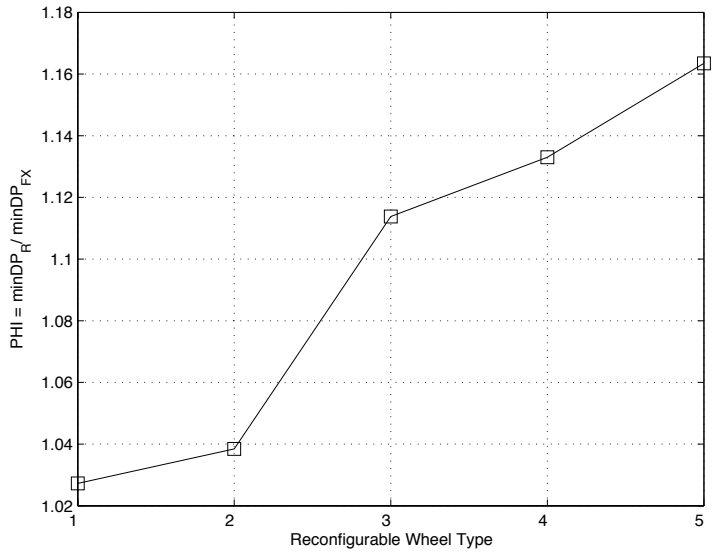

Figure 4-23: Comparison of minimum DP (over drive cycle) of wheel with fixed and reconfigurable dimensions

system. It can be seen that each case of reconfigurable wheel is better in terms of improving the DP of the vehicle as compared to a fixed wheel. It is also not surprising to see that with increasing reconfigurability (going from case 1 to 5) the ratio gets higher. In summary, from Figures 4-21 and 4-23, one can observe that reconfigurable wheels with variable dimensions increase robustness by enhancing the minimum DP of the vehicle over the course of its travel thus avoiding failure (by getting stuck). In a manned mission, where a stuck vehicle can in the worst case cause loss of life (if crew runs out of life support), reconfigurability of the locomotive system can play a very important role in ensuring mission success.

4.5 Technologies

Recently several concepts have started to appear for reconfigurable wheels. Figure 4-24 shows a design concept for a wheel in which the diameter can be altered. The larger diameter configuration can be used for on-road travel, while the smaller diameter configuration can be used on a racetrack without having to change out the wheels. The wheel has movable tread sections, designed to go from the road to the track without changing any parts. The center cap moves outward on a piston, thus articulating the spokes like a car jack. This motion decreases the diameter of the wheel from it's road-going 'expanded' state, while closing the gaps in the tread to create a slick tire surface. A smaller wheel is advantageous for racing because of the smaller amounts of rotational energy needed. Acceleration is also enhanced by using a smaller wheel with the same transmission gearing [19].

A prime enabler for reconfigurability is modularity. In the PSV case study discussed above, it

Figure 4-24: Reconfigurable Wheel with Variable Diameter [19]

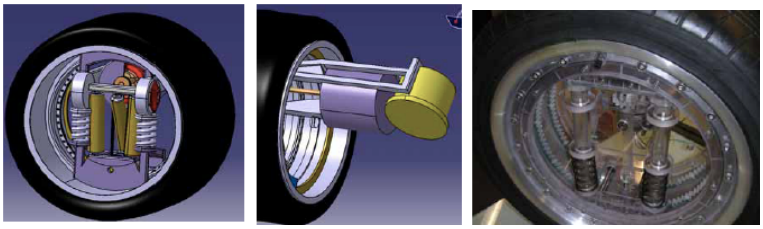

(a) Modular Drive System for a Concept Car [98]

(b) Prototype of Wheel-Drive Module [98]

Figure 4-25: Modular Drive System for a Concept Car with GM

was shown that for different configurations the drive system elements may have to be changed (either by adding on more modules or taking some away to keep the vehicle light). In recent years there have been several developments in automotive sub-systems that can directly enable an architecture in which is it easy to conceive a modular, easy changeable drive unit for planetary surface vehicles. An innovative prototype wheel with integral brake, steering, suspension, and drive motor has been developed as part of design and development of *GM's Concept Car* [98] (see Figure 4-25).

In addition to the drive system, sub-systems such as the crew station maybe able to undergo required reconfiguration (perhaps to adjust for passenger and/or cargo capacity as desired) by using a concept similar to what some new GM prototype cars such as HyWire [8] and Autonomy [7] are using. These are fuel cell driven cars. The fuel cell systems can be designed to fit almost any shape or body. They are inherently modular (in contrast to an internal combustion engine). The prototype vehicles house all of the drivetrain components on a skateboard-shaped chassis. The drive system instead of being one large electric motor, has four smaller motors connected directly to each wheel [7]. The mechanical interfaces are minimized between the passenger compartment and the drive system. For instance, the steering and brake commands are generated from a console with a joy-stick type controller and are communicated through wires or wirelessly to actuators on the wheels. This allows for great ease in changing the upper body of the vehicle in radical ways.

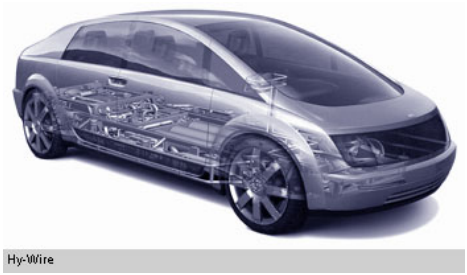

(a) GM HyWire prototype car [8]

(b) Skateboard Chassis [7]

Figure 4-26: Prototype Cars from GM

Chapter 5

Case Study-II: Communication Satellite Constellations

The previous chapter addressed multi-ability and survivability for reconfigurable systems. This case study addresses the issue of evolvability. Evolution is particularly relevant for large systems such as manufacturing systems, or space assets that require extensive capital and are subject to various uncertainties. The system chosen for analysis in this case-study is a communication satellite constellation. It has been previously shown that system deployment in stages, or evolution over time, can reduce economic risks for large capital intensive systems [49]. This case study explores how the design decisions of a satellite constellation can be affected if reconfigurability for evolvability is factored in.

Communication satellite constellations are normally designed for a fixed capacity and type of service. The economic troubles of Iridium and Globalstar, however, have illustrated the significant risks associated with large commercial satellite constellations. Both of these Low Earth Orbit (LEO) satellite communication systems projected a large customer base for a certain type of service (telephony along with fax, messaging, *etc.*) which did not materialize after the constellations were deployed. In service providing systems, one of the greatest uncertainties lie in the subscriber base, and due to increasingly dynamic markets it has become important for systems to be responsive to new or changed needs. A large amount of work addresses RMS in the context of stochastic demand [29, 145]. In the case of space systems however, the reconfigurability is inherently more difficult due to physical inaccessibility. This poses many technological and practical challenges that are not present in many other large systems (as discussed in earlier in detail in Section 3.1).

It was previously shown [49] that deploying and subsequently reconfiguring a LEO communication satellite constellation in stages can mitigate economic risks due to the uncertainties in subscriber demand. Such an evolution provides an "as-needed, as-afforded" approach which may allow system managers to delay decisions until there is greater certainty of market requirements. A few different methods have been proposed (and patented) for growing constellations in stages [77, 53].

In the traditional design process of systems that are fixed (*i.e.* consist of only one stage/state) the design that fulfills the requirements and is lowest in cost is generally selected for final implementation. If however, a system is to be designed with the capability of future reconfiguration to meet a new need, then it is unclear what the initial design (or state) should be. There can be several designs that are low cost and meet the fixed initial objectives of the system, but are not practically reconfigurable since they entail large costs (*i.e.* switching costs) for future adaptation. Similarly, there can be designs that meet the current objectives at somewhat higher cost but are capable of meeting new objectives at a later time at a lower comparative cost. This case-study focuses on evolvable satellite constellations and presents a methodology for determining the optimal design of a constellation that needs to reconfigure at a later time to meet a higher capacity demand.

In the case of satellite constellations, which is a System of Systems (SoS), one can envision reconfiguring the constituent elements (*i.e.* the individual satellites), or the whole SoS itself. In the former, the reconfiguration will essentially be intra-satellite reconfiguration, while in the latter it will be inter-satellite reconfiguration. There can be hybrid cases as well in which both inter- and intra-satellite reconfiguration takes place. This case-study focuses on an inter-satellite reconfiguration scenario.

5.1 Inter-Satellite Reconfiguration

The reconfiguration of a constellation for capacity expansion through inter-satellite reconfiguration can be achieved in a variety of ways. In one previous study [49] the reconfiguration involved moving existing satellites from higher to new and lower orbits and launching additional satellites. This allowed for reconfiguring from one 'optimal' constellation to another 'optimal' constellation, in which the optimality criteria is minimum number of satellites that provide global coverage and meet the capacity requirement. In such a case, for chemical propulsion the ΔV requirements for moving the satellites to different orbits that require plane changes can be prohibitive. If on the other hand, electric propulsion is used then communication outage costs become significant. Furthermore, changing the altitude of the satellites has inherent trades-offs of radiation shielding and hardening costs versus drag (which reduces the lifetime). At high altitudes, the radiation shielding and hardening costs are high, while at low altitudes the drag gets larger. A satellite deployed at a high altitude in order to change to a lower altitude orbit must have the amount of fuel to not only make an orbital change,

but also have enough to account for the higher station keeping requirements. On the other hand, if the altitude of the satellite is increased, then in addition to the fuel requirements of making the orbital change, it should have sufficient shielding as well. Its electronic components and other elements must have expensive radiation hardening, to withstand higher dosage levels and continue to function properly.

Keeping in view all these limitations, the method chosen here for reconfiguring the constellation to increase its capacity involves adding more planes and more satellites per plane in the constellation. The analysis presented here focuses only on this type of reconfiguration.

5.2 Designing for Evolvability

In some cases, evolution can often be for planned states (for strategic reasons, or resource availability issues *etc.*) in which the future states are known in advance. A more common situation is, however, when the future states are not known. In such a case, a comprehensive analysis should be undertaken in which all the possible scenarios are explored, and a design that performs best in a spectrum of different possibilities should be investigated. The implicit assumption is that the various scenarios, to which the system will be subject to, can be modeled and in doing so the possibilities are essentially finite. So the modeled uncertainty for the system will be bounded.

In the context of evolution, the fundamental question is that what should be the design of the system in its first state, so that it can readily reconfigure to future states, although the future choice of states are not exactly known.

In the case when the objective/goal for the first state is known, the first step can be to find the iso-performance surface for the initial objective in the design space [48]. The various objectives/goals to which the system will need to respond to are then modeled, and their corresponding iso-performance surfaces are also found. The problem then is to find the design that can reconfigure from a design that existed in the initial objective iso-performance surface, to one that exists in the future possible objective iso-performanc surface.

Suppose, the objective the system needs to fulfill in the first state or initial state is J_o. The set of objectives the system may need to fulfill in the future can be defined by a vector $\mathbf{J} = [J_1, \cdots, J_i, \cdots, J_k]$. The future objective may be one of the elements of $\mathbf{J}$. All the design vectors, $\mathbf{x}$, now need to be found where $\mathbf{x}_o \in \mathbf{I}_o$ and the set $\mathbf{I}_o$ is defined as:

$$\mathbf{I}_o = \{\mathbf{x} | J(\mathbf{x}) \equiv J_o\} \tag{5.1}$$

$$g(\mathbf{x}) \leq 0, \quad h(\mathbf{x}) = 0 \tag{5.2}$$

$$\mathbf{x}_{LB} \leq \mathbf{x} \leq \mathbf{x}_{UB} \qquad \mathbf{x} \in \Re^{n \times 1} \tag{5.3}$$

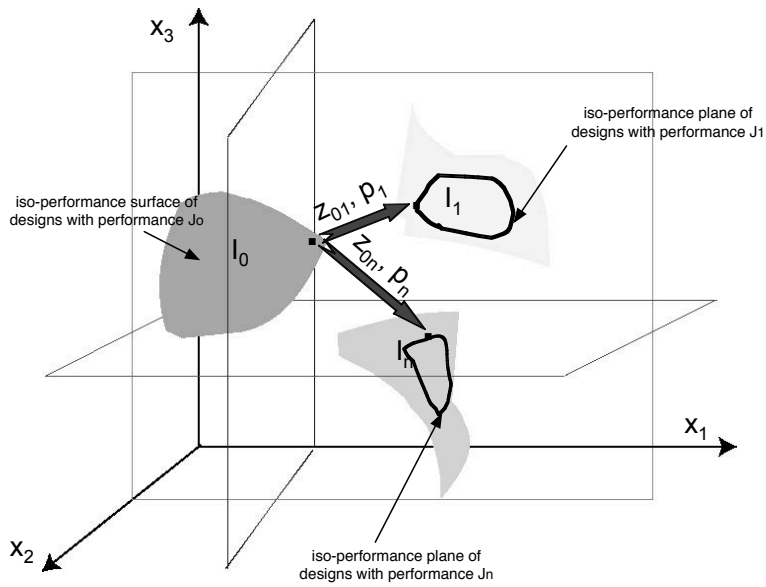

Figure 5-1: Design Selection for Future Evolution

For each $\mathbf{x}_o \in \mathbf{I}_o$, and $J_i \in \mathbf{J}$, the optimal design vector $\mathbf{x}_i^{'*}$ is found such that

$$Z_i(\mathbf{x}_o, \mathbf{x}_i^{'*}) \leq Z_i(\mathbf{x}_o, \mathbf{x}_i^{'}) \; \forall \; \mathbf{x}_i^{'} \in \mathbf{I}_i \tag{5.4}$$

$$\mathbf{I}_i = \left\{ \mathbf{x}_i^{'} | J(\mathbf{x}_i^{'}) = J_o \right\} \tag{5.5}$$

$$g(\mathbf{x}_i^{'}) \leq 0, \quad h(\mathbf{x}_i^{'}) = 0 \tag{5.6}$$

$$\mathbf{x}_{iLB}^{'} \leq \mathbf{x}_i^{'} \leq \mathbf{x}_{iUB}^{'} \qquad \mathbf{x}_i^{'} \in \Re^{m \times 1} \tag{5.7}$$

$$m \leq n \tag{5.8}$$

where $Z(i\ ,\ j)$ is reconfiguration cost in reconfiguring from design/state i to j. Note, that m is less than or equal to n here, which essentially means that in the initial problem when the iso-designs for state A are being found the design vector can be large and have several variables. However, once the initial designs have been selected, usually only a sub-set of the design variables can be chosen in determining the designs of the future states. The rest remain fixed. This is notionally illustrated in Figure 5-1. The figure shows the case for a 3 variable design vector, $\mathbf{x} = [x_1,\ x_2,\ x_3]$. One may chose an iso-performance surface I_o that has performance J_o. From this surface, some designs may represent a system that is able to reconfigure to achieve states that are equal to designs present in surfaces I_1 up to I_n. These surfaces are sets of designs that fulfill some potential future requirements J_1 to J_n. However, suppose only variables x_1 and x_3 can be assumed to be reconfigurble, while x_2 cannot change once it has been assigned a value in I_o. Then essentially the problem reduces to finding designs that exist in the plane of $x_1 - x_3$, that have minimum reconfiguration costs z. In some

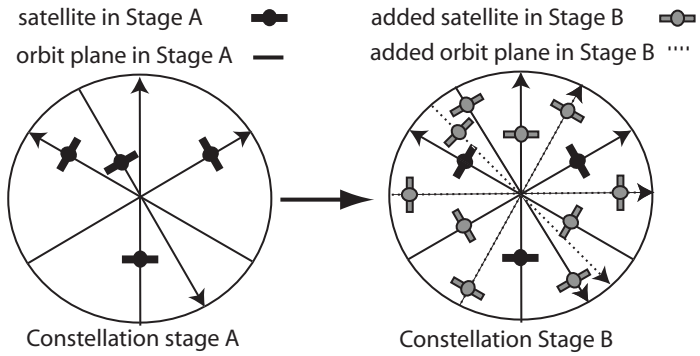

Figure 5-2: Constellation Reconfiguration from Stage A to Stage B

analyses, the future objectives J_i can have associated probabilities, p, and expected reconfiguration costs can be computed.

With the iso-capacity designs, $\mathbf{x}_o$, and their corresponding optimal future states determined, the evolvability is computed as described in Equation 2.44. The selection of final design candidates from the set $\mathbf{I}_o$, is then based on how the evolvability of the various $\mathbf{x}_o$ compares.

5.3 Initial Constellation State Determination

The methodology described above is applied in this case-study. In this analysis only polar constellations are considered [25]. It is assumed for simplicity that the constellation can have two states, A, and B. The first state/stage is designed to meet a known capacity demand (which is based on current market demand and can be assumed to be known with reasonable certainty). The second stage is an extension of the first stage in which more planes and satellites per plane are added so that a higher capacity demand is met. The design of the first stage thus needs to be such that it fulfills current requirements but is reconfigurable so that it can fulfill a new but unknown requirement at a later time. The set of potential new requirements is however bounded by a discrete set of future scenarios. Figure 5-2 shows the top view of the Earth's pole and illustrates the reconfiguration process.

The specific problem investigated in this analysis is the determination of the optimal initial stage, A, of the constellation that fulfills an existing capacity requirement C_A, and has minimum reconfiguration cost for meeting an uncertain demand by reconfiguring into stage B that has a higher

capacity.

The initial capacity, C_A , which the first stage, A, has to provide is chosen as a fixed parameter. To make the problem amenable for computation, the future uncertain demand is modeled as a vector of discrete capacities $\mathbf{C}$. It is also assumed that the constellation only undergoes a reconfiguration for a higher capacity demand, *i.e.* $\forall\, C_i \in \mathbf{C},\ C_i > C_A$. The methodology followed for obtaining a solution for this problem consists of the following steps:

- Specify set of discrete capacities $\mathbf{C}$ that could potentially be needed in the future:

$$\mathbf{C} = [C_1 \cdots C_i \cdots C_m] \tag{5.9}$$

  These are the capacity levels that the constellation will have in stage/state B.

- Find the set of iso-performance designs $\mathbf{I}_o$, (in which each design has same capacity C_A within some specified percent, ϵ_{tol}). One of the elements of the set $\mathbf{I}_o$ is the initial constellation that should be deployed to provide the known capacity C_A. However, it needs to be determined which particular element, $\underline{\mathbf{x}a}_i$, of $\mathbf{I}_o$ is the optimal solution given the requirement of reconfiguration for a higher capacity in the future.

- For each constellation $\underline{\mathbf{x}a}_i \in \mathbf{I}_o$, the optimal new constellation, $\underline{\mathbf{x}b}_{ij}$, that meets capacity demand $C_j \in \mathbf{C}$ is found such that reconfiguration cost between $\underline{\mathbf{x}a}_i$ and $\underline{\mathbf{x}b}_{ij}$ is minimized.

- The reconfiguration cost of each $\underline{\mathbf{x}a}_i$ is computed for reconfiguration into the corresponding optimal $\underline{\mathbf{x}b}_{ij}$ for each capacity requirement C_j. For n elements in $\mathbf{I}_o$, and m elements in $\mathbf{C}$, a cost matrix $\mathbf{R}$ of dimensions $[n\ m]$ is generated in which element r_{ij} is reconfiguration cost with $\underline{\mathbf{x}a}_i$ as initial constellation that reconfigures into $\underline{\mathbf{x}b}_{ij}$ to meet new capacity demand C_j.

$$\mathbf{R} = \begin{bmatrix} \overbrace{r_{11}}^{C_1} & \overbrace{\cdots}^{C_i} & \overbrace{r_{1m}}^{C_m} \\ \vdots & \vdots & \vdots \\ r_{n1} & \cdots & r_{nm} \end{bmatrix} \tag{5.10}$$

- The best initial constellation, denoted as $\underline{\mathbf{x}a}^*$, is determined by finding the constellation $\underline{\mathbf{x}a}_i$ that has greatest evolvability (as defined earlier in Equation 2.44).

Figure 5-3 summarizes the steps graphically.

It should be noted that although reconfigurable system as defined in this work are those that can reversibly achieve different configurations, in this particular case the reversibility is not factored in. Given the specific context of the problem, it is meaningful to consider expansion (rather than contraction of the deployed space assets). So in this case, a more limited focus on the reconfigurations is used.

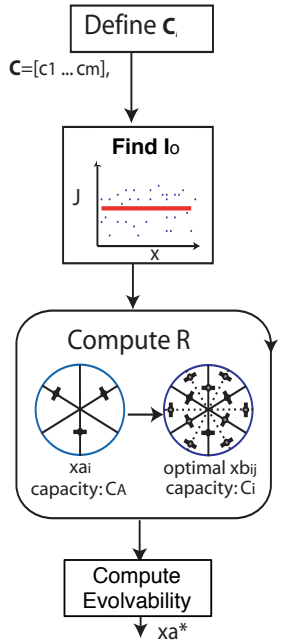

Figure 5-3: Flowchart for determining optimal initial constellation

5.4 Satellite Constellation Reconfiguration Modeling

A MATLAB framework, for modeling polar, global coverage, LEO communication satellite constellations providing telephony service, was used in this study. The framework had several benchmarked and validated modules [52], and several new modules were created to carry out the necessary analysis as outlined in the previous section. Figure 5-4 illustrates the solution framework schematically. A description of the main modules is provided below (the 'fixed constellation design selector' and 'Evolvability Analyzer' are discussed later in Section 5.6).

5.4.1 Constellation Capacity

INPUTS: constellation altitude, h, minimum elevation angle ϵ_{min}, total number of satellites N_{sat}, satellite antenna diameter D_a, satellite transmit power P_t, and type of multi-access scheme, MA.
OUTPUTS: Total number of channels in constellation, $N_{chConstel}$, and total number of subscribers, C.

The constellation capacity in this analysis is defined as the number of subscribers that the constellation can support. The module uses some fixed parameters which are given in Table 5.1. The values of the parameters are based on the Iridium satellite constellation which uses an MF-TDMA multi-access scheme and Globalstar constellation which uses MF-CDMA. These values are chosen so that the results from the analysis are close to a realistic scenario. It is assumed that

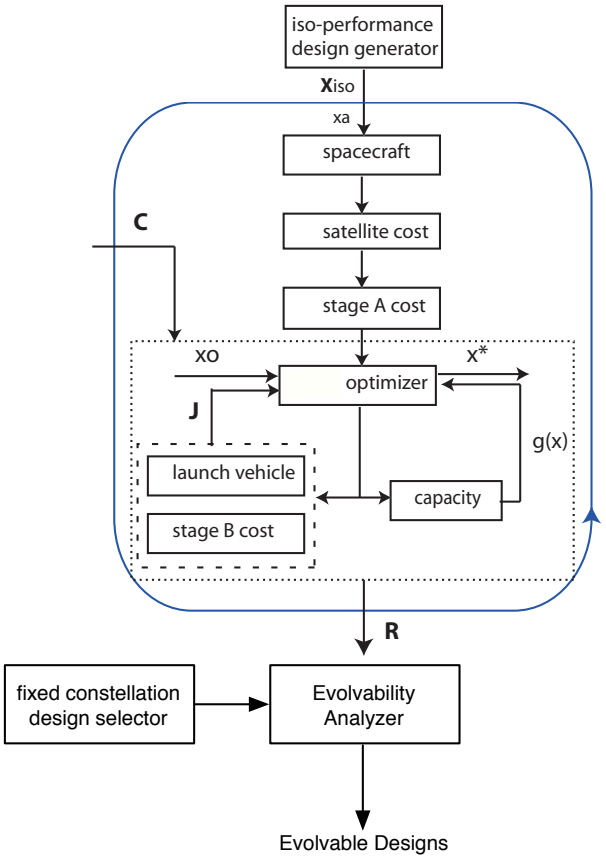

Figure 5-4: Block diagram of framework modules.

Table 5.1: Link parameters of Iridium and Globalstar used in calculating capacity for MF-TDMA and MF-CDMA systems

Parameter	MF-TDMA	MF-CDMA
downlink frequency [GHz]	1.6239	2.5
BER	0.001	0.01
Convolutional code rate	0.75	0.5
T_f [ms]	90	-
R_b [bps]	4800	2400
T_g [ms]	0.36	-
B_{sat} [MHz]	5.15	11.35
B_T [kHz]	41.67	1230
B_g [kHz]	1.236	-
K	12	-
Channels per cell	10	9
Modulation Scheme	QPSK	QPSK
l_m [dB]	16	6

the satellites use multiple spot beams to allow for frequency re-use. It is also assumed that the increased beam interference due to the addition of satellites and planes in the constellation will be compensated with power control and position-dependent frequency assignment [85].

In the current implementation, the module computes the capacity for only two types of multi-access schemes: MF-TDMA and MF-CDMA. For the MF-TDMA scheme, the number of channels per cell (spot beam) is computed as [40]

$$N_{ch} = \frac{1}{2K} \frac{B_{sat}}{B_T + B_g} \frac{R_b T_f - F}{n_{bits} + R_b T_g} \tag{5.11}$$

In the MF-CDMA scheme, N_{ch} is calculated as [40]

$$l_d = \frac{k_B T_s R_b l_m}{P_{cell} G_t G_r L_{tot}} \tag{5.12}$$

$$B_d = \frac{B_{ch} T}{R_b \alpha (1 + f)} \tag{5.13}$$

$$N_{ch} = \frac{T + B_d \frac{I_{tot}}{E_b}}{1 + B_d l_d} \tag{5.14}$$

In the present analysis only polar constellations are considered, therefore after accounting for the polar overlap factor the total number of channels per satellite is given as [40]:

$$N_{chConstel} = 0.68 Z N_{ch} N_{sat} \tag{5.15}$$

Note, that since it is reasonable to assume that not all the subscribers will be using the system simultaneously, the actual number of channels in the system will be less than the total subscriber base of the communication satellite constellation. Lutz and Werner [86] have defined how the total number of subscribers can be calculated based on the number of channels, a global utilization factor, U_s and user activity level A_{user}:

$$C = \frac{U_s \frac{365}{12} 24 \cdot 60 N_{chConstel}}{A_{user}} \tag{5.16}$$

This module has been benchmarked using data from the Iridium and Globalstar satellite constellation. For the Iridium case, the number of channels in the constellation is computed to be 75,000 (Iridium had 84,000). According to Lutz the typical values for U_s are between 10% to 15%. Using a mean value of 0.12 for U_s and 125 min/month [49] for A_{user} the number of subscribers is 2.5 million (Iridium designed the system for a target subscriber base of 3 million). For Globalstar, the number of channels per satellite were reported to be 2500. The module computes the number of channels to be 2900. The results are therefore in reasonably good agreement.

5.4.2 Iso-Performance Design Generator

INPUTS: Tradespace of constellation designs, desired capacity, tolerance, ϵ_{tol}

OUTPUTS: set of iso-capacity designs, $\mathbf{I}_o$

Iso-performance designs are designs that have equal performance. There are a few different algorithms that can be used for determining iso-performance contours in a multi-variable design space [48]. However for simplicity, this module performs a full factorial evaluation of a constellation design space and selects all the designs that provide full global coverage and meet a required capacity level with a tolerance of ϵ_{tol}. The variables in the design space are number of planes, p, number of satellites per plane, s, altitude, h, minimum elevation angle, ϵ_{min}, satellite antenna diameter, D_a, satellite transmit power, P_t, and multi-access scheme, MA. The design space used in the case study for finding the iso-performance designs was

$$
\begin{aligned}
&3 \leq p \leq 7 \\
&8 \leq s \leq 14 \\
&h = [800 : 50 : 1450] \ km \\
&\epsilon_{min} = [8 : 0.5 : 10] \ deg \\
&D_a = [0.4 : 0.4 : 2.0] \ m \\
&P_t = [150 : 50 : 500] \ W \\
&MA = [1, 2]
\end{aligned}
$$

A value of 1 in MA was for MF-TDMA, and a value of 2 was for MF-CDMA. It should be noted that p and s are variables in the trade space in addition to h and ϵ_{min}. Usually only h and ϵ_{min} are treated as independent variables, since for polar constellations (which were the only type considered here) the minimum number of planes and satellites per plane can be determined analytically for global coverage based on only these two specifications [25, 112]. However, the goal in this problem is not to be limited by constellations that minimize number of satellites (which is the traditional approach). Therefore, p and s are treated independently. This reconfiguration strategy (of addition of planes and satellites) thus essentially turns an initial single-fold coverage constellation into an n-fold coverage constellation (in stage B).

All the designs that are generated by the combination of the variables are tested for single-fold global coverage and those that do not meet full coverage criteria are discarded.

In the specific problem analyzed, designs with a capacity C_A of 150,000 subscribers within a tolerance of $\pm 0.5\%$ were obtained from the isocapacity generator module. This level of capacity was picked to reflect the approximate subscriber base that Iridium and Globalstar actually achieved during the intial years of full operation. The generator produced 24 iso-capacity designs, $\underline{\mathbf{x}a_i}$, shown in Figure 5-5. The $\mathbf{I}_o$ set thus initially had 24 elements in this case study. A few designs however

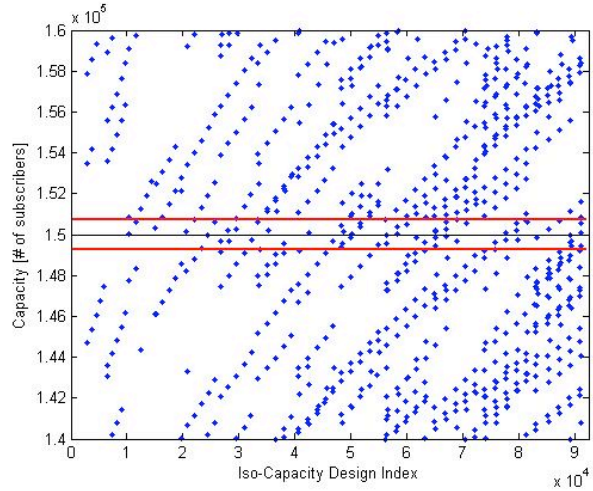

(a) iso-capacity designs

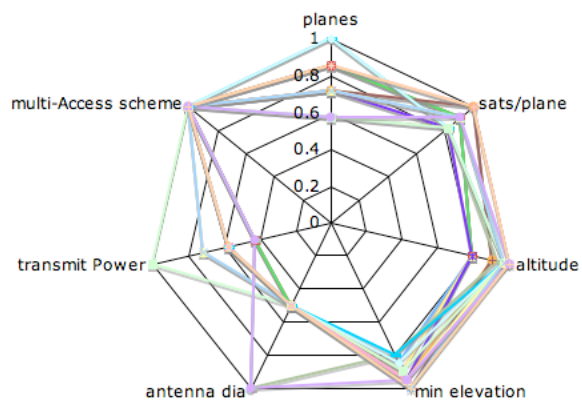

(b) radar plot

Figure 5-5: Iso-Capacity designs generated for capacity of 150,000 subscribers.

were later found to be infeasible in the sense that they could not reconfigure to all the capacity levels in **C**. Those were discarded, and the final set of designs were 16 in total. The radar plot (normalized with maximum value of each variable) of those design vectors, $\underline{\mathbf{x}a_i}$, shows that there was an even spread in values of p, s, h, ϵ_{min}, and P_t, however the values for D_a were limited to only a few specific ones, while the multi-access scheme was always MF-TDMA. Table 5.2 shows the design variable values in the 16 selected vectors.

5.4.3 Spacecraft

INPUTS: altitude, h, transmit power, P_t, antenna diameter, D_a number of inter-satellite links (ISLs) on a satellite, and satellite design life, T_{sat}

OUTPUTS: satellite total power, P_{tot}, wet mass, M_{sat-w}, dry mass, M_{sat-d}, and volume, V_{sat}

Table 5.2: Designs with 150,000 subscribers capacity

#	p	s	h [km]	ϵ [deg]	D_a [m]	P_t [W]	MA
1	6	10	1150	8.5	0.4	150	1
2	6	10	1150	9	0.4	150	1
3	5	9	1150	9	0.4	200	1
4	6	10	1150	9.5	0.4	150	1
5	5	9	1150	9.5	0.4	200	1
6	5	11	1300	9.5	0.4	200	1
7	5	11	1300	10	0.4	200	1
8	4	9	1350	8	0.8	150	1
9	7	9	1400	8	0.4	200	1
10	7	9	1400	8.5	0.4	200	1
11	4	9	1400	9	0.4	350	1
12	5	10	1400	9.5	0.4	250	1
13	5	10	1400	10	0.4	250	1
14	6	11	1450	9.5	0.4	200	1
15	4	10	1450	9.5	0.8	150	1
16	6	11	1450	10	0.4	200	1

The spacecraft module is based on a parametric non-geostationary satellite model originally developed by Richharia [111], and improved by Springmann [130]. This module is used for estimating the mass and volume of a LEO satellite based on basic input design parameters. The outputs provided by this module are subsequently used for selecting launch vehicles and estimating satellite costs.

5.4.4 Launch

INPUTS: M_{sat-w}, V_{sat}, altitude h, inclination of the orbit i, max allowed satellites per launch vehicle, number of planes in stages A and B, p_A and p_B, and number of satellites per planes in stages A and B, s_A and s_B respectively.
OUTPUTS: launch vehicle type, number of launches required, number of satellites per launch vehicle, launch costs.

This module uses a Matlab database to select a suitable launch vehicle that gives minimum total launch cost. The database is populated with information from Isakowitz's launch reference guide [74] and contains information of US, European, Chinese, and Japanese launchers. It is assumed that international launches are permissible (which may not always be the case in reality due to policy issues).

The module, based on the satellite data, selects all launch vehicles that are capable of delivering that payload to the specified orbit, computes the number of required launches, and based on the costs selects the vehicle that has the minimum total launch cost. It is assumed that a particular

launch delivers payload to a single plane and does not make plane changes within the same launch mission.

5.4.5 Cost

The constellation initial deployment (state A) costs are computed as the sum of satellite development, manufacturing, and launch costs. Reconfiguration costs include manufacturing costs of additional satellites and launch of additional satellites only. Other programmatic cost segments such as operation costs *etc.* are not factored in.

The satellite costs are determined from a simple cost model, SVLCM [14], that provides a rough-order-of-magnitude cost estimate based on the dry mass of the spacecraft. The model gives estimates of the development and production cost of un-manned Earth orbiting spacecraft. The SVLCM is a top-level model derived from the NASA/Air Force Cost Model (NAFCOM) database.

Radiation shielding costs are also included in the satellite costs. The radiation shielding cost estimator takes the altitude of a circular polar orbit, the lifetime of the satellite, and the thickness of its aluminum shielding in centimeters and approximates the hardness required of the vehicle and the percent total cost of the vehicle to include that hardness. The cost relationship was obtained from [142]. The total dose equation was developed by running the CRRESRAD model in the Air Force Geospace modeling environment for polar orbits from 350 km to 2050 km in 50 km increments for 1 year. The data was then surface fitted to obtain a parametric relationship. The additional costs incurred in making electronic and other components radiation hardened were not factored in here.

5.4.6 Constellation State B Determination

The second stage of the constellation that meets a given capacity demand occurring in the future with some probability is determined through optimization. For each iso-performance design, $\underline{\mathbf{x}a}_i$ at a capacity level of 150,000 subscribers, the optimal constellation it should reconfigure into (based on minimization of the reconfiguration cost) is determined for each capacity $C_j \in \mathbf{C}$. A range of capacity values from 300,000 subscribers to 1.5 million subscribers was used. Their were 9 different capacity levels that were modeled:

$$\mathbf{C} = 10^6 \times [0.3, 0.45, 0.6, 0.75, 0.9, 1.05, 1.2, 1.35, 1.5] \tag{5.17}$$

The optimal state B for each possible starting design $\underline{\mathbf{x}a}_i$ for each C_j is found by solving the following optimization problem:

$$
\begin{aligned}
&\min J = ReconfigCost(\underline{\mathbf{x}})_{A\rightarrow B} \\
&\text{s.t.} \\
&p_A \leq p_B \leq 5p_A \\
&p_B = kp_A,\ k = 1, 2, 3 \ldots \\
&s_A \leq s_B \leq 35 \\
&C_B \geq C_j\ (C_j \in \mathbf{C})
\end{aligned}
$$

The design vector $\underline{\mathbf{x}}$ used in this optimization problem consists of only two variables $\underline{\mathbf{x}} = [p, s]^T$. It is important to note that although in the iso-capacity design generator the design vector was $\underline{\mathbf{x}} = [p, s, h, \epsilon_{min}, P_t, D_a, MA]^T$, in this case the design vector is only a subset of that and is $\underline{\mathbf{x}} = [p, s]^T$. This is because once the constellation stage A has been fielded, satellite design parameters such as antenna diameter and transmit power are fixed (so that the same satellite designs could be reused in stage B). Since the reconfiguration process in this analysis was only considering addition of planes and satellites per plane, the design vector used for determining the reconfiguration cost to stage B only involves these variables.

For n iso-capacity designs, and m capacities (in $\mathbf{C}$), the optimization is performed nm times. In a particular optimization run, the p_A and s_A are the number of planes and satellites per plane in a particular $\underline{\mathbf{x}a_i}$.

The number of planes in stage B is restricted to be a multiple of the number of planes in A so that the inter-orbit spacing remains uniform in order to ensure uniform level of local capacity over the globe. A maximum limit of 35 satellites per plane is also set. The optimization was done by doing a full-factorial search (this was possible since the design vector had been reduced to only two variables).

Figure 5-6 shows an OPD of the modeled problem. It is easy to see that variables related to individual satellites (the antenna diameter, the transmit power, the multi-access scheme) are not affected by the reconfiguration. The reconfiguration process consists of two sub-processes of adding new planes and new satellites in existing planes. The addition of satellites in existing planes will require a change in the phasing of each previously deployed satellite within its orbit, however this is not specifically modeled, since the ΔV involved is expected to be small [39]. The colored objects highlight the two things that are changed. There are new satellites that get added to the constellation, and therefore the total capacity of the constellation changes.

5.5 Data Analysis for State A

Using the modules described above, the first set of data that was generated was the collection of iso-capacity design vectors that meet the initial demand of 150,000 subscribers. The details of those vectors were discussed earlier in Section 5.4.2. Using these vectors, the cost of deploying these various

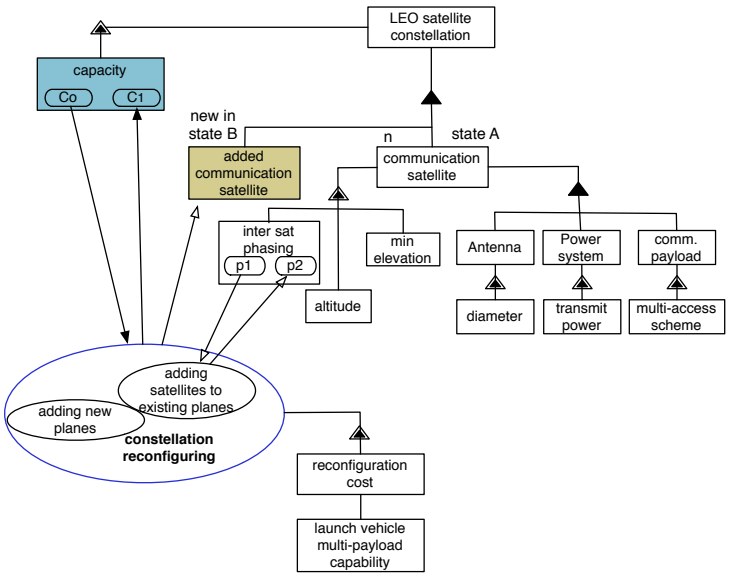

Figure 5-6: Object-Process Diagram of the Constellation Reconfiguration

designs was computed, and is shown in Figure 5-7. This is the cost of developing, manufacturing, and launching the satellites of the 16 iso-capacity constellations. It can be seen that there are clearly a set of designs that are better (*e.g.* 8, 9, 10, 14, 15) than another group of designs which are much higher in cost (*e.g.* 3, 5, 12, 13 and 16).

It is also interesting to note the effect of launch capability on cost. Since it was recognized that multi-payload capability of a launch vehicle, and risk issues can significantly affect the total costs when the deployment of a large constellation is being considered [124], six different launch scenarios were used. In the first case, each launch vehicle was allowed to carry a maximum of two satellites only (given that their mass and volume were feasible for its payload capacity). This limitation was imposed due to risk considerations, in which a large number of satellites may not be launched at once since the failure of the launch would entail the loss of many satellites. For instance, during the deployment of the Global Star constellation a failed launch of the Zenith vehicle caused the loss of 12 on-board satellites. In the second, third, fourth and fifth cases, the maximum allowable satellites per launch were 3, 4, 5, and 6 respectively. In the last case no limit from a risk perspective was imposed, and a launch vehicle was allowed to carry as many satellites as it could given its mass and volume capacity. All these six cases are shown in Figure 5-7, and the impact of the multi-payload issue on the deployment costs is clearly evident.

In the traditional approach, if the aim was to deploy a constellation that provides service to 150,000 subscribers, and would later not be reconfigured, the lower cost designs would be picked and given further consideration. However, the problem here is to determine which one should be used as the first stage, A, so that future reconfiguration is cheaper. Evolvability computations therefore

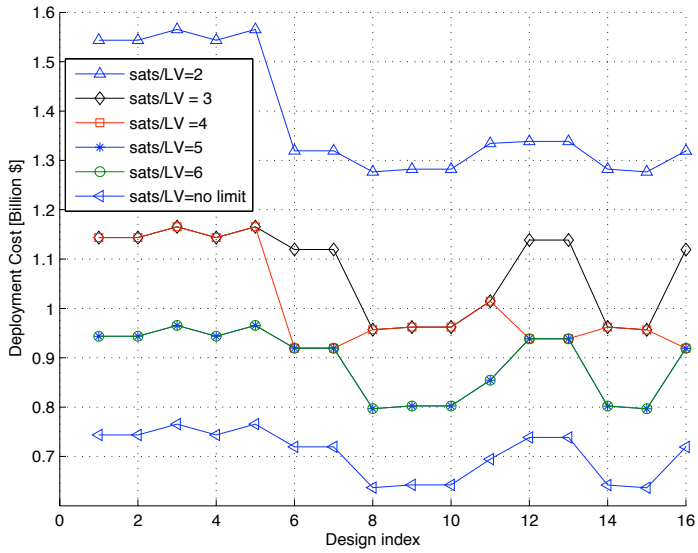

Figure 5-7: Stage A costs of iso-capacity designs

also have to factor in.

For each of the 16 potential state A designs, the best state B for each new capacity level (that is given in **C**) was determined. Thus 16 pairs of A-B configurations for each capacity level were found. The best B for each case was the one with lowest reconfiguration cost and could still meet the new and higher capacity level. The matrix **R** was thus generated as a result of this step.

Figure 5-8 shows the mean reconfiguration cost (across the different capacity levels), for each iso-capacity design. The value on the y-axis is essentially $mean([r_{i1}, \cdots, r_{i9}])$, for the ith design. This was also computed for varying launch cases, and the results are shown in the figure.

5.6 Evolvability Considerations

Once the data for potential state A candidates had been obtained and analyzed, another set of data was then generated to perform evolvability calculations. Recall that the evolvability had been defined earlier in Equation 2.44 as

$$\begin{aligned}\Delta_e &= \left(1 - \frac{C_r}{C_{new}}\right)\frac{J_r}{J_{new}} \\ &= \delta_C\ \delta_J\end{aligned}$$

In this case, C_r is the reconfiguration cost of the existing constellations (state A) to a new state B for some new capacity requirement. The performance J_r, is the capacity of the constellation in state B. The data for C_{new} is now also needed which is in this case the cost of deploying a new

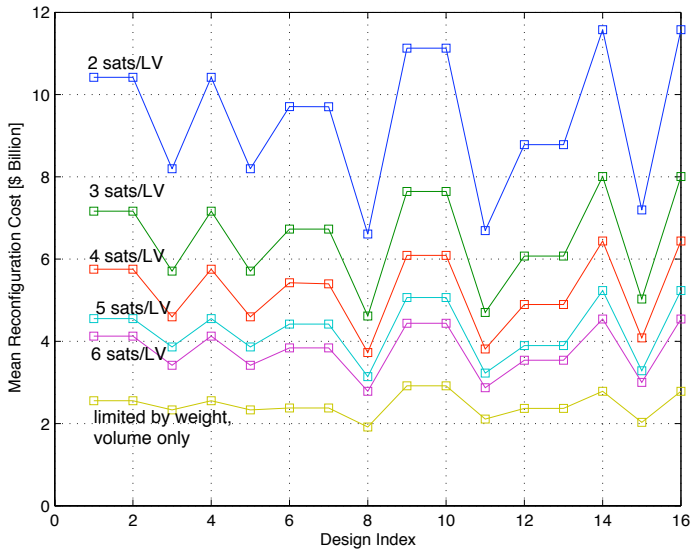

Figure 5-8: Reconfiguration Costs of state A constellations for varying capacity levels

constellation altogether to meet a new capacity demand at a later time. The J_{new} will be the capacity of the newly deployed constellation at the later time. Reconfiguration for evolution will be feasible if reconfiguration is cheaper to do, rather than deploying a new system altogether. It was discussed previously that the values of δ_C should be positive and δ_J should be equal or greater than one for reconfiguration to always be the better option.

Using the capacity values in **C**, that model the future demand levels a constellation may need to fulfill, a set of designs were found that are optimal in fulfilling those demands. The optimal designs were found by exploring a large trade space (see Figure 5-9), and picking the minimum cost designs for the given capacity level. This plot has the cost values for the case when the a maximum of 5 satellites are allowed per launch vehicle. As mentioned earlier, since the launch restriction issues factor in heavily in defining the constellation costs, the minimum cost constellations for each capacity level were found for each of the six launch scenarios described earlier. Figure 5-10 shows this result. As before, it can be seen that the minimum costs are when there are no restrictions (from a risk sense) on the maximum number of satellites a launch vehicle can carry at a time.

On comparing Figures 5-8 and 5-10 it is clear to see that the reconfiguration costs are high in general (as compared to deploying a new constellation altogether). For higher number of allowable satellites per launch, the deployment cost of new constellation will be lower. Reconfiguring an existing constellation will then be even more unfavorable. The only situation in which evolving an existing constellation will be advantageous, is when the number of satellites that can be deployed in a single launch is small. Figure 5-11 shows how the reconfiguration costs for each iso-capacity design (which is a potential candidate for state A) increase for increasing capacity levels (which

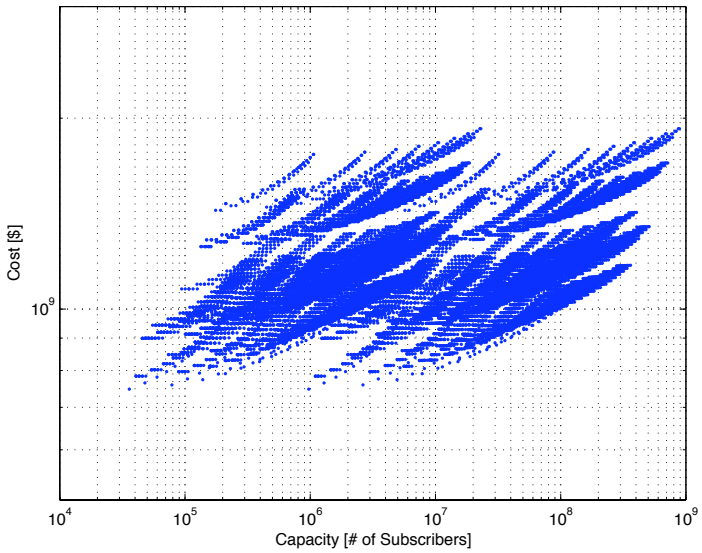

Figure 5-9: Trade space of satellite constellation designs

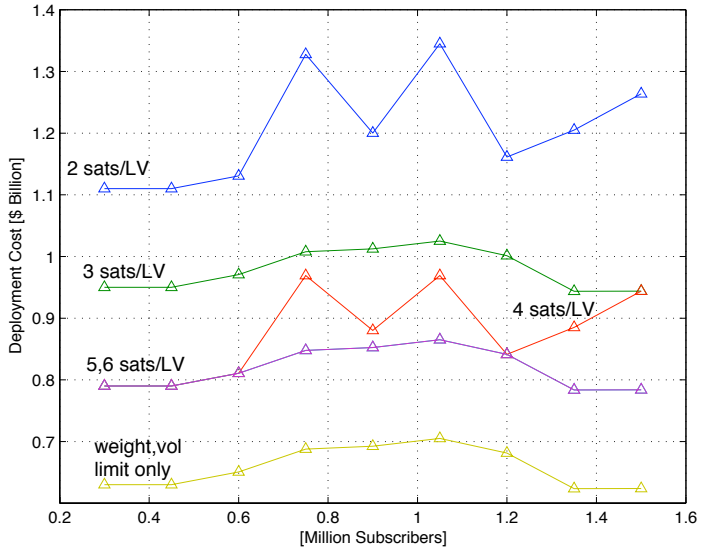

Figure 5-10: Costs of Constellations Serving Different Capacity Levels for Various Launch Restriction Cases

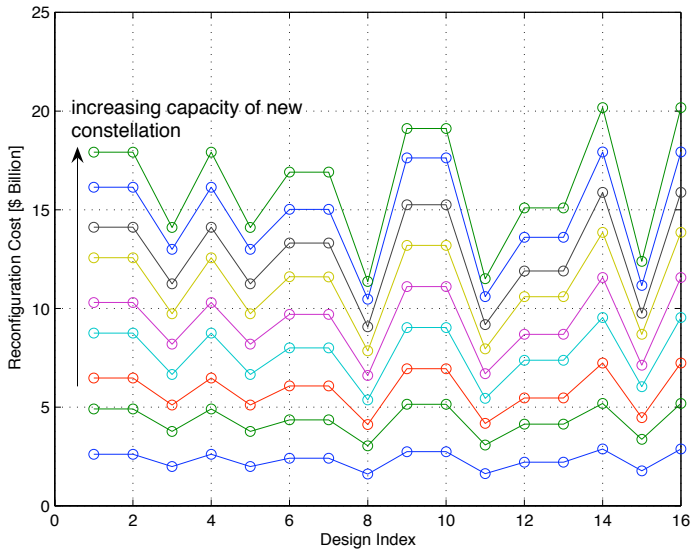

Figure 5-11: Reconfiguration Costs of state A constellations for varying capacity levels

state B has to achieve). The plot shows the case when launch vehicles have a limit of a maximum of two satellites per launch (since this is closest in comparison to the option of deploying a new constellation).

Using the cost data for reconfigurations, and the cost data of deploying a new constellation for the different capacity demands that may arise in the future, the δ_C was computed. Figure 5-12 confirms the results from the previous two figures that in most cases, and for most capacity levels, it is cheaper to deploy a new constellation (only the first three capacity levels of 0.3, 0.45 and 0.6 million are shown). The value of δ_C should be positive for reconfiguration to be favorable. However, it can be seen that except for a few designs (where it is close to zero but still negative), all other options give a negative value. This is due to the fact that there is a severe limitation on the reconfigurability that in order to ensure uniform coverage only multiples of planes in state A can exist in state B. Thus, if state A has 5 planes, state B can only have 5, 10, 15 planes *etc.* If planes are not added in multiples, then the coverage will not be uniform. Therefore the addition of only one or two planes was not considered. If only one or two planes were to be added, then in order for the coverage to remain uniform, the existing satellites will have to make orbital changes (which is prohibitive from a fuel sense). A further limitation arises when additional satellites are inserted in existing planes. Since a launch vehicle is assumed to not carry out a plane change, and only deliver satellites in a particular plane, there will be say 6 launches required to add 6 satellites, one each in one plane in a 6 plane constellation. A new constellation, however, does not have all these limitations. It can be designed for minimum number of satellites that give global coverage, and the satellites can be made more capable (large antennas, higher power *etc.*) to deliver the higher capacity. The only case

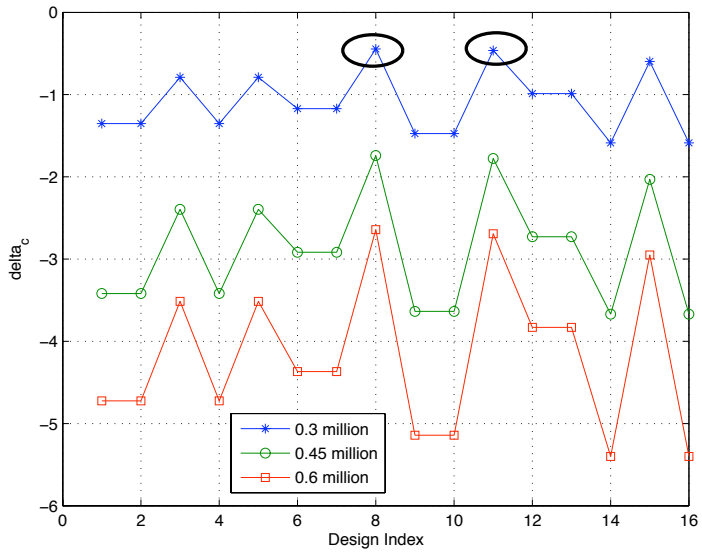

Figure 5-12: δ_C of state A constellations for varying capacity levels

when the cost of a new constellation becomes comparable, with reconfiguration option is for the 0.3 million subscribers capacity case, and when only few satellites are allowed to be carried on a launch vehicle. It can be seen as shown in Figure 5-12, that designs 8 and 11 come close to zero for the 0.3 million capacity case, indicating that the reconfiguration option cannot be completely ruled out.

The comparison of performance (which in this case is capacity), was also carried out to make sure that the fixed constellations are not worse off than the reconfigured state B solutions. Figure 5-13 shows the δ_J for the different cases and designs. It can be seen that it is very close to one. The value of δ_J was expected to be close to 1, since only solutions that satisfied the capacity levels had been selected for analysis. Recall that the iso-capacity designs that could not provide the required capacity levels in state B had been discarded earlier on.

Figure 5-14 shows the δ_C and δ_J plotted in the same graph. As pointed out earlier, for the 0.3 million capacity case (and no more than 2 satellites per launch), a few designs from the set of iso-capacity sate A designs can be reconfigured with perhaps almost equivalent costs as compared to deploying a new constellation altogether.

5.6.1 Best and Worst Designs

In summary, from the above analysis the general result that emerges in terms of evolvability of a LEO communication satellite constellation is that for some lower capacity levels (that are higher than the initial level however) can merit reconfiguration in the future. However if the capacity requirement is very high, it might be better to deploy a new constellation altogether. A review of designs 8 and 11 (that seem to be the best in terms of evolvability as compared to the other iso-designs of state

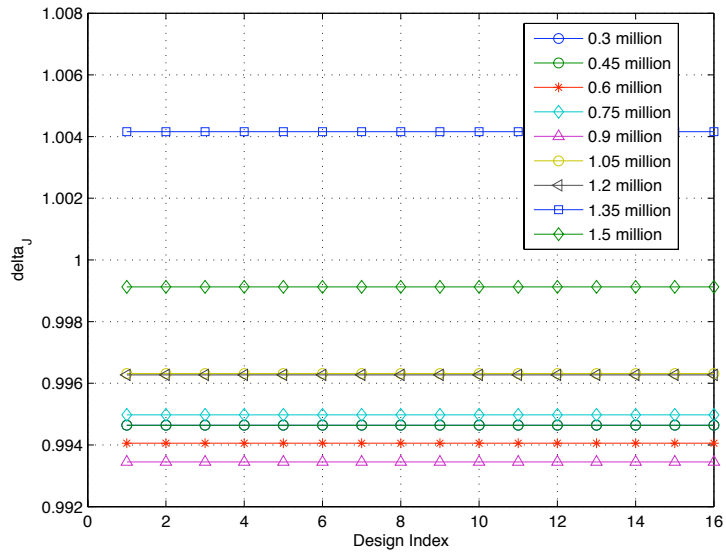

Figure 5-13: δ_J of state A constellations for varying capacity levels

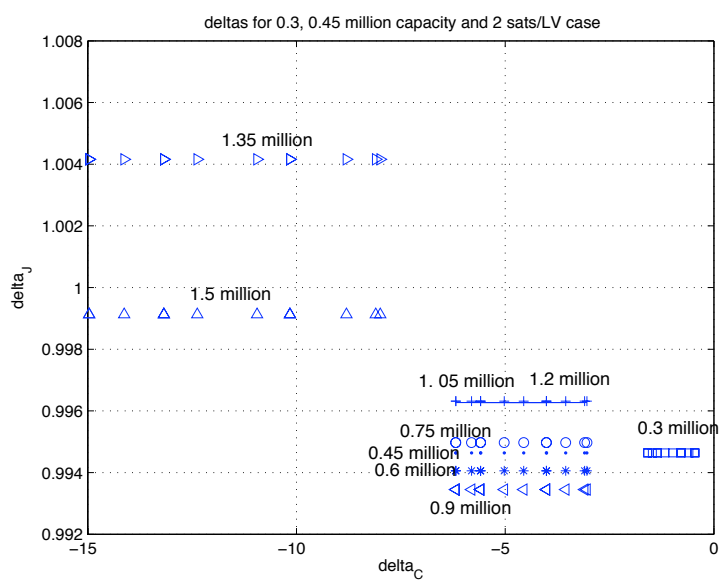

Figure 5-14: δ_J and δ_C for varying capacity levels

Table 5.3: State B Constellations for Reconfigurable State A Designs

#	C_1	C_2	C_3	C_4	C_5
8	[4, 27]	[8, 21]	[8, 27]	[8,34]	[12, 2]
11	[4, 27]	[8, 21]	[8, 27]	[8, 34]	[12, 2]
15	[4, 30]	[12, 15]	[8, 30	[12, 25]	[12, 30]

A) reveals that these are the constellations with few planes and satellites per planes (see Table 5.2). Each of these has 4 planes, and 9 satellites per plane. The design of the satellites is slightly different between the two (with larger diameter and lower power in #8 while smaller diameter and higher power in #11). Design 15 is also somewhat reasonable (with a δ_J close to zero). It also has 4 planes, but 10 satellites per plane.

The state B constellations into which the initial constellations of design 8, 11 and 15 need to reconfigure into for the first five capacity demand possibilities are shown in Table 5.3. The first element of each vector denotes the number of planes and the second element denotes the number of satellites per plane. For instance, in case of design 8, with originally 4 planes and 9 satellites per plane in state A, it will reconfigure into a constellation of 4 planes with 27 satellites per plane in State B to increase its capacity to C_1 (of 0.3 million subscribers). Figure 5-15 shows the evolution of design 8 from its state A to B. The particularly bad designs (such as 9, 10 and 16) are those with highest number of planes and satellites per plane. Design 9 and 10 have 7 planes and 9 satellites per plane each, while design 16 has 6 planes with 11 satellites per plane. Again, due the limitations of the reconfigurability (that only multiples of existing planes can be added), it is clear why this trend exists in the good and bad designs for evolvability.

In a previous study related to this problem [124], the expected life cycle costs had been computed for each initial constellation state A design, by assigning probabilities to the capacity values of **C**. The expected reconfiguration costs (which was the weighted sum of the reconfiguration cost for each possible future capacity level) was added to the initial deployment cost to get the expected lifecycle cost. Such an approach was not used here, since assigning the probabilities can be an arbitrary step (unless a very good forecast model is available which is usually not the case for the type of system being analyzed here). Furthermore, the results get combined and it can be hard to determine some key findings. For instance in this case, one can see that the lower capacity level is favorable for considering the reconfiguration option.

It should be noted that in many analyses where future 'switching' or reconfiguration of some sort is being considered for such large systems, an NPV computation is performed, in which the future 'switching costs' are discounted. There is thus a great dependence of the results on *when* the switching occurs, and the value of the discount rate. In this case an NPV analysis is not conducted, since the ratio δ_C will cancel out the discounting factor from both the C_r and C_{new}. Since the comparison is being made between a future reconfiguration cost and a future deployment cost, their

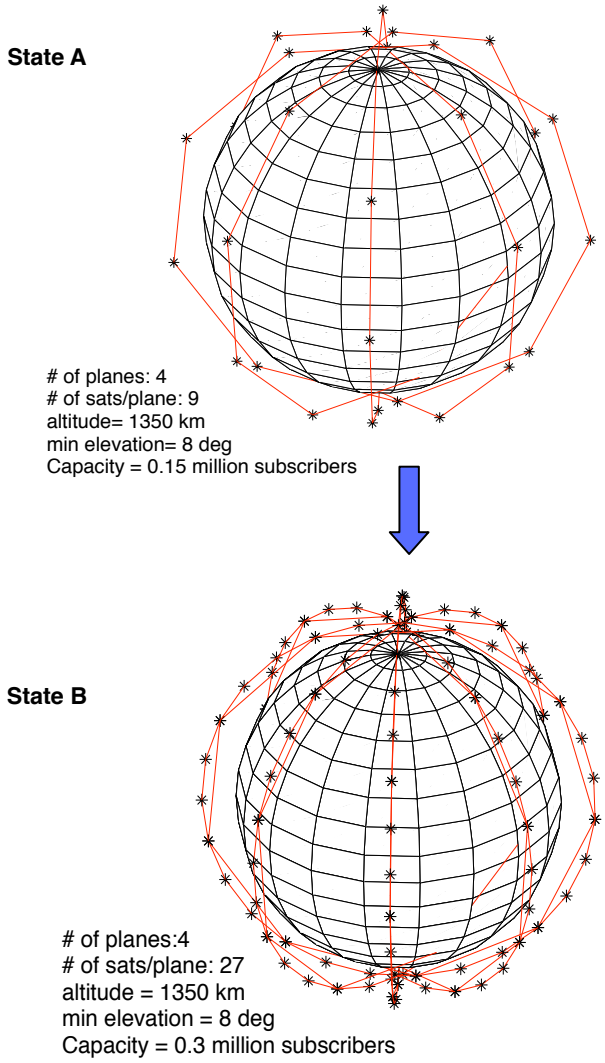

Figure 5-15: Evolution of Satellite Constellation Through Addition of Planes and Satellites

discounting factors will be the same (assuming that both occur within same period of time). In more detailed analysis, one could compare the difference in time that would be needed to deploy a new system, versus simply expanding an existing one *etc.* which can affect the outcome of the results.

5.7 Summary

In the specific case study analyzed in this work, the optimal solutions for stage A constellations consist of small satellites and lower number of total satellites as compared to the Iridium and Globalstar constellations. Furthermore, the evolution of an existing constellation can be favorable if the new capacity demand is not very large, and multi-payload launches are not carried out.

On the whole, it can be seen that the large launch costs, make constellation reconfiguration (through planes and satellites insertion) very expensive. It is apparent how the physical inaccessibility, and large ΔV requirements (as pointed out in Chapter 3) makes this problem so challenging. Nonetheless the desirability of making deployed constellations responsive to new needs remains strong given the large capital that is involved in these systems along with the high uncertainties. It should be noted that the results of this study are based on the specific assumptions (of allowing only addition of multiple planes for expansion). If others types of reconfigurations are considered along with more detailed financial analysis (factoring in NPV considerations), the results can be different.

Intra-satellite reconfiguration can potentially herald a new era of managing constellations to respond to new needs. Recent work in application of Software-Defined Radio for satellite transponders [99] holds great promise for future intra-satellite reconfigurability. The new Galileo satellites are already using on-orbit reconfigurable transponders for TT&C [37]. Radiation hardened FPGAs are also now commercially available and a few satellites have already flown using these devices [46]. Regenerative payloads are increasingly becoming common due to higher computational capabilities being available [50]. A significant amount of research in reconfigurable antennas has produced prototypes of systems that can reconfigure their operating frequency, beam-width and other relevant characteristics [148]. All of these technologies combine to make truly reconfigurable satellites a reality in the not too distant future. Such satellites will be able to change their type or level of service, use new multi-access schemes, and communication protocols *etc.*, to evolve with changing needs.

Chapter 6

Architecture of Reconfigurable Systems

The preceding chapters elaborated on the fundamental notions of reconfigurability (its definition, quantification *etc*), and used a few case studies to illustrate the systems-level trades offs for multiabiliy, evolvability and survivability. This chapter now focuses on a lower level in which components, modules and other architectural aspects are analyzed in the context of reconfigurability. For this end, a survey of 33 reconfigurable systems is first presented, along with a discussion of various common themes and trends that can be observed.

6.1 Reconfigurable Systems Survey

In order to assess how reconfigurable systems have been typically engineered, a set of 33 systems of different kinds was selected for analysis. There were three main types:

- Commercial/Consumer Items
- Air/Space Systems
- Manufacturing/Test

These categories weren't chosen apriori when the systems were selected, rather they became obvious after the selected systems were grouped in terms of their application/usage domains. Table 6.1 and Figure 6-1 show a listing and pictures of these systems respectively. A description of each of these systems is provided in Appendix B.

The *Functional Type* and *Complexity* in Table 6.1 have been assigned based on the definitions given in [87] and [69] respectively. For the functional types, the letters E, M and I are for energy, matter and information respectively. The number 1 is associated with functions that transform or

Figure 6-1: Some selected reconfigurable systems

Table 6.1: Set of Systems Used for Reconfigurability Analysis

#	Name	Functional Type	Compl-exity	Mass [kg]	Volume [m^3]	Cost [$]
1	Potentiometer	E1	1	0.01	1×10^{-6}	2.5
2	Airpot	E1	1	0.07	7.6×10^{-5}	20
3	LEGO	M1	1	1	3×10^{-3}	14
4	Vaccum	M4	2	7.5	6.88×10^{-2}	650
5	Food Processor	M1	2	6	1.5×10^{-2}	150
6	Sewing Machine	M1	2	9.18	4.7×10^{-2}	130
7	Convertible Stroller	M2	2	4.09	2.9×10^{-1}	70
8	Digital Photoframe	I3	2	0.82	8.6×10^{-4}	200
9	USM Haller Table	M3	2			5000
10	3-in-1 Crib	M3	2	36.4	1.44	250
11	Sofa Bed	M3	2	41.8	2.74	550
12	Adjustable Bed	M3	2	61.4	1.02	2700
13	Convertible Car	M2	3	1590	12	35,000
14	SMART car	M2	3	730	5.63	14,000
15	Flexible Race Car	M2	3	500	7.99	99,500
16	NI-RIO	I1	3	2	9.35×10^{-4}	2000
17	Reconfigurable Discrete Die	M1	3	3980	2	500,000
18	RMS	M1	4	32,700	166	1,000,000
19	Polybot	M2	3	3.6	2.3×10^{-3}	10,000
20	LARA	M2	3	50		
21	SRR	M2	3	10		
22	SMM	I1	3	2320	6.36	120,000,000
23	SWARM	I2	3	25	3.16×10^{-2}	
24	Xilinx Virtex II Pro FPGA	I1	3	0.001	7.29×10^{-6}	250
25	EHW	I1	3		6.25×10^{-6}	
26	Long life SC Avionics	I1	3		4.05×10^{-3}	180
27	SmartSat-I RCE	I1	3	16	1.82×10^{-4}	500
28	MEMS patch antenna	E4	2		1.25×10^{-6}	80
29	TTC Transponder	I1	3	2.9	6.97×10^{-3}	
30	Morphing UAV	M2	3	1360		
31	F-14 Tomcat	M2	4	33,800	1820	38,000,000
32	VDCH	M2	4	9,550	90.6	100,000,000
33	VLA	I4	4	6,210,000	376,000	79,000,000

process the operand, 2 is for transport or distribute, 3 is for store or house, 4 is for exchange or trade, and 5 is for control or regulate [87]. It can be seen that the selected systems mostly are described by M1, M2, M3 and I1 types, *i.e.* most of these systems are matter or information processing (M1, I1), or mass transportation (M2) or storage/housing (M3). There are however, a few other types also present. Note that these types are associated with the *primary* function of the system, for there are certainly several other sub-processes that are of different types and enable the primary function to be carried out. The definition of the complexity levels is as follows 1: component/part, 2: group, mechanism, sub-assembly, 3: machine, apparatus, device, 4: Plant, equipment, complex machine unit [69]. Most of the systems that were analyzed are at complexity level 2 or 3 (as can be seen from the table), however there are a few at level 4s.

It should be noted that these systems range from conceptual stage (*e.g.*Variable Diameter Compound Helicopter) all the way to full production and deployment stage (*e.g.*SMART car). Although it would be more suitable to only consider systems that have actually been deployed, the conceptual and prototype systems were included because reconfigurability (especially on a large scale at the architectural level) is a fairly new area of interest in system design. Consequently, many reconfigurable systems are currently only in the prototype or even proof-of-concept stages. Nonetheless, some useful information can still be obtained from these examples, and they have therefore been used in studying reconfigurability. Some kind of data such as cost *etc.* however could not be obtained for these cases (which is why there are some empty cells in Table 6.1).

Figure 6-2 shows a plot of the mass and volume of the systems on a log-log scale to provide a sense of the scale of variation of these quantities across the sample systems. Note that the volume was computed by simply multiplying the length, width, and breadth of each system (thus the volume of a box in which the system can fit was essentially obtained). The volume is therefore a first order estimate (and in some cases its more accurate value may be lower).

Figure 6-3 shows the cost (price in case of commercial items) in a log-scale graph to indicate the scale of cost among the sampled systems. The index on the x-axis corresponds to the system number in Table 6.1.

6.2 Requirements

The first aspect that can be probed are the requirements that drove the choice of having some kind of reconfigurability in these systems. For this purpose, the three application categories of commercial/consumer items, air/space systems and manufacturing/test systems were analyzed separately. System number 1 through 15 (*i.e.* from potentiometers to race car in Table 6.1) were the commercial/consumer items, from 16-18 (NI-RIO to RMS) were manufacturing/test, and 19-33 (Polybot to VLA) were designated as air/space systems. In this analysis, the multi-ability category was refined

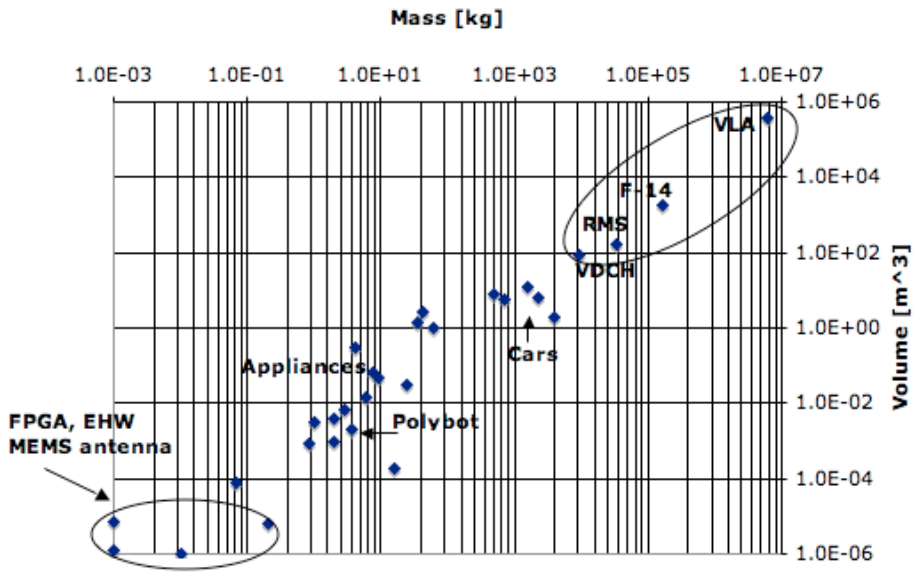

Figure 6-2: Mass and Volume of the Reconfigurable Systems That Were Studied

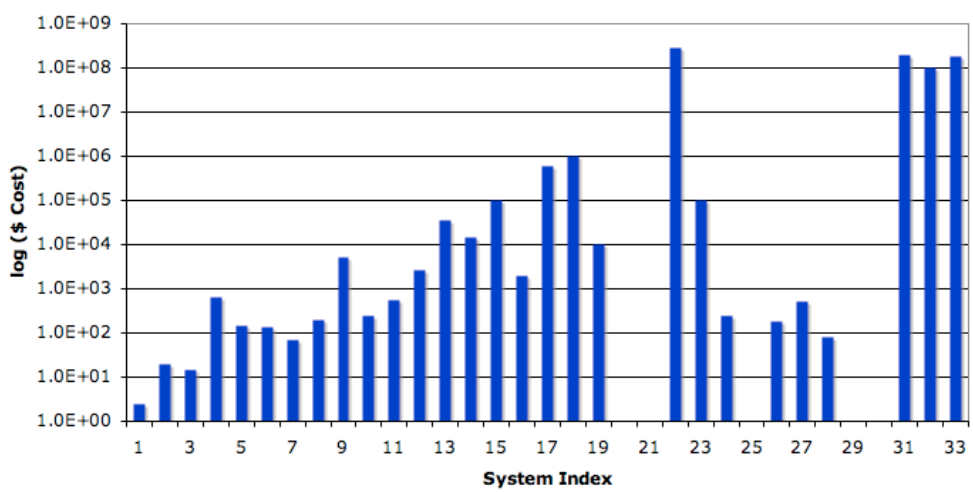

Figure 6-3: Cost of Reconfigurable Systems

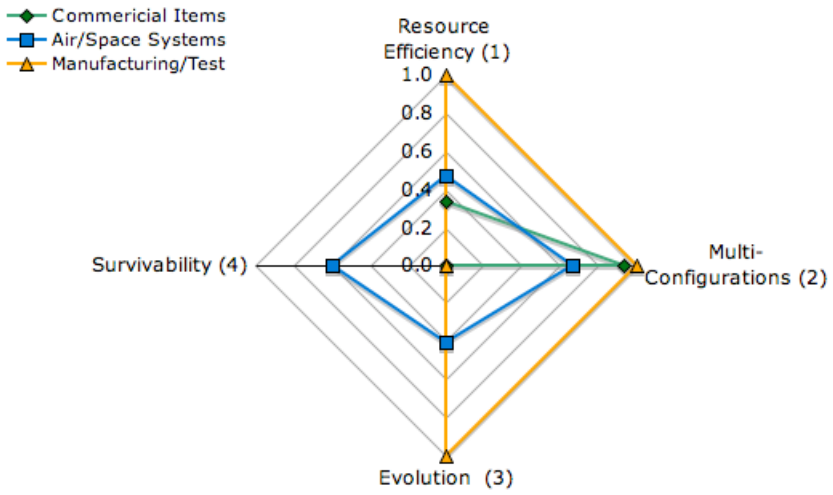

Figure 6-4: Reconfigurability Drivers for Systems in Three Application Domains

into two subcategories of 'resource efficiency' and 'multiple configurations' (that had been discussed in Section 2.2.1). The other two were Evolution and Survivability (as discussed in Section 2.2). These categories were then assigned to each system based on their stated objectives as found in their description and other relevant literature sources. A 33×4 matrix was created in which a value of one was assigned to the element in the ith row and j^{th} column if the ith system fulfilled the jth need sub-category. The percentage of systems assigned to each of these four categories (for each of the three application domains) was determined, and is shown in a radar plot in Figure 6-4. The detailed data for this figure is shown in tabular form in Figure B-25 in Appendix B.

It can be seen that the different classes show varying trends in the reasons for their reconfigurability. The consumer items are dominated by the two sub-categories of multi-ability. They either are reconfigurable due to resource efficiency requirements, or have multiple configurations for some planned or unplanned usage needs. Space systems on the other hand are motivated by requirements of survivability and evolution for unknown configurations in addition to multi-ability. In manufacturing, the systems resource efficiency, multiple-configurations, and evolution aspects all play a role. Although the number of systems in this application domain was very small (only 3), the results do seem to represent the characteristic nature of these types of systems.

Figure 6-5 shows the information for the Air/Space Systems in which the two sub-categories of resource efficiency and multi-configurations have been recombined into 'multi-ability'. A category will have a value of 1.0 if all the systems exhibit this particular category in their requirements. It can be seen that the multi-ability is the most often reason why air/space systems are made reconfigurable (80% from among the systems studied). The next big reason is survivability (60% in this case). It is interesting to note that evolution is the lowest category and indicates that air/space systems have

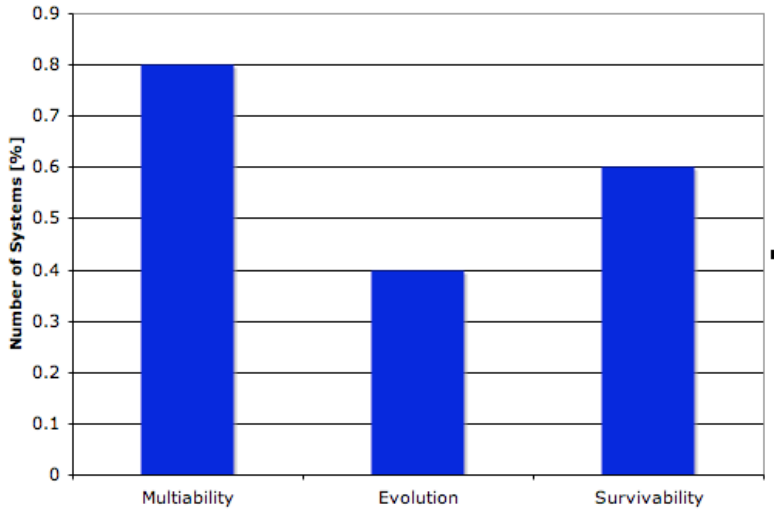

Figure 6-5: Reconfigurability Needs in Space Systems

not been traditionally designed and built for evolving over time as new needs unfold. In fact it is the mainly new systems (still in the conceptual or prototype stages) such as EWH, ANTS *etc.* that specifically are motivated by this issue.

6.3 Reconfigurability and Time

The time related aspects were studied for the systems for which relevant data could be obtained. The analysis was done from two perspectives. In the first a relationship between the reconfiguration time and state occupancy time was determined, and in the second the reconfiguration with respect to operational cycle of the system was studied.

6.3.1 Reconfiguration Time

Reconfiguration time, denoted as T_r, is the time a system takes to reconfigure from one state or configuration to its next state/configuration. Depending on the context it may include the total time spent in perhaps designing and finding the new configuration (*e.g.* in case of evolution) in addition to the actual time spent in carrying out the reconfiguration processes on/by the system. The agent (human or machine), and the processes used will have a direct effect on the minimum limits of the reconfiguration time. The reconfigurable systems that were studied (with details in Appendix B) were analyzed in terms of their reconfiguration times and the data is shown in Table 6.2.

For consumer items such as vacuum cleaners, food processors *etc.* the time was estimated from personal experience as a user of these systemss, where as for other systems such as the F-14, VLA *etc.* the reconfiguration time was obtained from actual data. In case of the Solar Maximum Mission

Table 6.2: Reconfiguration Times

#	Name	Reconfiguration Time	Average State Occupancy Time	Life [yrs]
4	Vaccum	30 [sec]	15 [min]	2+
5	Food Processor	60 [sec]	20 [min]	2+
6	Sewing Machine	10 [sec]	3 [min]	2+
7	Convertible Stroller	3 [min]	30 [min]	1+
8	Digital Photoframe	5 [min]	1 [day]	3+
10	3-in-1 Crib	30 [min]	12 [months]	2+
11	Sofa Bed	5 [min]	8 [hrs]	5+
12	Adjustable Bed	60 [sec]	2 [hrs]	2+
13	Convertible Car	3 [min]	30 [min]	
14	SMART car	2 [days]	3 [months]	
16	NI-RIO	15 [min]	8 [hrs]	5-7+
17	Reconfigurable Discrete Die	30 [min]	20 [hrs]	5+
19	Polybot	30 [sec]	5 [min]	
22	SMM	2 [days]	5 [yrs]	5+
23	SWARM	120 [sec]	30 [min]	
31	F-14 Tomcat	6 [sec]	15 [min]	30+ (7200 op hrs)
33	VLA	14 [days]	3 [months]	30+

(SMM) the reconfiguration time was taken to be the total time it took for servicing the craft (which was 2 days, since the first attempt to capture the satellite failed on the first day of the mission). It does not include the time of getting the mission approved, ready, and launched to carry out the reconfiguration. In case of SWARM also, the time is the docking time for the various modules based on the assumption that the docking-undocking procedures are what primarily constitute the reconfiguration process in the SWARM system [96]. For NI-RIO the data is again based on personal experience as a user, and for the reconfigurable discrete die, the data is based on a first order estimate and is meant to only capture the order of magnitude of the time.

The average time the system spends in a particular state or configuration, denoted as T_s, was considered to be the average state occupancy time. For instance the VLA stays in each of its four configurations A,B,C, and D for three months on average. So the T_s for the VLA is 3 months. For consumer items, and other items such as NI RIO or the reconfigurable discrete die, the T_s was again estimated from general experience and basic assumptions.

The log of the ratio of T_s and T_r was computed and plotted as shown in Figure 6-6. An interesting observation that can be made is that there is a lower bound of approximately 1 for this ratio, *i.e.* the reconfiguration time is never more than *at least* 1/10 of the time the system spends in a particular configuration. One might state that reconfiguration times that exceed 10% of the useful time in any given state render reconfiguration undesirable. This is a rule of thumb. The truly acceptable maximum T_r depends on the exogenous dynamics (also discussed earlier in Section 2.5). Note that this fact distinguishes reconfigurable systems from pure re-design or unplanned re-modeling.

It should be noted that where the data has been estimated from experience or on a first order

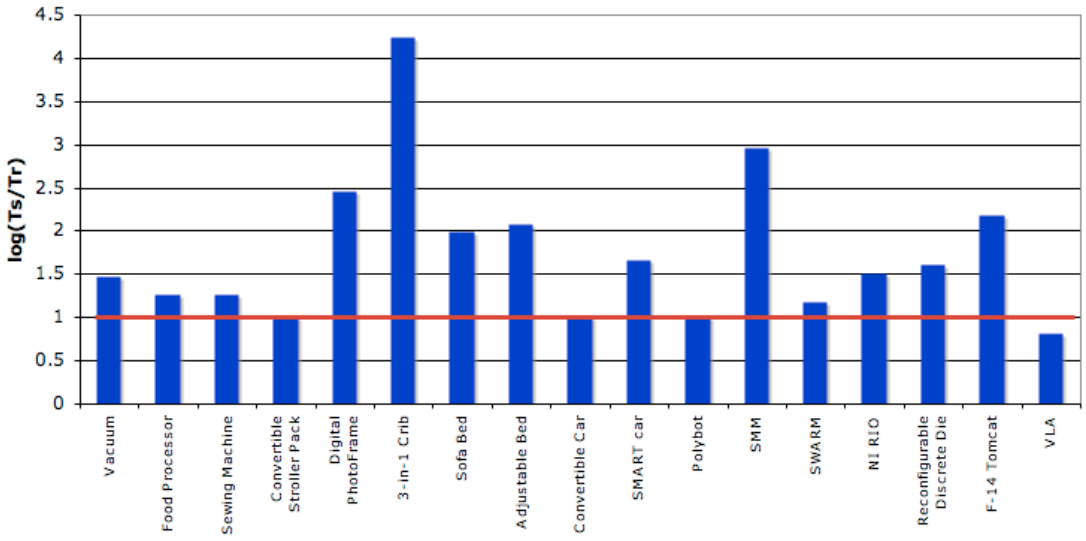

Figure 6-6: Reconfiguration Time Ratios

level, the lower limit for the state occupancy time, and an upper limit for the reconfiguration time has been used. Therefore, in reality, on average the state occupancy time for most of these systems will be longer, and the reconfiguration time will be shorter. The ratio will therefore be even higher and the proposed ratio of at least one tenth should still hold.

6.3.2 Operational Cycle

As discussed earlier, the differentiation of systems along on-line reconfiguration and off-line reconfiguration may provide some useful insights. The 33 systems that were studied, were grouped in these two categories, and it was found that there were sets of systems that fall into either one of these two categories, and there was also a set which can undergo both types of reconfigurations depending on the particular usage case.

The reconfiguring agent was also factored in this study. The reconfiguration agent can be external or internal to the system. Convertibles (with an electric mechanism) have an internal agent (which moves the roof), while in a SMART car the agent is external to the system (the body panels are manually changed out).

The set of systems was grouped according to the nature of their reconfiguring agent. Again, it was found that there were three types. In the first type, the reconfiguring agent is always a machine, in the second type it is a combination of humans and machines, and in the third type it is mostly humans (a manual process). This categorization is of course somewhat subjective. It can be argued that in almost all systems there is a combination of humans and machines involved in their reconfiguration. The assumption made here was that systems that undergo reconfigurations mostly through machines with the human input perhaps being limited to only touch of a button,

	Online	Online & Offline	Off-line
Machine	Adjustable Bed Convertible Car Flexible Race Car SRR EHW LongLifeSC Avionics SmartSat-I RCE MEMS patch Antenna Morphing UAV TTC Transponder F-14 Tomcat VDCH	Xilinx Virtex II Pro FPGA	Reconfigurable Die
Machine and Human		Potentiometer Airpot NI RIO RMS Polybot LARA SWARM	SMM VLA
Human			LEGO Vacuum Food Processor Sewing Machine Convertiable Stroller Digital PhotoFrame USM Haller Table 3-in-1 Crib Sofa Bed SMART car

Figure 6-7: Reconfiguration Agent and Operational Time Relationship

or a few simple commands will be designated as those that undergo 'machine' reconfiguration. For systems in which both humans and machines play equal/important roles, will be designated as the second type, and the third type will be those in which machines serve as mere tools, but the major role is carried out by humans. Figure 6-7 shows a 3 X 3 matrix in which all the 33 systems can be grouped. The instant observation that can be made is that only the diagonal blocks are populated. The lower left portion is conspicuously empty, while the upper right portion has barely any members (nonetheless it is not totally empty). This grouping however is logically obvious, since it can be seen that systems that can only reconfigure on-line are always machine actuated. So systems such as the morphing UAVs, the F-14, the Polybot *etc.* undergo reconfigurations through actuators and mechanisms built into them. They can therefore reconfigure on-line. The systems that can undergo both on-line and off-line reconfigurations (depending on particular use/application) employ both humans and machines. These are things like potentiometers, airpots, FGPAs, NI RIO, RMS. The third group can only reconfigure off-line. These are mostly the consumer items (vacuum cleaners, food processor *etc.*) that require human agents.

6.4 Quantification

Some of the metrics for quantifying reconfigurability that were introduced earlier, were applied for the systems (for which relevant data was available). This section illustrates the use of these metrics. Table 6.3 shows two kinds of information. For the systems where the states are discrete, the total

Table 6.3: Configurations Data

Name	# of Configurations	Name	Range
Vaccum	7	Potentiometer	5k-50k Ω
Food Processor	7	Airpot	0-30 lb/(in-sec)
Convertible Car	2	Flexible Race Car	0.329-0.52, 0.284-0.67, 0.31-0.508
Digital Photoframe	inf	Digital Photoframe	1-80 photos
Convertible Stroller	2	Reconfigurable Die	0-0.3 m (pin stroke)
USM Haller Table	510	USM Haller Table	3-38 (seats)
3-in-1 Crib	3	SRR	$\pm 45^o$ range in shoulder angle
Sofa Bed	2	Morphing UAV	233% wing area change
Adjustable Bed	6	VDCH	29.3 - 17.58 [m] rotor diameter
MEMS patch antenna	2	Sewing Machine	3-7,1-4 [mm] width, length of stitch
F-14 Tomcat	2	F-14 Tomcat	64.2, 38.2 [ft] wing span
VLA	4	VLA	200-0.05 arcsec (resolution)
SmartSat-I RCE	3,inf		1-36 [km] (separation)
TTC Transponder	2		

number of useful, distinct configurations are shown, while systems that have a continuous (or almost continuous) range of states, their limit or range information is shown. For the flexible race car, the data in the Range column gives the limits of the center of gravity, roll-stiffness and aerodynamic down force distribution. For more details see [106]. For the digital photoframe, and the SmartSat-I RCE the 'inf' is added to indicate that there are potentially infinite configurations that can be achieved through change of pictures or software respectively. So in case of the photoframe, at a time it can hold up to 80 different photographs, its different configurations (*i.e.* state of having a particular photograph) are limitless. Photos can be added on and removed infinitely. Similarly for the RCE, it has three main configurations for graceful degradation (discussed in Appendix B), however through change of software it can also change several functional attributes (like operating frequency, data processing *etc.*).

6.4.1 Reconfigurability Index and Coefficient of Variation

The use of the Reconfigurability Index (RI) as defined in Section 2.7.2 can be demonstrated here for the USM Haller table. Recall that the RI provides a measure of the range of capabilities the system can provide. So in this case the seating capacity can change from 3 to 38. So the RI is 35. As noted earlier, the RI is an absolute measure and is therefore only useful when comparing similar systems.

The data for most of the systems was more at the component/sub-system level (such as wing span limits, or resolution limits *etc.*) This is applicable for the coefficient of variation, c_v metric. However, data about the 'nominal' operating point or the most frequent operating point for most of these systems was unavailable, so the c_v was not computed here.

Table 6.4: Combinatorial Efficiency

Name	# of Configurations n_c	# of Modules N_m	Combinatorial Efficiency μ_c
Vaccum	7	8	0.88
Food Processor	7	8	0.88
USM Haller Table	510	9	56.67
3-in-1 Crib	3	8	0.38
Polybot	inf	18	inf
SmartSat-I RCE	3	7	0.43
VLA	4	27	0.15

Table 6.5: Relative Functional Efficiency (Ξ_f)

Name	F-System [$]	R-System [$]	Ξ_f	F-System [kg]	R-System [kg]	Ξ_f
Convertible Stroller	44.99+39.99	69.99	1.2	4.6+1	3.5	1.6
3-in-1 Crib	291 + 145	413	1.05			
Reconfigurable Discrete Die	$300 \times 19,000$	500,000	11.4			

6.4.2 Combinatorial Efficiency

For calculation of the combinatorial efficiency, only systems with discrete states, and modules were considered. Those systems and their total number of modules are shown in Table 6.4. For the polybot case (where a system of 18 modules had been considered as a sample), the number of configurations (in which the system can usefully operate) are practically infinite. Its μ_c, which is the ratio of n_c and N_m is then also infinite. The thing that should be noted is that systems with identical modules, or with very similar modules that have few connectivity restrictions, will end up with very large values of μ_c. The USM Haller table and Polybot therefore have significantly large values as compared to others. Although the VLA also has identical modules (the telescopes), their connectivity restrictions are fairly high (only can be arranged in 4 ways), and therefore its μ_c is low. For LARA, it can be expected that the μ_c will also be very high, but since information about its number of modules (in a representative system) was not available, its μ_c was not computed. It can be assumed however that in most cases it too will be infinite (similar to the Polybot case).

6.4.3 Relative Functional Efficiency

The Relative Functional Efficiency, Ξ_f can be employed for systems where resource efficiency was a motivating factor for making the system reconfigurable. Considering the data that could be obtained in this regard, (along with the requirement of resource efficiency), Ξ_f was computed for three systems shown in Table 6.5. The 'F-System' denotes a fixed system counterpart, and the 'R-System' column has data for the reconfigurable system under study. For the fixed system, there are two or more systems that combine to give the equivalent functionality of the reconfigurable system. The plus or

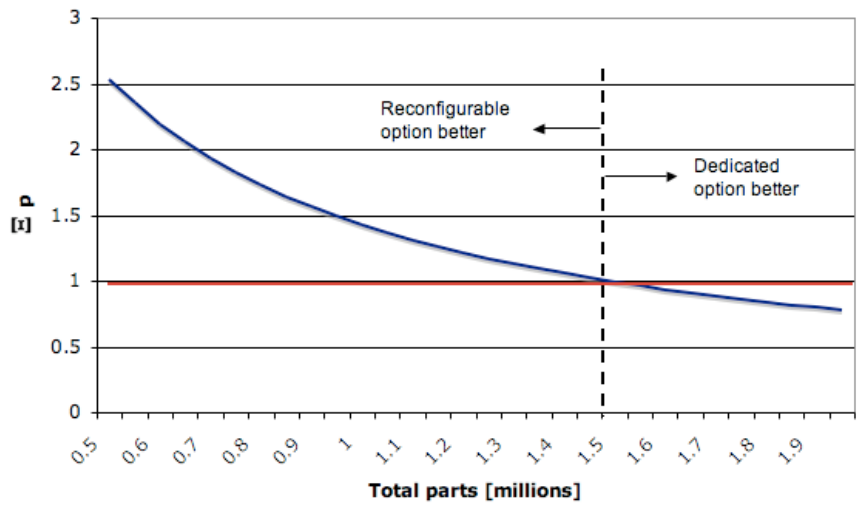

Figure 6-8: Relative Performance Efficiency of Reconfigurable Die

multiply signs indicate this. So for the stroller case, the reconfigurable version can be a stroller or a baby carrier back-pack. Thus, a fixed stroller and baby carrier (of comparable design) was used for comparison. For the 3-in-1 Crib, a separate crib (that is not reconfigurable), and a toddler bed was used for comparison with the reconfigurable crib that can convert into both. For the reconfigurable die, a set of 300 dies were used for comparison (since this was the motivating case for its design as described in its literature [137]). It was assumed in each case that the functionality/capability *etc.* for both fixed and reconfigurable systems was the same (for lack of data and simplicity here). From Equation 2.37, the Ξ_f thus ended up being simple ratios of the price and masses respectively.

The convertible stroller is primarily marketed as an item that can help in saving mass/volume when traveling with a baby. The mass efficiency is therefore a relevant metric for this product. The Ξ_f was computed for both price and mass as a resource to be efficiently utilized. In both cases it comes out favorable as compared to fixed systems. However, its Ξ_f for the mass as a resource is higher, 1.6 as compared to 1.2 for price (which is indicative of its design intent).

In case of the Reconfigurable Die where there the non-recurring and recurring cost are significant and can be computed in monetary terms, the Relative Performance Efficiency Ξ_p, as described in Section 2.7.1 was also computed. The full details of the reconfigurable die are given in Appendix B, however as a brief summary, this system was assumed to require an Elvax Interpolator Sheet for every 100 forming runs (which is not required for a dedicated, fixed die). The cost for this sheet was \$350, the cost of the reconfigurable die was \$500,000 and cost of a fixed die was \$19,000. This die was to serve in the production of 300 different types of aircraft body panels (therefore 300 fixed dies would have been required). With these assumptions, the plot shown in Figure 6-8 was generated in which the Ξ_p is computed using Equation 2.42. Both the cost of the die and the recurring cost of the interpolator (in case of the reconfigurable option) are factored in. For this particular case, the

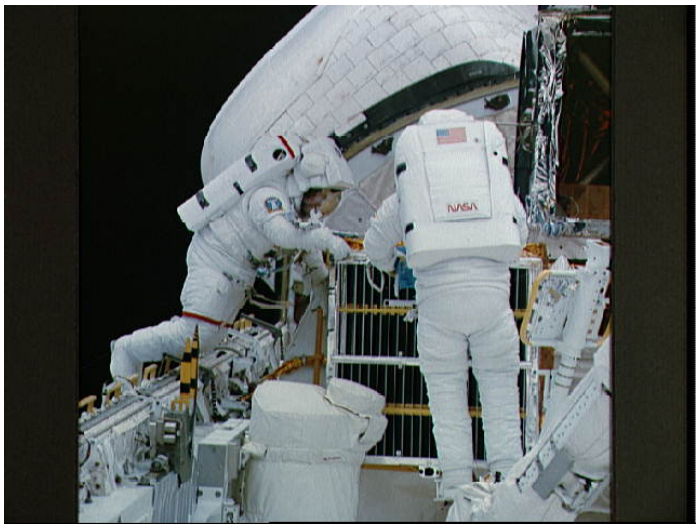

Figure 6-9: Repair of the Solar Maximum Mission Satellite onboard Shuttle Challenger [3]

value of Ξ_p indicates that the reconfigurable die is a cheaper option if fewer than 1.5 million total parts are to be manufactured. After that its value goes below 1, indicating that the fixed die option will come out cheaper. Note, that the calculation does not account for time value of money, and it is assumed that the recurring cost of the interpolator sheets are not phased out over years. If that accountability is factored in, the break even point will get pushed out even further. The 1.5 million parts is therefore a lower bound, and it can in fact be higher if the production is over a few years and the discounting rate is high.

6.4.4 Evolvability

The Solar Maximum Mission (SMM) was used as a sample system to illustrate how the evolvability metric can be potentially employed. Equation 2.44 was used for this purpose, and for simplicity (and also lack of information), it was assumed that the performance in both cases was same. The SMM was a satellite deployed, by a Delta rocket, to study the sun (during a period of maximum solar activity), however it soon underwent a failure (in December 1980) in its attitude control system and could not carry out any useful function. The SMM had been built on the Multi-Mission Spacecraft (MMS) platform which was specifically designed to allow for on-orbit servicing (in addition to manufacturing benefits). The cost of the satellite was $120 million in 1980. Four years later, a Challenger shuttle mission (STS-41C) was sent to service the spacecraft. Figure 6-9 shows the repair being carried out by a shuttle astronaut. The repair was carried out successfully, however the orbit of the satellite was greatly reduced from ($512 \times 508\ km$ to $405 \times 408\ km$) [1]. For a first order analysis, using

Table 6.6: Solar Maximum Mission

Shuttle Launch Cost	\$245 million
SMM Cost (1980)	\$ 120 million
SMM Cost (1984)	\$ 151 million
Delta II Launch Cost	\$ 67 million

Equation 2.44, Δ_e was found to be:

$$\Delta_e = \left(1 - \frac{C_r}{C_{new}}\right)\frac{J_r}{J_{new}} \tag{6.1}$$

$$= (1 - \frac{245}{151 + 67}) \tag{6.2}$$

$$= -0.12 \tag{6.3}$$

Note, that although the performance was affected (the orbit was lowered *etc.*), for lack of information about the exact detrimental effect, it is assumed that both J_r and J_{new} are the same. If the J's are properly accounted, the value of Δ_e may further decrease. However, even from cost considerations alone, it can be seen that the servicing mission was more expensive (by 12%) as compared to launching a new satellite. There are however several other factors that need to be considered (such as the ability to produce another identical satellite in the first place, additional missions that could be carried out (and probably were) by the Challenger flight which would then effectively reduce the cost of the shuttle mission directed towards the SMM alone *etc*).

6.4.5 Survivability

Several systems could be used to illustrate how the two metrics of graceful degradation, Λ, and robustness, Φ_r, can be computed. The SmartSat-1 RCE (which has three degraded states), Polybot, LARA, EHW *etc.* are all applicable however enough data was not available. For the SRR however, the data was found that its fixed version had a stability margin of 2.1^o, while the reconfigurable version always had 15° or more. Thus , Φ_{rSRR} is the ratio of these quantities and is 7.14.

6.5 Cost

A reconfigurability cost analysis was also carried out. The relevant data could only be obtained for the commercial and manufacturing systems however, and therefore the analysis is only applicable to those domains.

In terms of cost aspects, two main trends were noticed. In the systems where there is no fundamental change in their architecture or nature, on average the cost of the reconfigurable version was found to be 35% higher as compared to its fixed/non-reconfigurable counterpart. For instance,

Table 6.7: Cost Differences of Reconfigurable and Fixed Systems

Name	R-System [$]	F-System [$]
Airpot	16.5	12
LEGO	14	10
Vaccum	700	550
Food Processor	117	90
Sewing Machine	950	690
Convertible Stroller	70	45
3-in-Crib	413	335
Sofa Bed	550	420
Convertible Car	39,600	32,200
NI-RIO	1895	1395

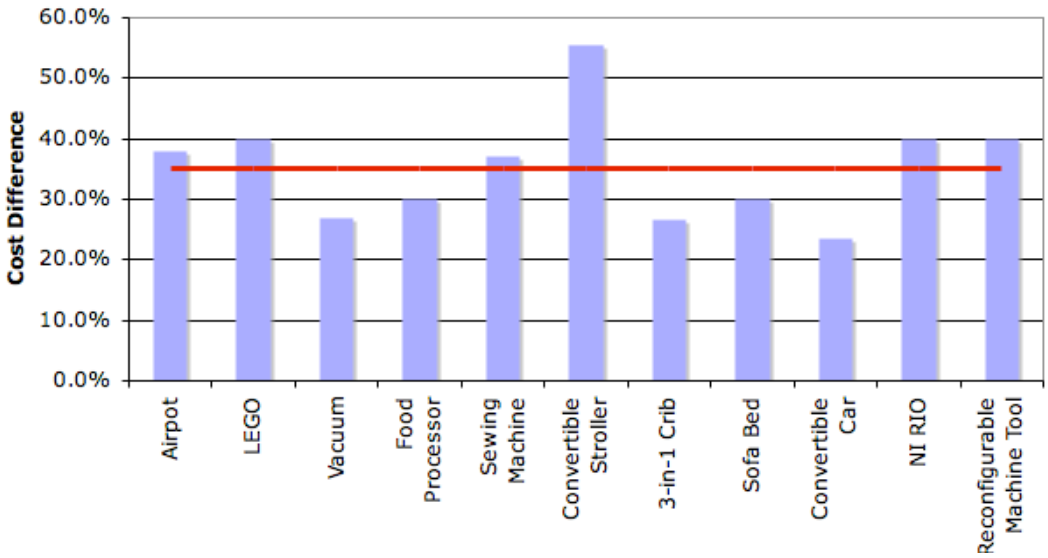

Figure 6-10: Cost of Reconfigurability in Commercial Items

a convertible car is 23.5% more expensive than a non-convertible car of the same size, make, model *etc.*, an NI-RIO data acquisition (DAQ) system is 40% more expensive then a non-reconfigurable DAQ system and so on. Table 6.7 shows the cost data for the systems for which this could be found. It should be noted that for each reconfigurable system, only one fixed (almost similar) counterpart was used for comparing price. So for instance, for the convertible stroller, that can both be a stroller and a child carry pack, only a similar fixed stroller was used for comparison. If the whole set of fixed systems that can collectively deliver the range of functionality that is achieved from the reconfigurable system are to be considered, then the Ξ_f, Ξ_p are better measures. Figure 6-10 shows the % increase in price in going from a fixed system to an (or almost) equivalent reconfigurable system. It is computed as $(C_r - C_{fx})/C_{fx}$, where C_{fx} and C_r are costs of fixed and reconfigurable systems respectively. An additional data point of Reconfigurable Machine Tool has been added in

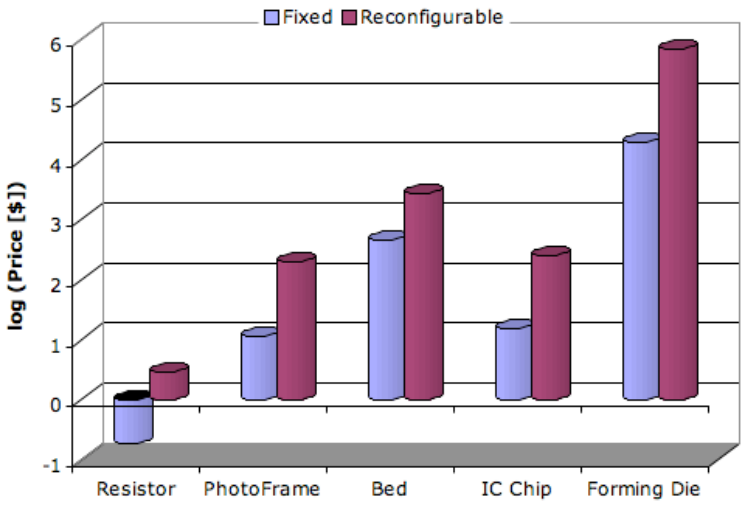

Figure 6-11: Cost Comparison Between Architecturally Different but Functionally Similar Reconfigurable and Fixed Systems

based on the fact that CNC machines are usually 1.4 times the price of a dedicated machine [129]. Since CNCs can be considered as the 'reconfigurable' version here, this data is also added in. The average cost difference is found to be 35% (with a standard deviation of 9%) in this data. This is can serve as a first order estimate for the cost of reconfigurability in a commercial items.

Another interesting observation was made about the cost of making a system reconfigurable in which its fundamental nature (from perhaps only mechanical) changes to a more complex electro-mechanical-informational kind. In essence, the DSM of these systems is radically different between the reconfigurable version and the fixed version. In both cases (fixed and reconfigurable) the externally delivered function is the same, but in terms of many form attributes and sub-processes/functions, there may be little similarity. From among all the systems studied, there were 5 such systems: the potentiometer, the digital photo-frame, the adjustable bed, the FPGA, and the reconfigurable die. The prices of the potentiometer with a simple fixed resistor, the digital photo frame with a regular photo frame, the adjustable bed with a regular bed, the FPGA with an Application Specific Integrated Circuit (ASIC), and the discrete die with a regular integral die were compared. Figure 6-11 shows that there is usually a difference of an order of magnitude in cost. The value for the resistor is negative in the chart since its price was $0.19 and since the log of the prices was plotted, it came out negative. It however can still easily be seen that there is an order of magnitude of difference between its price and that of a potentiometer. The set of systems in this case however is very small, and a more comprehensive survey will be needed to corroborate this observation.

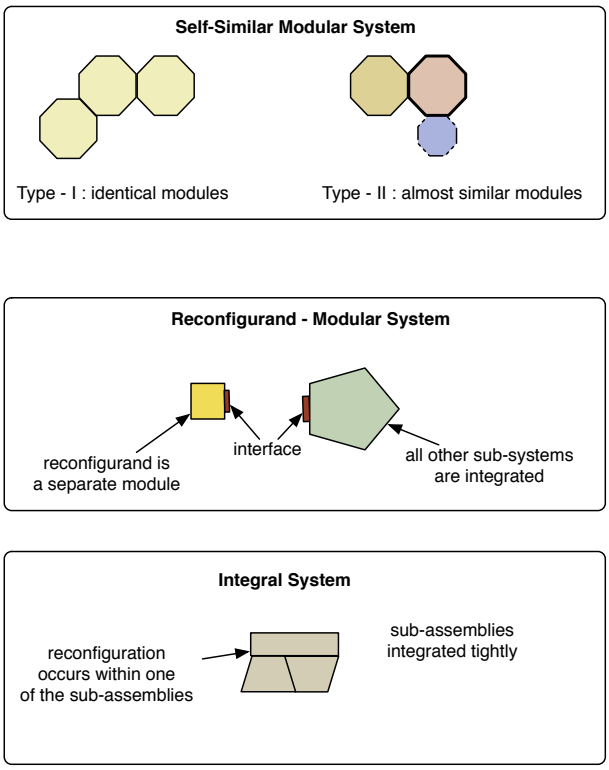

Figure 6-12: Types of Architectures in Reconfigurable Systems

6.6 Architecture

The set of 33 systems were also studied from various architectural aspects. Their form, processes, interfaces *etc.* were all analyzed. From the review of their form/physical design, it emerged that all the systems could be categorized into three main types:

- 1. Self-Similar Modular: all modules are exactly or almost identical
- 2. Reconfigurand Modular: only the component that is reconfigured is modular
- 3. Integral: sub-systems, components are linked in an integral manner

There is thus an increasing degree of integration in going from the first to the third type. Figure 6-12 shows a notional schematic of these types. It is important to clarify that the modularity (and 'modules') considered here are from the perspective of reconfigurability. Thus, 'reconfigurable modularity' *i.e.* one that is intended for *reconfigurability* is implied here. An architecture can be modular from different perspectives and due to different needs. It may be modular for manufacturing or packaging purposes for instance. In the context of reconfigurability, the intent of the modularity is to enable easy reconfiguration after the system has been fielded.

Depending on the extent and degree of reconfigurability it may or may not need to be modular (which is indeed found to be the case). In self-similar modular architectures, there are fundamentally two kinds. In the first kind each module is exactly the same. In the second kind, perhaps only the encapsulation/interfaces/and outer form is identical or very similar, but the functionality of each module maybe different.

The Reconfigurand Modular systems are those in which only the reconfigurand is implemented as an independent module in the system (*i.e.* has well defined interfaces *etc.*) while the rest of the parts/sub-assemblies are well integrated. These are things like vaccums, food processors and SMART cars. This is somewhat similar to the 'component swapping modularity' defined by Ulrich and Tung in the context of how the final product configuration is built from modular sub-systems/components [118]. That specific type is not used here because firstly it was primarily defined from a manufacturing sense, and also it is specifically for 'swapping' only (whereas in some cases of reconfiguration there maybe a transposition instead of substitution).

Integral systems are classified here as those that do not exhibit any modularity from a reconfigurability perspective. Modularity usually has a specific intent (*e.g.* for manufacturing, testing, packaging). In this context the modularity is considered from a reconfiguration aspect.

In the self-similar modular systems, large constitutive chunks of the system can (and do) undergo a reconfiguration, while in the Reconfigurand Modular systems only a smaller chunk relative to the rest of the system is reconfigured. In the integral case, the chunk is also small and its degree of reconfiguration is also limited (*i.e.* mostly transposition) and cannot be removed from the system easily and is well integrated with the rest of the system. Table 6.8 shows some architecturally relevant information about the modular systems.

The *Modularity* column indicates the type of modularity (as defined by Ulrich [133]) in the system. Figure 6-13 shows the four kinds, integral, slot-modular, sectional-modular, and bus-modular systems. In slot modularity, each of the interfaces between components is of a different type so that the various components cannot be interchanged. In a bus architecture, there is a common bus to which the other components connect via the same type of interface, and in a sectional architecture, all interfaces are of the same type and there is no single element to which all the other components attach [133].

It should be noted that the architecture types defined by Ulrich are primarily defined by their interfaces/link relationship, whereas the three types discussed above (self-similar, reconfigurand-modular, and integral) are fundamentally based on module form/function in addition to their connectivity relationships. The *Processes* column shows the fundamental reconfiguration processes that are carried out, where T denotes transposition, A denotes addition, and S denotes subtraction/removal. The *Outcome* column shows what is changed as a result of a reconfiguration in the system. The abbreviation Fa denotes Form Attribute, Pa denotes Process (Function) Attribute

Table 6.8: Architectural Data for Modular Systems

#	Architecture Type	Name	Interface Types	Modularity	Module Types	Configurations
1	Self-Similar (I)	Polybot	1	Sectional	2	inf
2	Self-Similar (I)	LARA	1	Sectional	1	inf
3	Self-Similar (I)	Xilinx FPGA	1	Sectional	1	inf
4	Self-Similar (I)	EHW	1	Sectional	1	inf
5	Self-Similar (I)	SC Avionics	1	Sectional	1	inf
6	Self-Similar (I)	SmartSat-I RCE	1	Bus	1	inf
7	Self-Similar (I)	Reconfigurable Die	1	Bus	1	inf
8	Self-Similar (I)	VLA	1	Bus	1	4
9	Self-Similar (II)	LEGO	1	Sectional	4+	
10	Self-Similar (II)	USM Haller Table	1	Sectional	3	510
11	Self-Similar (II)	SWARM	1	Sectional	4	
12	Self-Similar (II)	NI-RIO	1	Bus	25	inf
13	Self-Similar (II)	RMS				
14	R-Modular	Vaccum	1	Bus	7	7
15	R-Modular	Food Processor	1	Bus	7	7
16	R-Modular	3-in-1 Crib		Slot		3
17	R-Modular	SMART car	1	Bus	1	inf
18	R-Modular	SMM	1	Slot	6	inf

Table 6.9: Additional Architectural Data for Modular Systems

#	Name	Processes	Outcomes	Op Cycle
1	Polybot	All	All	Online/Offline
2	LARA	All	All	Online/Offline
3	Xilinx FPGA	All	All	Online/Offline
4	EHW	All	Fa,Pa	Online
5	SC Avionics	All	All	Online
6	SmartSat-I RCE	All	Fa,Pa	Online
7	Reconfigurable Die	T	Fa,Pa	Offline
8	VLA	T	Fa, Pa	Offline
9	LEGO	T	All	Offline
10	USM Haller Table	All	Fa,Pa	Offline
11	SWARM	All	All	Online/Offline
12	NI-RIO	All	All	Online/Offline
13	RMS	All	Fa,Pa	Online/Offline
14	Vaccum	A,S	Fa,Pa	Offline
15	Food Processor	A,S	Fa,Pa	Offline
16	3-in-1 Crib	T	Fa,Pa	Offline
17	SMART car	A,S	Fa	Offline
18	SMM	A,S	Fa,Pa	Offline

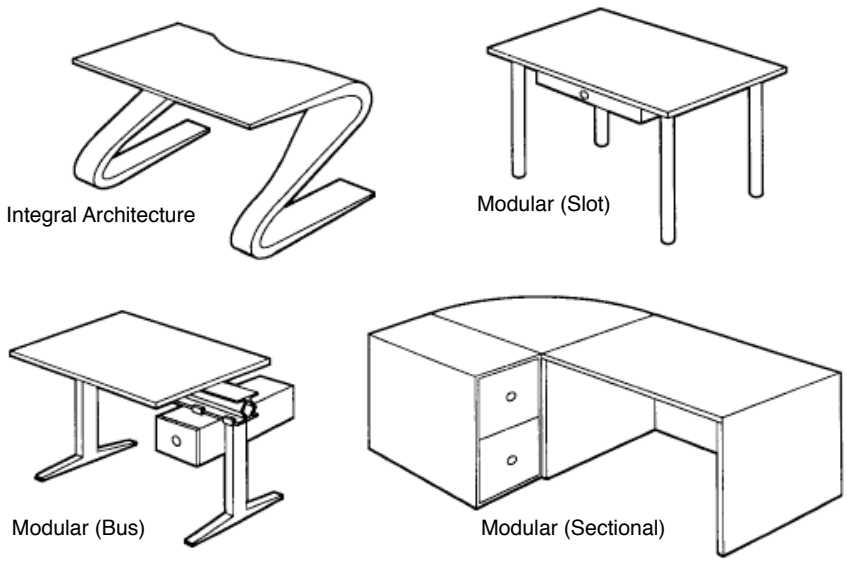

Figure 6-13: Types of Architectures [133]

and, P denotes Process.

6.6.1 Objects

From the inspection of the data in Table 6.8, several trends in modular systems are immediately obvious from a physical perspective. The number of interface types is always one (even for the Reconfigurand-Modular systems). The interfaces here considered to be those that exist between the modules that are reconfigured (and not between other sub-systems/components of the system). Note that the interface maybe transferring mechanical loads, information, energy *etc.* For instance SWARM has a Universal Docking Port (UDP) that connects all the modules together [113], Polybot has identical interfaces between the segments that have electrical and mechanical connections. The number of module types is also very low (especially in the self-similar modular systems and hence their definition). The reconfigurand-modular systems on the other hand show larger number of types of the modules.

The modularity type in the self-similar systems is overwhelmingly sectional, where 8 out of 12 (or 66%) self-similar systems are sectional-modular. The 13th system, RMS was not counted here since its modularity was not known. The slot modularity is conspicuously absent and logically so. In the Reconfigurand-Modular systems however, slot modularity does seem to appear along with Bus modularity. Out of the 5 such systems, 2 had slot and 3 had bus modularity.

Since the modularity here is for reconfigurability, there will be some choices that will be inherently favorable such as sectional modularity as opposed to slot. When the intent of the modularity is for

Table 6.10: Architectural Data for Integral Systems

Name	Configurations	Processes	Outcome	Op Cycle
Potentiometer		T	Pa	Online/Offline
Airpot		T	Pa	Online/Offline
Sewing Machine		T	Pa	Offline
Convertible Stroller	2	T	Fa, Pa	Offline
Digital Photoframe		A,S	Fa, Pa	Offline
Sofa Bed	2	T	Fa	Offline
Adjustable Bed	6	T	Fa	Online
Convertible Car	2	T	Fa	Online
Flexible Race Car		T	Fa,Pa	Online
SRR		T	Fa,Pa	Online
MEMS patch antenna	2	T	Fa,Pa	Online
TTC Transponder		T	Pa	Online
Morphing UAV		T	Fa,Pa	Online
F-14 Tomcat		T	Fa,Pa	Online
VDCH		T	Fa,Pa	Online

manufacturing and assembly ease it might be okay to have slot modularity (as was the case for MMS). But for reconfigurability that occurs in the operation phase, identical interfaces lend them selves to greater ease and degree of reconfigurations. For instance, there will be fewer tools and resources available in the field typically then as compare to a manufacturing facility. So it will be easier to have a set of standard tools to carry out the reconfiguration. Also, in general the modularization will be at a higher level of abstraction and will result in larger functional assemblies [64]. This is again due to the fact that reconfiguration will be carried out on a fielded system. These notions are confirmed from the data in Table 6.8.

6.6.2 Processes

The architectures are intimately linked to the processes that are involved in the reconfiguration. If things have to be added or removed, the reconfigurand is made modular. However depending on the degree of transposition relative to the other system components, the architecture can be integral (for less), or modular (for high) level of transposition/transformation. It is interesting to note from the data in Table 6.10 that except for the digital photo frame (which is an informational system), all other systems only undergo a transposition process during their respective reconfiguration. Their integral architectures (in terms of reconfigurability) therefore seem suitable in this context. On a similar note, the data in Table 6.8 shows that the self-similar systems overwhelmingly undergo all the three kinds of processes. Again their architectures allow for this and the link between the form and reconfiguration process is clear. Almost all the reconfigurand-modular systems happen to undergo substitution in the set of systems selected, and it is suspected that this could very well be the dominant trend in this type of architecture.

6.6.3 Outcomes

The consequence of reconfigurability from an architectural standpoint is that form attribute, function (process) attribute or even the externally delivered function itself is changed. For each system, these three types of outcomes were identified, and are shown in Tables 6.8 and 6.10. The most common outcome in most cases is that of a change in the form attribute and process attribute. This is to be expected since it is usually much easier to change the system's attributes rather than to change its externally delivered function. Only the self-similar modular systems exhibit all three types of outcomes, where in 7 out of 13 (or 54%) self-similar systems the form attribute, function attribute and function can all be changed. So systems like LEGO, SWARM, ANTS, and Polybots which are essentially a collection of highly similar modules allow for the highest extent of reconfigurability. In integral systems, 6 out of 15 cases have only one outcome (of either form or function attribute). In the modular systems however, only 1 out of 18 systems exhibits a single outcome (SMART cars in which the body panels are changed to allow for color variation). All the other modular systems exhibit two or more outcomes.

6.6.4 Agents

The close relationship between the reconfiguring agent and the time in the operational cycle of the system when reconfigurations take place (*i.e.* whether online or offline) was illustrated in Figure 6-7 previously. From an architectural standpoint this aspect is important to account for, since it directly affects the complexity and design of the system. An external agent can allow for much desirable reduction in system components and beneficially affect reliability and complexity. An external agent however will almost always make it very hard to do on-line reconfigurations, while an agent internal to the system will allow for both on-line and off-line reconfigurability.

6.7 Role of Requirements, Constraints, and Technology

A review of previous programs in which modularity (and reconfigurability) was designed in the architecture to cut costs reveals that as budgetary cuts occurred over time, more emphasis on short term savings drove towards eliminating modularity and reconfigurability. For instance the multi-mission satellite platform that NASA developed in the 1970s was abandoned later on. It was noted that "the main objective concerning the design of the MMS has been related to aspects of cost effectiveness. Maximum use was to be made of NASA standard components. The basic concept has been to design a core spacecraft which has inherent flexibility to meet a range of mission needs without modification of its hardware elements [33]." The MMS was touted as being a system in which upgrades would be possible: "Space-based and ground refurbishment and payload changeout are offered among other features, such as propulsion options for orbit adjust, ground support and flight support systems,

refueling, STS interface, and housekeeping services [120]." So while desirable qualities such as maintainability, serviceability, upgradeability *etc.* are nice to have they can get sacrificed at the altar of short term cost constraints fairly quickly. Therefore, reconfigurable architecture maybe abondoned due to budgetary constraints (to which space systems are especially vulnerable) if it allows for short term savings in the program. However if it is the *enabling* quality that allows for the fundamental functionality (*e.g.* in sub-category 2 in which it has to fulfill roles at different times *e.g.* in morphing UAV, VLA *etc.*) it is more likely to not be traded off from the system's architecture, and in fact actively pursued.

An important aspect is the impact of technology that enables the reconfigurability in the architecture. A good case in point is the F-14 aircraft that had a mass penalty of 2300 kg due to its swinging wings. The central actuation force for the wing transformation had to be transmitted across the aircraft which caused large penalties in mass and complexity. This added weight and complexity led future aircraft generations (F-18, F-22 *etc.*) to abandon this design. The renewed interest in wing morphing, particularly in UAVs is now concurrent with the development of smart elements, new materials (smart memory polymers, instead of the more traditional alloys) *etc.* The small, distributed actuators will contribute significantly to the success of the reconfigurable wing design in UAVs but might also cause maintenance challenges.

Chapter 7

Conclusions

This chapter summarizes the key results of the preceding chapters, proposes a set of principles and guidelines for designing for reconfigurability, and discusses future research and applications of this work.

7.1 Summary

The research presented in this thesis, attempts to lay essential foundations for studying reconfigurability in systems. The definition of reconfigurability is first disentangled from other related terms, and the meaning is elaborated to clearly differentiate from other '-ilities'. The identification of the fundamental properties that reconfigurability enables in a system, *i.e.* multi-ability, evolvability, and survivability, and their associated metrics allow for a value-based assessment of the architectures. In general, the metrics for evaluating a system's architecture should be tied to the intents. This ensures value delivery by measuring how well the intent or requirements are being met. The relative metrics of functional efficiency, performance efficiency, evolvability, and degradability therefore allow for the evaluation of the essential qualities for which reconfigurability is being incorporated in the system. Another key notion described in this work relates to the categorization of reconfigurability in terms of when it occurs in the operational cycle of the system. A reconfigurable system can essentially be modeled as a system that tries to produce a *desired* output (*i.e.* fulfill some objective) at various points during its operation by undergoing some form of *on-line* reconfiguration. When the desired output requires a change in the system that is outside its existing capability or *on-line reconfiguration bandwidth*, it then undergoes a more radical form of reconfiguration which may require the system to be 'shut down' but alters its capabilities to meet the new objectives when it is operational again after the reconfiguration process. By treating the reconfigurations through such a meta-model, systems level aspects such as accrued losses/benefits, effects of reconfiguration time *etc.* can be investigated.

The fundamental limitations encountered by space systems are also elaborated to highlight why reconfigurability can be especially desirable for these systems. The benefit of efficiently utilizing the transported mass to a planetary surface is elaborated. Along the lines of mass efficiency, a model is developed for reconfigurable spare parts requirements. This model can quantify the effect of having reconfigurable (or common) spares on the logistics resource requirements for space exploration missions.

The two case-studies of reconfigurable planetary surface vehicles and satellite constellations are then used to illustrate in detail some of the trades that are involved in assessing the benefits and limitations of reconfigurability. The PSVs are analyzed for resource efficiency where it is found that up to 27% mass savings can be achieved with a reconfigurable fleet as compared to a non-reconfigurable fleet of vehicles. The degradability is also almost 3 times less for the reconfigurable case. Issues such as impact on crew-time (which can be adverse if a lot of time-consuming reconfigurations are required), and energy costs *etc.* however were not factored in the analysis. In the second case-study of communication satellite constellations shows how evolvability analyses can be carried out. It was found, for the particular problem studied, that reconfiguration only seems feasible for certain capacity levels and specific launch scenarios.

The high-level '-ility' analysis was then complemented with a more detailed view on architecture, costs, and reconfiguration time issues for a set of different reconfigurable systems. Through a survey of 33 different systems, several common trends in the context of reconfigurability were identified ranging from architectural type to reconfiguring agents. Based on the analysis of the systems, three types of architectures from a reconfigurability perspective *i.e* self-similar modular, reconfigurand modular and integral, are identified. It was found that for commercial items, the reconfigurable systems cost 35% more on average. It was also found that in general the average useful state occupancy time of a reconfigurable system is 10 times or more than that of the reconfiguration time. These empirical generalizations can be used in preliminary design and evaluation processes for certain classes of systems.

In short, the results and observations from collected data show that reconfigurability can provide a number of benefits and is important when the underlying aim is to design not just for the short term cost and performance goals, but also for'-illities' such as evolvability, survivability *etc.* There are however several issues such as potentially increased costs, reliability aspects, and operational/maintenance factors that can adversely impact a system due to its reconfigurability.

7.2 Principles and Guidelines

Based on the results and summary discussed above a few general principles can be synthesized for reconfigurabililty in systems.

7.2.1 Principle of Reconfigurability

For every configuration of a reconfigurable system,
there exists a corresponding dedicated system that is
AT LEAST equal in performance
A good reconfigurable design is one in which the
performance of each configuration approaches that
of the corresponding dedicated system

This principle can be easily proved by comparison of an ASIC and an FPGA (for which a similar specific 'law' has been proposed [65]). An ASIC solution can be implemented on an FPGA and then if the extra (unused) elements *i.e.* interconnects, logic blocks *etc.* are removed, the resulting system will be one that uses less power, is more dense and is even cheaper when produced in volume. This notion can be extended to any system in general. For instance, consider the case of a morphing UAV. A fixed aircraft can also potentially be built that matches exactly the configuration of the morphable UAV, so that fixed aircraft cannot be worse off from the UAV's configuration. However it can potentially (and frequently) be made a bit better than the UAV configuration and so on. Although it can be argued that such a principle is self-evident, it is useful to clearly enunciate this fact. Keeping this principle in view, comparison metrics can be developed for specific systems to test the 'goodness' of the reconfigurable designs. The relative functional efficiency and performance efficiencies (discussed in Chapter 2) are partly motivated by this fact/principle.

7.2.2 Principle of Self-Similarity

Systems with self-similar modules,
have highest degree of reconfigurability.
Common modules should be maximized across configurations.

Systems composed of identical or very similar modules are the easiest to reconfigure radically (hence are greatly *reconfigurable*). This has been qualitatively proposed earlier [62], however the analysis in Chapter 6 illustrates this notion empirically. LEGOs, ANTS, Polybot, SWARM, avionics based on identical generic modules [41] *etc.* are all self-similar systems that exhibit a high degree of reconfigurability. Their form can be radically altered, and their functions (not just functional attribute) can be completely different.

It should be noted that the first principle outlines the fact that in each configuration a reconfigurable system should strive to be as close as possible to a corresponding dedicated system that is optimized to fulfill the requirements of that state. This would lead to a high degree of differentiation in the components. On the other hand however the principle of self-similarity will tend to push designs towards higher commonality, in which the extreme case will be that the system modules are exactly identical.

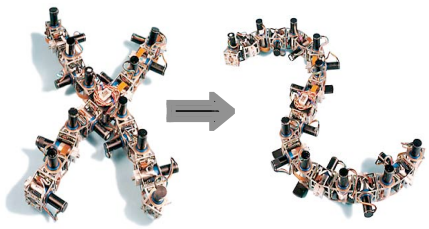

Figure 7-1: Self-Similar Modular Systems allow for Highest Reconfigurability

Figure 7-2: LEGO sets with varying level of commonality among pieces

Another point to note is that if there is a high degree of commonality such that every part/component is almost similar, then the resulting externally delivered function can be quite limited. On the other hand if the commonality is at a higher level of abstraction, *e.g.* modules consisting of many parts/sub-systems, then greater functionality and meaningful reconfigurability can be achieved. For instance, consider the case of the self-similar systems of Polybots, SWARM, ANTs *etc.* In these systems, the similarity or commonality is at high levels (large modules are identical). This causes a lot of redundancies, *e.g.* each segment in a Polybot has its own motor, its own computer *etc.*, however it also allows for highest degree of reconfigurability.

Figure 7-3(a) illustrates some of these observations. A set of three LEGO sets were compared (see Figure 7-2). The first set was DUPLO, meant for 1-3 year olds. All the blocks in the set are almost identical (very small variety), and the models that can be built have consequently very low fidelity and function. The second set was Land Busters, which allows for detailed model construction of vehicles (race cars, trucks, motor bikes *etc.*) It has numerous specialized parts in addition to the basic LEGO bricks. The third set was LEGO mindstorms, which has medium level fidelity

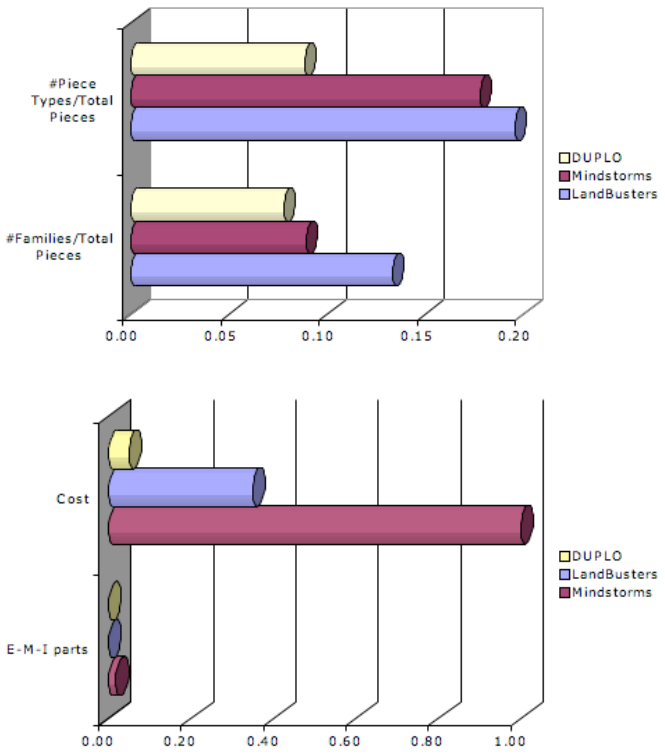

Figure 7-3: Commonality vs Model Fidelity and Functionality in LEGO Sets

in terms of creating models (fewer specialized parts as compared to Land Busters), however it has sensors, actuators and controllers that enable the system to actually carry out functions that it structurally represents. It can be seen that as the structural fidelity increases (in going from DUPLO to Mindstorms to Land Busters), there is an increasing number of part families and part types (shown normalized with total number of parts in each set). Although DUPLO has the highest level of commonality, *i.e.* lowest number of families and types, it has lowest level of actual structural and functional capability. Also, from Figure 7-3(b) it can be seen that the cost goes up with increasingly functionality among these sets (DUPLO is $9.99, Land Busters is $59.99 and mindstorms is $199.99). Furthermore, since DUPLO and Land Busters are capable of only structural representation their parts are all 'mechanical', while mindstorms has about 2% (or 13 out of its 718 total) parts that are electrical actuators, sensors *etc.* So not surprisingly, the number of specialized and unique parts increases when actual/more functionality starts to emerge.

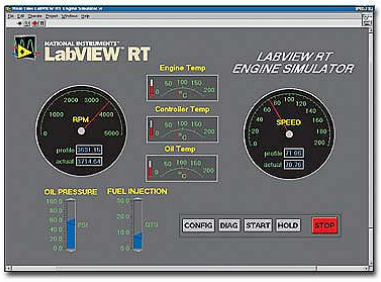

Figure 7-4: 'Virtual Instruments' allow for high reconfigurability in instrument's capabilities

7.2.3 Principle of Information Reconfiguration

Maximize the informational nature of the element under frequent reconfiguration
Physical nature of frequently reconfigured elements should be minimized

Maximizing the informational nature is desirable since it is easier to change information then physical matter/material. Making the system informationally reconfigurable however maybe more expensive and/or difficult upfront. However once it gets implemented the information reconfiguration process is usually faster, cheaper, and easier. The cost of 'reconfigurability' (non-recurring cost) maybe higher, but the cost of 'reconfiguration' (recurring cost) can be much lower. A common example are reconfigurable displays (ranging from digital photo frames to touch screen control panels). Virtual Instruments (that can be created through NI LabVIEW software) are another example of software implementation of traditional hardware systems.

The general reconfigurability of a system is enhanced when the hierarchy of functions has a one-to-one correspondence to the physical implementation. This allows for localization of change, since any modification in the structure of the artifact affects only its target function. Software (and to some degree electrical components) typically have structures that are suitable for reconfigurable design, as they are inherently function specific with little or no form constraints. However, in conventional mechanical design the hierarchy of physical assemblies does not reflect the function structure. A component often contributes to several functions. The components are product specific, as opposed to function-specific, and are difficult to use in a different product or different application other than the one originally intended [64].

With the advent of higher computing capabilities, it is becoming increasingly possible to implement many traditional hardware elements as software components. Figure 7-5 shows how in the proposed reconfigurable satellite transponders, the traditional hardware filters and other circuit elements will be replaced with software [99]

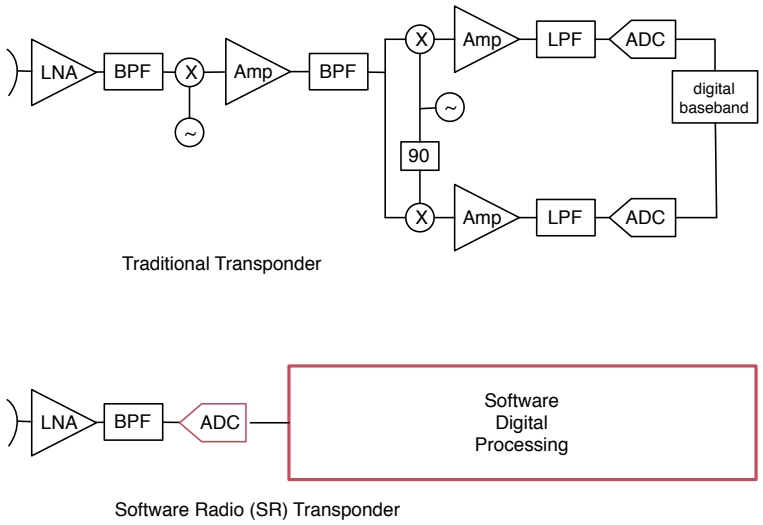

Figure 7-5: Reconfigurable Satellite Transponder

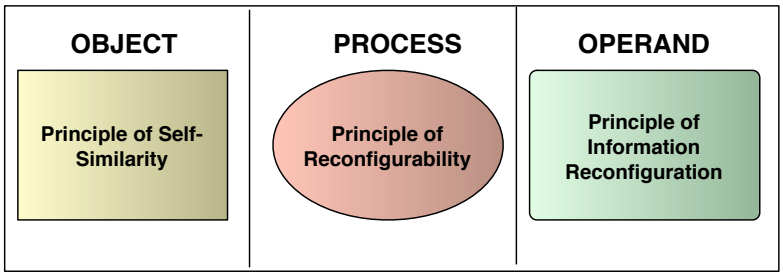

Figure 7-6: Reconfigurability Principles

This principle also fits in well with interfaces, where increasingly the wireless interface is enabling reconfigurations that were previously not possible. It has been recognized that the most adaptable interface is a wireless interface [64] which requires no physical connection between communicating entities. The nature of the interface inherently affects the degree of reconfigurability. On a related line, it has been empirically shown that information bandwidth is considerably easier to change than electrical energy flow (which requires a physical link) in design changes [67]. Physical interfaces have spatial constraints. Informational interfaces (such as wires) have this issue to a lesser extent, while wireless interfaces do not have this problem altogether. Reconfigurable modular spacecraft that fly in formation and communicate wirelessly [104], drive-by-wire technologies in cars (that allow for removal of all physical connections between the passenger compartment and the chassis [7]) *etc.* are among examples of a growing number of reconfigurable systems that increase the informational nature and minimize the physical nature of the interface.

The three proposed principles can be categorized as addressing the object, process and operand aspect of reconfigurability. Figure 7-6 shows this in an illustration.

7.3 Design for Reconfigurability (DFR)

Building upon the methods used for studying reconfigurability in systems in the previous chapters, a framework can be distilled that outlines the essential aspects of design for reconfigurability (DFR). It is useful to have a concise description of such a process, since a well-defined methodology assists the decision-making process. In modern engineering design and development practices, it has become fairly routine to follow some "design for X" (DFx) methodology, where X may correspond to a quality criteria such as variety, customizability, assembly, manufacturing, maintainability *etc.* It has been noted that in general any DFx should have metrics with which to compare alternative architectures/designs [134]. The X of relevance here is 'reconfigurability', and the metrics developed in this work can serve this purpose. Although it has been pointed out that DFx methods provide the most benefit when they are applied early in the design process, much of DFx deals with details that are unclear early in the design [143]. For instance in design for manufacturing (DFM), the intent is to reduce manufacturing costs, and recommendations include reduction of part count, choosing cheaper production processes *etc.*[134]. Similarly, in design for assembly (DFA) the intent is to have economical and efficient assembly. Some rules of thumb include having chamfers and other alignment aids, inserting parts from above, and providing ample space for insertion of tools or fingers [143].

The recommendations proposed/summarized for DFR in comparison are relatively at a higher architectural level so that they can be effectively employed in the early part of the design cycle and be of greater benefit. The main objective for DFR is to enable cost and time efficient reconfigurations such that the intended value (to be obtained from reconfigurability) is effectively delivered. Figure 7-7 describes the main recommendations for DFR. The first one simply states that the motivating factors for which reconfigurability is being sought should be reflected through applicable metrics. The second refers to the discussion in Section 2.4.3 about having differentiated states, so that for each operating/external condition there is a state that offers a clear advantage over the others (rather than having many states that offer lower and similar benefit). In the third recommendation, off-line reconfiguration is suggested (if allowed by the reconfiguration time requirements) since it will levy reduced requirements on the system design, there will be fewer parts needed (*e.g.* no actuators, controllers *etc.*), and overall the system can be lighter, cheaper, less complex *etc.* The fourth point is about using the reconfigurand-modular architecture where only a certain part of the system needs to be reconfigured, especially through substitution. This can allow for improvement/optimization of the remaining integral 'base' of the system, while still allowing for the necessary modularity to carry out reconfigurations easily. The fifth point refers to the use of self-similar modular architectures for achieving high degree of reconfigurability in form and function. The sixth recommendation is about reducing the number of interfaces, especially if they are physical (as opposed to informational) along with their extent and sensitivity. The reconfigurations are easier with minimal interfaces that do not

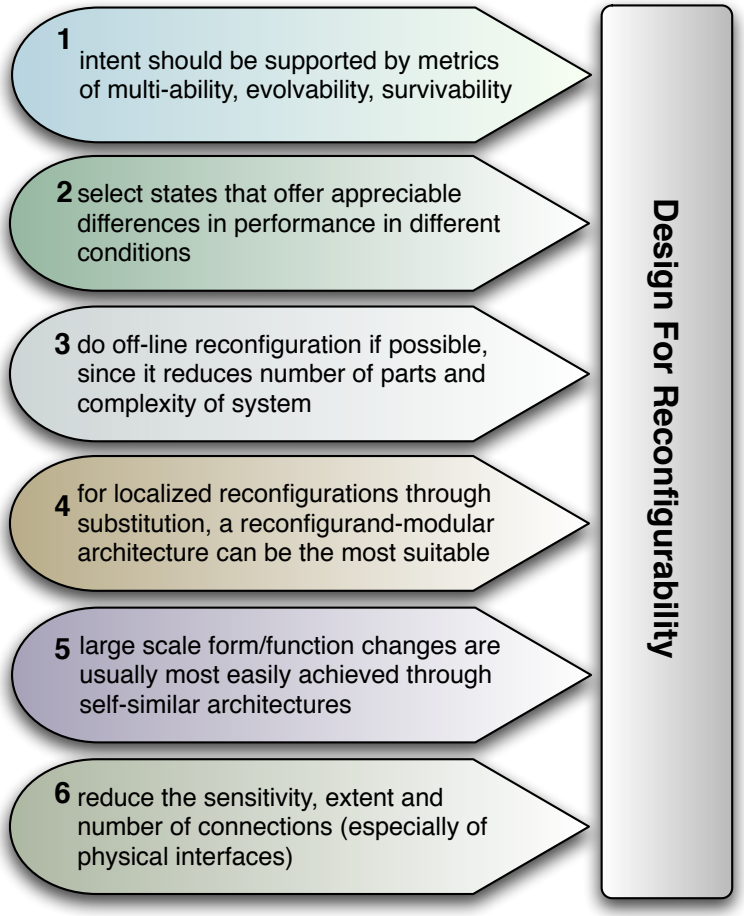

Figure 7-7: Design for Reconfigurability

require high precision, special tools/processes *etc.* Along these lines, the λ_c (defined in Section 2.7.2), should be kept as low as possible.

A complete framework based on the propositions, illustrations (through case-studies and examples), and observations made throughout this thesis is now summarized for studying reconfigurability in systems. Figure 7-8 describes this framework through an Object-Process Diagram. Firstly, the fundamental requirements that necessitate the possibility of having reconfigurability in the system have to be identified and categorized (*i.e.* does the system have resource efficiency requirements, or does it need to continue performing in degraded states *etc.*). Depending on the specific system being studied, one may need to model the usage scenarios that help define how the system will operate and be used. The system is then modeled with a reconfigurable and non-reconfigurable design. At this stage it is probably high-level analysis and the models may usually define the system with a few key variables. Depending on the type of reconfigurability/reconfigurable system the methodologies for determining a good design of a reconfigurable system (as discussed in Sections 4.2 and 5.2) can be employed. The various techniques for determining the states of the system (such as those discussed in Section 2.4.3) may also be used depending on the system.

The designs for the two cases are then compared using applicable metrics of functional efficiency, evolvability, survivability *etc.* This quantitative comparison, along with the consideration of other aspects/effects that might arise due to reconfigurability (such as increased risk-pooling as was the case in the analysis of reconfigurable spares) will define the boundary of using a reconfigurable vs non-reconfigurable system. For instance, in case of the specific example used for the reconfigurable spares, after the MTTF of the components falls below a certain level, the fixed and dedicated spares option comes out better. A similar situation of when reconfiguration should occur in an existing constellation and when deploying a new fixed system is better was highlighted in Chapter 5. Based on the results, either a non-reconfigurable or reconfigurable architecture will emerge as being a more suitable option. Due to the fidelity and level of modeling however, there maybe enough ambiguities that can warrant additional analysis.

Once/if the reconfigurable solution is found promising (*i.e.* it comes out better than the fixed option in the desired requirements such as evolvability, or survivability *etc.*), a more detailed design process will then be carried out. In this stage the reconfigurability design principles, along with the empirical observations that were highlighted in Chapter 6 can be particularly useful. With the detailed design information, some of the metrics introduced in Section 2.7.2 can be employed. This process can be done iteratively, in which the detailed design will be revised until a satisfactory solution is obtained.

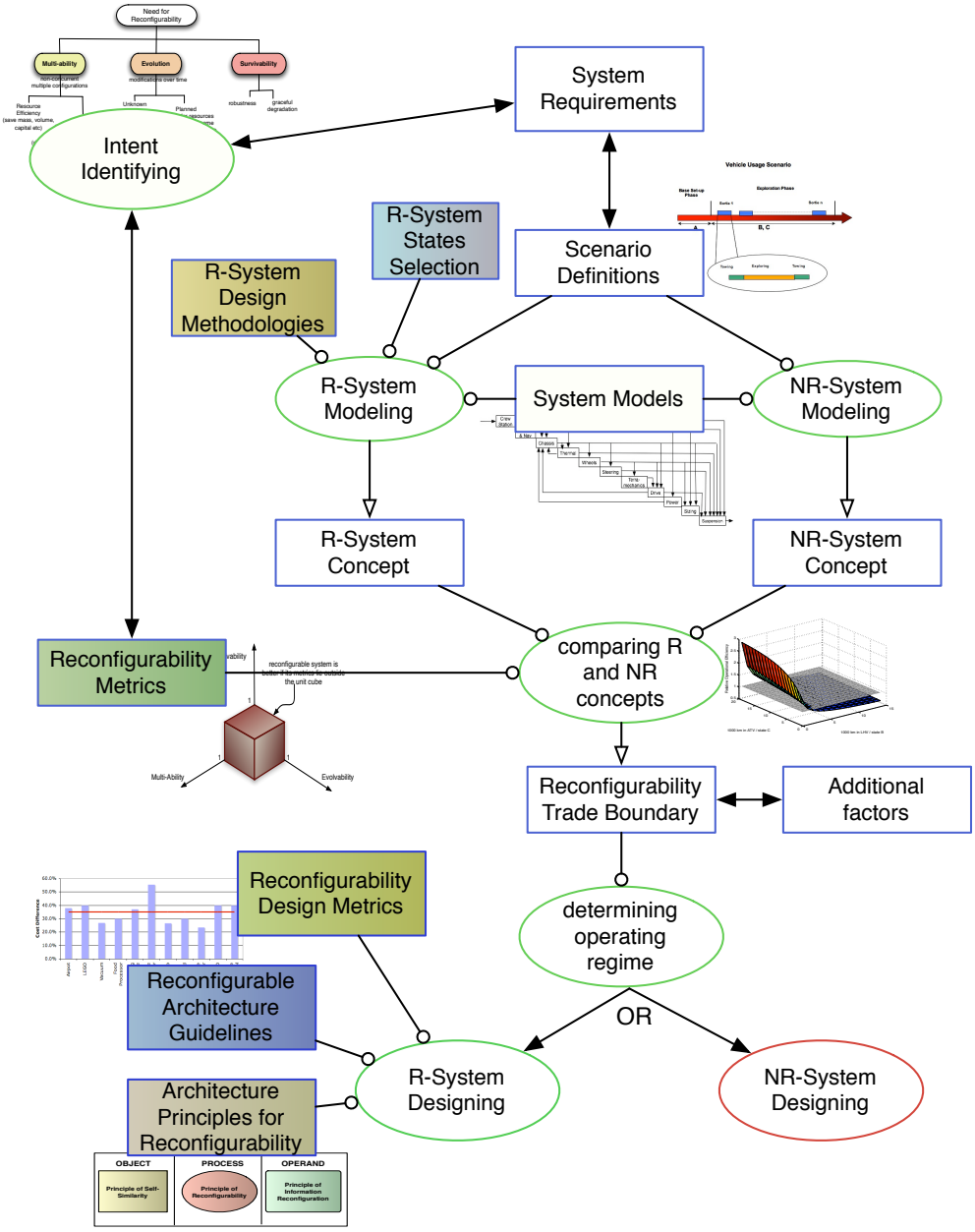

Figure 7-8: Framework for Reconfigurability Assessment

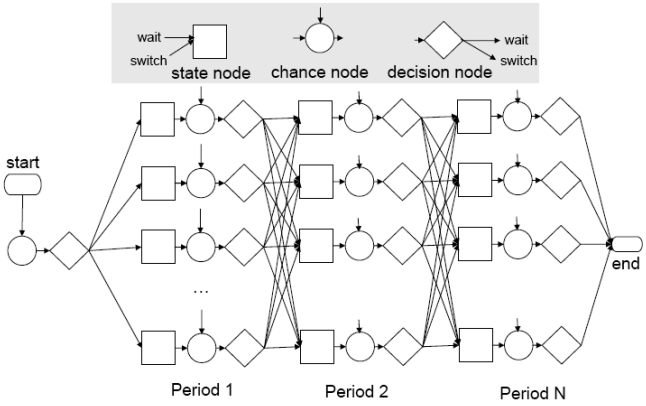

Figure 7-9: Time Expanded Decision Network [51]

7.4 Future Research

This thesis has identified and developed a few modeling frameworks that help in studying reconfigurability in systems. The control-theoretic and the Markov modeling approaches were illustrated with examples and shown how they can be applied for analyzing the various states a reconfigurable system may exist in over time. In future research, Time Expanded Decision Networks (TDN) will be employed as a tool for analyzing reconfiguration of large, complex systems in depth [51]. TDNs have recently gained attention due to the availability of larger computation capabilities. In a TDN, the time duration under consideration is discretized, and a copy of a static 'node' in the network is made for each of the time points. The node can essentially be a particular state of the system in this case. The nodes will be connected through arcs according to the rules that the connection moves forward in time, and that it represents a feasible reconfiguration. By modeling the reconfiguration over time between different states through a TDN, trades such as when a particular reconfiguration should take place, and the effect of various nodes or states in the network can be readily assessed. The TDN modeling framework is natural for studying evolvability, in addition to multi-ability (where specific capabilities are present at different instants of time), and degradation (where specific degraded states can be occupied as a function of time). Figure 7-9 shows a schematic of a notional TDN.

Additionally, as follow-up work the model developed for estimating the impact of reconfigurability on spares requirements for space exploration missions will be enhanced. In the present model issues such as redundancy of parts (that effects the availability computations), and impact on crew time (to carry out reconfigurations/scavenging) have not been factored in. In future enhancement to the model these will be taken into account.

The modeling framework for Planetary Surface Vehicles will also be expanded in future studies. Currently, the vehicle dimensions are only based on number of passengers. In future refinements a more explicit consideration for cargo capacity in determining the dimensions will be made. Furthermore, the mass penalties for reconfigurability (such as due to greater modularity) will be accounted

for. Additionally, new ways of reconfiguration will be explored. For instance, in the reconfigurable wheels analysis, only dimensional reconfiguration (of wheel width and diameter) was assumed. In future work, reconfiguration through variation of the wheel load will also be examined.

The communication satellite case study will also be refined through inclusion of additional reconfiguration schemes (presently only addition of multiple planes and satellites has been explored). Furthermore, reconfiguration for not only capacity expansion but also for failure management will be studied.

Appendix A

PSV Modeling Framework

This section describes the MATLAB modules developed for modeling Planetary Surface Vehicles. Collectively, the modules estimate model mass, power and dimensional requirements of different kinds of vehicles. The inputs, outputs, and description of each module presented below.

A.1 Crew Station Module

This module models two types of crew station based on the vehicle being open or pressurized. Table A.1 shows the inputs. The outputs are based on the type of the vehicle. For pressurized vehicles the outputs include data regarding habitability such as consumables mass and volume *etc.* Table A.2 shows the outputs in detail.

Open Vehicle Crew Station

For an open PSV, it is assumed that the crew station simply consists of seats made of Aluminum tubes (as was the case in the Apollo Lunar Roving Vehicle), and floor plates beneath the seats. The seats (and consequently the plates) are sized by using the dimensions of an average person in an upright sitting position. The dimensions were obtained from [34]. The seats were made 5% large to account for the fact the astronauts will be suited. The floor plates are also modeled to be made of Aluminum and their thickness is computed such that each plate under each seat can support the load of a suited astronaut. It is assumed that the number of seats is equal to the number of passengers

Table A.1: Inputs of Crew Station Module

Inputs	**Description**
nCrew	# of passengers the crew station can accomodate
sortieDays	days of continuous operation before vehicle is refueled
nEVA	# of EVAs performed during a sortie
PSVtype	'open' or 'pressurized'
planet	'moon' or 'mars'

Table A.2: Outputs of Crew Station Module

Outputs	**Open Vehicle**	**Pressurized Vehicle**
CSmass [kg]	crew station total mass	total mass including consumables
CSsize [m m m]	crew station length, height and width (array output)	
CSdata.crewFreeVol [m^3]	-1	free volume available to crew
CSdata.consumMass [kg]	0	mass of water, air, and food
CSdata.Energy [W-hr]	used by portable life support system during sortie	energy used by CO_2 scrubs, kitchen, hygiene, EVAs, and interior lights
CSdata.Power [W]	for portable life support	for CO_2 scrubs, kitchen *etc.*
CSdata.HabHeight [m]	-1	pressurized compartment height
CSdata.HabWidth [m]	-1	pressurized compartment width
CSdata.HabLength [m]	-1	pressurized compartment length
CSdata.ExtHeight [m]	-1	unpressurized compartment height
CSdata.ExtWidth [m]	-1	unpressurized compartment width
CSdata.ExtLength [m]	-1	unpressurized compartment length

and that they are arranged in rows of two (similar to the LRV configuration). This arrangement is used in determine the width and length of the crew station.

Some extra mass due to foot rests, seat belts and hand rails is also added. It is also assumed that all life support equipment is carried by the crew as payload on the vehicle and is not explicitly counted in with the crew station mass. Furthermore, the crew station is un-enclosed. The LRV was used as a sample to model the crew station for the open vehicle case. The power requirement due to the crew alone is set to 50W, assuming that the space suits or the portable life support system may have some power needs (although they will be primarily powered independent of the PSV). The crew station energy is thus computed by assuming that this level of power is required during the entire duration of sortie.

Pressurized Vehicle Crew Station

In case of the pressurized vehicle it is assumed that the crew station is a pressurized, cylindrical shell of some light metal (currently Aluminum and Titanium can be used). The pressurized compartment, at 1 atm of pressure P, houses the crew quarters, scientific equipment, and food. The thickness, t, of the shell is found by the hoop stress relationship.

$$t = \frac{Pr}{\sigma / s_f} \tag{A.1}$$

Radius of the shell is r. A safety factor, s_f, of 4 is assumed and σ is the yield strength of the material. Tanks of water, oxygen and other consumables are modeled to be outside of the pressurized shell. Figure A-1 shows a notional picture. The width of the shell is set to 7.5 feet (2.28m) to allow crew members to fully stand up. The length of the shell is then computed based on the volume needed for the given number of crew and duration. The volume is determined based on an empirical model

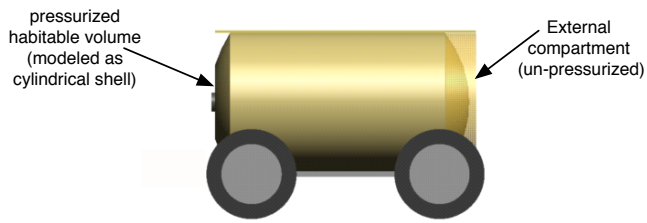

Figure A-1: Vehicle with Crew Station as Cylindrical Pressurized Volume

as given below.

$$V = \max(2, 10^{0.97 \log(sortieDays) - 0.28})) \tag{A.2}$$

The total volume required is the personVol multiplied with the number of crew in the PSV. This model was based on actual volume of manned vehicles used for missions lasting 14 days or less. This included Gemini, Apollo, and Space Shuttle missions [1].

The pressurized PSV is also modeled with an entrance hatch, and separate volumes for hygiene and kitchen equipment. The life support system is assumed to be open, with no regenerative equipment. The mass estimates for water per crew member are varied depending on duration of sortie. For sorties less than 5 days, the water allocation is 5 kg/crew/day, for sorties between 5 and 10 days, the water allocation is 10 kg/crew/day, and for sorties greater than 12 days the allocation is 12 kg/crew/day. This is based on estimates provided in [82] and accounts for the fact that for longer sorties the crew will want to shower or wash clothes etc. Estimates of power and energy requirements for the crew station include requirements due to CO_2 scrubs, interior lights, EVAs, hygiene, and kitchen.

A.2 Communication and Navigation Module

This module models the communication and navigation equipment that can be expected to be used on the PSV. Currently it models only navigation items, and it is assumed that any specialized communication equipment will be counted as payload for the PSV. Sunsors, gyroscopes, odometers, data processors, and inclinometer are presently modeled for open PSVs. For pressurized PSVs the mass is simply doubled as a rough estimate. The power requirements are set to 50W for open vehicles [2], and 1000 W for pressurized vehicles [3]. Table A.3 shows the inputs and outputs.

A.3 Chassis Module

The chassis is modeled as a simple ladder frame, square cross-section, tubular chassis. The wheelbase and track are first determined based on the size of the crew station and type of vehicle. For

Table A.3: Inputs and Outputs of Comm & Nav Module

Inputs	**Description**
PSVtype	'open' or 'pressurized'
planet	'moon' or 'mars'
Outputs	
mass	navigation equipment total mass
Pcomm	power requirement of comm & nav equipment

Table A.4: Inputs and Outputs of Chassis Module

Inputs	**Description**
nCrew	# of passengers seated in vehicle
nWheels	# of wheels in vehicle
frameLoadMass [kg]	mass supported by chassis frame
crewStationSize [m m]	length and width of crew station
material	material of chassis frame
PSVtype	'open' or 'pressurized'
gplanet [m/s^2]	g of planet on which vehicle operates
Outputs	
chassisFrameMass [kg]	mass of chassis
wheelbase [m]	vehicle wheelbase
track [m]	vehicle track/tread
chassisData.h [m]	frame cross-section height
chassisData.t [m]	cross-section thickness

pressurized vehicles the wheel base is computed as follows:

$$wb = l_{cs} \times f_{wb} \tag{A.3}$$

$$trk = w_{cs} \times f_{trk} \tag{A.4}$$

The wheel base factor is set to 0.85 (it is assumed that the distance between the center of the wheels will be slightly less than total length of pressurized shell. The track factor is 1.05 (assuming that the wheels will be farther apart than the width of the crew station to allow for better stability. These factors are purely assumptions and have not been estimated/computed from anywhere.

For open vehicles an empirical model is used to determine the wheel base and track given the number of passengers. This empirical model was obtained by using data of suitable terrestrial off-terrain commercial vehicles.

$$wb = 2.45 \times n_{crew}^{0.11} \tag{A.5}$$

$$trk = 1.9(wb)^{-0.116} \quad n_{crew} > 1 \tag{A.6}$$

$$trk = 41 \times 0.0254 \quad n_{crew} = 1 \tag{A.7}$$

Due to the lack of sufficient data for single passenger vehicles, the track is fixed at 41 inches if the

number of passengers is only one.

The dimensions (thickness and height of square cross section) are determined by a simple model of a beam in bending by assuming that each side-rail of the frame supports exactly half of the loaded weight of the vehicle. It is further assumed that the loaded is evenly distributed and the side rail is supported by two reaction forces due to the wheels/axles attached to it. The deflection of the beam is fixed (based on requirements that are set for race car chassis), and given the known distributed load and length of beam (taken to be equal to wheel base), the values for thickness and height of cross section are obtained. Note that this loading arrangement is also used if the number of wheels is modified (to six or eight for instance) and in which case the estimate will be conservative on the upper bound since in reality there will be three or four reaction forces on the beam for six or eight wheels. This correction to the model will be made in the future.

A.4 Thermal Module

The thermal modeling that is currently done is very basic. It is simply assumed that the thermal system is 3% of the sprung mass of the vehicle. The sprung mass is taken to be the sum of the crew station mass, m_{cs}, communication and navigation mass, $m_{c\&n}$, power system mass, m_{ps}, drive system mass, m_{ds}, and chassis frame mass, m_{ch}.

$$m_{sprung} = m_{cs} + m_{c\&n} + m_{ps} + m_{ds} + m_{ch} \tag{A.8}$$

$$m_{th} = 0.03 \times m_{sprung} \tag{A.9}$$

The input to this module are all the required masses, and the output m_{th}. In [82], it is suggested that it is usually 4-5% of the vehicle mass. For now the assumption of 3% is used since it is expected that improvements in thermal regulation technologies can reduce the weight.

A.5 Wheel Dimensioning Module

This module is used to size the wheels for the vehicle. The diameter and width of the wheels are sized for a specified sinkage and soil bearing pressure. Typically the sinkage is computed once the wheel dimensions are known (*e.g.* for a wheel of given dia and width its sinkage is computed based on the load is supports). However since there were more unknowns than equations available, an assumption was made for the sinkage that it is some fixed percent of the wheel diameter. In the current model it is assumed to be 1.4%. This means that a wheel of 80 cm diameter sinks 1 cm into the soft surface. In the future this module needs to be improved. In Figure A-2, the sinkage of the wheel, z, is shown along with the chord length , (labeled as l) of the wheel and contact patch width

Table A.5: Inputs and Outputs of Wheel Dimensioning Module

Inputs	**Description**
PSVtype	'open' or 'pressurized'
obstacleHeight [m]	max height of obstacle vehicle can cross
wheelLoad [N]	load supported by one wheel
sinkage [%]	fraction of wheel diameter allowed to sink
planet	'moon' or 'mars'
Outputs	
wheelDia [m]	diameter of wheel
wheelWidth [m]	width of wheel
wheelMass [kg]	mass of wheel

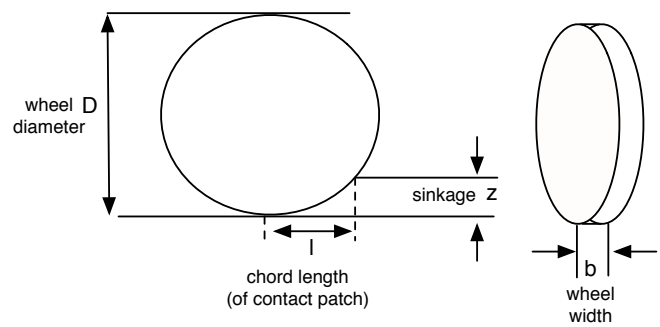

Figure A-2: Wheel Dimensions

b that is in contact with the soil due to sinkage. It is assumed that the width of the contact patch is the same as the width of the wheel.

The following three equations were used for sizing the wheels [144]:

$$p = \left[\frac{k_c}{b} + k_\phi\right] z^n \tag{A.10}$$

$$z = \left(\frac{3W}{(3-n)(k_c + bk_\phi)\sqrt{D}}\right)^{\frac{2}{2n+1}} \tag{A.11}$$

$$z = \alpha D \tag{A.12}$$

where p is soil pressure $[N/m^2]$, k is cohesive modulus of deformation $[N/m^{n+1}]$, k_ϕ is the frictional modulus of deformation $[N/m^{n+2}]$, n is the sinkage coefficient, z is the sinkage [m], W is wheel load [N], D is wheel diameter [m], and b is wheel width [m].

The values of the soil constants for moon and mars are obtained from [82] and [55]. The soil bearing pressure is set to be higher for pressurized vehicles as compared to open vehicles (it is assumed that the pressurized vehicles will traverse on surfaces that have capability of supporting a higher load).

Using Equations **??**, A.11, and A.12 the known quantities are p (set to soil bearing pressure),

Table A.6: Soil Parameters Used for Moon and Mars

Planet	k_c $[N/m^{n+1}]$	k_ϕ $[N/m^{n+2}]$	c [Pa]	ϕ [deg]	n	K [m]	Density $[kg/m^3]$
Moon	1400	8.2×10^5	170	35	1	0.018	1660
Mars	10000	8.5×10^5	1000	35	1	0.03	1300

Table A.7: Inputs and Outputs of Steering Module

Inputs	**Description**
nSteeredWheels	# of wheels that are steerable'
sprungMass [kg]	sprung mass of vehicle
wheelbase [m]	
track [m]	
Outputs	
mass [kg]	steering system mass
turningRadius [m]	turning radius of vehicle

the constant α (which is set to 1.4%) and W the wheel load. The unknowns are z, D and b. Equation A.12 is substituted in Equation **??** and an expression for b is obtained which is then substituted in Equation A.11). After simplification and solving for D the following relationship is obtained:

$$D^{n+1} + D^n \frac{3Wk_\phi}{(3-n)\alpha^{0.5}k_c p} - \frac{3W}{(3-n)k_c\alpha^{n+0.5}} = 0 \tag{A.13}$$

If n is assumed to be equal to 1 or zero, then the above equation becomes a polynomial of D. The model finds the roots of this polynomial to predict the wheel diameter required, however as noted above, it is restricted for the case of $n = 0$ or 1. For moon and mars $n = 1$, and for Earth the value of n for dry sand is 1.1 and is currently being approximated as 1 in the model for simplicity.

Once the diameter is determined the obstacle height is used to set the final value. The diameter must be twice the height of obstacle required to be traversed [82], and if the value from Equation A.13 is less, then it is increased to meet the obstacle traverse requirement.

The width of the wheel is then determined from Equation **??**.

The wheel mass is obtained from an empirical model based on data of light race car wheels.

$$m_{wheel} = 186 \times (D/2)^{2.81} b^{0.4} \times 0.7 \tag{A.14}$$

A.6 Steering Module

The steering module is very simple and assumes ackerman steering for the vehicle. It models the mass of a steering motor required for each set of wheels that are steerable, along with some additional mass for links etc. The additional mass is estimated to be 4 kg (based on data of electrically powered steering systems (EPS) in current vehicles given in [5]. It is assumed that the planetary vehicles

Table A.8: Inputs and Outputs of Terra-Mechanics Module

Inputs	**Description**
wheelDia [m]	
wheelWidth [m]	
wheelLoad [N]	load supported by one wheel
wheelSlip [%]	
sinkage [%]	fraction of wheel diameter allowed to sink
planet	'moon' or 'mars'
Outputs	
DP [N]	drawbar pull per wheel
slope [deg]	slope that vehicle can climb
R_c [N]	compaction resistance on wheel
R_b [N]	bulldozing resistance on wheel
H [N]	soil thrust per wheel

will have steer-by-wire systems (with no steering columns, rack and pinion assemblies etc), so the steering assembly additional mass is reasonable.

The motor power is estimated as:

$$P_{steermotor} = 960/(1600 \times 0.8) m_{sprung} \tag{A.15}$$

and is based on data from [6] and [11]. The motor power is then used to obtain mass of the motor from another empirical model based on masses of currently available motors and motor types. DC brushless motors are assumed to be used in this case.

The turning radius is based on the assumption that only one axle is steerable. This needs to be improved for the case of both front and rear wheel steering (as was the case in the LRV and hence the prediction of turning radius by this model is higher than the actual value for LRV). The wheel turn angle is assumed to be 50°. For ackerman steering the following equations hold [11]:

$$\cot\alpha = \frac{trk}{wb} + \cot\beta \tag{A.16}$$

$$\sin\alpha = \frac{wb}{R_{turn}} \tag{A.17}$$

where R_{turn} is turning radius and β is wheel turn angle in degrees. For known wheelbase, track and wheel turn angle, the turn radius is computed as

$$R_{turn} = \frac{wb}{\sin\left(\cot^{-1}\left(\frac{trk}{wb} + \cot\beta\right)\right)} \tag{A.18}$$

A.7 Terra-Mechanics Module

This module computes the motion resistances experienced by the vehicle. The wheels are assumed to be rigid (no pneumatic tires). Three kinds of resistances are computed that significantly affect motion of a rigid wheel on soft terrain: compaction resistance, bull dozing resistance, and rolling resistance.

A.7.1 Compaction Resistance

This is due to the compaction work done by the the wheels per unit length in pressing the ground to a depth of its sinkage. Loss of soil thrust in unprepared terrains is primarily due to the compaction resistance. It is given by [144]:

$$R_c = \frac{z^{n+1}}{n+1}\left(k_c + bk_\phi\right) \tag{A.19}$$

where R_c is the compaction resistance [N], and the other variables have been defined earlier.

A.7.2 Bulldozing Resistance

This is developed when a substantial soil mass is displaced by a wheel. This type of resistance is common when a wheel compresses the surface layers of the soil and pushes the soil fore and aft of the tire. It is worse for wheels that are thick [34, 27]. The bulldozing resistance is given as follows [34]:

$$K_{pc} = \left(N_c - \frac{2}{3}\tan\phi\right)(\cos\phi)^2 \tag{A.20}$$

$$K_{py} = \left(3\frac{N_\gamma}{\tan\phi} + 1\right)(\cos\phi)^2 \tag{A.21}$$

$$R_b = b\left(0.67czK_{pc} + 0.5z^2\gamma_s K_{py}\right) \tag{A.22}$$

where R_b is the bulldozing resistance [N], b is wheel width [m], ϕ is soil internal friction angle in degrees, c is cohesion [Pa], z is sinkage [m] and $\gamma_s[N/m^3]$ is specific soil weight.

A.7.3 Rolling Resistance

This captures the combined effects of various resistances to motion such as scrubbing at the wheel-soil interface, deflection of tread elements etc. It is given by:

$$R_r = \mu_r W \tag{A.23}$$

where R_r is the rolling resistance [N], μ_r is the coefficient of rolling resistance, and W [N] is the load on the wheel. The rolling resistance coefficient is assumed to be 0.03 based on an assumption made

in [138], however a more reliable estimate has not been found as yet. This can be further improved in the future.

A.7.4 Soil Thrust

This is the maximum thrust the soil can provide before undergoing shear failure. It is derived from the Coulomb's equation of shear failure. The maximum thrust, H, is given as:

$$H = (Ac + W\tan\phi)\left(1 - \frac{K}{sL}(1 - e^{\frac{-sL}{K}})\right) \tag{A.24}$$

where $A[m^2]$ is the area of the contact patch, K [m] is the coefficient of soil slip, s is wheel slip and L [m] is the wheel chord length. The wheel chord (labeled 'l' in Figure) is computed by

$$L = \sqrt{(}(D - z)z) \tag{A.25}$$

where D is wheel diameter, z is sinkage [m]. The contact patch (see figure 5) area A is bL, with the assumption that the width of the contact path is equal to wheel width. The wheel slip, s, is defined to be the percent difference between speed of wheel and speed of vehicle:

$$s = \left(1 - \frac{V}{r\omega}\right)100 \tag{A.26}$$

V is linear speed of wheel center, r effective rolling radius and ω angular speed of wheel. A slip of 35% is assumed in the model.

A.7.5 Drawbar Pull

The drawbar pull, DP, is defined as the force available at the draw bar. It is the difference between the soil thrust developed by the vehicle and the total resisting force on the vehicle [**?**]. It represents the ability of a vehicle to pull or push extra machinery/implements *etc.*

$$DP = H - \sum R \tag{A.27}$$

$$DP = H - R_c - R_b - R_r \tag{A.28}$$

The gradeability of a vehicle at 20% slip can be approximated by the ratio between the drawbar pull and wheel load [27]:

$$slope = \tan^{-1}\left(\frac{DP}{W}\right) \tag{A.29}$$

Although in a slip of 35% is assumed in the model, this formulation is still used as a first order approximation.

Table A.9: Inputs and Outputs of Drive System Module

Inputs	**Description**
driveType	type of drive system, drivenWheel, or central
motorType	'AC', 'DCbrush', or 'DCbrushless'
soilR [N]	total motion resistance due to soil
R_r [N]	rolling resistance
grade [deg]	max slope vehicle can climb
wheelDia [m]	Diameter of wheel
wheelSlip	
wheelbase [m]	
track [m]	
nWheels	#of wheels in vehicle
speed [km/hr]	max speed of vehicle
mobilityDuration [hr]	total time vehicle is moving
slopeFraction	fraction of moving time spent on sloped terrain
gplanet [m/s^2]	gravitational acceleration of planet
Outputs	
levelPower [W]	power required for level motion
slopePower [W]	power required for motion on slope
levelEnergy [W-hr]	energy expended during level motion
slopeEnergy [W-hr]	energy expended during motion on slopes
driveSysMass [kg]	total mass of drive system including motor, controller etc
motorData.torque [Nm]	torque of drive motor
motorData.power [W]	power of drive motor
motorData.mass [kg]	mass of drive motor

The gravitational resistance R_g is the resistance encountered by the vehicle when climbing a slope of angle θ. It is given by:

$$R_g = W(\mu_r \cos\theta + \sin\theta) \tag{A.30}$$

Note that this R_g includes the rolling resistance as well. The normal forces on the wheels change when the vehicle is on a slope, therefore the rolling resistance component is different and is given by the $W\mu_r \cos\theta$ term. The term $W \sin\theta$ is due to the force of gravity.

A.8 Drive System Module

This module models two kinds of drive systems: 'drivenWheel', or 'central'. In the first type each wheel is driven individually by its own motor (as was the case in the Apollo LRV). In the second type it is assumed that one central motor drives the vehicle, and the drive system includes a drive shaft. See Figure A-3

An empirical model for determining mass of motor (based on its power and type such as AC, DCbrush, or DCbrushless) and its controller is used to obtain mass estimates.

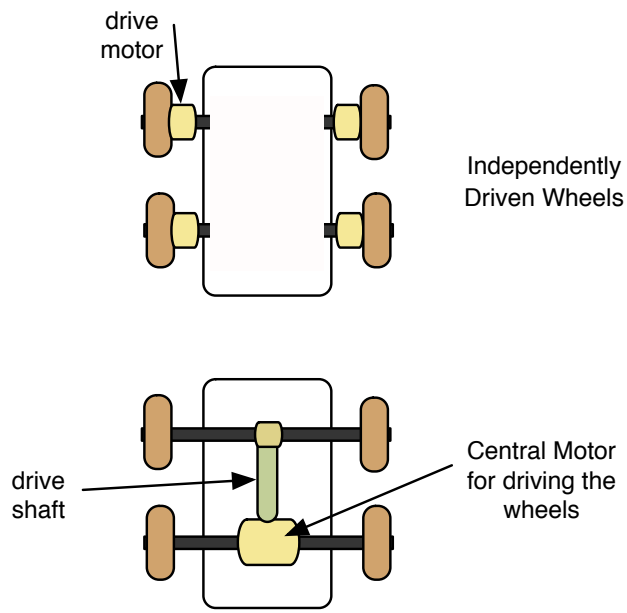

Figure A-3: Modeled Drive System Types

Independent Drive System

The required torque per wheel for moving the vehicle on level surface is determined by:

$$T_{level} = R_{soil} D/2 \tag{A.31}$$

and for moving on a slope by

$$T_{slope} = (R_{soil} + R_g + R_r) D/2 \tag{A.32}$$

The R_r is subtracted since R_g includes the rolling resistance on a slope.

The motor sizing is done separately for the two types of drive systems. For the 'drivenWheel' case, the efficiency η is estimated to be 98%, and harmonic drives with 80:1 ratio (similar to the ones that were used on the LRV) are considered. The motor power is then estimated as:

$$P_{motor} = \frac{v R_{soil}}{(1-s)\eta} \tag{A.33}$$

where v [m/s] is the top speed of the vehicle on level surface. The motor power is sized for full speed drive on flat surface, and it is just assumed that the speed on a slope will be lower.

The torque required from the motor is however sized for the worst case scenario (since the motor must be able to supply the maximum torque needed for traverse) and is given by:

$$T_{motor} = \frac{\max(T_{slope}, T_{level})}{i_g \eta} \tag{A.34}$$

where i_g is the speed reduction ratio of the harmonic drive.

The total drive system mass for the vehicle is the sum of motor mass, harmonic drive mass, and motor controller mass multiplied with number of wheels in the vehicle (since each wheel has separate motor, harmonic drive and controller).

Central Drive System

For the case of central drive type, an efficiency of 95% is assumed (as given in various references for this type of configuration). A gear ratio of 30:1 is assumed (although in terrestrial electrically drive vehicles the ratio is usually 10:1). The power required for the motor is obtained by:

$$P_{motor} = N_{wheels} \frac{vR_{soil}}{(1-s)\eta} \tag{A.35}$$

where N_{wheels} is the number of wheels in the vehicle. Note that R_{soil} is the total resistance experienced by a single wheels. The torque is sized as:

$$T_{motor} = N_{wheels} \frac{\max(T_{level}, T_{slope})}{i_g \eta} \tag{A.36}$$

The mass of the gearbox is obtained by an empirical model given in [83]. The drive shaft is a circular cross-section hollow shaft assumed to be made of carbon-fiber reinforced polymer. The thickness is assumed to be 3 mm and length to be 90% the length of the wheel base. The diameter of the shaft is determined based on the torque it needs to transmit (which is the torque delivered to wheels and is given by: $i_g T_{motor}$) and a safety factor of 4 for the shear strength. The axle shafts are also sized similarly with the assumption that that their length is equal to the vehicle track and need to withstand the wheel torque. Total mass of the drive system is the mass of the motor, motor controller, drive shaft and axle shafts.

The total power required for level motion at top speed is given by

$$P_{level} = P_{motor} F \tag{A.37}$$

where F is N_{wheels} for the case of independently drive wheels and is equal to 1 for central drive system. The total power required for traversing a slope is obtained by assuming that top speed is half of level speed:

$$P_{slope} = N_{wheels} \frac{v(R_{soil} + R_g - R_r)}{2} \tag{A.38}$$

Note, that this computation is not entirely accurate (since the gradeability of the vehicle given Plevel should be determined and then the power traversing that slope be calculated. This correction will be made in the future.

Table A.10: Inputs and Outputs of Power System Module

Inputs	**Description**
contP [W]	continuous power needed during operation of vehicle
levelP [W]	power needed for level driving
slopeP [W]	power needed for traversing slope
actP [W]	power for extrs activities such as drilling
contE [W-hr]	continuous energy needed duration operation
levelE [W-hr]	energy needed for level-terrain driving
slopeE [W-hr]	energy for traversing slope
actE [W-hr]	energy for exploration activities
TotalETime [hr]	Total time required for energy calculation
Source [-]	'batteries', 'FuelCells', 'solar' etc.
Type [-]	type of source e.g 'Li-Ion', 'AgZn' or 'InP', 'Si'
powercase [-]	1 or 2
gplanet [m/s^2]	gravitational acceleration of planet
Outputs	
PowerMass [kg]	[Primary Source Mass, Secondary Source Mass
Power Size	[m^2 or L etc]
P_all [W]	[PrimarySourcePower, SecondarySourcePower]
E_all [W-hr]	[PrimarySourceEnergy, SecondarySourceEnergy]
H [N]	soil thrust per wheel

The slope and power energy requirement is then computed as follows:

$$E_{slope} = P_{slope} t_{slope} \tag{A.39}$$

$$E_{level} = P_{level}(t_{mobility} - t_{slope}) \tag{A.40}$$

where t_{slope} is the total time [hrs] spent in traversing slopes, and $t_{mobility}$ is the total time the vehicle is moving and is computed by dividing vehicle range with speed.

A.9 Power System Module

The contP is power that is needed at all times while the vehicle is operating (it may or may not be moving). The model assumes the contP to be the sum of communication and navigation power and crew station power.

This module computes mass of power system given all the energy and power requirements of the vehicle. In addition to power required for driving, other subsystems such as crew station and perhaps additional activities require extra power.

The power source can be single or of two different kinds (such as solar and batteries). The total energy is first computed as the sum of contE, levelE, slopeE, and actE. The average power, P_{avg}, is obtained by dividing total energy with TotalETime.

If only single source is specified then power is obtained as the maximum power load required to

provide continuous power along with powering the drive of the vehicle or a high power activity.

If two sources are given then computation is done in two ways depending on powerCase variable. If powerCase equal to 1, the first source provides average power, and second source provides $P_{peak} - P_{avg}$ and $E_{total} - E_{avg}$. P_{peak} is the max power among contP, levelP, slopeP and actP. If powerCase equal to 2, then first source powers life support system, communication and nav, and mobility power and energy, while second source provides extra power for slope mobility and activities.

A power management and distribution mass of 17.4 kg/kW is included in the power system mass.

A.10 Dimensions Module

This module determines the overall length, width and height of the vehicle. The dimensions are estimated as follows:

$$L_{vehicle} = \max(D + wb, L_{cs}) \tag{A.41}$$

$$W_{vehicle} = \max(b + trk, W_{cs}) \tag{A.42}$$

$$H_{vehicle} = D/2 + H_{cs} \tag{A.43}$$

where L_{cs}, W_{cs} and H_{cs} are the length, width and height of the crew station.

A.11 Suspension Module

The suspension system is modeled as a simple percentage of the vehicle mass. The sprung mass of the vehicle is obtained and the suspension is assumed to be 12% of that mass (as indicated in [11] for commercial passenger vehicles).

$$m_{susp} = 0.12 \times m_{sprung} \tag{A.44}$$

A.12 Soil Parameters

A.13 Markov Model of Reconfigurable Vehicles Fleet

Table A.11: Parameters for Various Soil Types [144]

Type	n	k_c $[kN/m^{n+1}]$	k_ϕ $[kN/m^{n+2}]$
Dry sand	1.1	0.99	1528.43
Sandy loam	0.7	5.27	1515.04
Sandy loam (LLL)	0.2	2.56	43.12
Sandy loam MI (Strong)	0.9	52.53	1127.97
Sandy loam MI (Buchele)	0.4	11.42	808.96
Sandy loam	0.3	2.79	141.11
Sandy loam (Hanamoto)	0.5	0.77	51.91
Clayey soil	0.5	13.19	692.15
Clayey soil (Thailand)	0.7	16.03	1262.53
Heavy clay	0.13	12.7	1555.95
Heavy clay (WES)	0.11	1.84	103.27
Lean clay	0.2	16.43	1724.69
Lean clay (WES)	0.15	1.52	119.61
LETE sand	0.79	102	5301
Upland sandy loam	1.10	74.6	2080
Rubicon sandy loam	0.66	6.9	752
North Gower clayey loam	0.73	41.6	2471
Greenville loam	1.01	0.06	5880

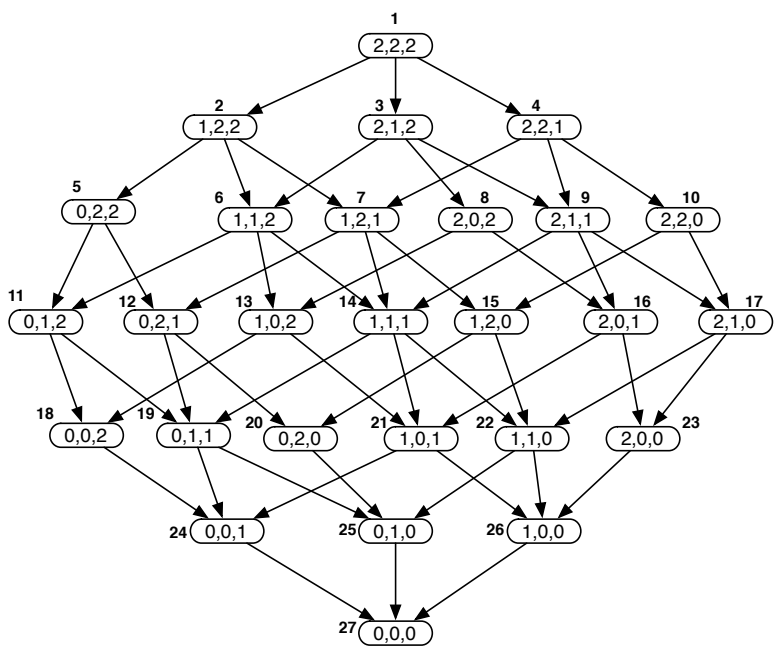

Figure A-4: Failure modeling of reconfigurable vehicles at fleet level

Appendix B

Reconfigurable Systems Descriptions

A set of representative systems, that fulfill the definition in Section 2.1, is described here. Each system is discussed in terms of its functional type, its reconfigurand (the thing that is reconfigured in the system), the outcome of reconfigurability, and the prime reconfiguring agent. The objective of studying these sample systems is to gain a better understanding of reconfigurability, and to identify any common trends or similarities across various aspects. Starting from simple components and consumer items, more complex air and space systems are progressively described here.

1. Potentiometers: The most simple example of reconfigurability is in a potentiometer. It is a variable resistor, that can provide different resistances in a circuit as desired. The outcome in this case is 'variable resistance', or more generally a reconfiguration in the system's functional attribute. The actual thing that undergoes a reconfiguration (or the *reconfigurand*) is a contact piece whose position is altered along the resistive strip. The length of the effective conductor gets changed which then produces a change in the resistance. The reconfiguring agent (the thing that produces or carries out the reconfiguration process) can be both humans or machines.

2. Adjustable Shock Absorbers: Another example is that of adjustable shock absorbers, in which the damping force can be changed to accommodate a wide range of conditions. These adjustable shock absorber can be used for a diverse array of energy absorption applications when input parameters vary or are not clearly defined [23]. These systems work by converting kinetic energy to thermal energy. More specifically, motion applied to the piston of a fluid-based shock absorber pressurizes the fluid and forces it to flow through restricting orifices, causing the fluid to heat rapidly. The thermal energy is then transferred to the cylinder body and dissipated to the atmosphere. The

(a) Potentiometer (b) Adjustable Shock Absorber

Figure B-1: Simple Reconfigurable Systems

size of the orifice can be changed by turning an adjustment knob and the damping coefficient gets altered. The reconfigurand in this system is the orifice, while the main outcome of reconfigurability is variable damping force, or more generally, reconfiguration of the system's functional attribute. The reconfiguration can be carried out both by humans or machines depending on the application. A typical adjustable shock absorber is shown in Figure B-1(b).

3. LEGO: These are perhaps the most well known and often-quoted products/systems in studies regarding modularity and/or reconfigurability. LEGO kits or toy sets, typically consist of a collection of various types of blocks (pre-dominantly) with identical interfaces that allow for constructing many different kinds of models. From toy gas-pumps to space ships, all sorts of things can be conceived and built. An important thing to note however is that LEGO blocks only structurally represent (to some basic extent) a system. In most of the cases, they do not carry out the associated functions, *e.g.* a LEGO airplane cannot fly, or a gas-pump cannot pump gas. Fundamentally, the main function of LEGO kits is to allow for model construction through reconfiguration of a fixed set of building blocks. The reconfigurand are the blocks, and the reconfiguring agent is usually a human. The outcome of the reconfigurations (*i.e.* when blocks are added, removed, or transposed in a model) is a change in the model's form, function (in some cases), form attribute, or function attribute.

4. Vacuum: Most vacuums for domestic use are equipped with a set of end-pieces that allow for cleaning surfaces of different types and sizes. There are pieces for cleaning narrow, small corners, and there are other types of pieces that allow for picking up dirt with an additional (and sometimes motorized) brush. The reconfigurand is the suction hose pipe (whose end gets substituted with different types of parts). The outcome is a change in the system's form attributes (since various pieces are added/removed or transposed) and function attributes (suction area, speed *etc.* get varied.).

5. Food Processor: Many kitchen items have some sort of reconfigurability. Food Processors are one such example, in which the cutting blades can be changed to produce different kind of 'pro-

(a) LEGO Blocks (b) Vacuum Attachments (c) Food Processing System

Figure B-2: Some Common Reconfigurable Items

cessing functions' such as shredding, slicing, grinding, grating, and even juice extraction *etc.* The reconfigurand is the cutting piece, while the outcome is a change in the system's form, and function.

6. Sewing Machine: A variety of patterns and sewing-related functions can be carried out in modern sewing machines. Many models allow for selecting dozens of different stitch patterns by changing the motion of the needle (through mechanical adjustment of the needle head). The reconfigurand is the needle head, and the outcome is a change in the system's functional attribute (*i.e.* pattern style).

7. Convertible Stroller Backpack: These are child-carrying devices from that can either be configured as a 'back-pack', in which the child is carried on person, or can be in a stroller configuration. The basic function of carrying a child remains the same, however the process used in fulfilling that function (*i.e.* either carrying or rolling) is different in the two configurations. The operand (the things that undergo reconfiguration) are the structural members that are positioned differently for the the two configurations, and the outcome is a change in the system's form attributes and functional attributes.

8. Digital Photoframe: This gadget, with a 5 by 7 inch wood finish frame, is a new way to display photos without PCs. Digital photos from a digital camera, or MemoryStick can directly be loaded onto this MemoryFrame via its built-in USB port. It has an active-matrix TFT LCD display for high resolution digital images. It can store 32-80 digital images that can also be played as a slideshow in the home or office. On an abstract level, this system can be considered as an 'information storage' system, in which the reconfigurations take place through exchange of information via its USB interface.

9. USM Haller Table: The Swiss company USM produces designer modular furniture for home and office use. Steel spherical joints, tubes, and panels (Figure B-5(a)) are the principal elements of

(a) Reconfigurable Sewing Machine

(b) Convertible Stroller

Figure B-3: Some Common Reconfigurable Items

(a) Digital Photo Frame

(b) Installing Pictures on the digital photo frame

Figure B-4: A digital photo frame allows for easy change of pictures

(a) USM joint

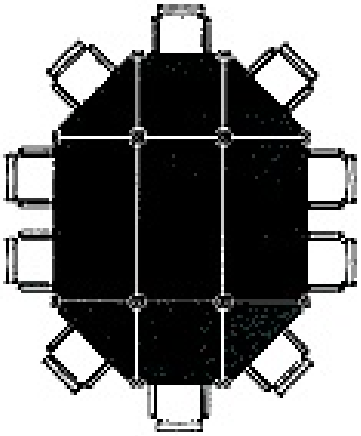

(b) Table Configuration 1

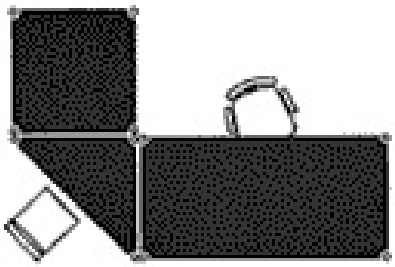

(c) Table Configuration 2

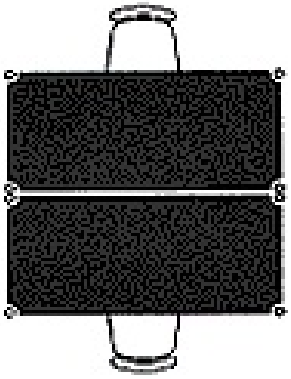

(d) Table Configuration 3

Figure B-5: USM Haller Reconfigurable Table

USM's furniture system [45]. There is a high degree of commonality, and from a basic set of parts, a variety of furniture items ranging from shelves to tables to displays are manufactured. The particular item used as a sample system is the USM Haller Table. Figures B-5(b), B-5(c) and B-5(d) show some of the numerous configurations that can be created with the modular, reconfigurable table building blocks.

10. Cribs: Some of the most commonly encountered reconfigurable systems in daily life are reconfigurable furniture that run the gamut from reconfigurable chairs to reconfigurable office cubicles. There are many cribs that can be reconfigured into seating furniture, or a toddler bed. The reconfigurand are the structural elements (wooden parts/pieces) of the furniture, while the outcome of the reconfiguration is a change in the system's form (*e.g.* from a crib to a bed), and function attribute (*e.g.* the sleeping area changes when reconfigured from crib to toddler bed). Figure B-6(a) shows a

typical 3-in-1 reconfigurable crib.

11. SofaBed: Futons or Sofa-Beds are often used when space is at a premium. They serve as convenient pieces of furniture that provide for seating in the day time and sleeping at night. They are also useful for providing a 'bed' to the occasional guest, while mostly serving as a 'sofa' in a living area. The reconfigurand here also are the structural parts that are shifted/moved in some fashion to produce the bed or sofa configuration. The outcome is a change in the system's form attribute and functional attribute.

12. Adjustable Bed: There are some types of beds with mechanized adjustment of height, and angle to allow for various positions. Hospital beds are routinely adjustable, and some models are also available for home use. These systems are electro-mechanical in nature and employ AC motors, hand-held position adjustment remotes etc. The reconfigurand are the structural parts (portions for head rest, back rest, lower body support etc) whose angle and height is adjusted, while the outcome is a change of the system's form attributes.

13. Convertibles: Cars have recently begun to exhibit reconfigurability in various ways. Minivans with reconfigurable seating (in which the seats can be removed entirely from the vehicle to create more space when desired), convertibles that can switch between an open bed truck and a small SUV *etc.* have been introduced in the last few years. In this study however, convertibles will be discussed. In a convertible, the roof is essentially reconfigurable in the sense that it can either be deployed or stowed (Figure **??** provides an illustration). The reconfigurand is the roof, and the outcome is a change in the system's form attribute.

14. SMART Cars: These cars have become very popular recently in Europe. Their typical models are 2-passenger vehicles that are very small but safe. They are meant for city driving, extremely economical on fuel, and include numerous features to appeal to urban-living. It has introduced a novel interlocking design that allows owners to change the car's color panels as often as they change cell phone faceplates [92]. The plastic body panels allow for easy reconfiguration and enable a different look for the car as often as the owner may want. Figure B-7(c) shows a SMART car undergoing such a change. The reconfigurand in this system are the body panels, while the outcome of the reconfiguration is a change in system's form attributes.

15. Reconfigurable Race Car: Some conceptual studies about reconfiguring critical design features in race cars as they traverse different types of segments on a race track have been carried out. It has been shown that the ability to reconfigure the center of gravity, roll stiffness and aerodynamic

(a) 3-in-1 Reconfigurable Crib

(b) Sofabed

(c) Adjustable beds

Figure B-6: Reconfigurable Furniture

(a) Convertible With Roof Down

(b) Convertible With Roof Up

(c) SMART car with easily changeable body panel

Figure B-7: Reconfigurable cars

(a) Polybot Segment (b) Various Configurations

Figure B-8: Polybot: A self-reconfigurable modular robot [147]

down force, while the car operates along different sections of the track (such as curves, straight-aways etc.) can greatly benefit race times. Even though such a system is currently only conceptual, it is included in this study for analysis. The operand here will be the components that are shifted to affect the dynamic properties, while the outcome is a change in the system's form attributes and function attributes.

16. Polybot: These are reconfigurable robots under development at the Xerox Palo Alto Research Center (PARC). The Polybot is a modular self-reconfigurable robot system composed of two types of modules called *segments* and *nodes*. Most of the functionality is is in the segment module. It has one degree of freedom (DOF) and two connection ports, a DC motor and a computer. The node module is rigid with no internal DOF, six connection ports and a computer. Its primary purpose is to allow near arbitrary topologies (chains, star, loops *etc*). The potential applications of the Polybot for space missions include maintenance operations (in which the robot can configure in various forms to conform to varying volumetric constraints) and planetary surface mobility for exploration. Its versatility allows it to be able to traverse a very wide range of terrain and overcome a large variety of obstacles [147].

17. Lander Amorphous Rover Antenna (LARA): This is a concept application based on the Autonomous Nano-Technology Swarms (ANTS) architecture being studied at Goddard Space Flight Center (GSFC). The ANTS basic structure is a robot consisting of identical struts arranged in a tetrahedron shape. In the prototype electric motors are located at the corners of the tetrahedron, which are called nodes. The nodes are connected to struts which form the sides. The struts telescope like the legs of a camera tripod, and the motors in the nodes are used to expand or retract the struts. This allows the robot to move: changing the length of its sides alters its center of gravity, causing it to topple over. It thus produces motion by toppling successively. The nodes also pivot, giving the robot great flexibility [22]. Figure B-9(a) The tetrahedron modules will be made much

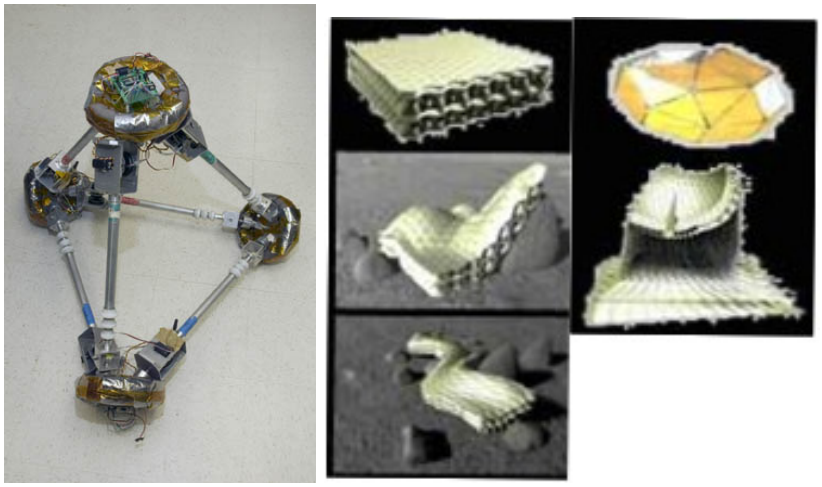

(a) ANTS robot (b) LARA Concept

Figure B-9: Reconfigurable Space Systems based on ANTS architecture

smaller by replacing their motors with Micro- and Nano-Electro-Mechanical Systems. The struts will be replaced with metal tape or carbon nanotubes to reduce size. It will also greatly increase the volume efficiency for space transportation since tape and nanotube struts are fully retractable. The miniature tetrahedrons, when joined together in "swarms", will have abundant flexibility by changing its shape to accomplish highly diverse goals. For example, while traveling through a planet's atmosphere, the swarm might flatten itself to form an aerodynamic shield. Upon landing, it can shift its shape to form a snake-like swarm and slither away over difficult terrain. If it finds something interesting, it can grow an antenna and transmit data to Earth. Highly-collapsible material can also be strung between nodes for temperature control or to create a deployable solar sail. Additionally, the nodes will be designed to disconnect and reconnect to different struts. If a meteoroid or rough landing punches a hole in the swarm, the system can heal itself by rejoining undamaged nodes and still carry out its mission [22]. The specific system chosen for study is the Lander Amorphous Rover Antenna (LARA) concept which is estimated to be a 50 kg spacecraft that can radically change shape to carry out some of the above described tasks [44]. Figure B-9(b) shows some of the functional concepts.

18. Sample Return Rover The JPLs Sample Return Rover (SRR) is a small, 10 kg class, autonomous rover with actively controlled shoulder pose, a positionable arm, and high performance real-time stereo navigation and obstacle avoidance. It has four 20 cm diameter wheels with independent steering. The SRR has been developed with the ability to actively modify its kinematic configuration to enhance rough terrain mobility. For example, when traversing an incline, SRR can lower one side of its suspension to increase its stability margin for tip-over failure. It accomplishes this using two active shoulder joints. The left and right side shoulder joint angles are independently

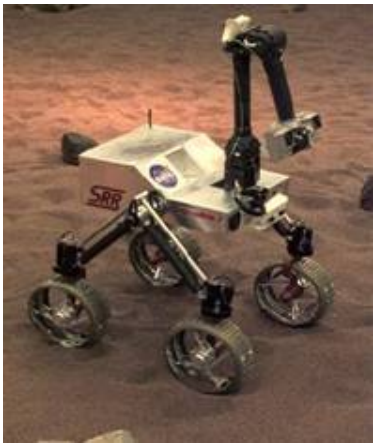

(a) SRR Pose 1

(b) SRR pose 2

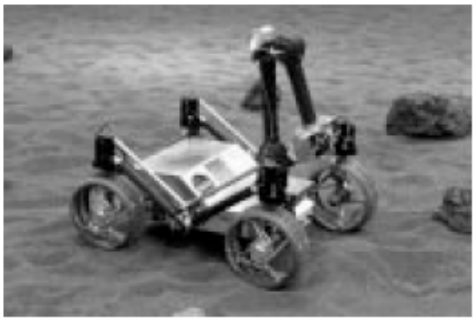

(c) SRR pose 3

Figure B-10: JPL Sample Return Rover [59]

controllable and can be manipulated to change the robot's stance. SRR can also redistribute its center of mass by repositioning its manipulator [59]. Figure B-10 shows some of the various configurations this robot can achieve.

19. Solar Maximum Mission: This spacecraft was based on the multi-mission modular spacecraft (MMS) platform designed by NASA in the 1970s (see Figure B-11(a)). The MMS had modules for propulsion, power, attitude control, command and data handling etc. The MMS design was for a system of serviceable and re-usable satellites and satellite components. The modular design was intended to make satellite design assembly (integration) and test faster and less expensive. It was the implementation of a vision of regular access to space, modular and interchangeable spacecraft components, easy integration of new technology, the establishment of design standards, and other concepts [84]. The Solar Maximum Mission was launched in 1980 to study solar flares. A malfunction in the satellite in January 1981 essentially rendered it useless. The SMM was later recovered by the space shuttle Challenger in April 1984, and became the first satellite in history to be serviced in orbit. The servicing took two days since on the first day the astronauts were unable to capture

the satellite. However once it was retrieved on the second day of the servicing mission, the actual replacement of the failed component with the new was done in 40 minutes [110]. The SMM served out its productive life until burning up in the Earth's atmosphere on 2 December 1989 [24].

20. Self-Assembling Wireless Autonomously Reconfigurable Modules (SWARM): This system is a functional prototype of a modular, wireless, spacecraft which minimizes hard interfaces between subsystems and standardizes those which remain [96]. Figure B-12(a) shows an assembled SWARM system. The main sub-systems (such as propulsion, Attitude Control, Command and Data Handling etc) are implemented in separate modules, with similar packaging, that all connect together through a 'Universal Docking Port' (as shown in Figure B-12(b)). The potential target benefits (from development and manufacturing aspects) are reduced inventory complexity, customization at assembly, simplified integration and verification and re-use of design and test processes among others. The potential In-orbit applications that can come about with such a system include inspection applications in which the spacecraft can separate into multiple smaller spacecraft for inspection, long baseline sensing applications can also benefit from such system. On-orbit upgrade, due to either failure, or obsolescence becomes possible (without requiring human servicing) in which the failed or old module is jettisoned and replaced with a new one that docks with the spacecraft.

21. Field Programmable Gate Array (FPGA): These are devices that have software programmable logic components and interconnects. The logic components can be programmed to have basic logic functionality (*e.g* AND, OR, NOT), or more complex math functions *etc*. The interconnects can be programmed to connect the various logic blocks as desired. The result is a custom circuit for an application, that can be readily changed into another circuit as and when desired. The implementation of the circuit is in hardware (the logic blocks and interconnect are hardware elements), but its description is in software, which makes the system highly reconfigurable. The reconfigurand in this case are the logic blocks and the interconnects, while the outcome of the reconfiguration process is modified function attribute. A Xilinx Virtex II Pro chip is considered in this study since its a widely used FPGA, and is also employed for space applications.

22. Evolvable Hardware (EHW): This refers to self-configuration of electronic hardware by evolutionary/genetic search mechanisms. Evolvable hardware can maintain existing functionality in the presence of faults and degradations due to aging, temperature, and radiation. It can also reconfigure for new requirements when mission changes occur. A prototype system has been developed at the Jet Propulsion Lab (JPL) based on Field Programmable Transistor Arrays (FPTA)[78]. Devices based on FPTAs have high degree of reconfigurability since the circuit is reconfigurable at the transistor level, whereas in the more common FPGA-based systems, the reconfiguration is done at at a more

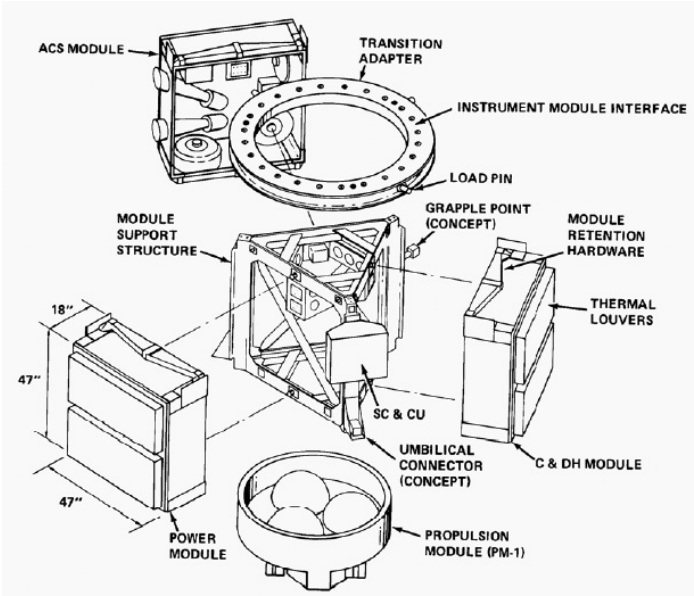

(a) Multi-mission Modular Spacecraft[84]

(b) Solar Maximum Mission Spacecraft [17]

Figure B-11: Multi-Mission Modular Spacecraft for Reconfigurability during Manufacturing and Servicing

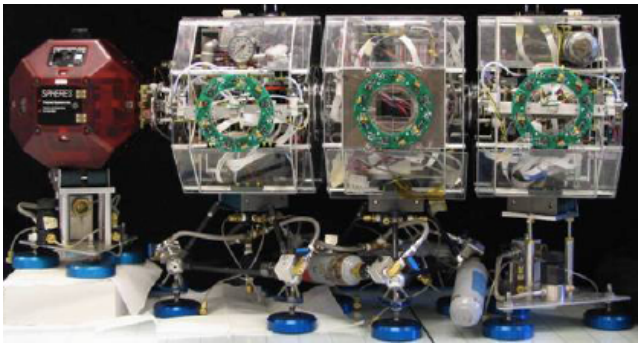

(a) SWARM[96]

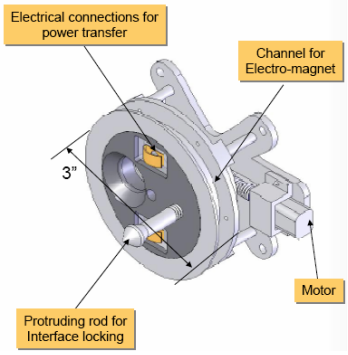

(b) Universal Docking Port used in SWARM modules[96]

Figure B-12: Self-Assembling Wireless Autonomously Reconfigurable Modules

(a) Actel's Radition Hardened FPGA

Figure B-13: FPGA with 2 million gate density, and upset rate of $< 10^{-10}$ error/bit-day

coarse level of granularity (*i.e.* at the logic cell level which itself is a collection of transistors). The FPTA module is an array of transistors interconnected by programmable switches, whose ON or OFF status determines a specific topology of the circuit. As the conditions or requirements change over time, the circuit is allowed to 'evolve' in real time through Genetic Algorithm based optimization to select the best configuration for the given state of conditions. A fitness function is specified for the system and the circuit tries to evolve to the best configuration (defined by the states of the transistors) that gives the best performance. Figure B-14(a) shows the complete prototype system consisting of a reconfigurable circuit hooked up with a PC. A number of fault-tolerance experiments have been performed that show how this system can self-recover in case of anomalies [132]. Two cascaded FPTA cells connected by 6 switches and comprising of 88 bits were 'evolved' to have the functionality of an analog multiplier. After generation 59 of the GA, when the best individual was sufficiently close to the target, one fault was induced by cutting one connection between the two FPTA cells, degrading the multiplier response. After 20 generations the GA was able to recover the desired circuit functionality. In another set of experiments, a NOR gate was implemented for normally operating at 27 C. It was then placed in a 330 C environment. The FPTA first produced a degraded response, but was then able to evolve and recover functionality under the new thermal conditions.

23. Ultra Long-Life Avionics: This is a avionics prototype system developed by the former NASA Exploration Team, NEXT [41] (which is now the NASA Space Architecture Team at head quarters) for ultra-long life space systems that require long-term survivability and adaptability. The architecture essentially consist of identical *generic function blocks*, communicating over wireless connections, that can be programmed to replace a wide variety of components in-flight (as shown in Figure B-15(a)). Hence each individual generic block is equivalent to an entire redundant string of components in a conventional approach. In this way a greater level of reliability can be potentially

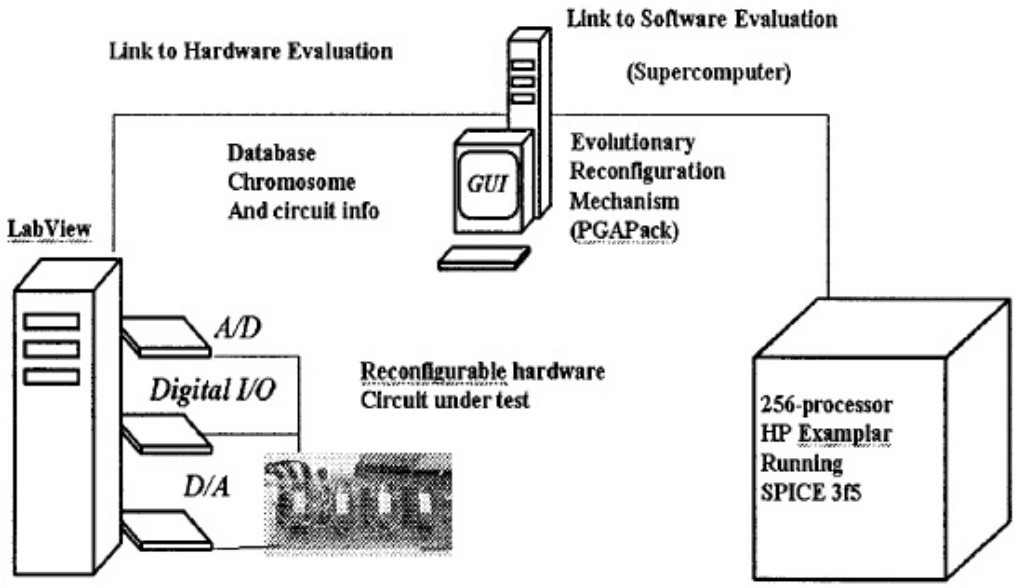

(a) Evolvable Hardware Prototype System

Figure B-14: FPTA circuit connected to a computer and software that evaluates optimal state for the circuit using a Genetic Algorithm technique.

achieved with less components. The prototype implements a navigator that has a gyroscope, star tracker, and accelerometer. Each of the sensors has its own controller, which collect data from the sensor and send it to the a local controller for processing. See Figure for a schematic. Each sensor's controller is implemented in a 600,000 gate FPGA (which is the generic function block). This prototype can detect failures in any one of the 'generic function blocks' by means of autonomous testing through wireless communication among the blocks. Once the failed block is identified, the tasks of the failed block are reallocated to a healthy block.

24. Reconfigurable Communications Equipment: This is the communications payload currently under development for the Japanse SmartSat-1 program in which twin 150-kg small satellites will be launched in 2008 into GEO. These satellites are using a Reconfigurable Communications Equipment (RCE) which will serve to flight qualify the onboard software radio technology, and concepts of functional redundancy and graceful degradation of systems with reconfigurability (see Figure **??**). The RCE consists of two patch antennas for transmitting and receiving, an X-band transponder, and onboard software-defined radio (OSDR). The OSDR has two banks of 3 FPGAs each, and a seventh FPGA controls the two banks. A multi-rate QPSK modulation and demodulation function from 2 kbps to 2 Mbps has been implemented. There are three operating modes: triple-redundancy, daisy-chain, and degenerate. Figure B-16 shows these configurations. The first mode has highest accuracy and can be used for tasks such as receiving configuration stream from Earth and writing it to non-volatile memory installed onboard). With the triple redundancy the

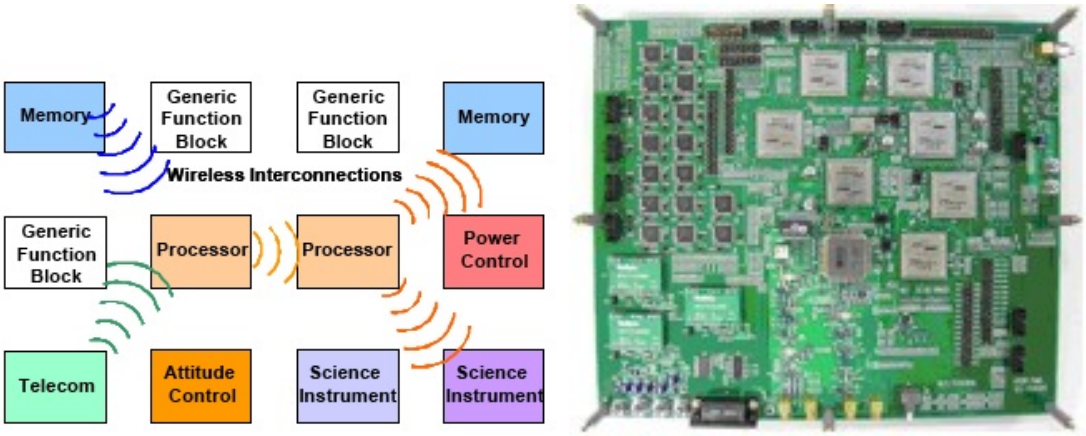

(a) Avionics Using Generic Function Blocks[41]

(b) RCE on SmartSat-I

Figure B-15: Reconfigurable Electronic Systems

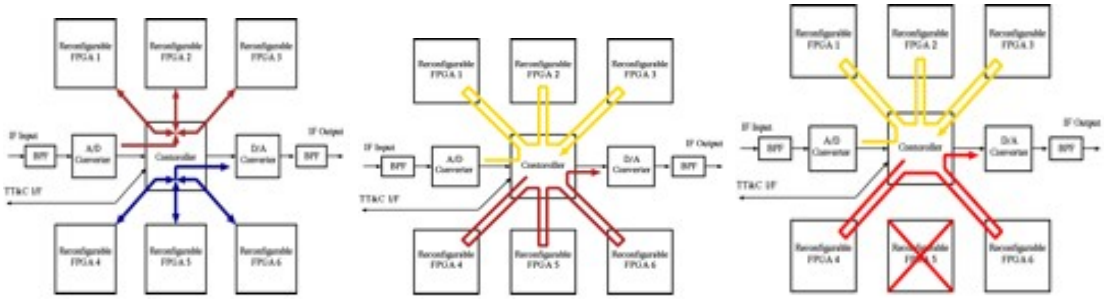

(a) Triple Redundancy Mode

(b) Daisy Chain Mode

(c) Degenerate Mode

Figure B-16: Three modes of the Onboard Software Defined Radio (OSDR) on SmartSat-I

data is checked from among the FPGAs and any discrepancy is corrected. In the daisy chain mode however the throughput is greatest and can be used for tasks that benefit from this configuration. In the degenerate mode one of the FPGAs is detached logically from use. A bank that includes a collapsed FPGA is assigned modulation/encoding function that requires lighter computational complexity than the demodulation/decoding function [105].

25. MEMS Patch Antenna: This is a prototype system consisting of a micro-electro-mechanical (MEMS) actuator for reconfiguring a patch antenna (see Figure B-17(a)). The actuator consists of a moveable metal overpass suspended over a metal stub. The overpass can move up and down and is actuated by an electrostatic force of attraction set up by a voltage applied between the metal overpass and the stub. A metal strip attached to the metal stub behaves as a parallel plate capacitor. The patch antenna operates at its nominal frequency when the actuator is in the OFF state. The actuator is in the ON state when the overpass is pulled down by the electrostatic force and the capacitance of the metal strip appears in shunt with the input impedance of the patch antenna. This capacitance tunes the patch to a lower frequency of operation. For specific prototype that has

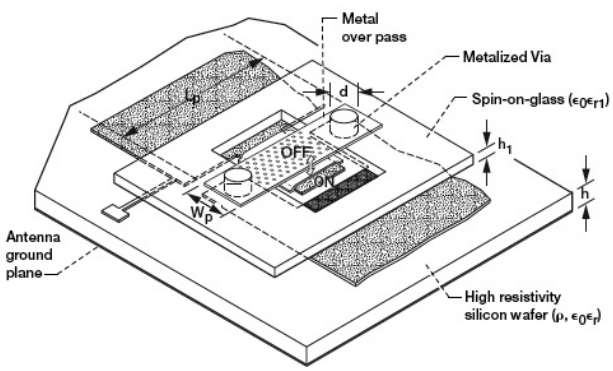

(a) MEMS Patch Antenna Actuator

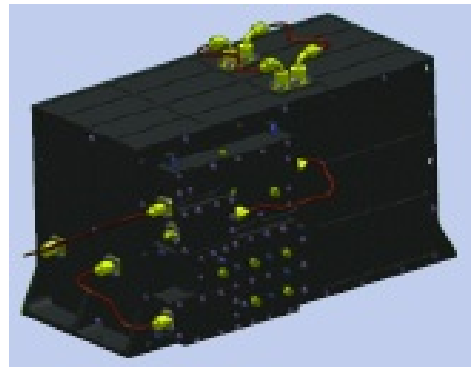

(b) On-orbit Reconfigurable TT&C Transponder

Figure B-17: Reconfigurable Communication Systems

been implemented, the antenna resonates at 25.4 GHz when the actuator is in the ON state, and at 21.5 GHz when in the actuator is in the OFF state. The patch can thus be dynamically reconfigured to operate in two different bands separated by a few gigahertz [125].

26. Reconfigurable Transponder: Alcatel Espacio's Tracking, Telemetry and Command (TTC) transponder for the Galileo satellites is a modular, dual-mode reconfigurable transponder. The receiver and transmitter frequency and signal modulation and coding schemes can be reconfigured on-orbit. The reconfigurand is the information that resides in the transponder's DSP (that processes the signals according to the appropriate scheme), and the outcome of a reconfiguration is a change in the function attributes of the system.

27. Reconfigurable Data Acquisition Devices: In PC-based data acquisition (DAQ) and measurement systems (as opposed to stand-alone devices such as oscilloscopes or signal analyzers with dedicated functionality), there has traditionally been a a fair degree of reconfigurability. Since the measurement and acquisition applications are defined in software, there has always been great versatility in these systems. A new set of devices employing FPGAs however have further increased the reconfigurability for the end-user, and in this study National Instruments Reconfigurable Input/Output (NI RIO) devices are included in the set of systems to be discussed. The RIO hardware can have custom high-speed digital proctocols, and user-defined onboard decision making and triggering. In the RIO system there is a controller, a chassis (in which the FPGA chip resides), and hot-swappable Compact I/O modules (*e.g.* Analog Input Module, AO module, Digital Input module, Digital Output *etc.*) that connect to sensors, transducers, and other devices. The controller allows signal processing and analysis applications to run, and it receives data from the chassis through a PCI bus. By varying the module types, and number (multiple chassis can be hooked together), a highly modular, reconfigurable data acquisition and analysis system is realized. The reconfigurand

(a) RIO Chassis

(b) RIO Modules

(c) Complete RIO DAQ System

Figure B-18: Reconfigurable Data Acquisition Measurement System

are the RIO modules, and the FPGA chip, while the outcome of the reconfigurations is a changed form attribute, function attribute, or even the function.

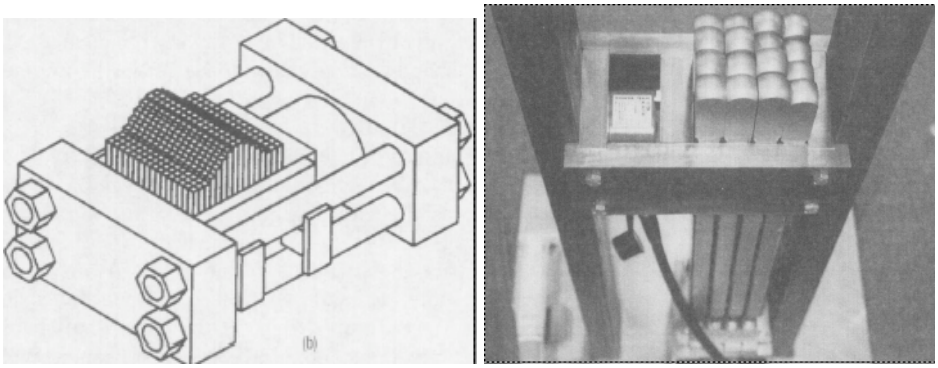

(a) Schematic of a the Discrete Die Concept (b) Prototype of Discrete Die

Figure B-19: Reconfigurable Discrete Die for Forming Aircraft Body Panels

28. Reconfigurable Discrete Die: This die, for forming aircraft body panels, was developed to cut time and cost of tooling development in the late 1990s [137]. A custom die for one panel type can cost about $19000. A typical aircraft can require hundreds of types of panels, *e.g.* each F-14 fighter aircraft has about 300 stretch-formed fuselage panels. The total development cost and fabrication time for stretch forming tooling was more than $5 million to make only 750 planes [137]. In order to reduce the time and effort of tooling fabrication for low volume products, a reconfigurable discrete die, consisting of a matrix of close packed individually actuated pins was prototyped. Each pin is a simple hydraulic actuator fitted with an in-line solenoid valve to control its vertical position. Pin positions can be either set in a closed or open-loop fashion. Once the pins are 'set', then the entire matrix is clamped into a rigid tool. Since aircraft body panels have very gentle curvatures and few if any, small part details, large pins (widths of 25 mm) were used in the prototype. Figure B-19(b) shows the concept schematically and the smaller prototype that was built. The dimpled surface of the discrete die, is covered with a deformable elastomer, called an interpolator, during forming and is expected to be changed after every 100 or so forming jobs. The required shape is input to the die control system, through a GUI, by specifying parameters of standard shapes like cylindrical, saddle, biconvex shapes *etc.*, or the height of each individual pin can be specified. The cost of such a tool for a 1.0 X 2.0 m forming area is around $700,000.

29. Reconfigurable Manufacturing Systems (RMS): These are systems designed at the outset for rapid and easy reconfiguration to allow for manufacturing to respond to changing needs. An RMS has been described as "a machining system which can be created by incorporating basic process modules-both hardware and software-that can be rearranged or replaced quickly and reliably. Reconfiguration will allow adding, removing or modifying specific process capabilities, controls, software, or machine structure to adjust production capacity in response to changing market demands or technology. This type of system will provide customized flexibility for a particular part

(a) Supertrack programmable pallet conveyor [95]

(b) Morpheum (Modular Reconfigurable Parallel Upgradeable Machine) in 4 DOF configuration [135]

Figure B-20: Reconfigurable Manufacturing Systems

family, and will be open-ended, so that it can be improved upgraded, and reconfigured, rather than replaced [93]." It is important to differentiate RMS with CNC machines. The CNC systems have multi-functionality and a high degree of flexibility in the types of jobs they can do, however the system design is not motivated nor intended to be changed in any significant way once the CNC system has been deployed. An RMS however is specifically meant to undergo reconfigurations as required. Figure B-20(a) shows a conveyor system which has been built on RMS design principles and can undergo various kinds of reconfigurations fairly quickly and easily [95]. Figure B-20(b) shows Morpheum, which is 4 DOF reconfigurable machine also built for RMS [135]. A particular manufacturing system consisting of 30 machines is assumed in this study (to obtain approximate mass, volume, cost estimates for comparison with other systems).

(a) NextGen UAV Concept with Sliding Wings[89]

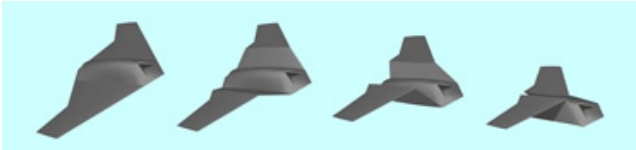

(b) Lockheed-Martin Concept with Folding Wings[89]

Figure B-21: Concepts for a Morphing Wing Unmanned Air Vehicle

30. Morphing Aircraft: The Defence Advanced Research Programs Agency (DARPA) has been spearheading an effort to develop aircraft capable of radical wing area changes, more than 150%, in-flight. The changes will be both in wing sweep and wing span, which would allow a single aircraft to 'morph' into various configurations appropriate for the mission (attack, reconnaisance *etc.*) at hand. A morphing wing capability will give drastically different mission roles during a single flight to an aircraft. The aircraft can thus configure according to a planned mission, or it can adapt to changing mission needs as they evolve over time during its flight. DARPA is also developing, very efficient, very volumetrically small, piezoelectric actuators through the Compact Hybrid Actuators Program (CHAP). They can be installed in the wing and provide actuation where it's needed. This eliminates the need of having large actuators and doing force transmission from a central location which can add a lot of material and weight . The CHAPs are very good at operating at low frequencies for periods of several seconds or even minutes to move the wing to a new configuration. But they can also operate at tenths of seconds to give control forces. A number of concepts and prototypes are being developed by various researchers and organizations in this regard. NextGen is looking at a sliding skins idea, Raytheon at telescoping wings and Lockheed Martin at rotating and folding wings [89]. The specific system chosen for study is a concept vehicle studied using the NextGen Aeronautics firebee UAV as a baseline [75].Figure B-21(a) shows one of the concepts being explored.

31. Grumman F-14 Tomcat: This supersonic, twin-engine, fighter aircraft has variable-sweep wings that allow optimum efficiency throughout the plane's flight envelope (see Figure B). Minimum sweep is used during low-speed flight to reduce takeoff and landing speeds while maximum sweep reduces drag during supersonic flight. Varying the wing geometry in-flight allows the F-14 to maximize range and endurance in its primary air patrol and escort mission[4]. The sweep range is

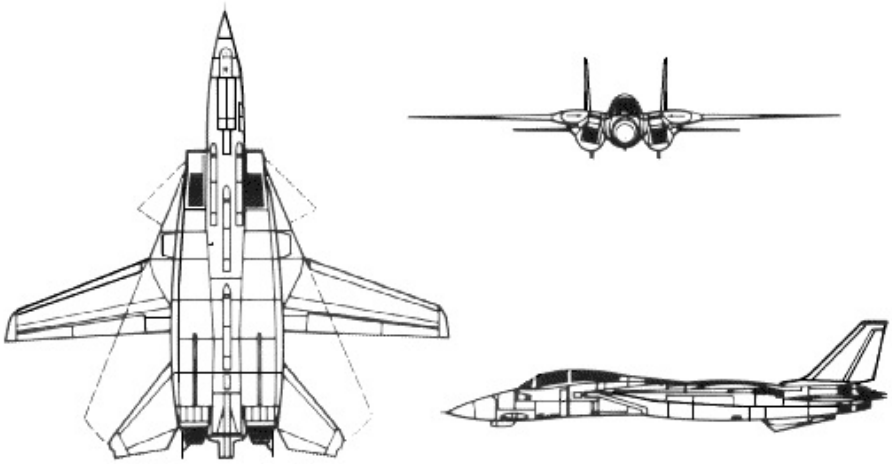

Figure B-22: F-14 Tomcat fighter with variable-sweep wings[21]

20 to 68 degrees and sweep speed is 7.5 deg/sec[20]. The unit cost of an F-14 was $38 million. It had a mass penalty of 2300 kg due to additional actuators and elements that were required to have a variable sweep wing as compared to a fixed wing[18]. The airframe design life was 7200 hours, and the plane was in military service for approximately over 30 years.

32. Variable Diameter Compound Helicopter: This is a concept rotorcraft studied in the late 1990s [140]. The design concept consisted of a variable-diameter main rotor, turboshaft/turbofan convertible engine, virtual-canopy cockpit, and reconfigurable payload bay. The rotorcraft was designed to be adaptable for various kinds of missions: Attack, Armed Recon, Scout, Combat Search and Rescue, and Utility (transportation of cargo *etc*). The high-speed dash, efficient hover, and vertical take off and landing (VTOL) requirements led to consideration of the class of vehicles known as "high speed rotorcraft" which have the ability to take off and land vertically but can also convert to a forward flight mode for achieving cruise speed and performance similar to that of a fixed-winged aircraft. Most high-speed rotorcraft reconfigure from helicopter to fixed-wing modes through transferring of lift from rotating blades to fixed wings. At the same time, propulsion maybe shifted from one source to another. In each case, the air vehicle reconfigures inflight enabling it to achieve the performance of either a helicopter or a fixed-wing airplane. In the VDCH the vehicle makes use of two convertible turbofan engines, able to provide shaft power to drive the main and tail rotors and jet thrust either separately or simultaneously. The wings allow for off-loading of the main rotor so that rotor stall and compressibility effects do not hinder the vehicle performance at high forward speed. In contrast to other high-speed rotorcraft, VDCH has no true "conversion". Instead the transition between helicopter and fixed-wing flight occurs continuously throughout the flight envelope. At speeds above the critical cruise velocity (200 kts for this aircraft), the rotor has been retracted to its smallest diameter and off-loaded. The variable-diameter rotor design is based on the Sikorsky

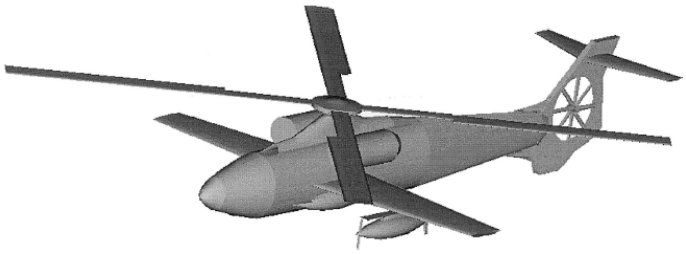

(a) VDCH Concept[140]

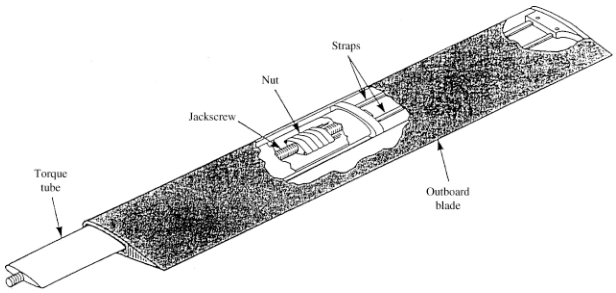

(b) Sikorsky TRAC-rotor[140]

Figure B-23: Variable-Diameter Compound Helicopter Concept

TRAC rotor which can extend and retract in flight using a jackscrew. A system of clutches in the rotor hub controls the extension/retraction. The convertible engine is used in turboshaft mode when gases are directed to the power turbine which drives the main rotor and tail rotor shafts. In turbofan mode, variable-inlet guide vanes direct inlet air through the fan and the shaft is de-clutched to provide jet thrust from the engine. The VDCH has some significant advantages over rotor-wing or stowed-rotor aircraft that require require complex mechanisms to stop, lock and stow the rotor. The VDCH can operate as a fixed-wing aircraft even in take off and landing, and if necessary, it can complete its mission with rotors inoperative.

33. Very Large Array (VLA): This consists of 27 radio antennas in a Y-shaped configuration in New Mexico. Each antenna (considered as a module in this system) is 25 m in diameter. The telescopes are arranged in 4 configurations, A, B, C, and D for approximately three months each during the year. Each change of configuration takes approximately two weeks. When they are in the A configuration, the telescopes extend over the 21 kilometer (13 mile) length of each arm. This simulates a single dish that is 36 kilometers (22 miles) in diameter. This configuration, has the most magnification and the greatest details can be seen. The size of the array gradually decreases with the B and C configurations until, in the D configuration, the telescopes are all placed within 0.6 kilometer (0.4 mile) of the center. In the smaller configurations, scientists can study the overall structure of the source they are observing. By observing the same source in each configuration, scientists can gather a great deal more information [9].

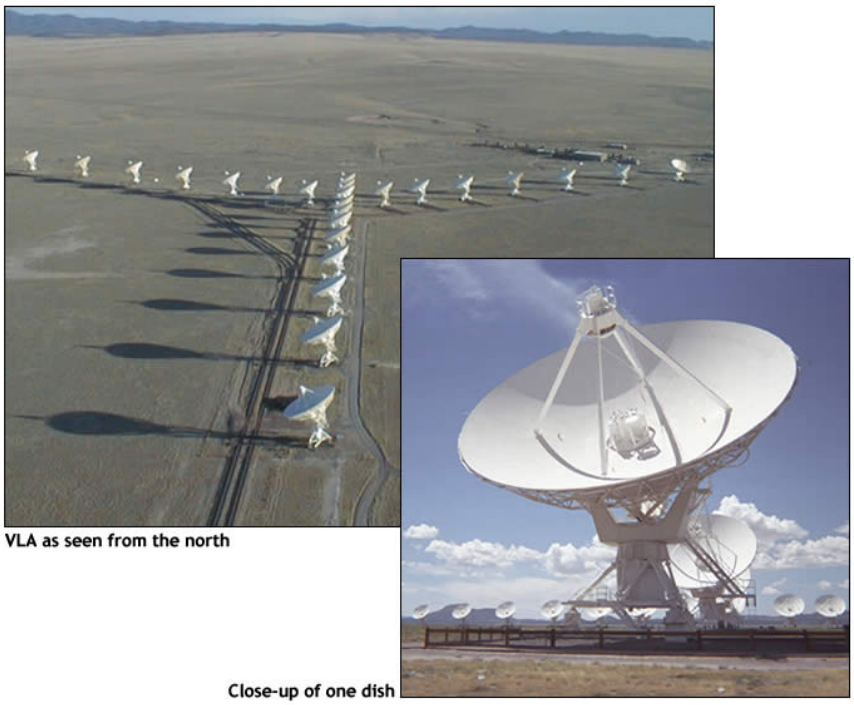

Figure B-24: The Very Large Array (VLA) Ground Telescope

		Resource Efficiency (1)	Multi-Configurations (2)	Evolution (3)	Survivability (4)
1	Potentiometer		1		
2	Airpot		1		
3	LEGO		1		
4	Vacuum	1	1		
5	Food Processor	1	1		
6	Sewing Machine		1		
7	Convertible Stroller Pack	1	1		
8	Digital PhotoFrame		1		
9	USM Haller Table		1		
10	3-in-1 Crib	1			
11	Sofa Bed	1	1		
12	Adjustable Bed		1		
13	Convertible Car		1		
14	SMART car		1		
15	Flexible Race Car		1		
16	NI RIO	1	1	1	
17	Reconfigurable Discrete Die	1	1	1	
18	RMS	1	1	1	
19	Polybot	1	1		1
20	LARA	1	1	1	1
21	SRR				1
22	SMM				1
23	SWARM	1	1	1	1
24	Xilinx Virtex II Pro FPGA	1	1	1	1
25	EHW			1	1
26	LongLifeSC Avionics	1			1
27	SmartSat-I RCE	1		1	1
28	MEMS patch Antenna	1	1		
29	TTC Transponder		1	1	
30	Morphing UAV		1		
31	F-14 Tomcat		1		
32	VDCH		1		
33	VLA		1		

Figure B-25: Table of Systems and Reconfigurability Need Categories

Bibliography

[1] http://directory.eoportal.org/pres_smmsolarmaximummission.html. Accessed: March 26, 2006

[2] http://moon.astronomy.cz/mise/lrv.jpg. Accessed: March 8, 2006

[3] http://science.ksc.nasa.gov/mirrors/images/images/pao/sts41c/10061449.jpg. Accessed: March 29, 2006

[4] http://www.aerospaceweb.org/aircraft/fighter/f14/. Accessed: February 23, 2006

[5] http://www.freescale.com/webapp/sps/site/application.jsp?nodeid=02wcbf07js1504. Accessed January, 2005

[6] http://www.freescale.com/webapp/sps/site/application.jsp?nodeid=02wcbf07js1504. Accessed March, 2006

[7] http://www.fueleconomy.gov/feg/fcv_benefits.shtml, Accessed: March 9, 2006.

[8] http://www.gmcanada.com/inm/gmcanada/french/about/overviewhist/images/hywire.jpg. Accessed: March 9, 2006.

[9] http://www.nrao.edu/intro/nm_astro.html. Accessed: February 23, 2006

[10] http://www.polarisindustries.com/en-us/atv/2006models/sportsman/sportsman700efi/specifications.htm. Accessed: May 2006

[11] http://www.worldautosteel.org/ulsas/general/background2.pdf. Accessed: March 2006.

[12] Nasa's Opportunity Rover Rolls Free On Mars. URL: http://www.nasa.gov/vision/universe/solarsystem/mer-060605.html Accessed: March 17, 2006

[13] Skunk Works Morphing UAV 3 Weeks Away From 1st Flight. URL: http://www.abovetopsecret.com/forum/thread147378/pg1 Accessed: June 2005

[14] www.jsc.nasa.gov/bu2/svlcm.html.

[15] *Oxford English Dictionary.* Oxford University Press, 1993.

[16] Paradigm Shift in Design for NASA's New Exploration Initiative. Final Report 16.89 Graduate Design Class Space Systems Engineering, 2004.

[17] http://heasarc.gsfc.nasa.gov/docs/heasarc/missions/images/solarmax_images.html, Accessed: February 26, 2006.

[18] http://www.aerosml.com/flightinternational91305.asp, Accessed: February 27, 2006.

[19] http://www.cardesignnews.com/features/2001/011214michelin-css/index.html, Accessed: March 9 2006.

[20] http://www.fas.org/man/dod-101/sys/ac/f-14.htm, Accessed: February 27, 2006.

[21] http://www.inetres.com/gp/military/ar/fighter/f-14.html, Accessed: February 26, 2006.

[22] http://www.nasa.gov/vision/universe/roboticexplorers/ants.html, Accessed: February 26, 2006.

[23] www.enidine.com, February 2006.

[24] http://heasarc.nasa.gov/docs/heasarc/missions/solarmax.html, February 25, 2006.

[25] W. Adams and L. Rider. Circular Polar Constellations Providing Single or Multiple Coverage above a Specified Latitude For Multi-Satellite Multi-beam Systems. *The Journal of the Astronautical Sciences*, 35, April 1987.

[26] Tom Allen and Joel Moses. ESD Terms and Definitions (version 12). Technical Report ESD-WP-2002-01, Massachusetts Institute of Technology, 2001.

[27] D.S. Apostolopoulos. *Analytical Configuration of Wheeled Robotic Locomotion.* PhD Thesis, Carnegie Mellon University, 2001.

[28] L. Apvrille, L. Dairaine, P. Senac, and M. Diaz. Satellite Telecom Software Dynamic Upgrade with QoS Continuity. In *20th AIAA International Communication Satellite Systems Conference and Exhibit*, number AIAA 2002-2014, Montreal, Canada, May 2002.

[29] F.M. Asl and A.G. Ulsoy. Capacity Management in Reconfigurable Manufacturing Systems with Stochastic Market Demand. In *2002 ASME International Mechanical Engineering Congress and Exposition*, number IMECE2002-MED-32872, 2002.

[30] F.M. Asl, A.G. Ulsoy, and Y. Koren. Dynamic Modeling and Stability of the Reconfiguration of Manufacturing Systems. In *Japan-USA Symposium on Flexible Automation*, Ann Arbor, MI, 2000.

[31] T.C. Bachman and R.C. Kline. Model for Estimating Spare Parts Requirements for Future Missions. In *Space 2004 Conference and Exhibit*, number AIAA-2004-5978, CA, September 2004.

[32] R.E. Barlow and F. Proschan. *Mathematical Theory of Reliability.* John Wiley & Sons, 1965.

[33] R.O Bartlett. NASA Standard Multimission Modular Spacecraft for Future Space Exploration. In *American Astronautical Society and Deutsche Gesellschaft fuer Luft-und Raumfahrt, Goddard Memorial Symposium*, number AAS 78-043, Washington, D.C, March 1978.

[34] M.G. Bekker. *Introduction to Terrain Vehicle Systems.* The University of Michigan Press, 1969.

[35] D.P. Bertsekas and J.N. Tsitsiklis. *Introduction to Probability.* Athena Scientific, 2002.

[36] Owen Brown. Reducing Risk of Large Scale Space Systems Using a Modular Architecture.

[37] J. Cabo, R. Bravo, E. Lopez, and O. Casas. Galileo TTC Transponder: A Multimode In-Orbit Reconfigurable Transponder.

[38] D. Caglar, C. Li, and D. Simchi-Levi. Two-Echelon Spare Parts Inventory System Subject to a Service Constraint. *IIE Transactions*, (36):1–12, 2004.

[39] M. Chaize. Enhancing the Economics of Satellite Constellations via Staged Deployment and Orbital Reconfiguration. Master's Thesis, Massachusetts Institute of Technology, June 2003.

[40] D. D. Chang and O. L. de Weck. Basic Capacity Calculation Methods and Benchmarking for MF-TDMA and MF-CDMA Communication Satellites. *International Journal of Satellite Communications and Networking*, 23(3):153–171, May/June 2005.

[41] S.N. Chau, A. Sengupta, T.A. Tran, and A. Bakhshi. Ultra Long-Life Spacecraft for Long Duration Space Exploration Missions. In *53rd International Astronautical Congress*, number IAC-02-U.2.05, Houston, TX, 2002.

[42] L. Chen, F. Xi, and A. Macwan. Optimal Module Selection for Preliminary Design of Reconfigurable Machine Tools. *Journal of Manufacturing Science and Engineering*, 127:104–115, February 2005.

[43] P.E. Clark and M.I. Rilee. Bees for ANTS: Space Mission Applications for the Autonomous Nano Technology Swarm. In *AIAA 1st Intelligent Systems Technical Conference*, number AIAA-2004-6303, Chicago, IL, September 2004.

[44] P.E. Clark and M.L. Rilee. LARA: Near Term Reconfiguration Concepts and Components for Lunar Exploration and Exploitation. Number IAC-04-IAA.3.8.1.08, Vancouver, Canada, October 2004. 55th International Astronautical Congress.

[45] A. Codrington. http://www.metropolismag.com/html/content_0602/usm/index.html, Accessed: 2002.

[46] A. Dawood and N. Bergmann. An Adaptive Instrument Module (AIM) for Satellite Systems. In *Fifth International Symposium on Signal Processing and its Applications, ISSPA '99*, Brisbane, Australia, August 1999.

[47] L. Dayaratna, G.L Ramos, and et.al. Multi-Output Frequency Generation System for AMC 15 and 16 Spacecrafts. In *22nd AIAA International Communications Satellite Systems Conference & Exhibit*, number AIAA 2004-3105, Monterey, CA, May 2004.

[48] O. L. de Weck and M.B. Jones. Isoperformance: Analysis and Design of Complex Systems with Known or Desired Outcomes. *Systems Engineering*, 9(1):45–61, 2006.

[49] Olivier L. de Weck, R. de Neufville, and M. Chaize. Staged Deployment of Communications Satellite Constellations in Low Earth Orbit. *Journal of Aerospace Computing, Information, and Communication*, 1(3):119–136, 2004.

[50] P. deSantis and P.S. Yeung. Regenerative Satellite Payload for Flexible Multi-Media Services. In *AIAA International Communications Satellite Systems Conference*, number AIAA-96-1037, Washington, February 1996.

[51] O.L. deWeck. Strategic Engineering: Designing Systems For an Uncertain Future. Presentation, January 2006. Presentation.

[52] O.L. deWeck and D. Chang. Architecture Trade Methodology for LEO Personal Communication Systems. In *20th International Communications Satellite Systems Conference*, number AIAA-2002-1866, Montreal, Canada, May 2002.

[53] D. P. Diekelman, G. T. Kroncke, and K. A. Olds. Method and Apparatus for Early Service Using Phased Satellite Deployment. Technical Report U.S. Patent No. 6,007,027, Motorola, December 28, 1999.

[54] Dov Dori. *Object-Process Methodology*. Springer, 2002.

[55] P. Eckart. *Lunar Base Handbook*. Space Technology Series. 1999.

[56] J.J. Zakrajsek et. al. Exploration Rover Concepts and Development Challenges. In *1st Space Exploration Conference: Continuing the Voyage of Discovery*, number AIAA-2005-2525, Orlando, FL, Jan-Feb 2005.

[57] J.R. Matijevic et al. Surface Transport Vehicles and Supporting Technology Requirements. In *AIAA Space Programs Technology Conferences*, number AIAA-92-1485, Hunstsville, AL, March 1992.

[58] W. Zhong et al. Performance Analysis of Machining Systems with Different Configurations. In *Proceedings of JUSFA: Japan-USA Symposium on Flexible Manufacturing*, 2000.

[59] P.S. Schenker et.al. Reconfigurable Robots for All Terrain Exploration. *Proceedings of SPIE*, 4196:454–468, October 2000.

[60] W. Feller. *An Introduction to Probability Theory and Its Applications, Volume 1.* John Wiley & Sons, third edition, 1968.

[61] S. Ferguson and L. Kemper. Effective Development of Flexible Systems in Multidisciplinary Optimization. In *10th AIAA/ISSMO Multidisciplinary Analysis and Optimization Conference*, number AIAA 2004-4309, Albany, NY, August-September 2004.

[62] E. Fricke. Fall 2003, System Architecture Notes: Design for Changeability, MIT. November 2003.

[63] W. Frisina. Modular Spacecraft. *Journal of Aerospace Engineering*, 7(4):411–417, 1994.

[64] P. Gu, M. Hashemian, and A.Y.C Nee. Adaptable Design. *CIRP Annals 2004*, 53(2), 2004.

[65] S. Hauck. The Future of Reconfigurable Systems. In *5th Canadian Conference on Field Programmable Devices*, number Key note address, Montreal, June 1998.

[66] S. J. Hoffman and D.I. Kaplan. Human Exploration of Mars: The Reference Mission of the NASA Mars Exploration Study Team. NASA Special Publication 6107, 1997.

[67] K. M. M. Holtta and K.N. Otto. Incorporating Design Effort Complexity Measures in Product Architectural Design and Assessment. *Design Studies*, 26:463–485, 2005.

[68] R.A. Howard. *Dynamic Probabilistic Systems Vol 1: Markov Models.* John Wiley & Sons, 1971.

[69] V. Hubka and W.E. Eder. *Theory of Technical Systems.* Springer-Verlag, 1988.

[70] K. Iagnemma and S. Dubowsky. *Mobile Robots in Rough Terrain: Estimation, Mobility Planning and Control with Application to Planetary Rovers.* Springer Tracts in Advanced Robotics, V. 12. Springer, 2004.

[71] K. Iagnemma and S. Dubowsky. Traction Control of Wheeled Robotic Vehicles in Rough Terrain with Application to Planetary Rovers. *The International Journal of Robotics Research*, 23(10-11):1029–1040, October-November 2004.

[72] K. Iagnemma, A. Rzepniewski, and S. Dubowsky. Mobile Robot Kinematic Reconfigurability for Rough Rerrain. In *Proceedings of the SPIE Symposium on Sensor Fusion and Decentralized Control in Robotic Systems III*, Boston, 2000.

[73] S. J. Isakowitz, J. Hopkins, and J. P. Hokpins Jr. *International Reference Guide to Space Launch Systems*. AIAA, third edition, 1998.

[74] S. J. Isakowitz, J. Hopkins, and J. P. Hokpins Jr. *International Reference Guide to Space Launch Systems*. AIAA, fourth edition, 2004.

[75] S. P. Joshi, Z. Tidwell, W. A. Crossley, and S. Ramakrishnan. Comparison of Morphing Wing Strategies Based Upon Aircraft Performance Impacts. In *45th AIAA/ASME/ASCE/AHS/ASC Structures, Structural Dynamics and Materials Conference*, number AIAA-2004-1722, Palm Springs, CA, April 2004.

[76] R.W. Fricke Jr. STS-61 Space Shuttle Mission Report. Mission Report NASA-TM-110545, NASA, 1994.

[77] T. P. Emmons Jr., R. S. Torkington, and J. E. Klekotka. Technique for Satellite Constellation Growth. Technical Report U.S. Patent No. 6,491,257 B1, Motorola, December 10, 2002.

[78] D. Keymeulen, R. Zebulum, Y. Jin, and A. Stoica. Fault-Tolerant Evolvable Hardware Using Field-Programmable Transistor Arrays. *IEEE Transactions on Reliability*, 49(3):305–316, 2000.

[79] M. Kifle and M. Andro et.al. Toward a Dynamically Reconfigurable Computing and Communication System for Small Spacecraft. In *21st International Communication Satellite Systems Conference and Exhibition*, number AIAA 2003-2285, 2003.

[80] S. Kirkpatrick, C.D. Gelatt, and M.P. Vecchi. Optimization by Simulated Annealing. *Science*, (220):671–680, 1983.

[81] R.G. Landers, B-K. Min, and Y. Koren. Reconfigurable Machine Tools. *Annals of the CIRP-2001*.

[82] W.J. Larson and L.K. Pranke, Editors. *Human Spaceflight Mission Analysis and Design*. McGraw-Hill.

[83] G. Lechner and H. Naunheimer. *Automotive Transmission: Fundamentals, Selection, Design and Application*. Springer, 1999.

[84] S. J. Leete. Design for On-Orbit Spacecraft Servicing. In *2001 Core Technologies for Space Systems Conference*, Colorado Springs, Colorado, November 2001.

[85] P. Loreti and M. Luglio. Interference Evaluations and Simulations for Multi-Satellite Multi-beam Systems for Multi-Satellite Multi-beam Systems. *International Journal of Satellite Communications*, (20):261–281, 2002.

[86] E. Lutz and A.J. Werner. *Satellite Systems for Personal and Broadband Communications*. Springer-Verlag, 2000.

[87] C. Magee and O. L. de Weck. Complex System Classification. In *Fourteenth Annual International Symposium of the International Council on Systems Engineering (INCOSE)*, Toulouse, France, June 2004.

[88] C.S. Marino and P.M. Chau. Reconfigurable Adaptive Interface Nulling (RAIN) Satellite Architecture. In *AIAA Space Technology Conference and Exposition, Albuquerque*, number AIAA-99-4495, Albuquerque, NM, September 1999.

[89] P. Marks. The Next 100 Years of Flight -Part Two,
URL http://www.newscientist.com/article.ns?id=dn4484, Accessed: February 26, 2006

[90] N.I. Marzwell, R.D. Waterman, K.Krishnakumar, and S.J. Waterman. How to Extend the Capabilities of Space Systems for Long Duration Space Exploration Systems. In *Space Technology and Applications International Forum-STAIF 2005*, number CP746, 2005.

[91] J.R. Matijevic, J. Crisp, and et. al. Characterization of the Martian Surface Deposits by the Mars Pathfinder Rover, Sojourner. *Science*, 278:1765–1768, December 5 1997.

[92] Douglas McGray. Hot Wheels. *Wired Magazine*, October 2004.

[93] M.G. Mehrabi, A.G. Ulsoy, and Y. Koren. Reconfigurable Manufacturing Systems: Key to Future Manufacturing. *Journal of Intelligent Manufacturing*, 11:403–419, 2000.

[94] M.G. Mehrabi, A.G. Ulsoy, and Y. Koren. Trends and Perspectives in Flexible and Reconfigurable Manufacturing Systems. *Journal of Intelligent Manufacturing*, (13):135–146, 2002.

[95] C. Mellor. Quick-Change Artists. *The Ontario Technologist*, Jan/Feb 2002.

[96] D. Miller. Self-Assembling Wireless Autonomously Reconfigurable Modules (SWARM). Presentation at the Marshall Space Flight Center, April 2005.

[97] J. Miller, J Guerrero et.al. Spaceframe: Modular Spacecraft Building Blocks for Plug and Play Spacecraft. In *16th Annual/ USU Conference on Small Satellites*, Utah, 2002.

[98] W.J. Mitchell. MIT Media Lab's Concept Car: With GM and Frank O. Gehry. Presentation, October 2004.

[99] M. Mondin, L.L. Presti, and A. Scova. A Software Radio-Based Reconfigurable Transponder for Space Applications. *Wireless Communications and Mobile Computing*, 2:839–845, 2002.

[100] Y-M. Moon and S. Kota. Design of Reconfigurable Machine Tools. *Journal of Manufacturing Science and Engineering*, 124:480–485, 2002.

[101] Y-M. Moon and S. Kota. Generalized Kinematic Modeling of Reconfigurable Machine Tools. *Journal of Mechanical Design*, 124:47–51, March 2002.

[102] W. Nace and P. Koopman. A Product Family Approach to Graceful Degradation. In *Proceedings of DIPES 2000, International IFIP WG 10.3 / WG 10.4 / WG 10.5 Workshop on Distributed and Parallel Embedded Systems*, Paderborn University, Germany, October 2000.

[103] E.O.A Naumann and E.A. Smith. A Manned Lunar Surface Vehicle Concept. In *AIAA/AFLC/ASD Support for Manned Flight Conference*, number AIAA Paper No. 65-250, Dayton, OH, April 1965.

[104] N. Nishinaga and Y. Ogawa et.al. SoftSAT: Reconfigurable Communication Satellite System. In *21st International Communications Satellite Systems Conference and Exhibit*, number AIAA-2003-2420, 2003.

[105] N. Nishinaga, M. Takeuchi, and R. Suzuki. Reconfigurable Communication Equipment on SMARTSAT-I.

[106] A. Olewnik, T. Brauen, S. Ferguson, and L. Kemper. A Framework for Flexible Systems and its Implementation in Multi-attribute Decision Making. *Transactions of the ASME*, 126(412-419), May 2004.

[107] et al Olivier L. de Weck. Modular Structures for Manned Space Exploration: The Truncated Octahedron as a Building Block. In *First Space Exploration Conference: Continuing the Voyage of Discovery*, number AIAA-2005-2764, Orlando, FL, February 2005.

[108] F. Pizzano and R.S. Kincade. Hubble Space Telescope Maintenance and Refurbishment Planning Analysis. In *AIAA and NASA, Symposium on the Maintainability of Aerospace Systems*, number AIAA-1989-5048, July 1989.

[109] R. Polidan and M. Steiner. Reconfigurable Systems and NASA - The GSFC Vision. In *2003 Core Technologies for Space Systems Conference*, Boulder, CO, 2003.

[110] J. Quinn. Repairman in Space.
URL http://www.inventionandtechnology.com/xml/2003/1/it_2003_1_dept_hofreport.xml

[111] M. Richharia. *Satellite Communications Systems: Design Principles*. McGraw-Hill, New York, third edition, 1999.

[112] L. Rider. Optimized Polar Orbit Constellations for Redundant Earth Coverage. *The Journal of the Astronautical Sciences*, 33(2), April-June 1995.

[113] L. Rodgers. Concepts and Technology Development for the Autonomous Assembly and Reconfiguration of Modular Space Systems. Master's Thesis, Massachusetts Institute of Technology, 2005.

[114] S. Romano and F. Pavlics. The Role of Roving Vehicles in Lunar Surface Exploration. In *AIAA 5th Annual Meeting and Technical Display*, number AIAA-68-1026, Philadelphia, PA, October 1968.

[115] A.M Ross, N.P. Diller, and D.E Hastings. Multi-attribute Tradespace Exploration with Concurrent Design for Space System Conceptual Design. In *41st Aerospace Science Meeting and Exhibit*, number AIAA 2003-1328, Reno, Nevada, January 2003.

[116] B. Roth, C. Peters, and W.A. Crossley. Aircraft Sizing with Morphing as an Independent Variable: Motivation, Strategies and Investigations. In *AIAA's Aircraft Technology, Integration, and Operations (ATO) 2002 Techical*, number AIAA-2002-5840, Los Angeles, CA, October 2002.

[117] Joseph H. Saleh, Daniel E. Hastings, and Dava J. Newman. Flexibility in System Design and Implications for Aerospace Systems. *Acta Astronautica*, 53:927–944, 2003.

[118] F. Salvador, C. Forza, and M. Rungtusanatham. Modularity, Product Variety, Production Volume, and Component Sourcing: Theorizing Beyond Generic Prescriptions. *Journal of Operations Management*, 20:549–575, 2002.

[119] F.M. Saverio. The Lunar Roving Vehicle Historical Perspective. In *Second Conference on Lunar Bases and Space Activities of the 21st Century*, 1988.

[120] W.R. Schindler and B. Raab. Multi-Mission Modular Spacecraft/MMS/ - A Natural Extension of STS. In *EASCON '80; Electronics and Aerospace Systems Conference*, Arlington, VA, Sept 29-Oct 1 1980.

[121] Lucy Sherriff. Spirit Reveals Mars' Violent Past.
URL http://www.theregister.co.uk/2005/05/25/mars_rovers_progress/
Accessed: March 17, 2006

[122] S.M. Shinners. *Techniques of System Engineering.* McGraw-Hill, 1967.

[123] R. Shishko. Calculating Space Station Resource Prices. In *Space 2000 Conference and Exhibit*, number AIAA-2000-5322, CA, September 2000.

[124] A. Siddiqi, J. Mellein, and O. L. de Weck. Optimal Reconfigurations for Increasing Capacity of Communication Satellite Constellations. In *1 st AIAA Multidisciplinary Design Optimization Specialist Conference*, number AIAA-2005-2065, Austin, TX, April 18-21 2005.

[125] R.N. Simons, D. Chun, and L.P. Katehi. Micro-electromechanical Systems (MEMS) Actuators for Antenna Reconfigurability. Technical Report NASA/CR-2001-210612, National Aeronautics and Space Administration, Glenn Research Center, 2001.

[126] R.M. Smaling. *System Architecture Analysis and Selection Under Uncertainty*. PhD thesis, Massachusetts Institute of Technology, 2005.

[127] M. Smotherman and K. Zemoudeh. A Non-Homogeneous Markov Model for Phased-Mission Reliability Analysis. *IEEE Transactions on Reliability*, 38(5), 1989.

[128] S.Y Son, T.L. Olsen, and D. Yip-Hoi. Economic Benefits of Reconfigurable Manufacturing Systems. In *Proceedings of the 2000 Japan-USA Flexible Automation Conference*, number 2000JUSFA-13193, Ann Arbor, Michigan, July 2000.

[129] P. Spicer, D. Y-Hoi, and Y. Koren. Scalable Reconfigurable Equipment Design Principles. *International Journal of Production Research*, 43(22):4839–4852, 2005.

[130] P.N. Springmann and O. L. de Weck. Parametric Scaling Model for Non Geo-Synchronous Communication Satellites. *Journal of Spacecraft and Rockets*, 41(3):472–477, 2004.

[131] Steve Squyres. Opportunity Stuck in Sand Dune.
URL http://www.spacedaily.com/news/mars-mers-05zq1.html, Accessed: March 17, 2006

[132] A. Stoica, R. S. Zebulum, D. Keymeulen, M.I. Ferguson, and A. Thakoor. Evolvable, Reconfigurable Hardware for Future Space Systems. In *53rd International Astronautical Congress*, number IAC 02-U.1.07, Houston, TX, 2002.

[133] K. Ulrich. The Role of Product Architecture in the Manufacturing Firm. *Research Policy*, 24:419–440, 1995.

[134] K.T. Ulrich and S.D. Eppinger. *Product Design and Development*. McGraw-Hill, 1995.

[135] A. Urbani and S.P. Negri. Example of Measure of the Degree of Reconfigurability of a Modular Parallel Kinematic Machine. In *3rd International Conference on Reconfigurable Manufacturing*, Ann Arbor, MI, August 2005.

[136] G. Walberg. How Shall We Go To Mars? A Review of Mission Scenarios. *Journal of Spacecraft and Rockets*, 30(2), March-April 1993.

[137] D.F. Walczyk, J. Lakshmikanthan, and D.R. Kirk. Development of a Reconfigurable Tool for Forming Aircraft Body Panels. *Journal of Manufacturing Systems*, 17(4):287–296, 1998.

[138] B.E. Wallace and D.L. Thrasher. A Preliminary Design Tool for Planetary Rover Subsystems. In *1992 Aerospace Design Conference*, number AIAA 92-1109, Irvine, CA, 1992.

[139] M.A. Walton and D.E. Hastings. Applications of Uncertainty Analysis to Architecture Selection of Satellite Systems. *Journal of Spacecraft and Rockets*, 41(1):75–84, January-February 2004.

[140] V.L. Wells, J.W. Rutherford, and A.M. Corgiat. Mission and Concept Evaulation for A Multirole, Mission-adaptable Air Vehicle. *Aircraft Design*, 2:65–80, 1999.

[141] J. Wertz. *Expected Productivity-Baed Risk Analysis in Conceptual Design: With Application to the Terrestrial Planet Finder Interferometer Mission*. PhD thesis, Massachusetts Institute of Technology, February 2006.

[142] J.R. Wertz and W.J. Larson, editors. *Space Mission Analysis and Design*. Space Technology Series. Microcosm Press and Kluwer Academic Publishers, third edition, 1999.

[143] D.A. Whitney. *Mechanical Assemblies: Their Design, Manufacture, and Role in Product Development*. Oxford Series on Advanced Manufacturing. Oxford University Press, 2004.

[144] J. Y. Wong. *Theory of Ground Vehicles*. Wiley-Interscience, third edition, 2001.

[145] Z. Xiaobo, W. Jiancai, and L. Zhenbi. A Stochastic Model of a Reconfigurable Manufacturing System Part1: A Framework. *International Journal of Production Research*, 38(10):2273–2285, 2000.

[146] A. S. Yigit and A. Allahverdi. Optimal Selection of Module Instances for Modular Products in Reconfigurable Manufacturing Systems. *International Journal of Production Research*, 41(17):4063–4074, 2003.

[147] M. Yim, K. Roufas, and D. Duff et al. Modular Reconfigurable Robots in Space Applications. *Autonomous Robot Journal*, Special Issue for Robots in Space, 2003.

[148] A.I. Zaghloul, E.C. Kohls, and O. Kilic. Active Phased Arrays for Satellite Communications: A System Perspective. In *20th AIAA International Communication Satellite Systems Conference and Exhibit*, number AIAA-2002-2031, Montreal, May 2002.